CERTIFICATE FROM THE SUPERVISOR(S)

This is to certify that the thesis entitled " **Nucleosome Remodelers in Mesenchymal Stromal Microenvironment** " Submitted by Sri / ~~Smt.~~ **Sayan Chakraborty** who got his / ~~her~~ name registered on **31.08.2016** for the award of Ph. D. (Science) degree of Jadavpur University, is absolutely based upon his own work under the supervision of **Dr. Amitava Sengupta** and that neither this thesis nor any part of it has been submitted for either any degree / diploma or any other academic award anywhere before.

Amitava Sengupta 30/3/22

Dr. Amitava Sengupta
प्रधान वैज्ञानिक, सह-प्राध्यापक
Principal Scientist, Associate Professor
भारतीय रासायनिक जीवनविज्ञान संस्थान
CSIR-Indian Institute of Chemical Biology
CN-6, Sector V, Salt Lake, Kolkata - 700091

(Signature of the Supervisor(s) date with official seal)

Nucleosome Remodelers in Mesenchymal Stromal Microenvironment

by

Sayan Chakraborty

Thesis submitted in partial fulfilment of the requirements

for the degree of

Doctor of Philosophy in Biology

At

Department of Life Science and Biotechnology

Faculty Council of Science

Jadavpur University

March 2022

Nucleosome Remodelers in Mesenchymal Stromal Microenvironment

by

Sayan Chakraborty

Thesis submitted in partial fulfilment of the requirements

for the degree of

Doctor of Philosophy in Biology

At

Department of Life Science and Biotechnology

Faculty Council of Science

Jadavpur University

Under the supervision of :

Dr. Amitava Sengupta

Cancer Biology Department

CSIR – Indian Institute of Chemical Biology

Nucleosome Remodelers in Mesenchymal Stromal Microenvironment

Sayan Chakraborty

ABSTRACT

Multipotency (*ability to differentiate into multiple mature cell types*) governed by asymmetrical division and self-renewal capacity (*ability to replenish the stem cell pool*) through symmetrical division are the two pivotal features of stem cells which ultimately help to maintain tissue homeostasis. In addition to regenerating tissue in response to normal wear and tear, trauma or disease, resident stem cells are now also understood to actively communicate with the tissue microenvironment as well as modulate immune components via secretion of various soluble paracrine factors and cell-to-cell interaction.

One of the most widely studied multipotent stem cells is ‘mesenchymal stem cells‘ (MSC) which was discovered in bone marrow stroma in 1960s and originally identified as the ‘colony-forming unit fibroblast‘. The ‘stemness’ is due to their trilineage differentiation potential into adipocytes, osteoblasts or chondrocytes. Some studies have shown that MSCs can also trans-differentiate into cells of ectodermal and endodermal lineages. MSCs were later named as ‘mesenchymal stromal cells’ because of their heterogeneous cell multipotency and fibroblast-like properties. The phenotypic profiles of both human and mouse MSCs are that they express CD29, CD51, CD73, CD90 and CD105 but not CD31, CD45 or markers of the hematopoietic lineage.

Dynamicity in epigenetic marks are known to be decisive regulatory factors in stem cell fate determination and differentiation. Investigation of epigenetic regulation of stem cell biology has mainly focused on embryonic stem cell (ESC) in past few decades but less is known about adult stem cells (AdSCs). MSCs are the most investigated AdSC population due to their enormous potential for therapeutic applications in regenerative medicine and tissue engineering. Although transcriptional regulation has been extensively investigated, little is known about the epigenetic mechanisms underlining key aspects of MSC biology.

Thus the epigenetics of MSCs is an intriguing area of investigation holding great promise for both basic and applied researches.

Recent evidences highlight importance of epigenetic regulation and their integration with transcriptional and cell signaling machinery in determining tissue resident adult pluripotent mesenchymal stem/stoma cell (MSC) activity, lineage commitment and multicellular development. Histone modifying enzymes and large multi-subunit chromatin remodeling complexes and their cell type-specific plasticity remain the central defining features of gene regulation and establishment of tissue identity. Modulation of transcription factor expression gradient *ex vivo* and concomitant flexibility of higher order chromatin architecture in response to signaling cues are exciting approaches to regulate MSC activity and tissue rejuvenation. Being an important constituent of the adult bone marrow microenvironment/niche, pathophysiological perturbation in MSC homeostasis also causes impaired hematopoietic stem/progenitor cell function in a non-cell autonomous mechanism. In addition, MSCs can function as immune regulatory cells, for instance by virtue of its regulation of TGF-β signaling. Research in the past few years suggest that MSCs / stromal fibroblasts significantly contribute to the establishment of immunosuppressive microenvironment in shaping antitumor immunity. Therefore, it is important to understand mesenchymal stoma epigenome and transcriptional regulation to leverage its applications in regenerative medicine and immune reprogramming.

The Nucleosome Remodeling and Histone Deacetylation (NuRD) complex is a multisubunit chromatin remodeling complex that couples ATP-dependent nucleosome sliding with histone deacetylase activity. Clinical trials using HDAC inhibitors like TSA, SAHA in various human and mice models of inflammatory diseases and autoimmune disorders have shown promising outcome in ameliorating the inflammatory burden. The involvement of class I HDAC complex like NuRD in regulating inflammatory response mediated by immune cells has also been well documented over the recent years. Altogether these initial findings have led us to investigate the role of NuRD complex during inflammatory response in non-immune cells like MSCs along with its possible pivotal role in MSC-driven osteogenesis which is highly connected to the inflammatory mileu present within the MSC niche.

Our findings identify Gatad2b as a positive regulator of MSC mediated inflammatory response in spite of the fact that as an integral component of NuRD it plays a role as transcriptional repressor. *Gatad2b* deficient stroma possess a molecular signature of being less immune-responsive or more immune-suppressive which determines the plasticity of its secretome. Our data showed that in variety of *in vitro* cellular model of stromal inflammation the optimal *Gatad2b* response was in between 6 hours to 12 hours and this time frame

mimics the acute stage of inflammation. So *Gatad2b* might be a regulator of acute inflammation and acute inflammation promotes osteogenesis. Hence we hypothesised that NuRD might also have a role during MSC-driven osteogenesis and this was demonstrated further when *Gatad2b* deficient stroma showed impaired osteogenesis and activation of BMP/SMAD signaling.

Altogether this work might be valuable for future strategies with the aim of maintaining stroma mediated tissue homeostasis, developing anti-tumor immunity as well as treating various inflammatory diseases.

ACKNOWLEDGEMENTS

This thesis work would have been impossible without the support of a great deal of people. I wish to take this opportunity to convey my sincere thankfulness to everyone who silently stood behind me to make this achievable.

I would like to thank my guide and mentor Dr. Amitava Sengupta for allowing me to work on this project. Without his help, recommendation and support, this thesis would not have been possible. His enthusiasm and mission of providing high quality work has been a spirit during my doctoral pursuit. I am also thankful to him for providing necessary funding to carry out the work. I am grateful to Dr. Debasis Banerjee, our clinical collaborator, for providing us with precious patient samples. I thank him for his constant support and inputs.

I appreciatively acknowledge the funding received towards my research award from the Council of Scientific & Industrial Research, Govt of India. I also thank all the other funding agencies whose contribution has enabled me to conduct this study smoothly.

My heartfelt thanks to my senior Shankha Subhra Chatterjee and and my colleagues Mayukh Biswas, Liberalis Debraj Boila and Sayantani Sinha for their help, cooperation and moral support. It was pleasure collaborating with them within the workplace. I would like to thank Shankha and Mayukh who helped me to acclimatize myself in the new work environment during the early days. I take this chance to also thank the next generation Ph.D. fellows of my lab namely Subham, Subhadeep, Wasim, Satyaki, Shinjan and Anwesha for their constant support and cooperation. It has been a gorgeous learning curve working with them and having fashioned recollections to hold dear always. This group has been a source of friendship as well as good counsel and collaboration.

I am thankful to my parents Mr. Saumitra Chakraborty and Mrs. Bani Chakraborty and to my wife Mousumi Bhattacharyya for their support, belief and advocacy. Their patience and sacrifice are going to be precious to me throughout my life. A special note of thanks to my teachers, whose teaching at different stages of education has made it possible for me to see this day. Since it is not possible to mention everyone due to lack of space, I express my gratitude to everyone for their love, cooperation and support. Finally, I am thankful to library staff, administrative staff and support staff of CSIR-IICB for their cooperation.

Sayan Chakraborty

Dedicated to my loving

Grandfather

The late Kamal Krishna Mitra

&

My beloved father

The late Saumitra Chakraborty

TABLE OF CONTENTS

SYNOPSIS

Stem cell niches are defined as the cellular and molecular microenvironments that regulate stem cell function together with stem cell autonomous mechanisms. This includes control of the balance between quiescence, self-renewal, and differentiation, as well as the engagement of specific programs in response to stress. In mammals, the best understood niche is that harboring bone marrow hematopoietic stem cells (HSCs). Adult bone marrow mesenchymal stem cells or marrow stromal cells (MSC) and osteolineage progenitors constitute major cell component of the HSC microenvironment or niche that regulates HSC proliferation and quiescence. A complex interplay of cytokines, chemokines, proteolytic enzymes and adhesion molecules maintain HSC integrity within the bone marrow niche (**4**). Genetic manipulation of the bone marrow stem cell niche may evolve as an important therapeutic approach to establish a conducive environment favoring proliferation of healthy cells and avert bone marrow failure or hematological malignancies.

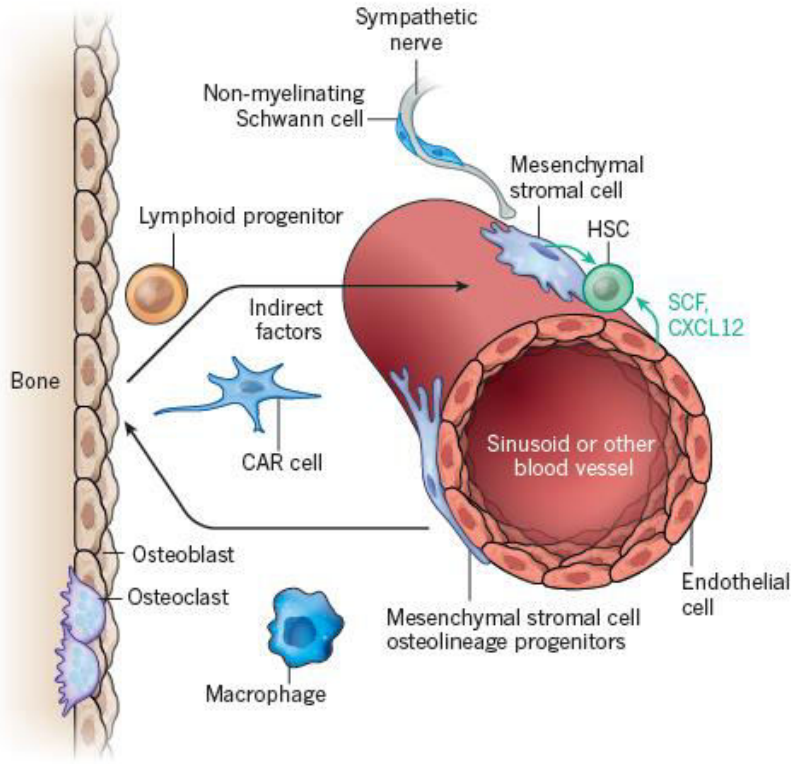

Fig. 1 : Hematopoietic stem cells and progenitors occupy specific niches of the bone marrow. SCF and CXCL12 secreted by the stromal cells helps in HSC maintenance. Osteoblasts arising from the MSCs also control hematopoiesis by secretion of a class of cytokines required by the HSCs. *Adapted from Nature 2014 Jan 16;505(7483):327-34*.

Haematopoietic stem cells (HSCs) and restricted haematopoietic progenitors occupy distinct niches in the bone marrow. HSCs are found mainly adjacent to sinusoids throughout the bone marrow where endothelial cells and mesenchymal stromal cells promote HSC maintenance by producing SCF, CXCL12 and other factors. Similar cells may also promote HSC maintenance around other type of blood vessels, such as arteriols. The mesenchymal stromal cells can be identified based on their expression of Lepr-Cre, Prx1-Cre, Cxcl12-GFP or Nes-GFP transgenes in mice and similar cells are likely to be identified by CD146 expressions in humans. Perivascular stromal cells, which probably include Cxcl12-abundant reticular (CAR) cells, are fated to form bone in vivo. It is likely that other cells also contribute to this niche, these probably include cells near bone surfaces in trabecular-rich areas. Other cell types that regulate HSC niches include sympathetic nerves, non-myelinating Schwann cells, macrophages and osteoclasts. The extracellular matrix and calcium also regulate HSCs. Osteoblasts directly do not promote HSC maintenance but do promote the maintenance and perhaps the differentiation of certain lymphoid progenitors by secreting CXCL12 and probably other factors. Early lymphoid restriced progenitors thus reside in an endosteal niche that is spatially and cellularly distinct from HSCs (**5**).

Adult mesenchymal stem cells (MSCs) can be isolated from bone marrow or marrow aspirates and because they are culture-dish adherent,they can be expanded in culture while maintaining their multilineage differentiation potential. The MSCs have been used in preclinical models for tissue engineering of bone, cartilage, muscle, marrow stroma, tendon, fat, and other connective tissues. These tissue-engineered materials show considerable promise for use in rebuilding damaged or diseased mesenchymal tissues. Moreover, MSCs secrete a large spectrum of bioactive molecules. These molecules are immunosuppressive, especially for T-cells and, thus, allogeneic MSCs can be considered for therapeutic use. In this context, the secreted bioactive molecules provide a regenerative microenvironment for a variety of injured adult tissues to limit the area of damage and to mount a self-regulated regenerative response. Therefore, MSCs appear to be valuable mediators for tissue repair and regeneration. The natural titers of MSCs that are drawn to sites of tissue injury can be augmented by allogeneic MSCs delivered via the bloodstream. Indeed, human clinical trials are now under way to use allogeneic MSCs for treatment of myocardial infarcts, graft-versus-host disease, Crohn’s Disease, cartilage and meniscus repair, stroke, and spinal cord injury (**6,7**).

One of the major clinical implications of MSCs involve with their capacity to produce osteoblasts and bone repair / formation which is highly orchestrated with the inflammatory mileu present within the stromal niche. Depending upon the extent of inflmmation MSCs do modulate itself as well as the local microenvironment to promote tissue remodeling and repair. Physiologically acute phase of inflammation promote osteogenesis but if inflammation persists then it becomes chronic which leads to bone resorption and bone loss.

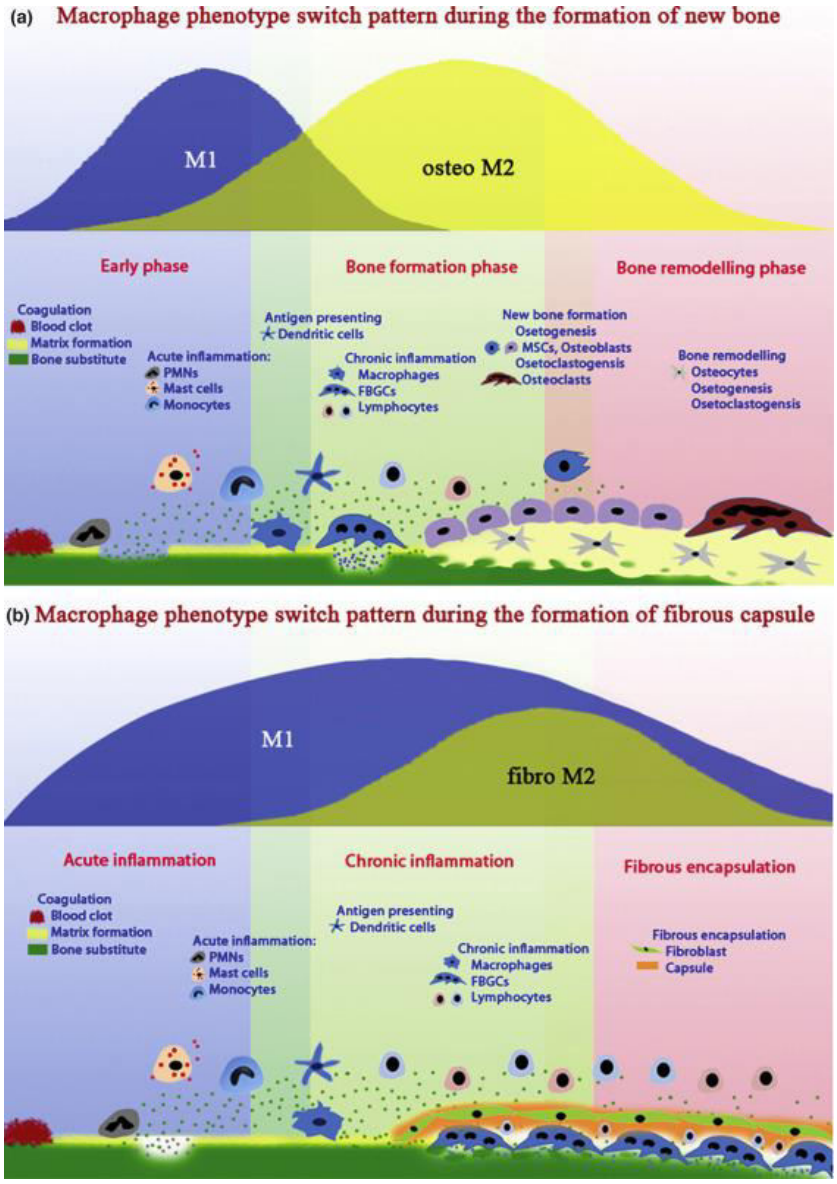

Fig. 2 : Schematic illustration of different phases of inflammation influencing *de novo* bone formation. (a) Different stages of bone formation and macrophage phenotype inflencing the process (b) During the early inflammation stage macrophages are predominantly of M1 phenotype and if the inflammation persists M1 to M2 switching occurs which result into an increase in fibrosis. *Adapted from Materials Today Volume 19, Number 6 July/August 2016*.

There are various mechanisms involved to maintain an efficient stroma. But not much attention has been given to the epigenetic regulation within the stromal niche particularly how chromatin remodeling complexes like NuRD can regulate the functional integrity of a stromal microenvironment.

In a previous study Ramirez-Carrozi et. al showed the anti-inflammatory function of NuRD complex in lipopolysacharide (LPS)-stimulated macrophages upon getting selectively recruited along with the SWI/SNF complexes to the control regions of secondary response genes and primary response genes with delayed kinetics (**157**). However the role in regulating the rapidly induced primary response genes were yet to be explored. In an another study by Pakala and colleagues metastasis-associated protein 1 (MTA1), a component of NuRD, was found to be a target of inflammation and stimulation of macrophages with LPS stimulated MTA1 transcription via NF-Kb pathway. MTA1 depletion in LPS stimulated macrophages impairs NF-Kb signaling and expression of inflammatory molecules. Subsequent studies found MTA1 protein to be involved in the regulation of the expression of myeloid-differentiation factor 88 and transglutaminase 2, both key components of NF-kB signaling in a variety of inflammatory diseases (**161**). Very recently El-Nikhely et. al showed metastasis-associated protein 2 (MTA2), another subunit of NuRD complex to be getting regulated by IKK2/NF-Kb signaling pathway in a c-Raf induced lung tumor (**158**). Trizzino et. al also demonstrated NuRD to be associated with EGR1, an important transcription factor for monocytic/macrophagic differentiation, leading to the repression of inflammatory enhancers in differentiating human macrophages (**159**). In addition Ikaros was shown to be functioning as a co-repressor upon binding with the CHD4 subunit of NuRD for the LPS-responsive genes in resting macropahges (**160**).

In recent years, a number of clinical trials using HDAC inhibitors are going on for treating several chronic inflammatory diseases and autoimmune disorders. HDAC inhibitors act as anti-inflammatory components in a dose-dependent manner, resulting in decreased proinflammatory cytokine production. Using animal models for rheumatoid arthritis have demonstrated that treatment with TSA, phenylbutyrate, or FK228 resulted in a decrease in the proinflammatory cytokine TNF-*α*. Since this initial work, numerous studies from both human and animal models of inflammatory or autoimmune diseases have documented the anti-inflammatory properties of several HDAC inhibitors. Two HDAC inhibitors (TSA and SAHA) have shown promise in future treatment for type 1 diabetes, a metabolic disease which has a substantial inflammatory component. In an *in vitro* study using pancreatic beta cells, both TSA and SAHA reduced cytokine-mediated cellular destruction in an NF-*κ*B dependent manner, indicative of a reduction in the inflammatory pathology (**162**).

In other immune-related pathophysiological mechanisms, TSA has been shown to reduce production of proinflammatory cytokines and ameliorate pathological destruction of myelin in a murine model of multiple sclerosis. As a key regulator of immune responses, monocyte and macrophage responses to HDAC inhibitor treatment are of particular importance. Human monocytes stimulated with proinflammatory lipopolysaccharide (LPS) or TNF-*α* and subsequently treated with the novel Class I HDAC1 inhibitor NW-21 decreased synthesis of the proinflammatory cytokines MIP-1*α* and MCP-1, suggesting that HDAC inhibitor treatment may help reduce synovial inflammation and be potentially useful in the management of rheumatoid arthritis. It is interesting to note that levels of other proinflammatory cytokines, notably TNF-*α* and IL-1*β*, were not affected when treated with NW-21. Finally, in both *in vitro* and *in vivo* models for inflammatory bowel disease (IBD), both valproic acid and SAHA drastically reduced TNF-*α* and IFN-*γ* levels, suggesting that HDAC inhibitors may prove fruitful as a novel therapy for the treatment of IBD (**163**).

When we talk about NuRD and the regenerative potential of MSCs in terms of osteogenesis and bone formation it has been found that specific components of the NuRD are required for fin regeneration in zebrafish. Transcripts of the chromatin remodeler chd4a/Mi-2, the histone deacetylase hdac1/HDAC1/2, the retinoblastoma-binding protein rbb4/RBBP4/7, and the metastasis-associated antigen mta2/MTA were specifically co-induced in the blastema during adult and embryonic fin regeneration, and these transcripts displayed a similar spatial and temporal expression patterns. In addition, chemical inhibition of Hdac1 and morpholino-mediated knockdown of chd4a, mta2, and rbb4 impaired regenerative outgrowth, resulting in reduction in blastema cell proliferation and in differentiation defects (**164**).

NuRD (Nucleosome Remodeling and Histone Deacetylase), also known as Mi-2 complex, is a repressive ATP-dependent chromatin remodeling complex which regulates various processes such as transcription, chromatin assembly, cell cycle progression, genomic stability. Formation of a functional NuRD complex requires association of both enzymatic and non-enzymatic subunits. Among the enzymatic components CHD3 and CHD4 have ATP-dependent chromatin remodeling activity and HDAC1 and HDAC2 catalyse histone deacetylation. In recent time, it has been shown that the lysine specific histone demethylase 1A (LSD1) can also be associated with NuRD complex in certain cell types. Other non-enzymatic subunits include MBD2 and MBD3; MTA1, MTA2 and MTA3; RBBP4 and RBBP7; GATAD2A and GATAD2B. These non-enzymatic components of NuRD is the structural counterpart among which some bind directly to histone tails (RBBP 4/7 and GATAD2A/2B) while others (MBD and MTA subunits) are implicated in recruiting the

complex to different genomic regions by associating with methylated DNA or with transcription factors respectively (**18-21**).

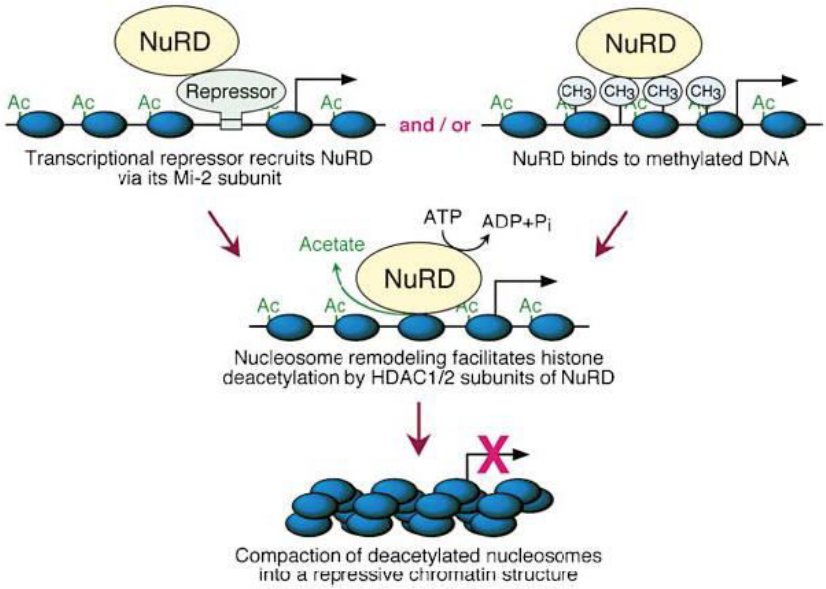

Fig. 3 : Mechanism of transcriptional repression by NuRD and other associating factors. NuRD gets recruited to the chromatin by associating with sequence specific transcriptional repressors and/or methylated DNA. HDAC1/2 activity of NuRD in turn makes the DNA more compact and repressed. *Adapted from Cell, Vol. 99, 443-446, Nov 24, 1999.*

So, NuRD being a HDAC-containing nucleosome remodeler and having certain epigenetic regulatory involvements in macrophage mediated inflammatory responses, has led us to investigate its role during inflammatory response in non-immune cells like MSCs along with its possible pivotal role in MSC-driven osteogenesis which is highly connected to the inflammatory mileu present within the MSC niche.

In our study we initially carried out a differential gene expression analysis of various NuRD subunits using multiple in vitro MSC/stromal fibroblast model of inflammation. LPS being a prototypical endotoxin binds to Toll-Like Receptor 4 (TLR4) and activates the NF-kB signaling pathway to subsequently release a series of pro-inflammatory cytokines which is a hallmark of a potent immune response. Stimulation of the murine MSC line OP9 and MS-5, and its human counterpart HS-5 as well as murine stromal fibroblast line NIH 3T3 with LPS resulted in a time dependent positive response of *Gatad2b* along with a couple of other NuRD subunits namely *Mbd2* and *Mbd3*.

Consistent with induction in *Gatad2b* mRNA, confocal imaging, western blot analysis and intracellular flow cytometry analysis showed a time-dependent upregulation and nuclear translocation Gatad2b protein level, accompanied with phosphorylated P65, in LPS primed OP9 as well as MS-5 cells. To evaluate whether this response was TLR4 specific we stimulated the MSC/stromal fibroblast lines with other pro-inflammatory stimuli like TNFα, IFNβ (Type 1 interferon) and IFNγ (Type 2 interferon) which also induced the expression of *Gatad2b* mRNA significantly along with other pro-inflammatory markers like *Interlukin-6*, *Cxcl 10*, *Ccl 2*.

Since *Gatad2b* was induced by LPS and other pro-inflammatory stimulus, we next explored whether it plays any role in mesenchymal stromal inflammatory response. Selective shRNA-containing lentivirus mediated knockdown of *Gatad2b* in MSC lines showed an overall compromised immune responsive status in steady state as well as during LPS treatment. Gene expression analysis showed reduced response to LPS-driven induction of NF-kB target genes like *Il1b*, *Il6*, *Cxcl8*, *Cxcl10*, *Tnf-α* in a time dependent manner when cells lacking *Gatad2b*. In addition, the *Tlr4* receptor response was also abrogated in absence of *Gatad2b* although other TLR4 signaling pathway components were shown to remain unchanged in terms of gene expression. Flow cytometry analysis illustrated reduced Tlr4 protein expression in *Gatad2b* knock down cells in basal as well as LPS treated condition. Immunoblot analysis further showed reduced levels of phospho-IRAK1 and phospho-P65 suggesting a perturbed NF-kB signaling pathway activation. However, no change was observed in total IRAK1, P65 and IKK protein expression. Overexpression of *Gatad2b* in wild type MSCs increased the expression of *Tlr4* and NF-kB target genes like *Il1b*, *Il6*, *Cxcl10*. Eventually we wanted to explore the transcriptomic and proteomic landscape in cells lacking *Gatad2b*. When compared between *shControl* and *shGatad2b* MSC lines in both untreated and LPS treated condition, RNA sequencing data reveals a significant downregulated profile for the pro-inflammatory genes, their associated receptors and transcription factors positively regulating the pro-inflammatory pathways. GO and pathway analysis showed various inflammation promoting pathways to be compromised when cells have inadequate level of *Gatad2b*. Bioplex assay confirms the same for the secretory interlukins and chemokines suggesting a less immune-responsive or more immune-suppressive stroma. Altogether these findings confirmed the possibility that *Gatad2b* might be a potent regulator of NF-kB signaling in LPS-stimulated mesenchymal stromal cells.

So far our findings have identified Gatad2b as a regulator of NF-KB signaling but it was still unknown what induces the expression of Gatad2b or to be more precise if NF-kB shares any positive feedback loop with Gatad2b in regulating its expression and subsequently upon differential gene expression analysis it was shown that Gatad2b induction was very much dependent on NF-kB as *RelA/P65* knockdown abrogated the induction of *Gatad2b*.

Altogether our findings identify Gatad2b as a positive regulator of MSC mediated inflammatory response in spite of the fact that as an integral component of NuRD it plays a role as transcriptional repressor. *Gatad2b* deficient stroma possess a molecular signature of being less immune-responsive or more immune-suppressive which determines the plasticity of its secretome. To assess whether this immune-plasticity reflects functionally in terms of regulating immune cells we performed an *in vitro* co-culture assay using RAW 264.7 murine macrophage cell line and MSC-derived cell free conditioned medium (MSC-CM) in presence or absence of exogenous M1/M2 stimuli and it was found that MSC-CM derived from *Gatad2b* deficient stroma polarised macrophages more towards M2 (Anti-inflamatory) and less towards M1 (Pro-inflammatory) compared to the MSC-CM derived from control stroma. This immunomodulating potential of MSC-CM upon MSC-intrinsic *Gatad2b* loss of function was also demonstrated in an in *vivo* system using female balb/c mice of 8-12 weeks. Murine breast carcinoma cell line 4T1 was injected orthotopically to induce the formation of tumor and MSC-CM from both control as well as *Gatad2b* knockdown stroma were injected intra-tumorally taking two different groups of mice. Within 18 hours of injection the mice were euthenised, tumors were isolated and single cells derived from the tumor mass were analysed for immune cells infiltration. Multicolor flowcytometry analysis showed tumors injected with *shGatad2b* MSC-CM had more percentage of immune-suppressive cells like CD206+ TAMs (Tumor-associated macrophage; resembles the M2 phenotype) and CD11b+ Ly6G+ MDSCs (Myeloid-derived suppressor cells). These findings further establish the functional role of stroma-intrinsic Gatad2b during MSC mediated inflammatory response.

Previously our data showed that in variety of *in vitro* cellular model of stromal inflammation the optimal *Gatad2b* response was in between 6 hours to 12 hours and this time frame mimics the acute stage of inflammation. So *Gatad2b* might be a regulator of acute inflammation and we have already discussed acute inflammation promotes osteogenesis. Hence we hypothesised that NuRD might also have a role during MSC-driven osteogenesis. Reduced self-renewal or tri-lineage commitment (Osteoblast, Adipocytes and Chondrocytes) potential of bone-marrow resident stromal cells is one of the major reasons of many bone related disorders and hematological malignancies.

Thus by monitoring the assembly and activity of NuRD in stromal cells during various physiological processes we can manipulate stromal fitness leading to its increased regenerative potential. OP9 cells have already been established as bonafied MSC line. Using OP9 cells as well as human primary MSCs as a model system we wanted to study how NuRD within the MSCs would affect bone marrow microenvironment organisation contributing to impaired stromal integrity.

Herein we observed that short term osteogenic cue using BMP2 stimulation and long term osteogenic differentiation of OP9 as an in vitro cellular model led to time dependent induction of specific NuRD subunits expression including *Gatad2b* along with *Alkaline phosphatase (Alpl)* a bonafied marker of osteogenic induction. This increase in expression correlated with phosphorylation of SMAD 1/5/8 which is activated upon BMP-2 signaling. Immunoblot and Immunofluorescence imaging also demonstrated nuclear translocation of certain NuRD components in BMP2 stimulated condition. Primary MSCs derived from bone marrow and expanded in vitro were also characterised and were differentiated in vitro by using osteogenic stimuli. Specific NuRD components were found to respond during osteogenesis. Stimulation of primary hMSCs with BMP4/7 also induced certain NuRD components along with the induction of phospho-SMAD 1/5/8 level. Co-immunoprecipitation studies further suggested that NuRD interacts with canonical transcriptional regulators of osteoblast differentiation and interestingly *loss of function* of NuRD components resulted in significant reduction in osteogenesis. Additionally, absence of NuRD subunits led to lower levels of phosphorylation of SMAD 1/5/8 upon BMP-2 (BMP4/7 for human MSCs) treatment. This suggests a probable module for reduced SMAD 1/5/8 phosphorylation and osteogenic differentiation. Collectively our findings demonstrate a possible NuRD dependent stromal differentiation regulation towards osteogenic lineage.

In summary we highlight the importance of NuRD complex in maintaining the functional integrity of MSCs in terms of inflammatory response and bone remodeling/repair within a resting as well as inflamed mesenchymal stromal niche.

INTRODUCTION

1. Mesenchymal Stromal Niche

The bone marrow (BM) stroma contains a heterogeneous population of cells, including endothelial cells, fibroblasts, adipocytes and osteogenic cells, and it was initially thought to function primarily as a structural framework upon which hematopoiesis occurs. Later evidence demonstrated, however, that at least two distinct stem cell populations reside in the bone marrow of many mammalian species: hematopoietic stem cells (HSCs) and mesenchymal stromal cells (also known as mesenchymal stem cells; MSCs), with the latter responsible for the maintenance of the non-hematopoietic bone marrow cells. Current models advocate two overlapping domains: the endosteal niche near bone surfaces as the primary location of dormant, quiescent HSCs; and the perivascular niche associated with the sinusoidal endothelium as the primary site of dividing, self-renewing HSCs (**5,6**).

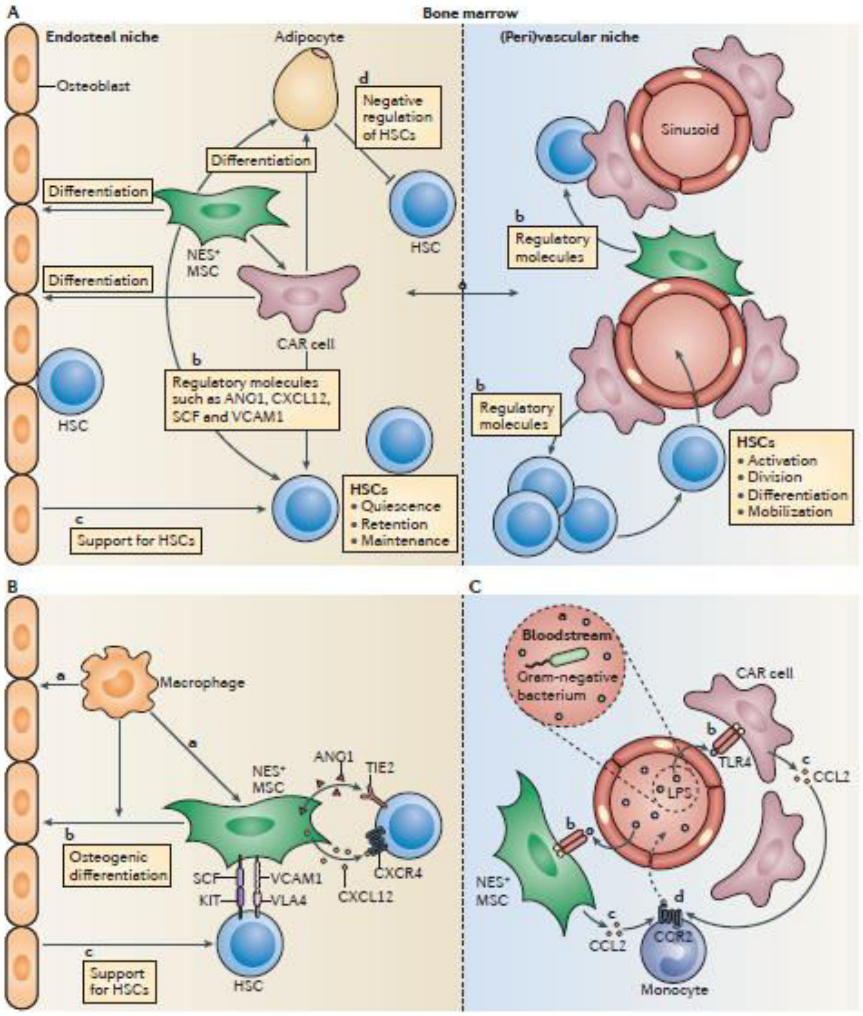

Fig. 4 : MSCs are critical components within the HSC niche of the bone marrow and confer a reciprocal regulatory mechanism in controling the local monocytes and macrophages. (A) Current model showing two functionally distinct areas within the bone marrow : the endostealniche and the (peri)vascular niche. (B) Bone marrow-resident macrophages promote the expression of HSC-supporting factors by MSCs, positively regulate MSC-driven osteogenesis which in turn also support HSCs. (C) Upon infection with gram-negative bacteria host MSCs and CAR cells respond to the bacterial LPS through TLR4 and mobilize the monocytes in a CCL2-CCR2 dependent manner as a part of the innate immune response against the bacterial infection. *Adapted from Nature Reviews Immunology Volume 12, May 2012, 387*.

1.1 Mesenchymal Stem/Stromal Cell (MSC)

MSCs, also termed multipotent marrow stromal cells or mesenchymal stromal cells, are a heterogeneous population of plastic-adherent, fibroblast-like cells, which can self-renew and differentiate into bone, adipose and cartilage tissue in culture. In the late 1960s, Friedenstein and colleagues established that single cell suspensions of BM stroma could generate colonies of adherent fibroblast-like cells in vitro. These colony-forming unitfibroblasts (CFU-Fs) were capable of osteogenic differentiation and provided the first evidence of a clonogenic precursor for cells of the bone lineage. The CFU-F assay is now widely used as a functional method to quantify stromal progenitors. Functional in vitro characterization of the stromal compartment by Dexter et al. in the 1970s then revealed its importance in regulating the proliferation, differentiation and survival of HSCs. CFU-F initiating cells in vivo have been shown to be quiescent, existing at a low frequency in human bone marrow. These cells can retain their multipotency for 30–40 cell divisions. However, their growth rate and replicative lifespan decline with somatic age, and their spindle-type morphology is gradually lost over time in culture. *In vitro* or *in vivo* differentiation of MSCs into mesenchymal tissue cells (osteoblasts, chondrocytes and adipocytes) has become the standard for demonstrating their multipotency (**1 - 4**).

1.2 Different sources and markers of MSCs

Since MSCs were originally isolated from bone marrow (BM-MSCs), this tissue has served as the foundation in this area of research. However, MSCs or MSC-like cells also referred to as MSCs, have also been found in adipose tissue, connective tissue of the umbilical cord and in cord blood. Although the MSC populations isolated from these different sources in many aspects are similar to one another, they display variations in both potential and phenotype. MSCs do not express known unique phenotypic markers, but the International Society for Cellular Therapy has proposed minimal criteria for defining the cells based on their plastic adherence, phenotype and trilineage multipotency. The phenotype definition requires expression of CD73, CD90 and CD105, together with a lack of expression of monocyte and macrophage markers (CD11b or

CD14), a haematopoietic progenitor and endothelial cell marker (CD34), a leukocyte marker (CD45), B cell markers (CD19 or CD79a) and HLA-DR (**7**).

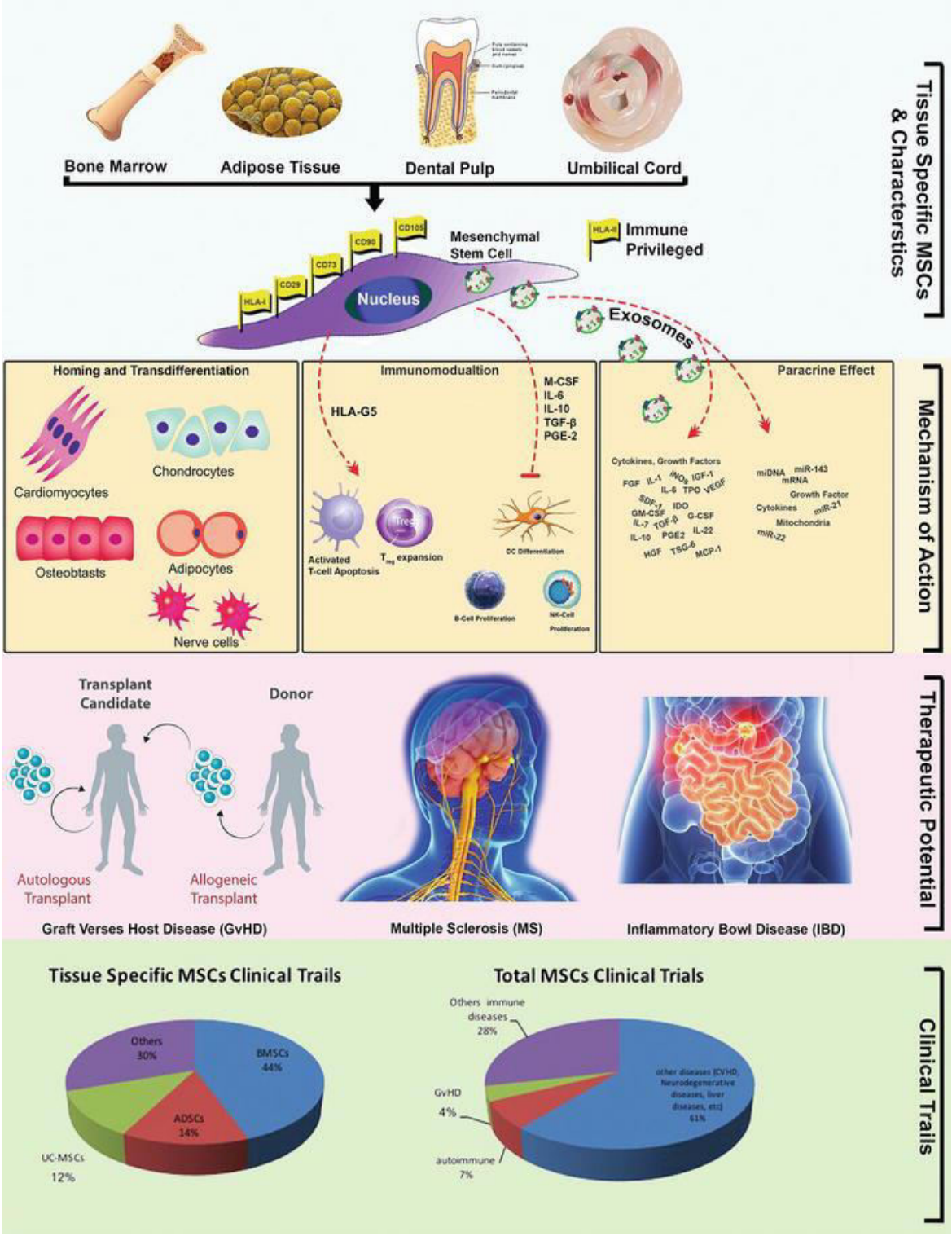

Fig. 5 : A diagramatic representation of cellular characteristics, mode of action and therapeutic potential of MSCs based on the current status of clinical trial. *Adapted from* 10.5772/intechopen.80772

1.3 MSCs in Osteogenesis

MSCs are capable of lineage commitment which can give rise to mature osteoblast cells (OB) and this process is known as osteogenesis which is a multi-step process involving an array of transcription factors, cytokines and growth factors. During the different stages of maturation developing osteoblasts do express a unique set of molecular markers. The maturation consists of three sequential stages : (a) cell proliferation, (b) extracellular matrix (ECM) secretion and matrix maturation, and (c) matrix mineralization. During the initial stages of osteogenesis immature osteoblsts undergo rapid proliferation and express collagen, fibronectin, osteopontin (OPN) and transforming growth factor-β (TGFβ) recceptor I. During the later stage immature OBs get transform into mature OBs and secrete collagen type 1 alpha 1 chain (COL1A1) and express alkaline phosphatase (ALP) to mature the ECM. Then comes the matrix mineralization where different osteoblast markers like osteocalcin (OCN), osteopontin (OPN), and bone sialoprotein (BSP) play a crucial role along with COL1A1 and ALP. Finally, these mature OBs undergo apoptosis, becomes part of the bone-lining or become an integral part of bone matrix as terminally differentiated osteocytes (OS) (**8**).

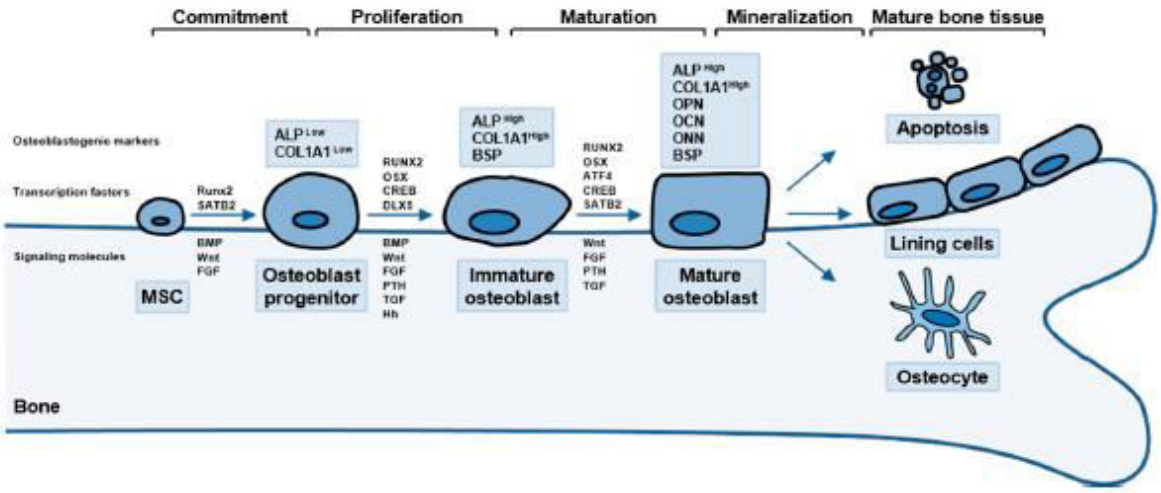

Fig. 6 : Involvement of specific transcription factors and expression of distinct OB markers define each stage of osteogenesis. *Adapted from Int. J. Mol.Sci.2021, 22, 2851.*

A highly orchestrated transcriptional regulatory network is involved in osteogenesis. Run-related transcription factor 2 (RUNX2) is considered as a master regulator for the expression of various osteogenic markers like osteocalcin (OCN), osteopontin (OPN), osteonectin (ONN), alkaline phosphatase (ALP), bone sialoprotein (BSP), and COL1A1. RUNX2 is marginally expressed in undifferentiated MSCs and its expression is highly elevated throughout the proliferation of pre-OBs. RUNX2 level is at its peak at the

immature OB stage and gradually its level decreases in the maturation stage. *Runx2*-deficient mice show defective endochondral and intramembranous bone formation. Another important transcription factor for OB commitment and differentiation is osterix (OSX/sp7) and its expression is positively regulated by RUNX2 which in turn also induces the expression of previously mentioned OB markers. Osx-deficient mice exhibit complete loss of OBs. However, RUNX2 expression remains unaltered in *Osx*-deficient mice, demonstrating that RUNX2 is upstream of OSX during osteogenesis. Another essential transcription factor is activating transcription factor 4 (ATF4) which promotes osteogenesis by interacting directly with RUNX2 to enhance OCN expression. ATF4-deficient mice are shown to exhibit severe osteoporosis, osteodysplasty, and altered bone mineralization with impaired terminal OB differentiation. Its expression is restricted in committed OB lineage cells (**9**).

A recent study identified RUNX1 to be a universal regulator of all of the three above mentioned transcription factors RUNX2, OSX and ATF4. In a conditional knockout study of *Runx1*$^{flox/flox}$/*Osx-Cre* mice, RUNX1 deficiency resulted in decreased bone density by downregulating RUNX2, OSX, and ATF4 expression in OB lineage cells. RUNX1 promotes RUNX2 and OCN expression by directly binding to the promoter regions of the *RUNX2* and *OCN* genes. It can also promote bone formation by upregulating the bone morphogenetic protein-7 (BMP-7) and Wnt / β-catenin pathways (**165**).

1.4 Signaling pathways in osteogenesis

Various signaling pathways are involved in the process of forming mature OBs and these include : Bone morphogenic protein (BMP), TGF-β, WnT, PTH, Fibroblast growth factor (FGF) and Hedgehog (Hh). Activation of the canonical Wnt signaling pathway results in β-catenin translocation into the nucleus followed by induction of the osteogenic target gene expression. Non-canonical Wnt signaling induced by Wnt5a or Wnt11 upregulate RUNX2 through c-jun N-terminal kinase (JNK) activation. The Wnt/calcium pathway, another non-canonical Wnt signaling pathway, increases intracellular calcium levels to activate calmodulin-dependent kinase II, protein kinase C (PKC), and calcineurin, leading to the induction of AP-1 transcription factors. BMP-2/Smad signaling pathway is also a potent regulator of osteogenesis and upon activation of this pathway Smad1/5/8 becomes phosphorylated which in turn translocates to the nucleus being complexed with Smad4 resulting in induction of RUNX2. BMP2/Smad signaling is also reported to induce OSX through distal-less homeobox 5 (DLX5) induction in a RUNX2-independent manner.

TGF-β signaling also plays a very crucial role in osteogenesis. Upon binding with its receptors TGFβRI and TGFβRII it activates Smad2/3 and being complexed with Smad4 undergoes nuclear translocation to trigger RUNX2-mediated osteogenic gene expression.

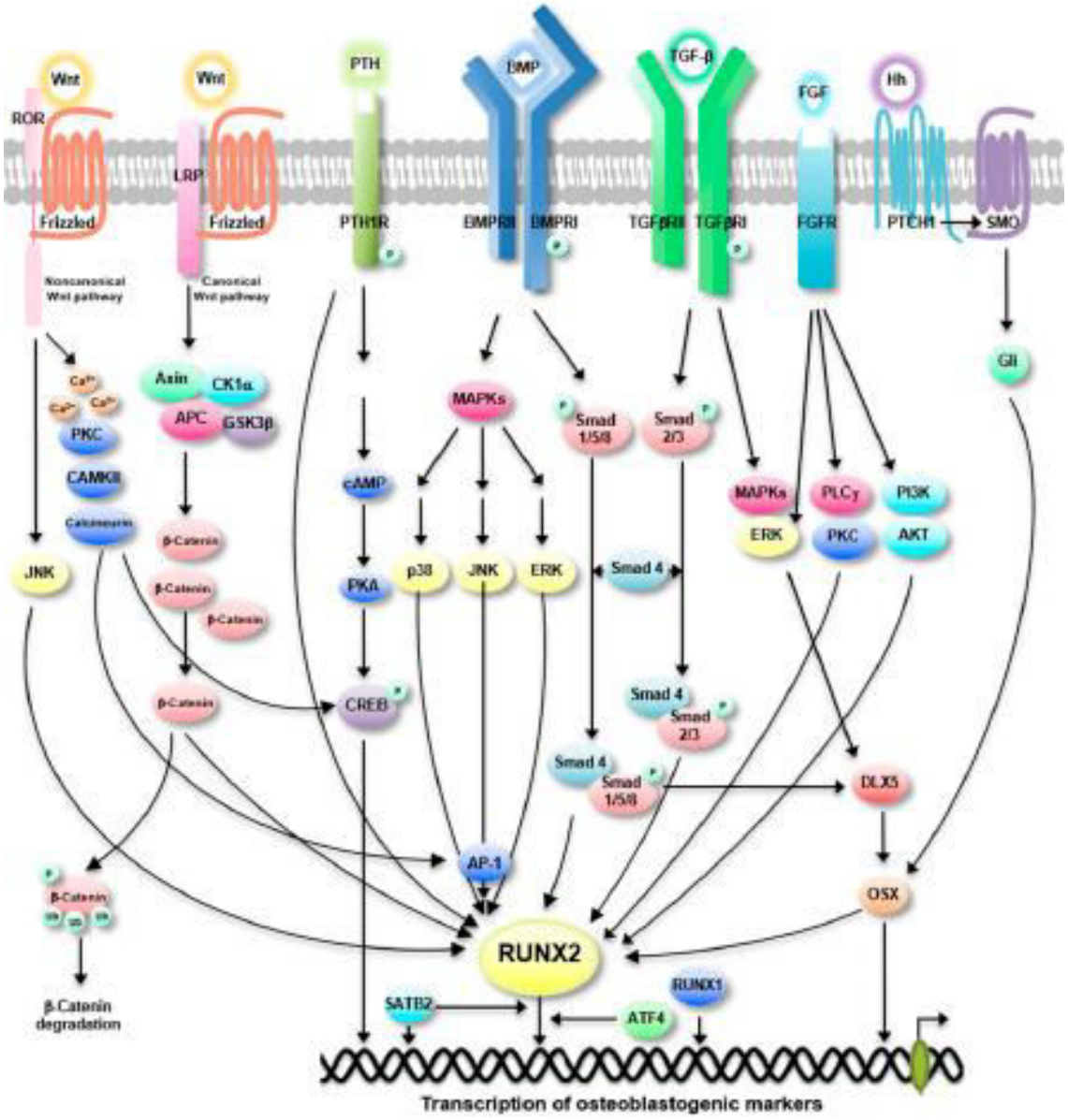

Fig. 7 : Signaling pathways involved in MSC-mediated osteogenesis. Schematic illustration showing various cell surface receptors and their ligands activating a series of interconnected signaling pathways converging at master transcriptional regulators of osteogenesis like RUNX2. *Adapted from Int. J. Mol.Sci.2021, 22, 2851.*

There are some other signaling pathways also which play a supportive role in MSC-driven osteoblast differentiation including FGF/FGF receptor (FGFR)-mediated signaling cascade acting through downstream signaling of phosphatidylinositol-3-kinase (PI3K)/protein kinase B (AKT), phospholipase γ/PKCα and extracellular receptor kinase (ERK)1/2; PTH signaling which upon activation phosphorylate cAMP-responsive element-binding (CREB) leading to induction of osteogenic markers as well as BMP-2 expression; and Hedgehog signaling triggering the activation og Gli transcription factor which in turn stimulates RUNX2/OSX activation (**165**).

2. Inflammation and Immune System :

Inflammation refers to the responsiveness of our body's immune system against a vast array of 'danger signals' like pathogens, tissue injury, toxic compounds or irradiation. Being a major component of innate immunity it provides a non-specific response. So followed by infection or tissue injury a properly functional immune system should induce inflammation by secreting variety of pro-inflammatory stimuli and thereby recruiting immune cells to the site of inflammation that will eventually neutralise toxins, clear away pathogens and bring back tissue homeostasis by healing / tissue repair. But the saying 'Too much of a good thing' applies strongly to the inflammation. Inflammation as per the demand is good which is termed as *Acute Inflammation* and characterised by rapid, severe onset and short lasting symptoms. In contrast, when inflammation gets up too high, 'switch off' machinery doesn't work and lingers for a long time then it becomes *chronic* which is detrimental to the organism, damaging normal tissue and may even develop into cancer. From the body's perspective, it's under consistent attack, so the immune system remains turned on indefinitely. Chronic inflammation can both be caused by, and lead to, various diseases like Atherosclerosis, Inflammatory bowel diseases (IBD), Rheumatoid arthritis (RA), Osteoarthritis, Psoriasis, Chronic obstructive pulmonary disease (COPD), Chronic kidney disease, Alzheimer's disease, Allergic asthma, Diabetes, Cancer and many more (**166**).

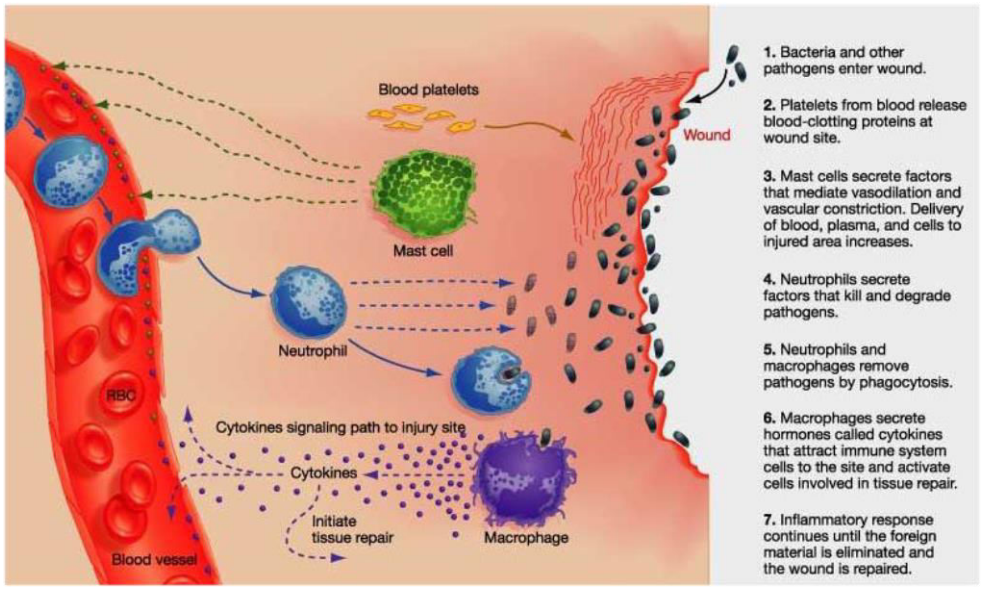

Fig. 8 : A schematic illustration for the pathophysiology of inflammation and immune system response.

2.1 Pathophysiology of Inflammation

Most of the features of acute inflammation continue as the inflammation becomes chronic, including the expansion of blood vessels (vasodilation), increase in blood flow, capillary permeability and migration of neutrophils into the infected tissue through the capillary wall (diapedesis). However, the composition of the white blood cells changes soon and the macrophages and lymphocytes begin to replace short-lived neutrophils. Thus the hallmarks of chronic inflammation are the infiltration of the primary inflammatory cells such as macrophages, lymphocytes, and plasma cells in the tissue site, producing inflammatory cytokines, growth factors, enzymes and hence contributing to the progression of tissue damage and secondary repair including fibrosis and granuloma formation.

Recruitment of immune cells to the site of inflammation consist of the following cellular events driven by a series of molecular changes involving the inflamed tissue, tissue resident innate immune cells / fibroblast and local blood vessels : **1.** Followed by infection or tissue injury various pro-inflammatory cytokines (IL-1, IL-6, TNF-α secreted by activated tissue-resident macrophages and fibroblast) and other inflammatory mediators (Histamine, Prostaglandins, Leukotrienes, Bradykinin, Fibrin, Plasmin released by tissue-resident macrophages as well as mast cells and due to blood clotting) act on the endothelial cells of the local blood vessel to render it activated or inflamed. Increased expression of endothelial CAMs (Cell Adhesion Molecule) namely E- and P-

selectin is the hallmark of inflamed endothelium; **2.** Neutrophils are generally the first cell type to bind to the inflamed endothelium by expressing L-selectin and mucin-like PSGL-1 on its surface to mediate the *rolling on* inflamed endothelium; **3.** Rolling is followed by *activation* of neutrophils by IL-8 and macrophage inflammatory protein 1β (MIP-1β) secreted either locally by the cells involved in the inflammatory response or by the inflamed endothelial cells lining the blood vessel; **4.** Binding of these chemokines to neutrophil membrane recptors makes them *arrested and adhered* strongly with Ig-superfamily adhesion molecules namely ICAM-1 (CD54) on endothelium with the help of integrins LFA-1 (CD11a/CD18) and MAC-1 (CD11b/CD18) present on neutrophils; **5.** Finally neutrophils migrate through the vessel wall into the tissues, a process called *transendothelial migration* which is mediated by PECAM-1 to PECAM-1 interaction. Once in tissues, the activated neutrophils start expressing more receptors for chemoattractants and consequently migrate up a gradient of chemoattractants to reach to the site of infection. Among the inflammatory mediators that are chemotactic for neutrophils are several chemokines, complement split products (C3a, C5a, C5b67), and many others. Neutrophil infiltration into the tissue peaks within the first 6 hours of an inflammatory respons; **6.** Activated neutrophils also express Fc receptors for antibody and receptors for complement proteins, thus enabling them to bind antibody- and complement-coated pathogens which results in phagocytosis. This clearance is followed by the release of more pro-inflammatory mediators (MIP-1α and MIP-1β) which act as signals for monocytes / macrophages to infiltrate to the site of inflammation. Macrophages arrive about 5 to 6 hours after an inflammatory response begins; **7.** The mechanism of monocyte infiltration from peripheral blood to the site of infection is almost the same as neutrophils except that monocyte-chemoattractant protein-1 (MCP-1 or CCL2) activates the integrin VLA-4 (CD49d/CD29) on monocyte membrane which binds strongly with VCAM-1 (CD106) of inflamed endothelium. Bacterial peptide fragments and complement fragments act as the chemoattractants for the infiltrated monocytes having complement receptor CR3 on its membrane and guiding them to the site of infection. Within the target tissue monocytes can differentiate into macrophages; **8.** IFN-γ acts in the later phase of acute inflammatory response and gets released from $CD4^+$ T_H1 cells. It activates macrophages and neutrophils, promoting increased phagocytic activity, increased cytokine production and increased release of lytic enzymes into the tissue spaces. In their activated state macrophges exhibit increased class II MHC expression making them more effective in antigen presentation; **9.** The duration and intensity of the local acute inflammatory response must be carefully regulated to control tissue damage and facilitate the tissue-repair mechanisms that are necessary for healing. TGF-β has

been shown to play an important role in limiting the inflammatory response. It also promotes accumulation and proliferation of fibroblasts and the deposition of an extracellular matrix that is required for proper tissue repair; **10.** When tissue damage or antigen persists, chronic inflammation develops which is characterised by constitutive accumulation and activation of macrophages, a synergistic role played by IFN-γ and TNF-α. IFN-γ activates the macrophages, while activated macrophages secrete TNF-α and this goes on in-loop. This large number of activated macrophages release various hydrolytic enzymes and reactive oxygen and nitrgen intermediates, which are responsible for much of the damage to surrounding tissue (**168**).

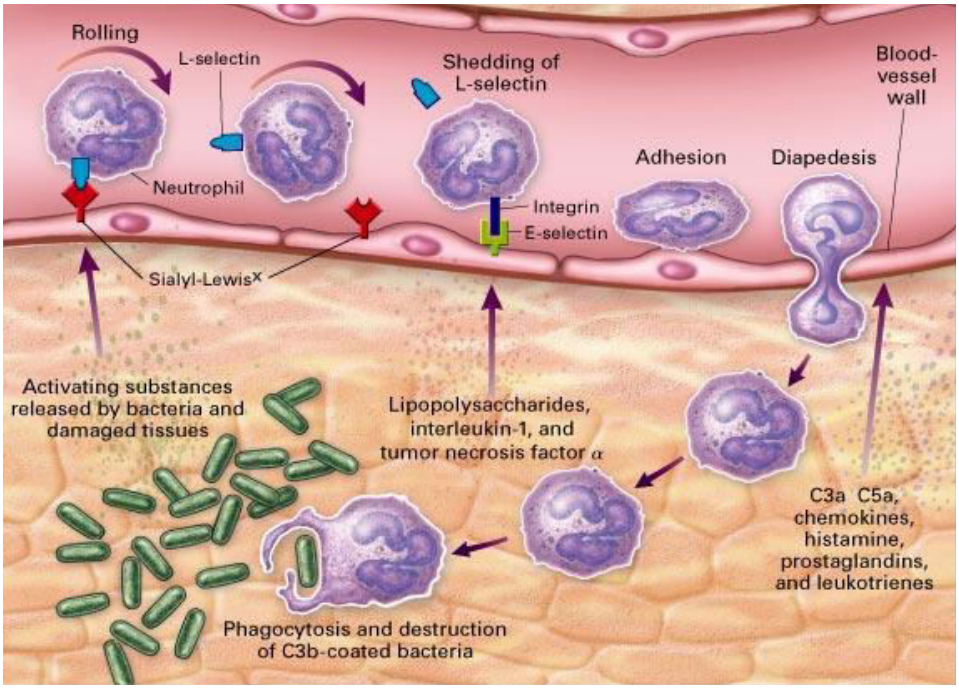

Fig. 9 : A model for cellular response during inflammation

Functionally inflammation can broadly be seperated into three sequential phases :

(1) *Initiation* Inflammation begins with an insult or stimulus to an organ. The source of inflammation can be a foreign body, like an invading bacteria or virus, though the source of inflammation can also be damaged cells, such as necrotic cells from a physical wound, or transformed tumor cells. The initial response may differ depending on the source of inflammation. For example, TLR2, TLR4, and TLR9 can be activated by lipoproteins on the surface of bacteria and prokaryotic DNA, causing the release of cytokines (such as IL-1β, IFNα, and IFNβ) and chemokines (such as IL-8, MCP-1 and MIP-1α) promoting immune cell activation and recruitment. It is also in this stage that the

complement pathway may become activated, initiating a cascade of events ultimately resulting in C3a activation enhancing inflammation and C3b, which will lead to generation of the membrane attack complex.

(2) *Elimination* At this point, C3a activation, histamine release from mast cells, and production of prostaglandin cause changes in the vasculature including vasodilation, increased blood flow, and increased vascular permeability allowing immune cells to more easily escape from blood vessels into the tissue. Immune cells, such as neutrophils and macrophages, recognize molecular patterns on the surface of invading pathogens or transformed cells and engulf these cells. The immune cells utilize cytotoxic mediators (such as reactive oxygen species) to destroy the targeted cells. Immune cells will also produce cytokines, such as TNF-α, IFN-γ, and IL-1β, which will enhance inflammation and recruit additional immune cells into the tissue.

(3) *Resolution* To prevent progression from acute inflammation to persistent, chronic inflammation, the inflammatory response must be suppressed to prevent additional tissue damage. Inflammation resolution is a well-managed process involving the spatially- and temporally-controlled production of mediators, during which chemokine gradients are diluted over time. Circulating white blood cells eventually no longer sense these gradients and are not recruited to sites of injury. Dysregulation of this process can lead to uncontrolled chronic inflammation. Inflammation resolution processes that rectify tissue homeostasis include reduction or cessation of tissue infiltration by neutrophils and apoptosis of spent neutrophils, counter-regulation of chemokines and cytokines, macrophage transformation from classically to alternatively activated cells, and initiation of healing.

Dead and dying cells present “find-me” and “eat-me” signals such as phosphatidylserine, oxLDL, and sphingosine-1 phosphate, which recruit scavenging phagocytes to engulf these cells and control further inflammation. Certain cells, such as macrophages, may switch to an anti-inflammatory phenotype promoting the depletion of cytotoxic mediators through arginase-1 activity. These cells also produce anti-inflammatory cytokines such as IL-10 and TGF-β. Fibroblasts activated by TNF-α and IL-1β begin tissue remodeling and repair by laying down collagen and extracellular matrix, which can produce scar tissue. Antigen presenting cells, such as dendritic cells, process antigen from the source of injury and then travel to lymph nodes where they present the antigen to naïve T cells and B cells. Naïve T cells can differentiate into helper T cells which may propagate the immune response through release of IFN-γ and IL-2. B cells differentiate into plasma B

cells, which produce antibody specific to the invading pathogen, which will more readily trigger an enhanced immune response the next time it is encountered (**167**).

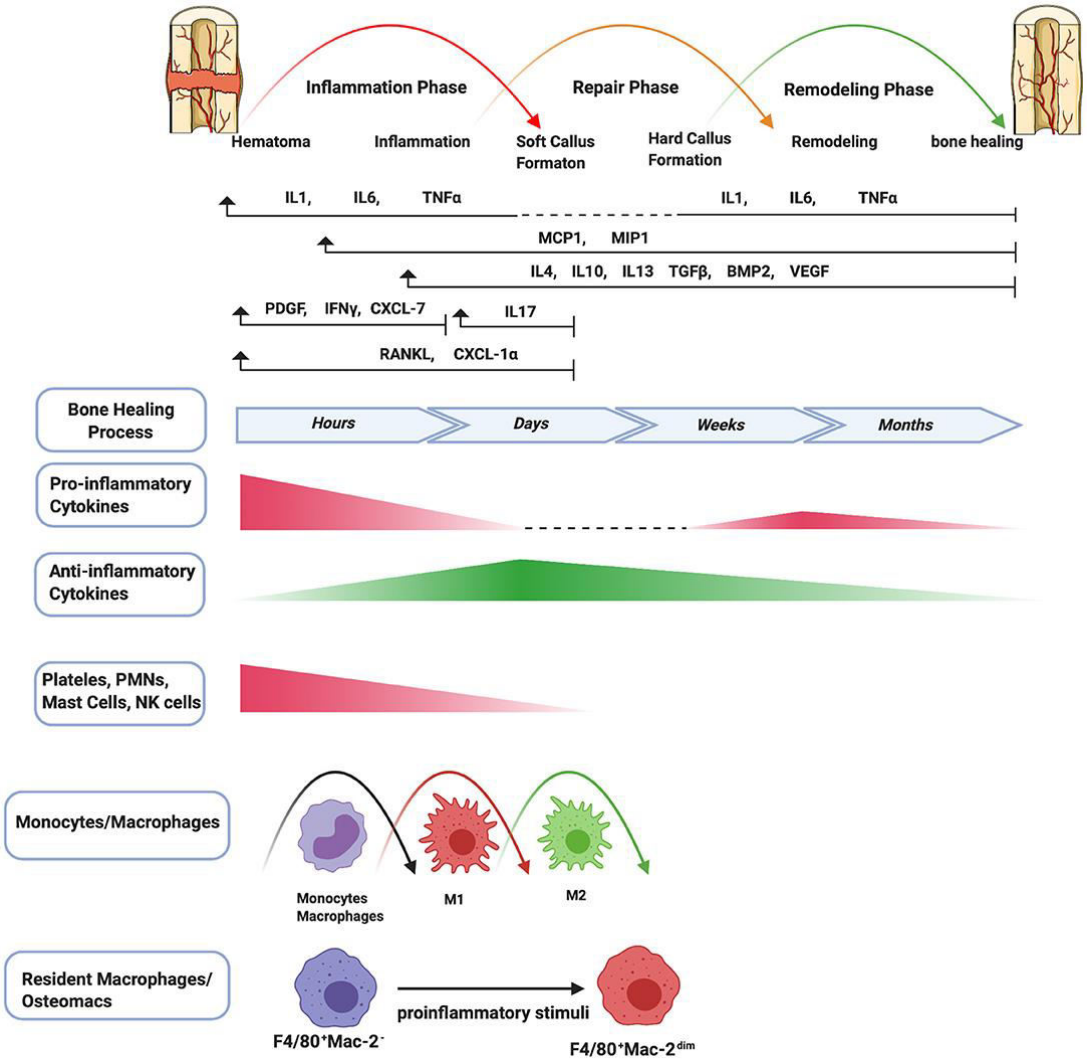

Fig. 10 : Schematic summary of the stages of bone healing and the temporal pattern of the relative immune cells and cytokines/growth factors expression. Bone healing can be viewed as a three-stage biological phase (inflammation, repair, and remodeling) which can be further divided into six main sub-steps: hematoma, inflammation, soft callus formation, hard callus formation, remodeling, bone healing. After fracture, immune cells including PMNs, NK cells, mast cells, and platelets are activated in the early stage of the inflammation and the secreted cytokines/chemokines subsequently recruit and activate monocytes/macrophages to further play important roles throughout this process. The pro-inflammatory cytokines including IL1, IL6, TNFα are essential signals during the early stages of bone fracture. In addition, TNFα increases again in the late repair phase, and several pro-inflammatory cytokines (e.g., IL1, IL6, TNFα) are highly expressed in the remodeling phase. The control switch of expression patterns from a pro-inflammatory to an anti-inflammatory response (IL4, IL10, IL13) in the late stages of inflammation is critical to fracture repair. *Adapted from frontiers in Endocrinology June 2020 Volume 11 Article 386.*

2.2 Signaling pathways associated with inflammatory response

A typical inflammatory response consists of four stages : (1) Inflammation inducers depending on the type of infection (bactrial, viral, fungi or parasitic) known as pathogen-associated molecular patterns (PAMPs) or endogeneous danger signals which are also termed as danger-associated molecular patterns (DAMPs); (2) Sensing the infection or injury by the receptors of the innate immune system such as Toll-like receptors (TLR), NOD-like receptors (NLR) and RIG-like receptors (RLR) which are known altogether as pattern-recognition receptors (PRRs) ; (3) Immune response induced by inflammatory mediators such as cytokines, chemokines and the complement system; (4) Modulation of the target tissues that have been affected by inflammatory mediators (**169**).

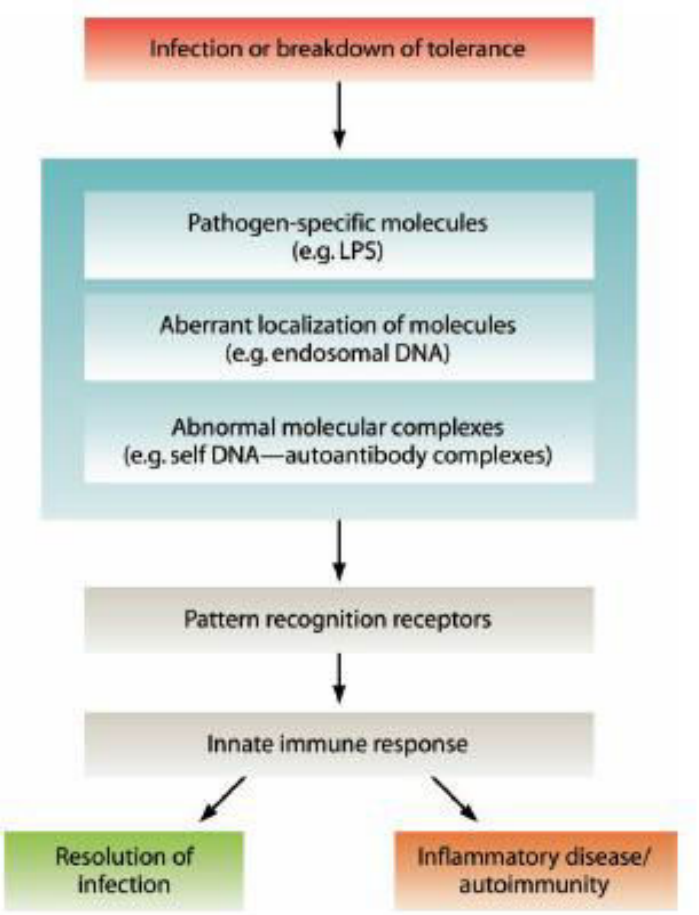

Fig. 11 : Schematic flowchart representation of different steps involved in innate immune recognition by PRRs. *Adapted from Clin. Microbiol. Rev. 2009; 22:240-273.*

Signaling pathways that operate in developing a complete immene response can be divided into two groups : (a) PAMP and DAMP associated signaling pathways inducing innate immune response; and (b) cytokines, chemokines and interferons-mediated signaling pathways which amplify the magnitude of innate immune response, connect innate immune response with adaptive immune response and finally imprint immune memory.

(a) Signaling pathways involving PAMPs/DAMPs and PRRs :

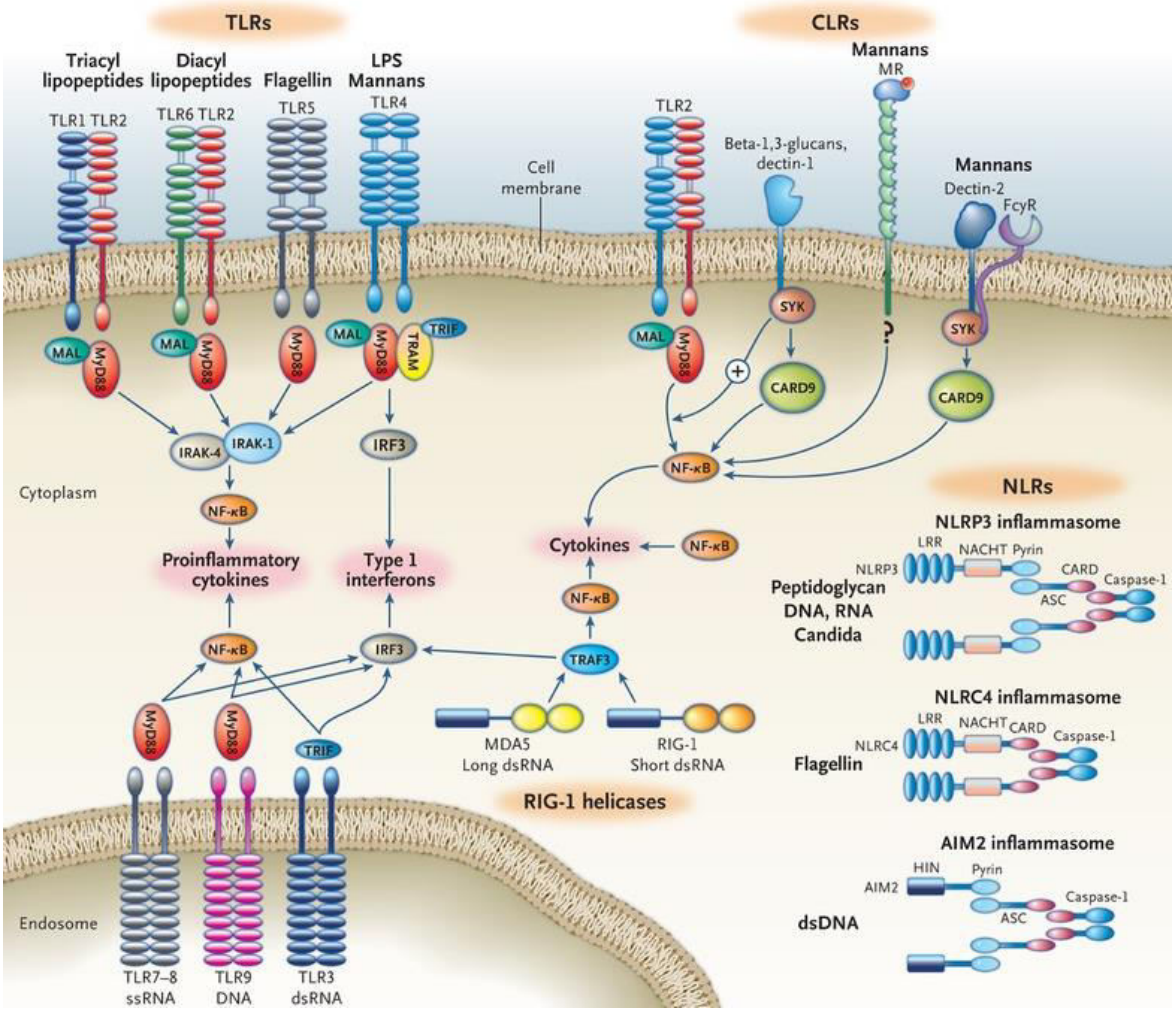

Fig. 12 : Graphical representation of different PAMP-associated signaling pathways. Different molecular patterns unique to bacteria, intracellular virus and their cytosolic derivatives like ssRNA, dsRNA, dsDNA and many other microbial components are detected by a broad range of PRRs to activate a series of signaling cascade as part of primary innate immune response ultimately activating many pro-inflammatory cytokines, chemokines and interferons. *Adapted from N Engl J Med 2011; 364:60-70.*

The onset of an inflammatory response occurs upon microbial infection (PAMPs) or from endogenous danger signals (DAMPs) which is nothing but activation of immune system governed by different families of PRRs. Three classes of PRRs play major role in recognition of PAMPs/DAMPs to initiate certain signal transduction pathways which include TLRs, RLRs and NLRs (**169**).

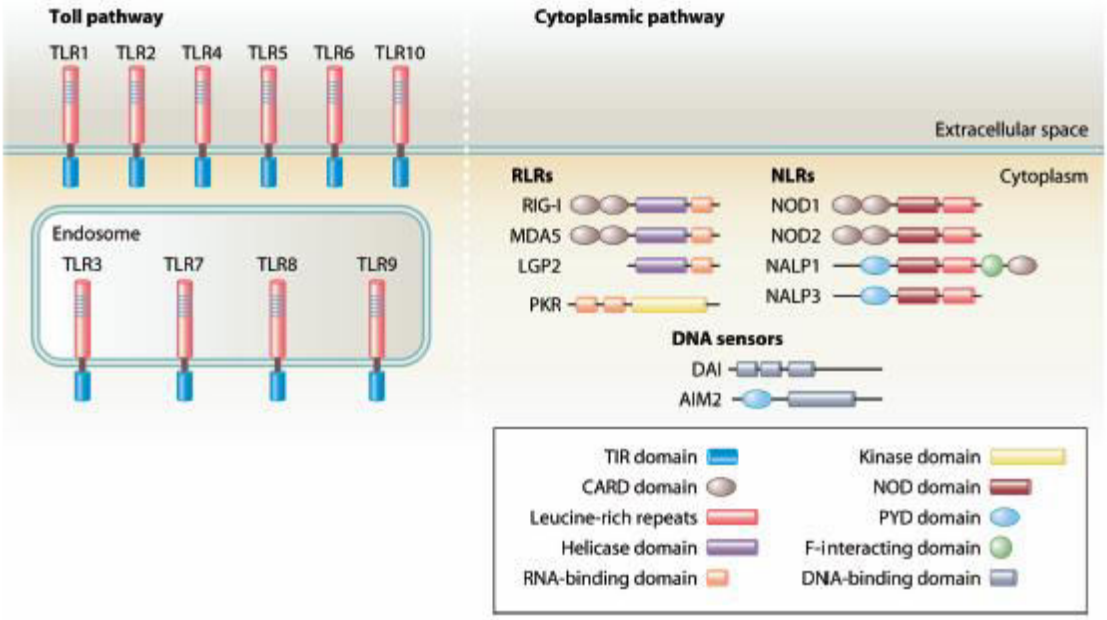

Fig. 13 : Schematic diagram showing different PRRs, their cellular localization and structural motifs/domains involved in PAMP binding followed by activation of several signaling pathways. *Adapted from Clin. Microbiol. Rev. 2009; 22:240-273.*

TLRs are the most well-studied group among these PRRs. Based on their cellular localisation they can be subdivided into two groups : cell surface TLRs which recognise mainly bacterial products unique to bacteria and not produced by the host (TLR1, TLR2, TLR4, TLR5, TLR6, TLR10) whereas others (TLR3, TLR7, TLR8, TLR9) are almost exclusively in intracellular compartments, including endosomes and lysosomes and recognise nucleic acids with self-non self discrimination. TLRs are not capable of recognising intracellular cytosolic pathogens and their derivatives like viral ssRNA, dsRNA and DNA as well as components of internalized or intracellular bacteria. A large group of cytosolic PRRs accomplishes this recognition which include RLR and NLR. Retinoic acid-inducible gene 1 (RIG-1) and melanoma differentiation-associated gene 5 (MDA5) are the well studied examples of RLRs; whereas NLR family consists of NOD1, NOD2, NALP1 and NALP3 (**170**).

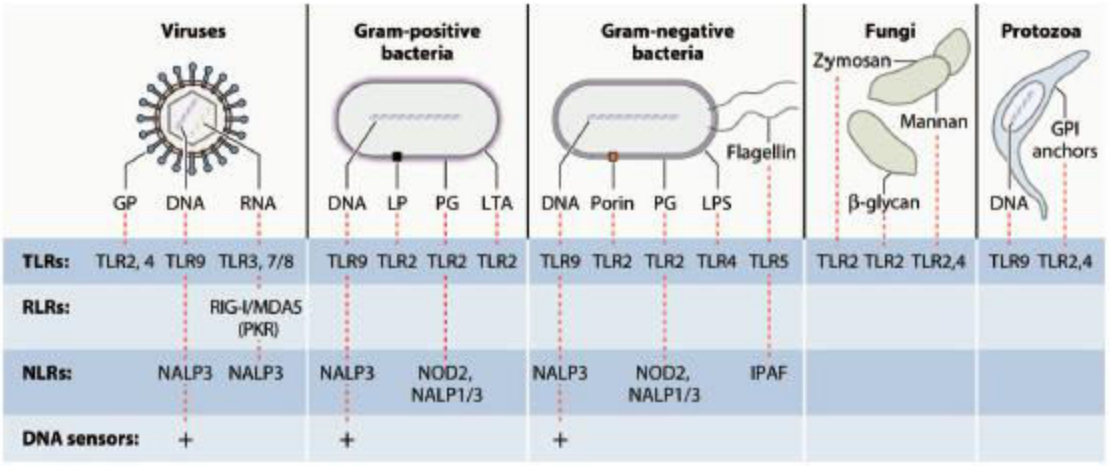

TABLE 1. Recognition of microbial components by PRRs

Receptor	Cellular localization	Microbial component(s)	Origin(s)
TLRs			
TLR1/TLR2	Cell surface	Triacyl lipopeptides	Bacteria
TLR2/TLR6	Cell surface	Diacyl lipopeptides Lipoteichoic acid	*Mycoplasma* Gram-positive bacteria
TLR2	Cell surface	Lipoproteins Peptidoglycan Lipoarabinomannan Porins Envelope glycoproteins GPI-mucin Phospholipomannan Zymosan β-Glycan	Various pathogens Gram-positive and -negative bacteria Mycobacteria *Neisseria* Viruses (e.g., measles virus, HSV, cytomegalovirus) Protozoa *Candida* Fungi Fungi
TLR3	Cell surface/endosomes	dsRNA	Viruses
TLR4	Cell surface	LPS Envelope glycoproteins Glycoinositolphospholipids Mannan HSP70	Gram-negative bacteria Viruses (e.g., RSV) Protozoa *Candida* Host
TLR5	Cell surface	Flagellin	Flagellated bacteria
TLR7/8	Endosome	ssRNA	RNA viruses
TLR9	Endosome	CpG DNA	Viruses, bacteria, protozoa
RLRs			
RIG-I	Cytoplasm	dsRNA (short), 5′-triphosphate RNA	Viruses (e.g., influenza A virus, HCV, RSV)
MDA5	Cytoplasm	dsRNA (long)	Viruses (picorna- and noroviruses)
NLRs			
NOD1	Cytoplasm	Diaminopimelic acid	Gram-negative bacteria
NOD2	Cytoplasm	MDP	Gram-positive and -negative bacteria
NALP1	Cytoplasm	MDP	Gram-positive and -negative bacteria
NALP3	Cytoplasm	ATP, uric acid crystals, RNA, DNA, MDP	Viruses, bacteria, and host
Miscellaneous			
DAI	Cytoplasm	DNA	DNA viruses, intracellular bacteria
AIM2	Cytoplasm	DNA	DNA viruses
PKR	Cytoplasm	dsRNA, 5′-triphosphate RNA	Viruses

Fig. 14 : Schema and table showing different microbial components from several different origins commonly refered to as PAMPs and their corresponding recognition partners classified as PRRs located at various cellular compartments. *Adapted from Clin. Microbiol. Rev. 2009; 22:240-273.*

(b) Cytokines and chemokines driven signaling pathways :

Cytokines are either pro-inflammatory which promote inflammation or anti-inflammatory which inhibit inflammation. Key pro-inflammatory cytokines include interlukin-1 (IL-1) family cytokines, IL-6 family cytokines, IL-17 family cytokines, type I interferons (IFNα, IFNβ), type II interferons (IFNγ), type III tumor necrosis factor (TNFα) whereas anti-inflammatory cytokines are IL-10 family cytokines, IL-12 family cytokines as well as IL-4, IL-13. Cytokines bind to their corresponding receptors which are majorly type 1 cytokine receptors. Pro-inflammatory chemokines are produced by cells mainly to recruit leukocytes to the sites of inflammation or injury and their signaling is activated downstream of G protein-coupled receptor (GPCR) superfamily.

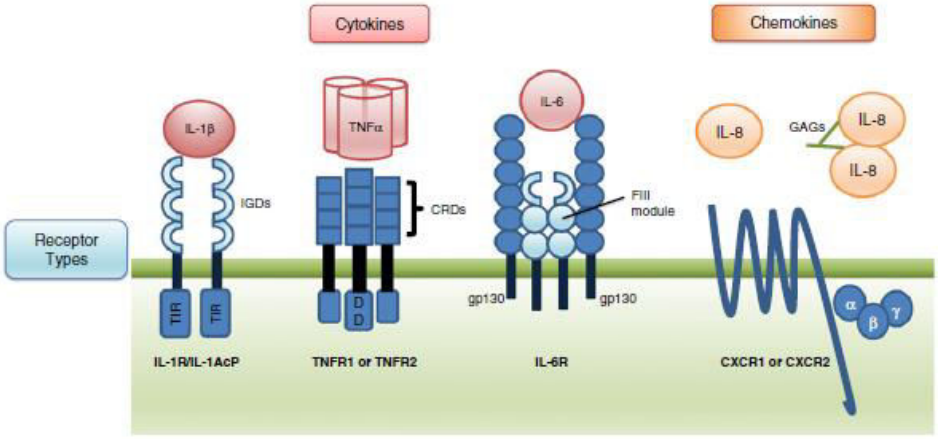

Fig. 15 : Different receptors for cytokines and chemokines and their domains for binding with ligands as well as adaptor molecules for signaling pathway activation. *Adapted from Biochimica et Biophysica Acta 1843 (2014) 2563–2582.*

Cytokine signaling occurs through various JAK-STATs. (**a**) Canonical type II IFN signaling occurs through receptors, IFNGR1 and IFNGR2, which constitutively associate with JAK1 and JAK2, respectively, leading to the phosphorylation of STAT1. Phosphorylated STAT1 homodimers translocate to the nucleus and bind to GAS elements, initiating the transcription of IFN- induced genes associated with immune activation. IFN- signaling can also lead to the phosphorylation of STAT3, which forms homo- or heterodimers that bind to GAS elements to induce inflammatory genes. (**b**) The type I IFN pathway can be stimulated by multiple family members, the most well-known being IFN-α and IFN-β. The receptors IFNAR1 and IFNAR2 are associated with TYK2 and JAK1, respectively. Canonical type I IFN signaling occurs through the phosphorylation of STAT1 and STAT2, which, together with IRF9, form the ISGF3 complex. ISGF3 translocates to the nucleus to initiate the transcription of IRGs through

the ISRE regulatory sequence. Non-canonical type I IFN signaling can occur through the CRKL or NFkB pathway. Subsequent to JAK activation, CRKL can become phosphorylated by TYK2, which leads to CRKL complexation with STAT5, which then binds GAS elements in the nucleus. (**c**) IFNAR1/2 signaling through TYK2 and JAK1 can trigger the activation of the NFkB pathway through phosphoinositide 3-kinase (PI3K), protein kinase B (AKT), and TNF receptor-associated factors (TRAFs) that act through IKKa and IKKb to drive NFkB induction of genes associated with survival and cell proliferation. The production of type I IFNs can also occur through activation of PRRs that converge on IRF7 to promote further production of type I IFNs and viral response genes. (**d**) Cytokines, both pro- and anti-inflammatory, signal through their associated receptor/JAK complexes, resulting in the downstreamphosphorylation of STATs (homo- or heterodimers). Translocation of these STAT complexes to the nucleus drives the transcription of genes involved in processes ranging from inflammation to angiogenesis and survival.

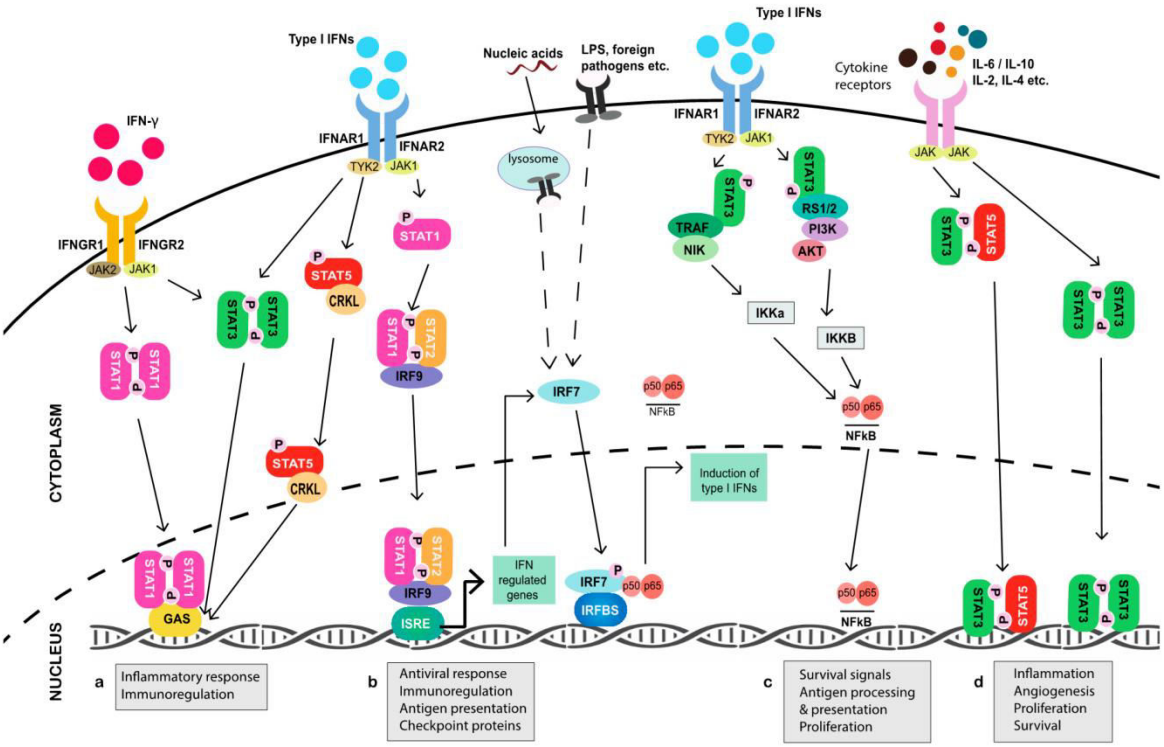

Fig. 16 : Various pro-inflammatory and anti-inflammatory cytokines act through different JAK-STATs. *Adapted from Cancers 2019, 11, 2002.*

IL-8 signalling pathway is an example of chemokine-activated signaling. IL-8 is thought to exist as monomers in the plasma but that local concentrations in the tissues favours dimer formation and these dimers are modified by the addition of glycosaminoglycans (GAGs). The GAGs facilitate binding of IL-8 to endothelial cells; they can then bind to a slow progression ofmigrating lymphocytes. Binding of IL-8 to the chemokine receptors CXCR1 or CXCR2 leads to activation of the heterotrimeric G-proteins (Gα, β, γ). The Gα subunit in particular activates themembrane-bound adenylate cyclase (AC), which generates cyclic AMP (cAMP) and cAMP can then activate protein kinase A (PKA). Alternatively, the Gβγ heterodimer can dissociate fromthe Gα subunit and stimulate phospholipase β (PLCβ) activity, which cleaves phospholipids to produce inositol 3,4,5-triphosphate (IP3) and diacylglycerol (DAG). DAG activates PKC, which then inducesMAPK activation, whereas IP3 triggers the degranulation by stimulating the release of Ca2+ from intracellular stores (**171,172**).

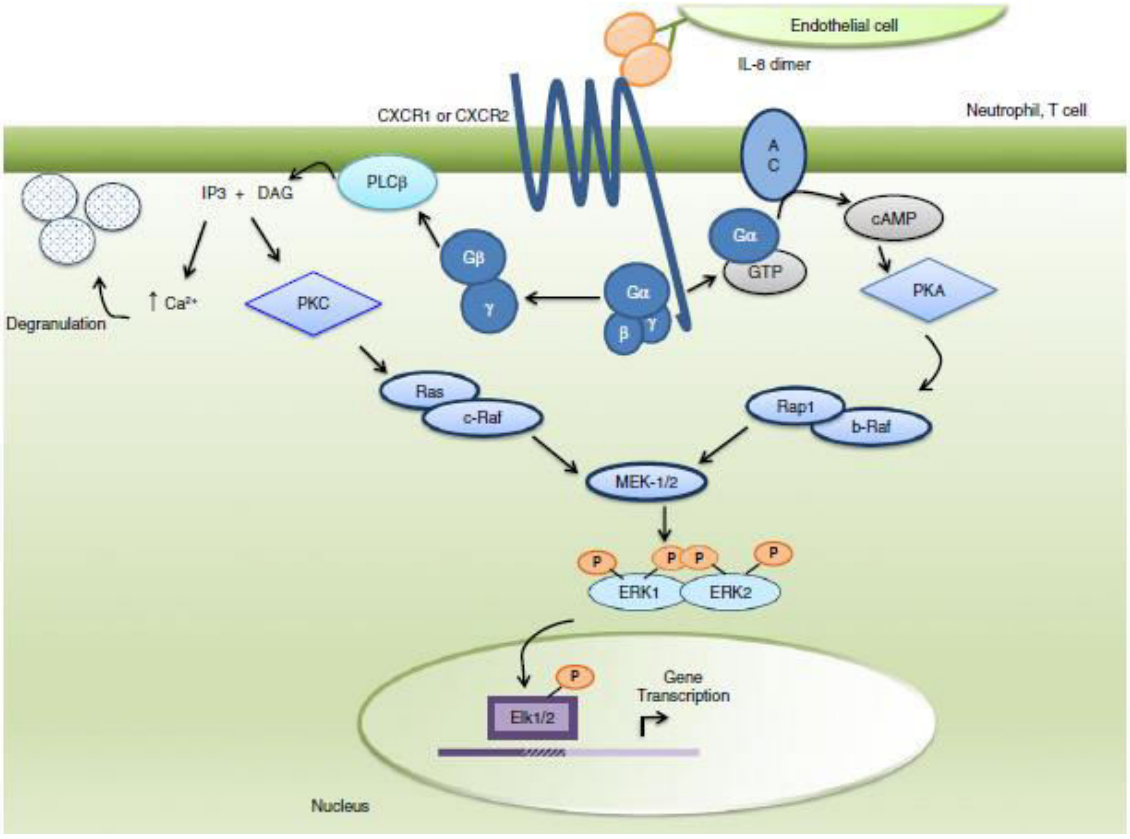

Fig. 17 : IL-8 signaling illustrating an example of chemokine signaling pathway. *Adapted from Biochimica et Biophysica Acta 1843 (2014) 2563–2582*

3. MSCs and Inflammation :

'Multipotency' and 'Immunomodulation' are the two determining factors of MSC maintaining tissue homeostasis upon injury and infection. Injured / Inflamed tissue requires an inflammatory response to clear away the pathogen which is mediated by the direct action of immune cells followed by resolution of inflammation to allow tissue regeneration and replacement of damaged cells. Endogenous MSCs govern this process as their secretome contains many of the paracrine immunomodulatory effector molecules which senses the extent of inflammation and based on that these MSCs control the 'switch on' and 'switch off' of the immune system. Secondly, these multipotent cells undergo differentiation and also deposit extracellular matrix during the immune resolution phase to replace damaged cells and tissues (**92**).

To fulfill their roles in tissue regeneration and fighting against infection, MSCs must be properly recruited to the site of damage. Inflamed tissue secrete various pro-inflammatory cytokines (IL-1, IL-6, TNF-α) which activate the MSCs. Additionally, a broad range of chemokines (MCP-1, MIP-1α, MIP-1β, RANTES, macrophage-derived chemokine or MDC, SDF-1 or CXCL12) and growth factors, like platelet-derived growth factor-AB (PDGF-AB), insulin-like growth factor-1 (IGF-1) are also released which induce the expression of tyrosine kinase receptors for PDGF and IGF, as well as chemokine receptors CCR2, CCR3, CCR4, and CXCR4 enabling the trans-migration of MSCs from bone marrow or adipose tissue to the site of inflammation, along with a gradient of chemoattractants. Alternatively, MSCs can also be recruited from within the tissues to site of injury via migration within the stroma or via micro-capillaries, refered to as cis-migration. In-vitro expanded MSC populations are often used for immunomodulation and regenerative therapy in pre-clinical models of inflammation-mediated disorders, transplantation or degenerative diseases. Following intravenous infusion, despite the large numbers that become trapped in the lungs, some MSCs subsequently do migrate to damaged tissue such as infarcted myocardium, traumatic brain injury, fibrotic liver and chemically damaged lungs, and to various types of tumors. In experiments tracing MSCs expressing green fluorescent protein–tagged nestin, endogenous MSC-like cells have been observed to migrate from bone marrow to lung tissue following the induction of asthma.

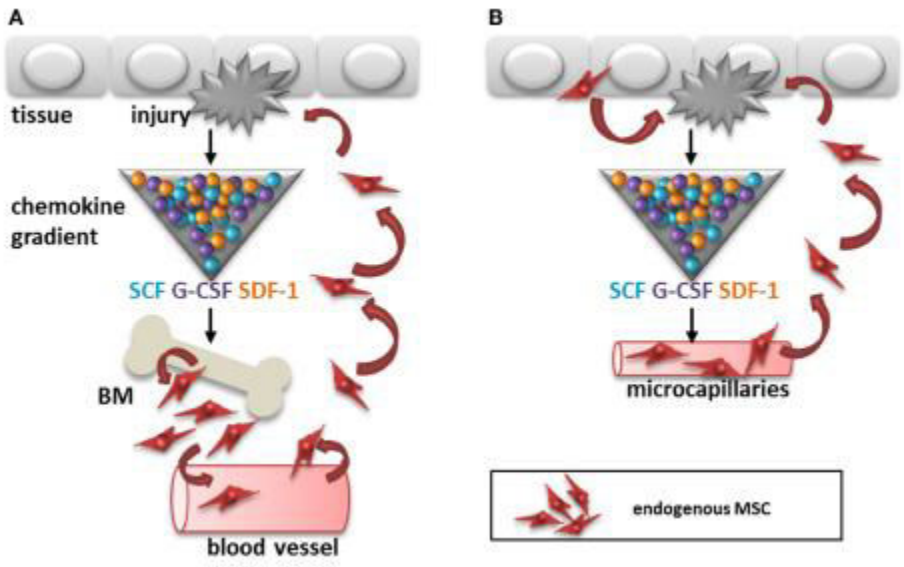

Fig. 18 : Two possible routes for homing of endogenous MSCs during tissue injury. (A) Various cytokines, chemokines and growth factors released from the damaged tissue trigger recruitment of MSCs from bone marrow to the sites of injury via circulation. (B) Alternatively MSCs can be recruited from within the tissues to the site of injury via microcapillaries or via migration within the stroma. *Adapted from Frontiers in Immunology 2014 May 16, Volume 5, Article 148*

Upon arriving in damaged tissue, MSCs are believed to exert their therapeutic effects in two ways: by cell replacement and by cell 'empowerment'. Being multipotent, MSCs do have the potential to differentiate and replace damaged resident cells, such as endothelial cells, smooth muscle cells, cardiomyocytes or hepatocytes, and thereby promote tissue regeneration in various organs such as the heart, kidneys and liver. Furthermore, inflammatory diseases have been effectively treated with only the culture supernatants of MSCs (the 'MSC secretome') containing growth factors, such as HGF or TSG6 ('tumor-necrosis factor (TNF)-stimulated gene 6'). Therefore, the therapeutic effects of MSCs may depend largely on the capacity of MSCs to regulate inflammation and tissue homeostasis via an array of immunosuppressive factors, cytokines, growth factors and differentiation factors. These include interleukin 6 (IL-6), transforming growth factor-β (TGF-β), prostaglandin E_2, HGF, epidermal growth factor, fibroblast growth factor, platelet-derived growth factor, vascular endothelial growth factor, insulin growth factor, stromal cell–derived factor 1 and, as discussed in more detail below, the tryptophan-catabolic enzyme IDO and nitric oxide (NO), a product of inducible nitric oxide synthase (iNOS). Together these secreted factors may inhibit inflammatory responses, promote endothelial and fibroblast activities, and facilitate the proliferation and differentiation of progenitor cells in tissues *in situ* (**94 - 97**).

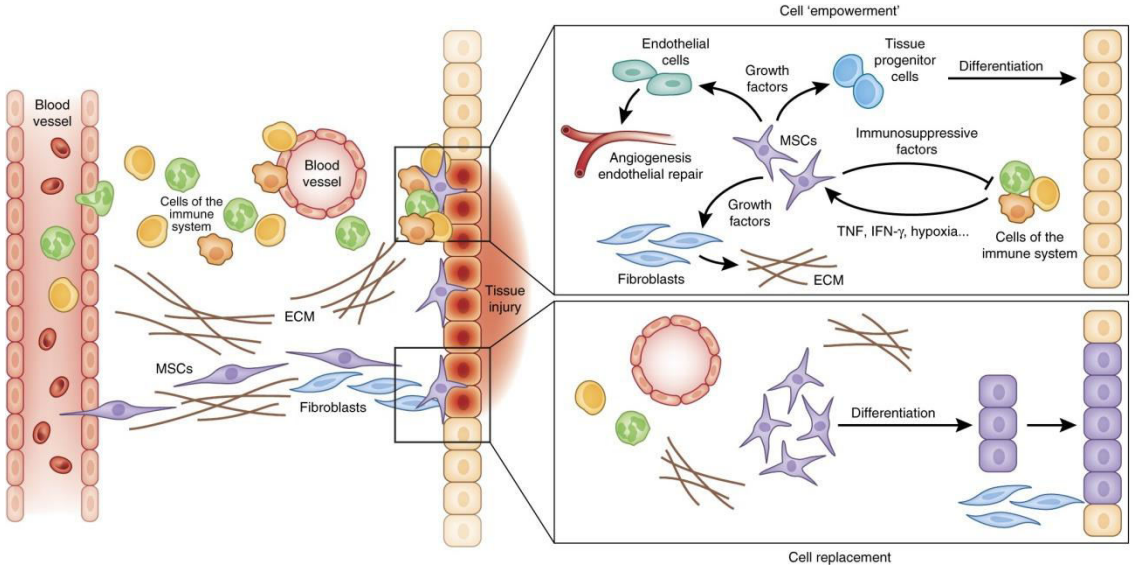

Fig. 19 : Modes of MSC-mediated tissue homeostasis. Cell replacement versus cell 'empowerment'. *Adapted from Nature Immunology Nov 2014, Volume 15, Article 11*

3.1 Mechanisms of MSC-mediated immunomodulation

As discussed earlier, the secretome of MSCs shows a very dynamic pattern during different stages of an inflammatory response. Although having a more or less constant profile of the released pro-inflammatory cytokines and chemokines, expression level of certain immunosuppressive factors in the MSC mileu does fluctuate based on the extent of inflammation and so, are the determining factors for whether MSCs will be immunostimulant or immunosuppressive. These broad panel of molecular factors include: indoleamine 2,3-dioxygenase (IDO), prostaglandin E2 (PGE2), inducible nitric oxide synthase (iNOS), transforming growth factor beta (TGF-β), interleukin-10 (IL-10), hepatocyte growth factor (HGF), histocompatibility locus antigen-G (HLA-G), CD39 and CD73, galectins, C-C motif chemokine ligand 2 (CCL2), haem oxygenase 1 (HO-1), tumour necrosis factor-stimulated gene 6 (TSG6), interleukin-1 receptor antagonist (IL1RA) and complement system-related factors.

During an overactivated immune response various pro-inflammatory cytokines can induce MSCs to acquire an immunosuppressive (MSC2) phenotype. Findings suggest that IFN-γ in combination with TNF or IL-1 induce the MSCs to secrete robust amount of chemokines along with the expression of inducible nitric oxide synthase (iNOS; in case of murine MSCs) or IDO (in case of human and other mammalian MSCs), resulting into subsequent inhibition of proliferation.

The majority of chemokines produced by cytokine-activated MSCs are CXC-chemokine receptor 3 (CXCR3) and CC-chemokine receptor 5 (CCR5) ligands, including CC-chemokine ligand 5 (CCL5), CXC-chemokine ligand 9 (CXCL9), CXCL10 and CXCL11, which are well-known chemoattractants for immune cells, including T cells. IDO is a catabolic enzyme that converts the essential amino acid tryptophan to kynurenine, which is further converted to kynurenic acid, anthranilic acid and other catabolites, depending on the enzymes present, whereas, iNOS is involved in the production of NO. iNOS mediated NO production leads to cell cycle arrest in T cells by impairing Janus kinase (JAK)-signal transducer and activator of transcription (STAT) signalling pathway. Increased NO production can also modulate mitogen-activated protein kinase (MAPK) and nuclear factor-κB (NF-κB) and thereby interfering with the production of pro-inflammatory cytokines by macrophages, NO indirectly inhibits T cell functioning. Immunosuppressive effects of IDO is mediated by the tryptophan catabolism leading to the depletion of this essential amino acid and thereby affecting the survival of immune cells. IDO secreted by MSCs also induce the differentiation of monocytes into M2-like macrophages, thereby attenuating inflammation and inhibiting effective repair processes. These findings together demonstrate the important implications of the interaction between chemokines and iNOS or IDO for the immunomodulatory functions of MSCs (**92,95**).

The MSC-derived secretome within an inflamed tissue microenvironment can also modulate the immune cells by the counterbalancing actions of various cytokines including TGF-β, IL-10, CCL-2, IL-6 and IL-7. TGF-β and IL-10 are the main immune-regulatory cytokines generated by quiescent MSCs. TGF-β is constitutively secreted by MSCs and further upregulated by inflammatory factors, such as IFN-γ and TNF-α. Induction of T_{reg} cells and inhibition of T cell activation have been shown to be driven by TGF-β as well as IL-10. TGF-β is one of the key regulators of Foxp3 expression. TGF-β inhibits IL-2, MHC-II (major histocompatibility complex II) and co-stimulatory factor expression in DCs and T cells. Both Th1 differentiation and Th2 differentiation could be inhibited by TGF-β. IL-10 expression could be further enhanced by TLR ligands and PEG2. IL-10 could inhibit antigen-presenting cell (APC) maturation and the expression of MHC and co-stimulatory factors. IL-10 inhibits pro-inflammatory cytokine production, T-cell proliferation and memory T-cell formation. IL-10 suppresses Th17 generation and promotes Treg formation. IL-10 exerts its anti-inflammatory effects through the JAK1-TYK2-STAT3-SOCS3 pathway (**99,101-103,108**).

MSC-secreted CCL2 plays an important role in regulating the expression of immune checkpoint molecule PD-L1 on T cells. It also inhibits the function of T_H17 cells and ameliorates experimental autoimmune encephalomyelitis (EAE). In a recent study, Giri et al. show that the chemokines CCL2 and CXCL12, secreted from bone marrow-derived mesenchymal stromal cells, upregulate IL-10 expression in CCR2+ macrophages. These polarized macrophages reduce tissue inflammation in colitis. While the full-length CCL2 binds to its receptor CCR2 expressed on T_H1, T_H17 and NK cells, and recruits them into the inflammation sites, there are other reports also which mention about a truncated version of CCL2, formed by the cleavage of metalloproteinases of the full-length CCL2, acting as a CCR2 antagonist and thereby inhibiting immune cell migration. On the other hand, IL-6 and IL-7 are the immune boosting factors of MSC secretome as they help in proliferation, survival and differentiation of T cells. Deletion of IL-6 in MSCs attenuates the pro-survival effects of MSCs on T cells. In a mouse model of colitis, IL-7 released by BM-MSCs was essential in supporting the survival of colitogenic memory T cells, which are responsible for disease relapse. Together, these observations indicate that the immunosuppressive versus pro-inflammatory properties of MSCs might be mediated, at least in part, by distinct cytokine components of the MSC secretome (**106,107**).

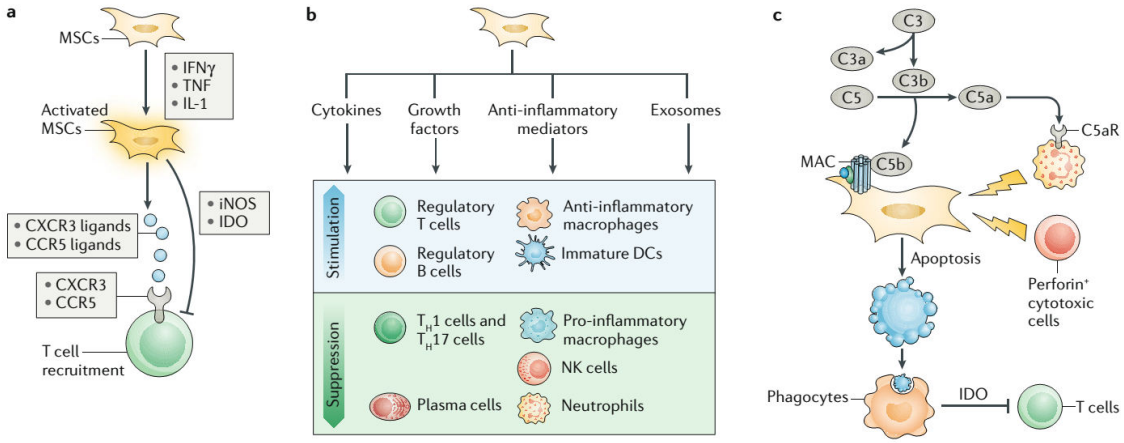

Fig. 20 : MSC-mediated immunomodulation. (a) iNOS / IDO axis for suppression of T cell. (b) Cellular target of immune-regulation by MSCs. (c) Even apoptotic MSCs can modulate the immune system. *Adapted from Nature Reviews Nephrology 2018 June Volume*

Among the MSC-derived growth factors, HGF (Hepatocyte growth factor) and LIF (Leukemia inhibitory factor) are known to have immunomodulatory effects with one study showing that administration of HGF alone can promote the recovery from EAE. HGF and LIF inhibit the differentiation of T_H1 and T_H17 cells. HGF also inhibits dendritic cell (DC) activation and promotes IL-10+ T_{reg} cells. Expansion of immune-suppressive myeloid derived suppressor cells (MDSC) is also promoted by MSC-generated HGF. LIF increases the expression of extracellular-signal-regulated kinases (ERKs) and suppressor of cytokine signalling 3 (SOCS3) and downregulates the activation of STAT3, which is a key factor that induces T_H17 cell differentiation. So altogether it seems like that MSC derived growth factors do participate to maintain immune homeostasis (**122-125**).

Among the other anti-inflammatory mediators of MSC secretome PGE2 and TSG6 are the two most extensively studied molecules. PGE2 is produced by COX-1 (cyclooxygenase-1, the constitutive isoform) or COX-2 (cyclooxygenase-2, the inducible isoform) from the arachidonic acid released from the membrane phospholipids. PGE2 interacts with EP2 and EP4 receptors expressed on the surface of immune cells and exerts its anti-inflammatory effects. The interaction between PGE2 and EP2 or EP4 receptors induces cyclic AMP (cAMP) upregulation, which then activates the PKA (protein kinase A) and PI3K (phosphatidylinositol-3 kinase) pathways. cAMP induces the expression of anti-inflammatory factors (IL-4, IL-5 and IL-10) and inhibits the expression of pro-inflammatory factors (IL-12p70, TNF-*α*, CCL3 and CCL4) through IL-2 pathway suppression. In addition, cAMP promoted M2 macrophage and T_H2 cell differentiation and inhibited T_H1 production. PGE2 promotes Foxp3+ T_{reg} cell production. PGE2 also promotes TGF-*β* secretion from monocytes and induces MDSC (myeloid-derived suppressor cells) generation, which could suppress NK cell and CD8+ T-cell activities. However, some studies have shown that PGE2 has pro-inflammatory effects with enhancing DC maturation and T-cell proliferation. Later studies have demonstrated that a low concentration of PGE2 promotes an inflammatory response, while a high concentration inhibits. PGE2 suppresses IL-12 and promotes IL-23 expression which is important for T_H17 production. TSG6 produced by TNF-stimulated MSCs, attenuates inflammation and enhances tissue repair in mouse models of arthritis, myocardial infarction, corneal injury, acute lung injury and peritonitis. TSG6 administration can suppress inflammation by inducing pro-inflammatory macrophages to adopt an anti-inflammatory phenotype and can attenuate LPS-induced acute lung injury. TSG6 inhibits the association of TLR2 with MYD88 and subsequently impairs NF-κB-dependent

activation of inflammatory gene transcription. Interestingly, TSG6 released by MSCs can bind to CD44 and inhibit the migration of neutrophils, monocytes and macrophages to inflamed tissues. Thus, anti-inflammatory factors such as PGE2 and TSG6 are key factors that contribute to the suppression of innate immune cells by MSCs. Both human and rat MSCs express a high level of HO-1 in the quiescent state. Blocking HO-1 reduced the immune-suppressive effects of MSCs. HO-1 could promote IL10+ Tr1 and TGFβ+ Tr3 generation, two types of T_{reg}. However, once MSCs are activated by pro-inflammatory factors, HO-1 expression decreases rapidly, and the immune-suppressive function of MSCs is taken over by other suppressive factors, such as iNOS. Galectins (Gal) are soluble proteins that bind to cell surface glycoproteins. MSCs express three isoforms of Gal, Gal-1, Gal-3 and Gal-9. Gal-1 binds to T_H1 and T_H17 but not T_H2 cells and induces cell apoptosis. Furthermore, Gal-1 promotes IL-10 production in T_H1 and T_H17 cells. Gal-1 suppresses the migration of immunogenic DCs. Gal-1 and Sema-3A bind to NRP1 (neuropilin 1, expressed on the T-cell surface) and arrest the T cells in the G0/G1 phase. Gal-9 suppresses B- and T-cell proliferation and is upregulated by IFN-γ. MSCs secrete HLA-G5 (one secreted isoform of non-classical class I MHC with immune-suppressive functions) under the stimulation of IL-10, IFN-γ and TNF-α. HLA-G binds to the receptors of ILT2 and ILT4, which are widely expressed by monocytes/macrophages, DCs, CD4+ and CD8+ T cells, B cells and NK cells. HLA-G inhibits the cytotoxic function of CD8+ T and NK cells, cytokine production of T_H1 and T_H17 cells, and induces T_{reg} generation and MDSC expansion. However, the immune-suppressive effects of HLA-G might also be concentration-dependent. It has been shown that a high concentration of HLA-G induces T_{reg} generation, while a low concentration promotes T_H1 development. HLA-G also confers the immune privilege characteristics of MSC differentiated derivatives. MSCs express CD39 and CD73. CD39 catabolizes ATP to AMP, and CD73 catabolizes AMP to adenosine. Extracellular ATP has pro-inflammatory effects, while adenosine has anti-inflammatory effects through the cAMP and PKA pathways. Thus, CD39 and CD73 could cleave extracellular ATP to adenosine and switch pro-inflammation to anti-inflammation. IL1RA expressed by MSCs could promote M2 macrophage polarization and T_{reg} generation with elevated IL-10 expression and suppress CD4+ T-cell activities. Furthermore, IL1RA could suppress B-cell differentiation and antibody production. Infused MSCs can be attacked by components of the complement system, complement-activated neutrophils and perforin-positive cytotoxic cells, inducing them to undergo apoptosis. Apoptotic MSCs can then be taken up by phagocytes, whereupon they induce the phagocytes to express IDO, with immunosuppressive consequences (**126-139**).

Apart from the soluble mediators exerting their effects on the neighbouring immune cells in a paracrine way or on the MSC itself in an autocrine manner, there are many immunomodulators present on the MSC surface. Presence or absence of these molecules serves as either co-stimulatory or co-inhibitory signals for the immune effector cells in a cell-cell contact dependent mechanism. These include : programmed cell death ligand 1 (PD-L1; also known as B7-H1 or CD274), programmed cell death ligand 2 (PD-L2; also known as B7-DC or CD273), TNF ligand superfamily member 6 (FASL; also known as FASLG), CD80 (B7-1) and CD86 (B7-2). hMSCs express few to none of the B7-1/B7-2 (CD80/CD86) costimulatory-type molecules; this appears to contribute, at least in part, to their immune privilege. MSCs express PD-L1 and PD-L2 under IFN-*γ* and TNF-α stimulation. Blocking the PD-L1 and PD-L2 pathways significantly impairs the immune-suppressive effects of MSCs. MSCs secreted PD-L1/L2 bind to PD-1 expressed on T lymphocytes and inhibit lymphocyte proliferation. PD-L1 and PD-L2 could suppress CD4+ T-cell activation, reduce IL-2 secretion, silence T cells and induce T-cell death. These factors could also inhibit AKT phosphorylation and upregulate Foxp3 expression, resulting in Treg production. Therefore, the ability of IFNγ-primed MSCs to suppress T cell proliferation is in part mediated by the upregulation of PD-L1/L2 on the surface of MSCs, whereas downregulation of PDL1 expression in MSCs blocks the immunosuppressive effects of MSCs. Similarly, TNF receptor superfamily member 6 (FAS)-FASL interactions enable MSCs to induce T cell apoptosis (**109-113**).

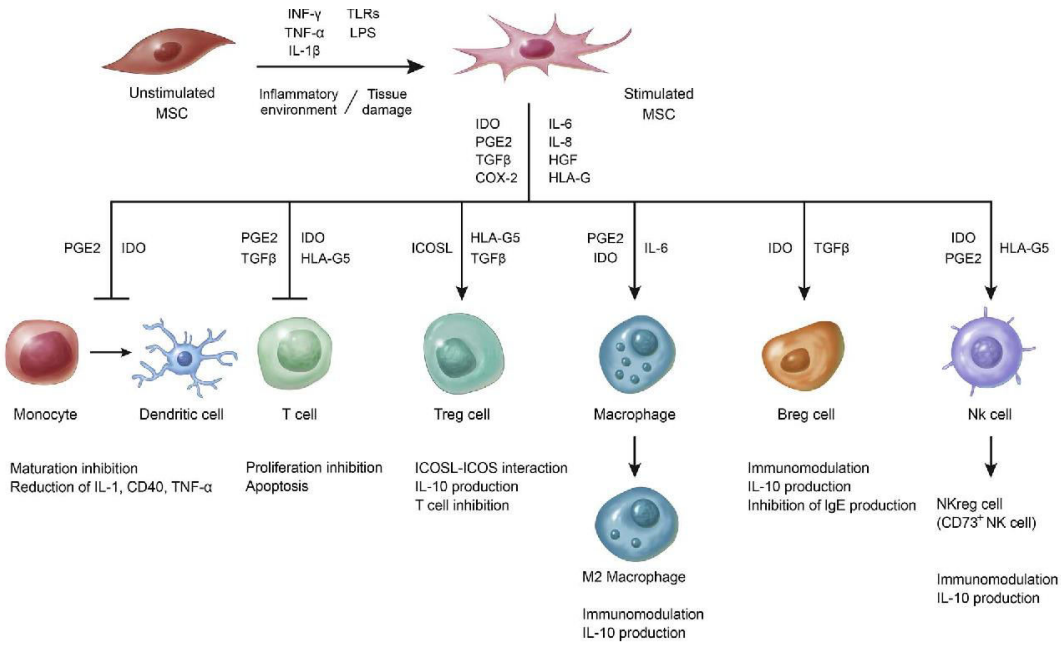

Fig. 21 : Immunomodulatory actions of stimulated MSCs on different cells of innate and adaptive immunity *Adapted from Cell Immunol. 2018 Apr 16; 326: 68-76.*

3.2 Inflammation dictates a new MSC paradigm

Depending on the severity of inflammation MSCs can switch between a pro-inflammatory (MSC1; Immunostimulant) or anti-inflammatory (MSC2; Immunosuppressive) phenotype. The kinds and concentrations of inflammatory mediators present in the tissue microenvironment largely determine the plasticity of MSC mediated immunoregulation. Under normal physiological conditions MSCs are immune tolerant due to their low level expression of class I MHC along with reduced expression levels of the major components of antigen processing machinery and the lack of class II MHC, FasL and co-stimulatory molecules like CD80 (B7-1), CD86 (B7-2), CD40 or CD40L. On the otherhand MSCs are known to constitutively express the non-classical HLA-G antigens and the co-inhibitory molecules like B7-H1 and B7-H4. But this immune tolerance property of MSCs is not constitutive.

Resting MSCs possess anti-apoptotic and supporting properties towards different cell types such as hematopoietic stem cells, T cells, B cell precursors, plasma cells, and neoplastic cells, and can't suppress immune reactions unless they are first activated by certain combinations of inflammatory cytokines. Thus, MSCs are 'licensed' to exert their immunomodulatory effects after stimulation with interferon-γ (IFN-γ) in the presence of one (or more) other cytokine(s), including TNF, IL-1α or IL-1β. The critical role in this process of IFN-γ and its receptor IFN-γR has been demonstrated in experiments with antibodies to IFN-γ or to IFN-γR, as well as MSCs deficient in IFN-γR1. During the initial stage of acute inflammation, when the immune system is not sufficiently actiivated, MSCs promote inflammation (MSC1) and once there is overactivation of immune system or more-than-required inflammation MSCs restrain it by switching towards a MSC2 phenotype to avoid self-overattack. So the reciprocity between MSC and inflammation is the major recipe to maintain a controlled and constructive immune response (**96,104**).

Molecules of acute phase inflammation, like IFN-γ, TNF-α, IL-1β or toll-like receptor (TLR) ligands provide the 'immune-licensing' of MSCs. Low levels of IFN-γ, TNF-α or any other pro-inflammatory cytokine shift MSCs towards a pro-inflammatory phenotype and enhance T cell responses by secreting chemokines (MIP-1α, MIP-1β, CCL5, CXCL9, CXCL10) which recruit lymphocytes to the site of inflammation. During this phase iNOS activity (for murine cells) and IDO activity (for human cells) are insufficient to suppress T lymphocyte proliferation. Moreover, antigen-pulsed MSCs stimulated with a low dose of IFN-γ have been found to act as antigen-presenting cells and can thus activate antigen-specific cytotoxic CD8+T cells. However when these cytokines are present in high levels

they induce the MSCs to secrete iNOS or IDO, as well as chemokines, such as the ligands of the chemokine receptors CXCR3 and CCR5, which are critical for recruiting various T cells into close proximity of MSCs, resulting in T cell proliferation inhibition and Treg induction. This immunosuppressive effects are more robust when IFN-γ acts in combination with the other pro-inflammatory cytokines, specially TNF-α and IL-1β. Therefore, the iNOS or IDO level is the determinant factor in switching MSCs between a pro- and anti-inflammatory phenotype (**104,105**).

The paradigm of MSC polarization into MSC1 or MSC2 might also depend upon toll-like receptor (TLR) activation expressed on their cell surface. Polarization into MSC1 phenotype, important for early injury responses, can be influenced by lipopolysaccharide (LPS)-dependent TLR4 activation, while double stranded RNA (dsRNA)-dependent activation of TLR3 is known to polarize MSCs into anti-inflammatory MSC2. In contrast other investigators have shown that TLR3 stimulation of MSCs leads to a pro-inflammatory response. The dichotomous pro- and anti-inflammatory effects of TLR3-stimulated MSCs may be time-related (**105,107**).

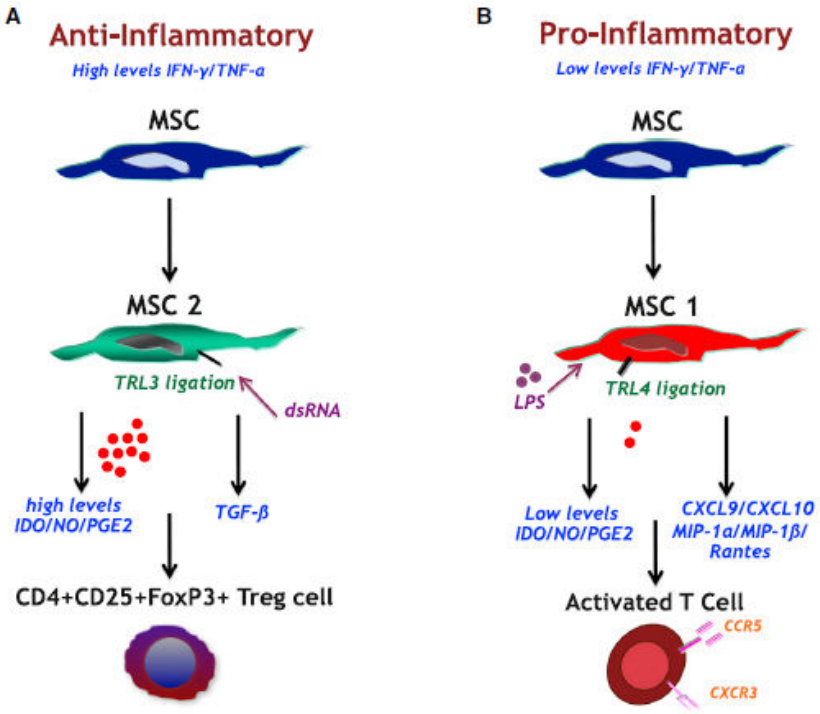

Fig. 22 : Polarization of MSCs into a proinflammatory and anti-inflammatory phenotype. (A) In presence of a hyperinflammatory microenvironment and upon TLR3 activation MSCs adopt an immune-suppressive (MSC2) phenotype (B) In presence of insufficient proinflammatory stimuli and upon TLR4 activation MSCs adopt an immune-stimulant phenotype (MSC1) to activate the immune system. *Adapted from Cell Stem Cell 2013 Oct 3; 505(7483):327-34.*

Anti-inflammatory cytokines like IL-10, TGF-β are also present within the inflammatory mileu and serve as counterbalancing components during the inflammatory response. TGF-β modulate the differentiation and regenerative capacities of MSCs. Surprisingly, when TGF-β1 or TGF-β2 is provided together with IFN-γ and TNF, the resulting MSCs are less immunosuppressive. The effects of TGF-β are a result of downregulation of the expression of iNOS (or IDO) in MSCs mediated by the signal transducer Smad3. Ironically, MSCs themselves can produce abundant TGF-β, which probably acts as a feedback loop to partially sustain inflammation, in addition to modulating the regeneration process. Despite that MSC-generated TGF-β, the immunosuppressive ability of MSCs can be inhibited by the addition of IL-10, which often works together with TGF-β. Such data reveal the other side of the coin: normally immunosuppressive cytokines can become immune enhancing through their effects on MSCs (**105**).

3.3 MSC-mediated tissue repair / remodeling during acute and chronic inflammation

In any tissue repair the inflammatory phase is transient, self-limiting and likely to be necessary for the subsequent regeneration and tissue healing. However, in the case of an infection, the inflammatory response will be persistent until clearing of invading microorganism is achieved, and if the microbial challenge cannot be eliminated, the infection can become chronic and result in tissue degradation and/or loss.

For example, chronic inflammatory diseases like rheumatoid arthritis (RA), diabetes mellitus and inflammatory bowel disease can affect bone quality, resulting in secondary osteoporosis. The mechanism behind this catabolic process is, at least partly mediated by the high prevalence of pro-inflammatory signals. This will lead to an imbalance between the activities of bone forming osteoblasts and bone resorbing osteoclasts, including RANK/RANK-L interactions and result in decreased bone mass.

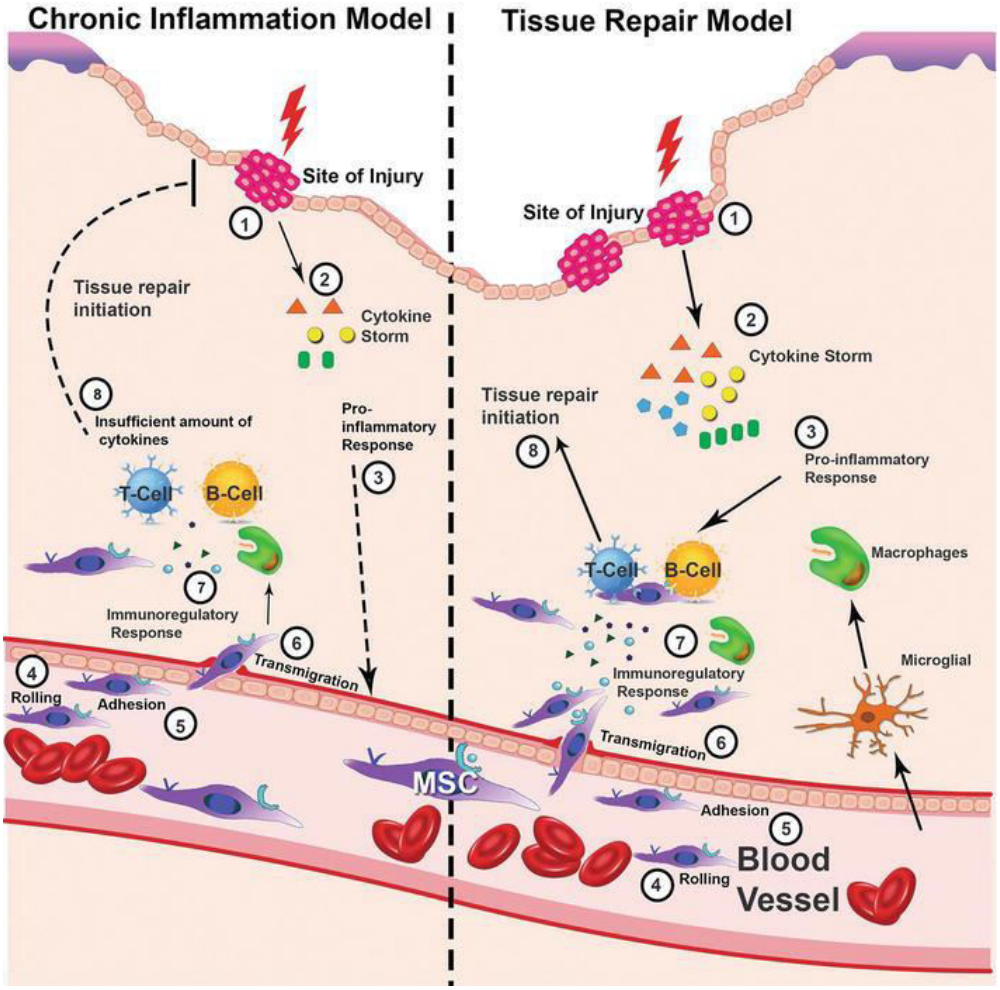

Fig. 23 : Immunoregulatory action of MSCS during chronic (left panel) and acute (right panel) inflammation. During acute phase of inflammation MSCs initiate the repair of the damaged tissue but if inflammation persists and becomes chronic then it leads to cellular fibrosis.

3.4 Comprehensive network between MSC, Inflammation and cancer

MSCs can both promote or inhibit tumor progression either by directly acting on the tumor cells via secreted mediators as well as cell-cell interactions or by modulating the immune cells recruited to the tumor microenvironment (TME), being a major characteristic of their immune-plasticity. Current experimental models suggest that the net effect of MSCs is considered to be pro-tumorigenic which might be due to imbalance between pro- and anti-tumorigenic activity dictated by the tumor type, intratumoral heterogeneity, the ecology of the host milieu, and possibly the composition of the MSC population itself. By inducing the expression of epithelial-mesenchymal transition (EMT)- and hypoxia-related genes in primary tumor, MSCs promote tumor cells to be invasive and metastatic. MSCs also deposit extra-cellular matrix (ECM) and thereby remodeling

the TME. TGF-β and IL-6, secreted by the MSCs, induce EMT and create a niche that promotes angiogenesis and tumor invasion. The activated TME in turn modulates the phenotype of tissue-resident and tumor-recruited MSCs (T-MSC). These tumor-associated MSCs are functionally distinct and different from the non-tumor MSCs (N-MSC). Presence of both TNF-α and IFN-γ is a major hallmark of TME mileu which induces the MSCs to produce TGF-β and VEGF. In addition, the synergistic effects of these two pro-inflammatory cytokines enhance the immunosuppressive nature of MSCs which altogether help to disseminate tumor cells. MSCs may adopt a CAF (Cancer-associated fibroblast) phenotype, which is highly a TME influenced phenomenon, characterized by upregulated α-SMA expression. Altogether tumor-associated MSCs (T-MSC) exhibit a significantly greater proliferative capacity, stronger migratory capability than N-MSCs and more potent immunosuppressive potential when compared to their normal tissue-associated counterparts. Finally, T-MSCs have been shown to promote tumor cell proliferation and to increase the proportion of cancer stem cells, suggesting a possible role in tumor cell reprogramming.

When it comes to the immunomodulatory potential of T-MSCs, TGF-β directly inhibits the function of anti-tumor effector cells (NK, CD8+ T cells, and γδ T cells) by downregulating the activating receptor NKG2D and generating and recruiting regulatory T cells and γδ T cells. T-MSCs have been shown to be more immunosuppressive than N-MSCs, by the action of PGE2 also. They decrease IFN-γ production and downregulate expression of the activating NK cell receptors NKp44, NKp30, NKG2D, DNAM-I, and NKG2A. T-MSCs also induce an inversion in the $CD56^{bright/dim}$ NK cell ratio in favor of the $CD56^{dim}$ phenotype. In addition, the chronic inflammatory nature of TME makes the MSCs immune-suppressive and facilitate tumor growth by modulating the immune cells in several ways - (1) MSCs can inhibit the proliferation, cytotoxicity, and cytokine production by NK cells by secreting several mediators, including PGE2, IDO, and sHLA-G5. In turn, MSCs can be killed by cytokine-activated NK cells through the engagement of NKG2D by its ligand ULBP3 or MICA expressed by MSCs, and of DNAM-1 by MSC-associated PVR or nectin-2. (2) MSCs inhibit differentiation of monocytes to DCs, skew mature DCs toward an immature DC state, and inhibit TNF-α and IL-12 production by DCs through PGE2 secretion. (3) MSCs dampen the respiratory burst and delay spontaneous apoptosis of neutrophils by constitutively releasing IL-6. (4) MSCs affect CD4+ T cells through PGE2, IDO, TGF-β, HGF, iNOS, and HO1 release. MSCs increase the production of IL-4 and IL-10 by T_H2 cells and reduce the release of IFN-γ by T_H1 and NK cells. IDO can reduce tryptophan levels and inhibit the growth of B cells, T cells, and

NK cells. Defective CD4+ T-cell activation impairs helper function for B-cell proliferation and antibody production. CD8+ T-cell cytotoxicity is inhibited mainly by sHLA-G5, as well as by the increase of the regulatory T-cell population, also induced by IL-10. (5) MSCs also polarise macrophage into anti-inflammatory M2 phenotype by the combined action of PGE2, IL-10, TGF-β. These tumor-associated macrophages (TAM) facilitate tumor growth and survival (**114-120**).

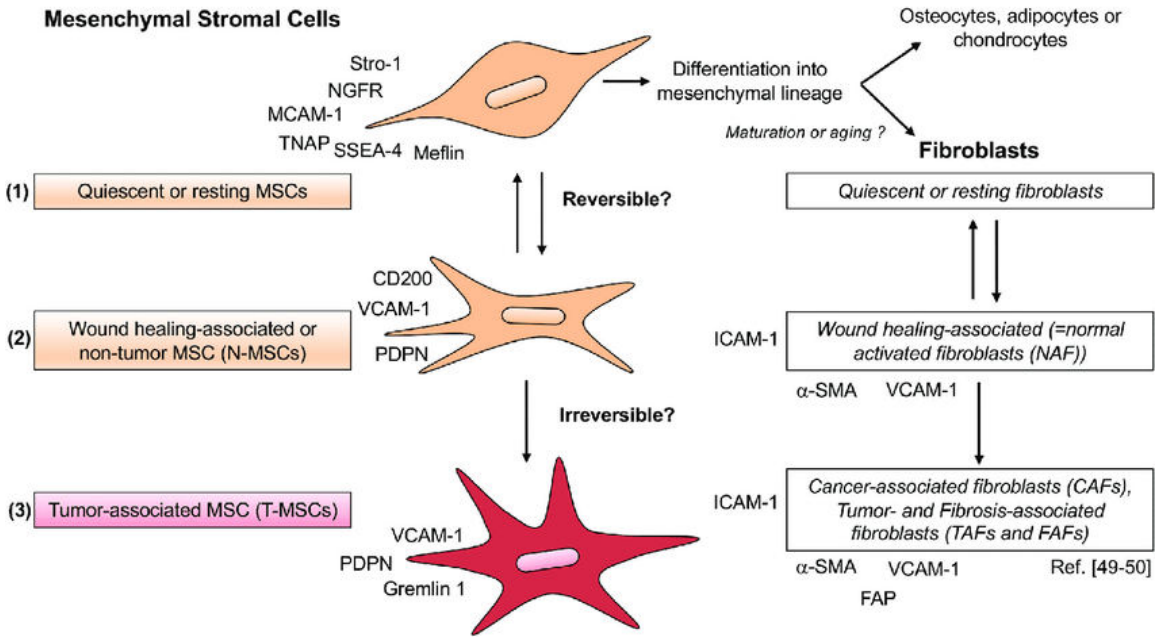

Fig. 24 : Possible mechanisms of MSCs transforming into cancer-associated fibroblast (CAF) in presence of chronic inflammatory tumor microenvironment (TME). MSCs and fibroblasts share overlapping characteristics and a reversible dynamics in course of maintaining tissue homeostasis. In presence chronic inflammation and tumor mileu MSCs undergo an irreversible transformation into CAF which in turn facilitates tumor progression, fibrosis and eventually are associated with many diseased conditions.

4. Epigenetic Mechanisms of Gene Expression

Epigenetics is defined as heritable and reversible changes in gene expression pattern without the alteration of the original DNA sequence. Epigenetic modifications are monitored by certain specialized enzymes that can act as 'writers' to deposit them and 'erasers' to remove them. The epigenetic landscape depicts the dynamic structure of chromatin that both restricts and permits the access of the transcriptional machinery to genes. Euchromatin is less condensed and more accessible region of chromatin associated with gene transcription whereas, heterochromatin is tightly condensed and restricts the access of the transcription factors. The dynamic balance between euchromatin and heterochromatin is subjected to various forms of epigenetic regulation such as DNA methylation, histone modifications and chromatin remodeling. The epigenetic marks regulating the expression of the molecular factors involved in MSC mediated immunomodulation and maintaining tissue homeostasis in order to intrinsically modulate the phenotype of MSCs without even changing its genotype can be a promising therapeutic target for future research.

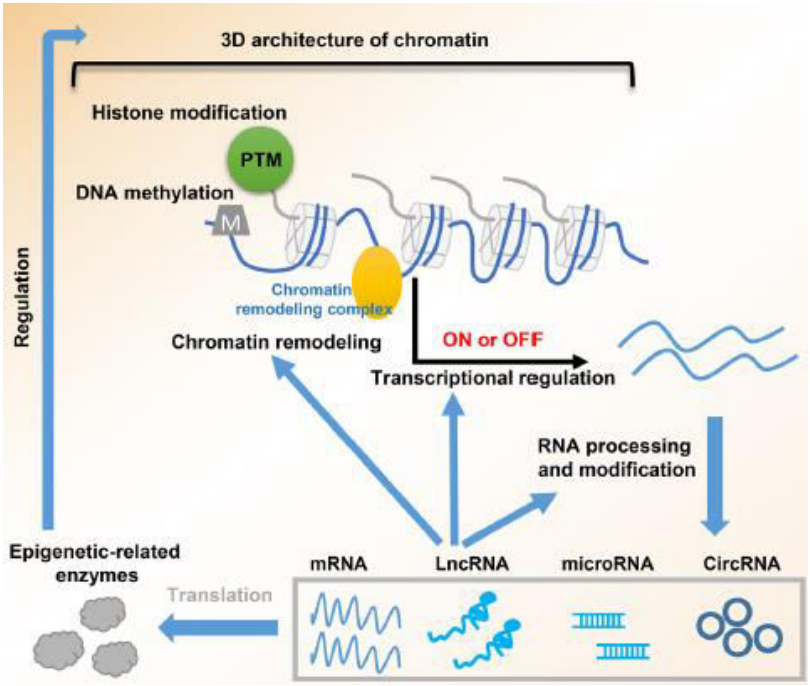

Fig. 25 : General schematic showing epigenetic factors regulating chromatin structure. The 3-dimensional (3D) architecture of chromatin is regulated by DNA methylation, histone post-transcriptional modifications (PTMs), and chromatin remodelers. These chromatin modifications act coordinately to control RNA transcription. On transcription, RNA processing and modifications add another layer of control on protein synthesis. The RNA products, including long noncoding RNAs (lncRNAs), microRNAs, and circular RNAs (circRNAs), in turn regulate chromatin remodeling, gene transcription, and mRNA processing and modifications. Notably, epigenetic modifications also regulate the expression of epigenetic players, such as epigenetic-related enzymes, which in turn modulate the 3D architecture of chromatin *Adapted from Front. Endocrinol. 2021 May 12; 351258.*

Within the nucleus DNA is tightly packaged into chromatin fibres. The fundamental unit of chromatin is the nucleosome, a core particle consisting of approximately 147 bp of DNA wrapped around histone protein octamers. Genome wide, areas of open chromatin with few nucleosomes form euchromatin, whereas the more condensed and nucleosome occupied stretches of DNA are known as heterochromatin. At more local levels the accessibility of DNA to the transcriptional machinery is regulated by nucleosome positioning and chromatin structure. Promoters and genes can either be maintained in a repressed state by the presence of nucleosomes or can be made open and accessible by the sliding of nucleosomes (**10-16**).

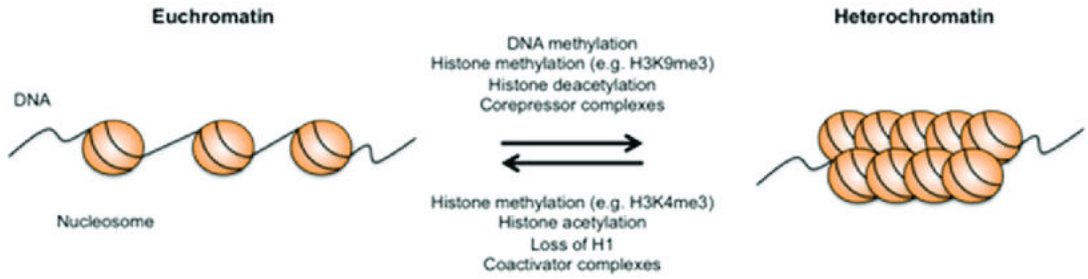

Fig. 26 : Schematic illustrating conformational transition between euchromatin and heterochromatin regulated by different epigenetic mechanisms. Euchromatin is open and accessible for gene transcription machinery whereas closed heterochromatin prevents transcription. *Adapted from MOJ Cell Sci Rep. 2016;3(1):26–28.*

4.1 DNA methylation

DNA methylation is characterised by methylation at the fifth position of cytosine (5-methylcytosine, 5-mC) in gene promoter CpG sites and is normally associated with gene silencing. The 'writers' of this DNA methylation mark are DNA methyltransferases : DNMT1 maintains the established methylation while DNMT3a and DNMT3b modify unmethylated DNA. This DNA methylation pattern can be reversed when ten-eleven translocation (Tet) family proteins convert 5-mC to 5-hmC (5-hydroxymethylcytosine) followed by DNA demethylation and gene transcription. In addition, N6-mA has recently been reported as another type of DNA methylation in mammals, and can be demethylated by the hydroxylase ALKBH1 (**173**).

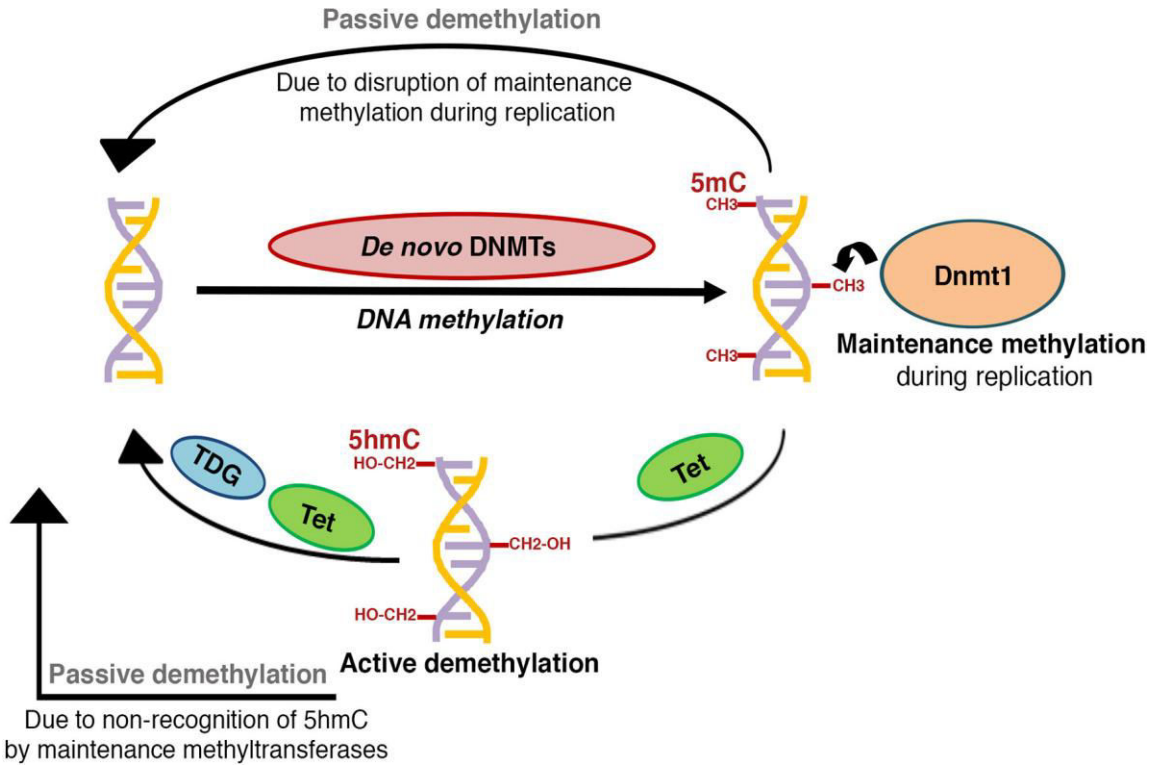

Fig. 27 : Schematic representation of DNA methylation patterning: The establishment of new DNA methylation patterns during development is regulated by the activity of de novo DNA methyltransferases, while activity of maintenance DNA methyltransferases serves to perpetuate these patterns during successive rounds of cell division. DNA methylation marks can be reversed through active or passive demethylation. Active demethylation involves the successive enzymatic oxidation of 5-methylcytosine (5mC) to 5-hydroxymethylcytosine (5hmC),5-formylcytosine (5fC), and 5-carboxylcytosine (5caC) by TET (Ten-eleven translocation) dioxygenases, followed by thymine DNA glycosylase (TDG) dependent removal of 5fC and 5caC, coupled with base-excision repair to a cytosine (C). A hemi-methylated 5hmC is not recognized by the maintenance DNA methyltransferases and can get diluted and lost during replication, thus contributing to passive demethylation. Disruption of maintenance methyltransferase activity can similarly result in replication dependent dilution of DNA methylation. *Adapted from Front. Endocrinol. 2021 May 12; 351258.*

4.2 Histone modification

Histones are primary protein components of eukaryotic chromatin and play a role in gene regulation. H3 and H4 histones have tails protruding from the nucleosome that can be modified post-translationally to alter the histone's interactions with DNA and nuclear proteins, leading to epigenetic changes for regulating many normal and disease-related processes. Histone modification consists of methylation, acetylation, phosphorylation, ubiquitinilation, and sumoylation.

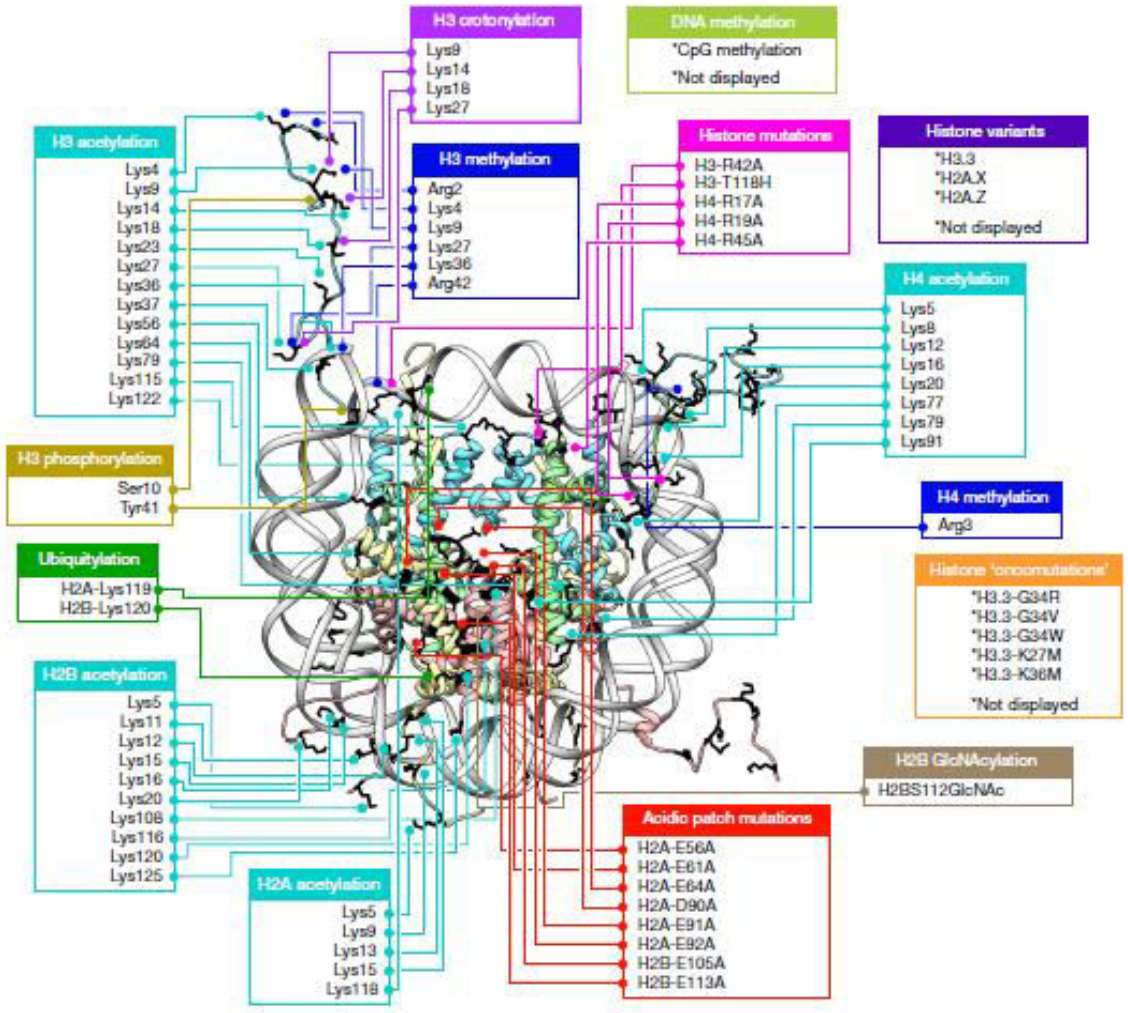

Fig. 28 : A diverse library of modified histones. *Adapted from MOJ Cell Sci Rep. 2016;3(1):26–28.*

Histone acetylation is the widespread and dynamic modification resulting from the interplay between histone acetyltransferase (HATs) and histone deacetylases (HDACs) that add or remove acetyl functional group at the lysine residues in the N-terminal tails of histones, respectively. HAT-acetylated lysines affect the overall charge of histones and weaken the interaction with DNA that is more accessible to transcription factors.

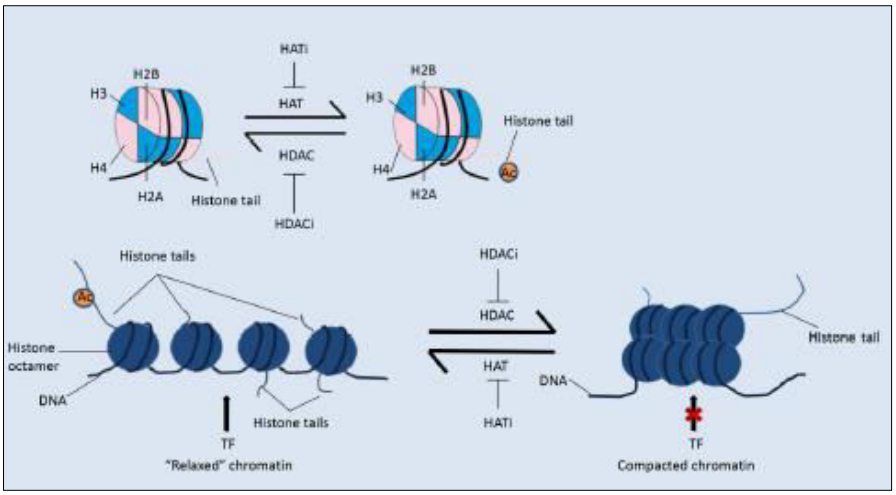

Fig. 29 : Histone acetylation and deacetylation controling the compaction state of chromatin. Acetylated histones facilitate transcription factor binding to DNA promoting gene expression. Deacetylation of histones induces the formation of tightly packed nucleosomes where transcription factors dont get the access to bind to DNA and therefore gene expression is suppressed. *Adapted from Genes 2018, 9, 633.*

On the other hand, histone methylation doesn't have to do anything with the charge of histones; rather it affects the chromatin structure which determines whether the DNA should be accessible for certain chromatin binding protein or not. Depending upon the accessibility provided by histone methylation, these epigenetic marks can both be activating or repressive and are maintained by a balancing act between histone methyltransferases (HMT) and histone demethylases (HDM) (**174**).

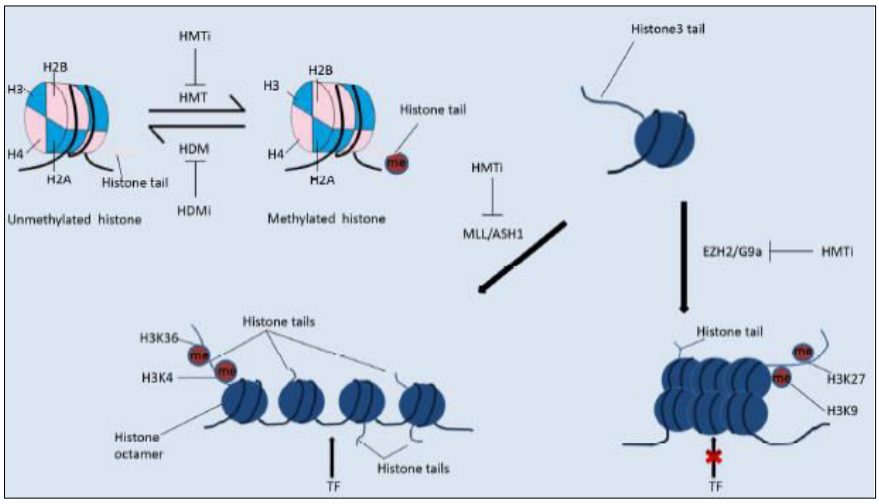

Fig. 30 : Histone methylation and gene expression. Methylation of histones can either suppress or enhance gene expression depending upon which residues in histones getting methylated.H3K4 and H3K36 methylation can promote gene expression; whereas methylation of H3K9 and H3K27 suppress gene expression by forming a compact chromatin structure. *Adapted from Adapted from Genes 2018, 9, 633.*

4.3 Chromatin remodeling complex

Active chromatin is decondensed to the extent that DNA binding factors can get access to DNA binding sites. Inactive chromatin is condensed and compact structure refractory to DNA binding factor. These two forms are temporally and spatially inter convertible by orchestra of various chromatin remodeling factors, including ATP dependent remodelers and chromatin modifiers. Remodelers are DNA dependent motors that utilize energy derived from ATP hydrolysis to non-covalently alter the chromatin structure. Remodelers can in vitro mediate (a) nucleosome sliding, in which the position of nucleosome on DNA changes, (b) the creation of a remodeled state, in which DNA becomes more accessible but histones remain bound, (c) complete dissociation of histone and DNA, or (d) histone replacement with variant histones (for a detailed discussion see below). At the same time, ATP dependent remodelers work in conjunction with histone chaperones and histone modifying enzymes. Currently, four different classes of ATP-dependent remodeling complexes can be recognized: SWI/SNF (switch/sucrose nonfermentable), ISWI (imitation SWI of drosophila melanogaster), NuRD (nucleosome remodeling deacetylase), and INO80 (chromatin remodeling ATPase INO80). Each class is defined by the presence of a distinct ATPase (**22-24**).

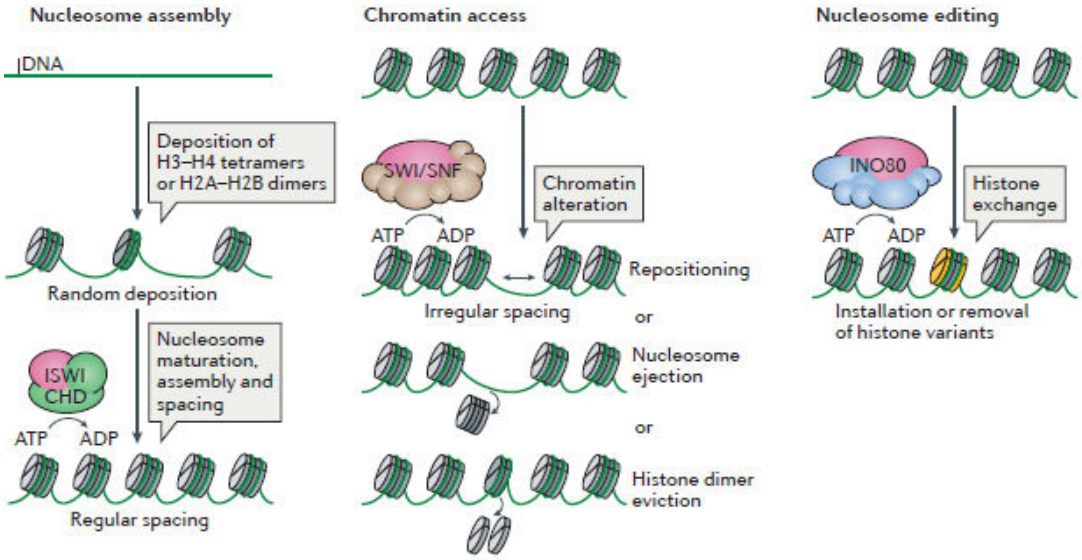

Fig. 31 : ATP-dependent chromatin remodelers and their mechanisms of functions. *Adapted from Nature Rev : Mol. Cell Bio. 2017, 18, 407-422.*

The mammalian switch/sucrose non-fermenting (SWI/SNF) family, also called BAF complexes (Brg/Brm Associated Factor) are thought to regulate gene expression by altering nucleosome positioning and structure. The ATPase subunit in SWI/SNF complexes is either BRM or BRG1; these molecules also contain bromodomains that allow binding to acetylated-lysine residues. BAF complexes exist in a wide variety of cell-specific, and more recently determined, disease-specific heterogenous configurations, each containing a total of 12-14 subunits that always include the core subunits BRM or BRG1, BAF170, BAF155, and BAF47 (also called hSNF5). The configurations change during cell-fate decisions; examples include esBAF in embryonic stem cells, npBAF in neural progenitor cells, and nBAF in postmitotic neurons, each of which contain specific subunit compositions. The genes encoding BAF complex components are mutated in over 20% of human cancers, and have jumped to the forefront of intense anti-cancer efforts (**18-21**).

The chromodomain helicase DNA-binding (CHD) family of ATPases is characterized by a signature chromodomain that elicits binding to methylated lysine residues. The ATPase subunits within this family include CHD1-9. However, CHD3 and 4 are most extensively characterized owing to their role in the the nucleosome remodeling and deacetylase (NuRD) complex. The large, multisubunit NuRD complex contains HDAC1 and 2 proteins and combines ATP-dependent chromatin remodeling with histone deacetylase activities to control both transcriptional activation and repression during embryonic development and cancer (**18-21**).

The imitation switch (ISWI) family controls nucleosome sliding and spacing. The catalytic ATPase in ISWI complexes is either SNF2L or SNF2H, which assemble with 1 to 3 accessory subunits to form 7 unique complexes. Nucleosome remodeling factor (NuRF), the founding member of this family, contains SNF2L and is essential for gene activation during development (**18-21**).

The ATPases within the human INO80 family include INO80, Tip60, and SRCAP, which assemble into large, multisubunit complexes that are responsible for exchanging variant histones into the chromatin structure. Human INO80 assists in the repair of double-strand breaks by evicting nucleosomes, thereby allowing repair factors to access the DNA (**18-21**).

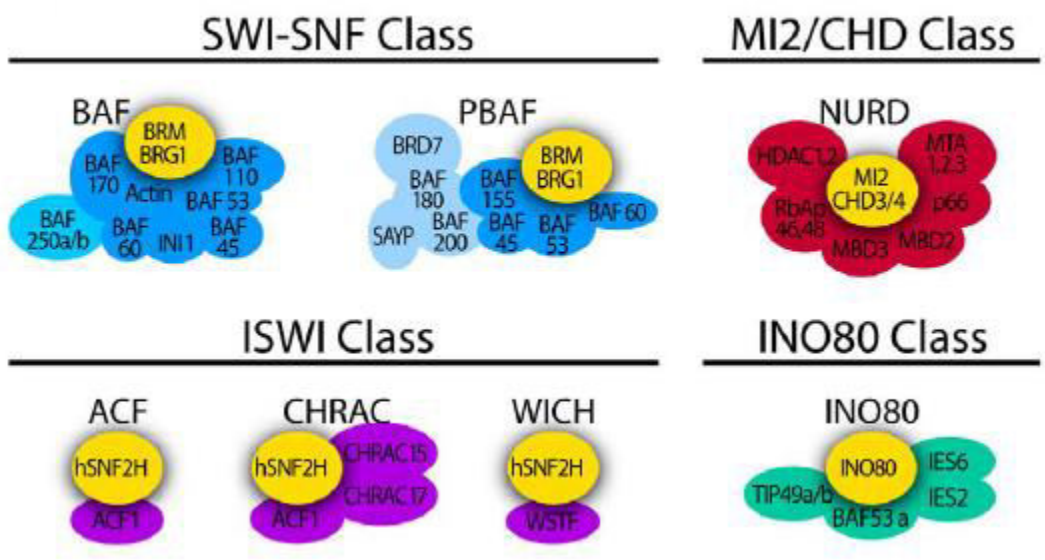

Fig. 32 : Four distinct families of chromatin remodeling enzymes. Families of mammalian ATP-dependent chromatin remodeling complexes are distinguished by their catalytic subunits : BRG1/BRM (SWI/SNF), ISWI, INO80 and CHD3/4 (Mi-2α/β). *Adapted from* PLoS Biol 9(11): e1001206

Materials & Methods

Cells

Mesenchymal Stromal cell lines OP9 (CRL-2749) and HS-5 (CRL-11882) cells were purchased from ATCC. Cells were grown and was maintained in DMEM media (Invitrogen) that was augmented with 20% and 10% non-heat inactivated FBS (Invitrogen) respectively, MS5 and NIH3T3 were also cultured in DMEM supplemented with 10% heat inactivated FBS. Murine macrophage cell line RAW 264.7 and murine breast carcinoma cell line 4T1 were cultured in RPMI-1640 media supplemented with 10% heat inactivated FBS. 100 µg/ml streptomycin (Invitrogen), 100 U/ml penicillin (Invitrogen) and 2 mM L-glutamine (Invitrogen). Human normal bone marrow-derived primary MSCs (PT-2501) were purchased from Lonza. These cells were cultured and maintained using human MSC media and supplements (Stem Cell Technologies). MSCs were passaged at 70% confluence, to avoid spontaneous differentiation and maintained at 37^0C with 5% CO_2 and 100% humidity. After informed consent of patients and according to institutional approval and guidelines from IICB human ethics committee, bone marrow samples were collected from MDS patients and age-matched healthy individuals. Bone marrow mononuclear cells (BMNCs) were either freezed or processed for isolation of human MSCs. These primary MSCs were also cultured and maintained using human MSC media and supplements. Irrespective of the cell type, all the cells were grown in their respective media along with penicillin, streptomycin and L-glutamine (all from Invitrogen). The cells were cultured at 37°C with 5% CO_2 and humidified condition.

Patient Cohort:

After informed consent of patients and accordingto institutional approval and guidelines from IICB human ethics committee, freshly diagnosed, untreated bone marrow aspirates of patient samples (1 -2 ml each) diagnosed with MDS (n = 20) were obtained from Park Clinic, Kolkata, India. Histopathological analysis of BM biopsies, immunophenotyping and karyotypic examination were used as inclusion criterions for this study. Individuals who were pathologically negative for MDS were considered as normal healthy donors. After informed from age-matched normal individuals BM aspirates were collected (n = 6). Mononuclear cells from samples were obtained using Ficoll (Low density 1.077g/cc Millipore Sigma, Burlington, MA, USA) separation. Cells were counted (trypan blue negative) and cryopreserved in liquid nitrogen for subsequent use if not processed for primary human MSC isolation. Ficoll method of mononuclear cell isolation briefly involves the following : Bone marrow was diluted 1:1 with sterile PBS and was layered on top of an equal volume of sterile room

temperature Ficoll very slowly. The tube was then centrifuged at 400xg for 30 mins with minimum deacceleration speed. Post centrifugation the mononuclear cell layer (visible as a separated white layer in between the RBC and serum layers) was carefully pipetted out in a fresh tube. Sterile PBS was used to wash the cellsbefore quantifying cell number using a hemocytometer. Cells were frozen in cryovials containing ice-cold 900µl of FBS and 100µl of DMSO mixture in sterile condition. Cells were gradually cooled to -80°C in a Frosty containing isopropanol and transferred to liquid nitrogen the next day.

Different pro-inflammatory stimuli for MSC driven immune response

For the establishment of our *in vitro* cellular model of inflammation MSCs were stimulated with different pro-inflammatory stimuli in a dose-specific manner. LPS which is a TLR4 agonist was used at 2.5µg/ml concentration for the optimal immune response elicited by MSCs. Other pro-inflammatory stimuli include recombinant human IFN-β, IFN-γ and TNF-α and all were used at a concentration of 10ng/ml.

BMP signaling, osteogenic differentiation

To carry out BMP stimulation of the MSCs, cells required to be serum starved. MSCs were cultured in presence of minimum serum containing media (DMEM containing 0.5% FBS) which was contained 50-100 ng/ml of recombinant murine BMP-2 (120-02, Peprotech) or recombinant human BMP4/7 heterodimer (3727-BP/CF, R&D). BMP receptor specific inhibitor Dorsomorphin (4 µM, Stem Cell Technologies) was used to inhibit BMP-2 signaling. BMP mediated differentiation for two and four days were carried out in a similar manner.Long-term osteogenic differentiation of MSCs is carried out in specific conditioned media. MSCs (having near 70% confluence) were maintained for a period of 3 weeks (21 days) in presence of osteogenic specific media containing DMEM (Invitrogen) supplemented with 20% or 10% FBS, 100 U/ml penicillin, 100 µg/ml streptomycin, 2 mM L-glutamine, ascorbic acid (0.25 mM) (Sigma),dexamethasone (0.1 µM) (Sigma) and β-glycerol phosphate(10 mM) (Sigma) at 37^0C with 5% CO_2 and 100% humidity. All stocks were prepared fresh every week and stored in dark condition. MSC differentiation media was replaced two to three times every week. It is essential to ensure that the cells are not exposed to direct light during the differentiation process.

Alkaline phosphatase staining

In order to monitor osteoblast differentiation weekly alkaline phosphatase staining using BCIP/NBT as a substrate was used. This process stains cells blue-violet when cells begin to express alkaline phosphatase. Briefly, to 10 ml of distilled water one BCIP/NBT tablet (Sigma Aldrich) was dissolved to prepare the substrate solution. Tween 20 (0.05%) was added to PBS to make washing buffer. Cells were removed from the incubator and media was aspirated without disturbing the cellular monolayer. Cells were wiped oncewith 1 x phosphate buffer saline (PBS) ensuring not to disrupt the cellular monolayer. 10% neutral buffered formalin was added to fix the cells for 60 seconds. It is critical to not over fix the cells. This might affect functioning of the enzyme Alpl. After completion of fixation formalin was removed and cells were thoroughly rinsed with washing buffer. Sufficient amount of substrate solution (BCIP/NBT) was next added to the monolayer of differentiated cells. Plates were maintained in absence of light or by covering with aluminium foil for 15 to 30 minutes. Progression of staining was checked every 2 to 3 minutes to avoid over staining. Substrate was discarded, cells were washed with washing buffer and analysed for staining. PBS was added to the wells to avoid drying up.

Quantitative RT-PCR analysis

Manufacturer's recommendation was followed to isolate total RNA using TRIzol (Life Technologies). After dissolving the RNA pellet in DEPC treated water, RNase-free DNase1 treatment (Roche) was performed to do away with any DNA contamination. Nanodrop was used to quantify total amount of RNA and 2-5 ug of RNA was used to prepare cDNA using reverse transcription reagents (TaqMan) from Applied Biosystemsin accordance to manufacturer's instruction. Real time PCR method (quantitative) was utilizedto determine gene expression levels using cDNA and SYBR green dye (SYBR Green Master mix from Applied Biosystems) on the 7500 Fast Real-Time PCR platform (Applied Biosystems). A housekeeping gene like *Gapdh* was used as a normalization control. Expression levels were calculated relative to *Gapdh* using $2^{-\Delta\Delta Ct}$ methods as described earlier (148-150).

Lentivirus preparation and transduction

Lentivirus preparation requires 293T cells cultured in DMEM media containing 10% heat inactivated FBS, 100 U/ml penicillin, 100 µg/ml streptomycin and 2 mM L-glutamine (Invitrogen) at standard growth conditions. Cells are co-transfected usingdesired plasmid DNA, *pMD2.G*and *PAX2* using calcium-phosphate transfection method maintaining cell density at 70% confluency in a T-225 cm^2 flask (148, 151, 152).The flask was poly-L-lysine coated. Cells were incubated in transfection media overnight following whichthey were washed with PBS without disturbing the cellular layer and butyrate induction was given for 8

hours. Post butyrate induction cells were washed with PBS and sufficient volume of collection media added. After 36-40 hours of incubation in normal growth condition supernatant containing lentiviral particles were collected. The viral particles were concentrated by ultra-centrifugation for 90 minutes, at 25,000 rpm maintained at 4°C (Sorvall, Thermo Scientific). X-VIVO media (Lonza) was used to resuspend the viral particles andsmaller aliquots were stored at -80°C. Viral titre was determined using 293T cells prior to transduction of desired cells. OP9 cell density was kept at 5x 10^3 cells/cm^2 and transduced for 12 hours using lentiviral particles at a MOI of 10 in presence of polybrene (8ug/ml). MS5 and NIH-3T3 cells were seeded as 1x10^4 cells/cm^2 and transduced for 8 hours using lentiviral particles at a MOI of 5 in presence of polybrene (8ug/ml). Following transduction cells were allowed to recover and checked for GFP percentage to determine the transduction efficiency.

Generation of *Gatad2b* deficient Stable Lines

In order to generate stable lines MSCs that were transduced were expanded.Cells were segregated using MoFlo XDP cell sorter (Beckman Coulter) to select GFP expressing cells or cultured in presence of puromycin (1ug/ml) for 48 hours to select the transduced cells. The GFP+ cells or puromycin selected cells were cultured further to carry out downstream experiments.

Flow cytometry analysis

For intracellular flow cytometry experiments, 100 µl of 16% paraformaldehyde was added to 1 ml of media to fix the cells at room temperature for 10 minutes.Following fixation FACS buffer was added and cells were pelleted down at 4^0C.Cells were permeabilized for 20 minutes at 4^0C using ice cold methanol after discarding the supernatant. Residual methanol was removed by washing the cells twice with FACS buffer. Cells were incubated with primary antibodies in FACS buffer. Antibodies against Gatad2b (1:100) or Tlr4 (1:100) or Total p65 (1:100) or Total Irak1 (1:100) were added at room temperature, in dark for 15 minutes. After incubation the cells were washed for 5 mins at 4^oC and resuspended in FACS buffer. Secondary antibodies Alexafluor 488-conjugated donkey anti-mouse secondary antibody (1:500) or goat anti-rabbit DyLight 568 (1:200) were added depending on the host species for primary antibody for 10 to 15 minutes in dark. For phospho flow analysis primary antibody was added for 1.5 hours followed by secondary antibody incubation for 1 hour respectively keeping the other steps constant. Cells were washed to remove non-specific binding, and resuspended in FACs buffer for analysis using LSRFortessa (Becton Dickinson). Data was analysed using FACSDiva software (Becton Dickinson). In order to determine cellular percentage of GFP^+ cells were multiplied by aggregate of viable cells at

specific intervals. For cell survival assay, cells in culture were stained for ten minutes at room temperature with Annexin V-APC (1:20) and 7-AAD (1 µg/ml) in Annexin-V buffer. The cells were then examined in LSRFortessa (Becton Dickinson) using FACSDiva software (Becton Dickinson).

Immunofluorescence

Cover slips were sterilized and coated with poly-L-Lysine before seeding of the cells. OP9 cells were allowed to adhere topoly-L-lysine (Sigma)-coated coverslips, serum starved overnight (in case of BMP-2 stimulation only) and subjected to LPS or BMP-2 treatment in presence for different time points at 37ºC with 5% CO_2. Ice cold PBS containing protease and phosphatase inhibitors were added to stop incubation and immediately fixed with 4% paraformaldehyde at room temperature for 10 minutes. Paraformaldehyde was removed by washing the cells and permeabilized using 0.2% Triton X-100 (Sigma) for 10 mins at room temperature. The cells were blocked for 30 mins at room temperature using 0.1% Triton X-100 and 2% BSA in PBS.Primary antibodies against Gatad2b (1:200) or p-P65 (1:100) or pSmad1/5/8 (1:50) were added for 1.5 hours at room temperature in a wet chamber. The cells were washed to remove the non-specific binding and Alexa fluor 568-conjugated donkey anti-rabbit secondary antibody (1:500) or Alexa fluor 488-conjugated goat anti rabbit secondary antibody (1:500) was added for 60 mins at room temperature in dark in a wet chamber. Ice cold PBS was used to wash the cells for five to six times and stained with DAPI (1 µg/ml, clone, cat) for 30 secs to 1min. The cells were thoroughly washed for seven to eight times with ice cold PBS. Vectashield (Vector Laboratories) was added to the slides prior to mounting of the cover slips and edges were sealed. FluoView (Olympus) confocal microscope was used for imaging purpose.

Immunoblot analyses

Cell lysates were prepared by disrupting cells in in presence of protease and phosphatase inhibitor cocktails using 1 x RIPA (Cell Signaling) for 15 minutes followed by short sonication of 25 secs (5 pulse for 5 second each). Lysate was centrifuged at 16,000g for 15 minutes at 4ºC to remove cellular debris and supernatant collected. Protein concentration was determined using Pierce BCA Protein assay kit (Thermo). 1x SDS gel loading buffer containing β-mercaptoethanol was used to resuspend the lysates. SDS-PAGE gel was used to separate the proteins and blotted onto PVDF membrane (Millipore). Primary antibodies against desired proteins were used to probe the blots overnight at 4^{o}C under rocking condition.Following day secondary antibody was added and incubated for 1 to 2 hours at room temperature. A 1:1000 dilution of antibodies was used for probing unless specified otherwise.

RNAseq analysis

TRIzol and PureLink RNA mini kit (Ambion) were used to isolate total RNA from 10 x 10^6 control or *Gatad2b*-deficient OP9 or MS5 cells. The quality of isolated RNA was determined using Agilent RNA 6000 Nano chips in 2100 Bioanalyzer (Agilent). The amount of RNA isolated was quantified with the help of NanoDrop spectrophotometer (Thermo). Keeping cut off at >8 for RNA integrity number samples were selected for Illumina sequencing library preparation. Ribo-Zero rRNA removal kit (H/M/R) from Illumina was used to remove ribosomal RNA from 5ug of total RNA. These ribosomal RNA depleted samples were used for library preparation using Illumina TruSeq RNA Library Prep Kit in accordance to the manufacturer's protocol rRNA-depleted fragmented total RNA was used to generate first and second strand of cDNA. The cDNA strands were repaired for adaptor ligation. Using limited PCR cycles the library was enriched. High sensitivity D1000 ScreenTape in Agilent 2200 TapeStation system was used to verify the quality of generated library. The library was finally quantified using quantitative Real Time PCR. Sequencing of these libraries (2 x100 bp paired end) were performed in HiSeq-2500 (Illumina) platform. NGSQC toolkit was used for quality control. Highquality reads of 89-91% were mapped to mm10 mouse genome reference sequence using TOPHAT. High percentage of alignment suggested good quality of RNA sequencing. Cufflinks-based maximum likelihood method was used for assigning a score to the transcripts for their expression. Cuffdiff validation identified a total of 35,771 transcripts to be expressed in both control and knockdown lines. "Full Length" or "Known Transcripts" percentage was approximately 95.5%.As per Cufflinks Class Code distribution"Potentially Novel Isoforms" of transcripts was found to be 4.5 %. For Significant Biology of Differentially Expressed Transcripts, GO-Elite_v.1.2.5 Software was used. P value ≤0.05 was used as a cut off for enrichment of GO terms and pathways.We considered $\log_2$FC >1 (up-regulation) and $\log_2$FC <-1 (down-regulation) to identify differentially regulated genes.

Gene ontology (GO) term enrichment analysis

For GO analysis the database for annotation, visualization and integrated discovery (DAVID) v6.8 was used. A modified p value, EASE score threshold (maximum probability) was used for analysis. GO term enrichment analysis utilizes a modified Fisher Exact P-Value, that ranges between 0 to 1 as the threshold of EASE Score. Fisher Exact P-Value = 0 corresponds to ideal enrichment. In the annotation categories p values <= 0.05 is reckoned to be highly enriched.

Preparation of conditioned medium from MSCs

Cells were seeded in complete DMEM medium containing 10% FBS at a density of 50,000 cells/cm^2 in a 60mm tissue culture treated dish. After 24 hours the complete medium was replaced with serum starved medium containing 0.5% FBS and the cells were incubated at 37ºC for another 24 hours. Then the medium was collected, centrifuged at 3000 rpm for 10 min at 4ºC to remove cell debris, filtered through 0.2 µm filters and then frozen in aliquots at -80ºC.

31-plex mouse chemokine assay

The presence of 31 different cytokines and chemokines in conditioned medium from MSCs was determined using the magnetic bead-based multiplex assay Bio-Plex Pro Mouse Chemokine Panel 31-plex kit from Bio-Rad Laboratories. The analysis was performed according to the manufacturers protocol and the outcome analyzed on the Bio-Plex 100 system. The expression of IL-1β, IL-2, IL-4, IL-6, IL-10, IL-16, GM-CSF, IFN-γ, TNF-α, CCL1, CCL2, CCL3, CCL4, CCL5, CCL7, CCL11, CCL12, CCL17, CCL19, CCL20, CCL22, CCL24, CCL27, CX3CL1, CXCL1, CXCL5, CXCL10, CXCL11, CXCL12, CXCL13 and CXCL16 were analyzed using this assay.

Polarisation of RAW 264.7 murine macrophage cell line in vitro

RAW 264.7 macrophages were seeded onto 12-well culture plates at 5×10^5 cells per 1 ml or 6-well culture plates at 1×10^6 cells per 2 ml of culture medium and cultured for 24 h. Subsequently the cells were incubated with 50% fresh serum starved medium or MSC derived conditioned medium. For M1 polarisation 100ng/ml of LPS and 40ng/ml of IFN-γ were added as stimuli and 20ng/ml IL-4 was used as M2 stimuli. The cells were cultured in presence of differentiation medium for 48 hours and analysed for the expression of M1 and M2 markers.

Mice and *in vivo* assay using MSC derived conditioned media

The Institutional animal ethics committee at IICB, Kolkata approved the animal experiments. Immunomodulating potential of MSC-CM upon MSC-intrinsic *Gatad2b* loss of function was also demonstrated in an in *vivo* system using female balb/c mice of 8-12 weeks. $1x10^6$ murine breast carcinoma cell line 4T1 was injected per mice orthotopically to induce the formation of tumor and MSC-CM from both control as well as *Gatad2b* knockdown stroma were injected intra-tumorally taking two different groups of mice. Within 18 hours of injection the mice were euthenised, tumors were isolated and single cells derived from the tumor mass upon type II collagenase/DNaseI treatment were analysed for immune cells infiltration. Multicolor flowcytometry analysis was conducted using 7-AAD and fluorochrome tagged

antibodies which consists anti-mouse CD45 V500c, anti-mouse CD11b BV711, anti-mouse Ly6G PE-Cy7, anti-mouse CD206 APC, anti-mouse F4/80 BUV395, anti-mouse CD68 BV421. The cells were then examined in LSR-Fortessa (Becton Dickinson) using FACSDiva software (Becton Dickinson).

Statistics

Data and statistical analysis were performed using GraphPad Prism 5.Forstatistical analysis Student's *t*-test was used. Mean ± s.d was used for quantitative analysis of data unless mentioned specifically. For overall statistical analyses, p-value significance was set at 0.05. RNA-seq data were deposited at NCBI.

RESULTS

Induction of *Gatad2b* and other NuRD subunits upon TLR4 pathway activation

As discussed earlier we wanted to explore the involvement of NuRD in MSC-mediated immunomodulatory response. Initially we used OP9 cells which is a *bona fide* murine MSC line derived from mouse calvaria, capable of trilieage differentiation into osteoblast, adipocyte and chondrocyte and hence can be considered as mesenchymal stem cells. To establish our *in vitro* cellular model of inflammation OP9 cells were treated with 2.5 ug/ml of LPS over a period of 24 hour. LPS is a gram-negative bacteria derived potent endotoxin which upon binding to its receptor TLR4 activates the NF-Kb signaling pathway and induces the expression of NF-Kb responsive genes which include a vast array of cytokines and chemokines. LPS treatment significantly induced the expression of *Gatad2b* and few other NuRD subunits as well which include *Chd4*, *Mbd2*, *Mta1/2/3* and *Rbbp4/7* along with its recptor Tlr4 and other classical pro-inflammatory markers like Il6, Il8, Tnfa, Ccl3 in a time-dependent manner (Fig. 33A). In addition to OP9 cells, human HS-5 cells were also treated with LPS followed by again a significant induction of NuRD subunits like *GATAD2B*, *CHD3*, *MBD2* along with other pro-inflammatory markers (Fig. 33D). We did not want to restrict our study among the mesenchymal stem cells only since mesenchymal stromal cells and/ stromal fibroblasts are also integral components of a MSC-niche and stroma-driven immunomodulation do involve these cells too. MS-5 is a murine bone marrow derived stromal line and NIH-3T3 is a mouse embryonic fibroblast line. Both MS-5 and NIH-3T3 were treated with LPS which resulted in induction of various NuRD subunits like we observed previously (Fig. 33E, 33H). Altogether after carrying out the differential gene expression study *Gatad2b* and *Mbd2* stand out to be the common LPS-responsive NuRD subunits across all the different cell lines. Consistent with the transcriptional activation, LPS treatment also promoted the expression of Gatad2b and Mbd2 proteins shown by intracellular flow cytometry, confocal imaging and immunoblotting (Fig. 33B, 33C, 33F, 33G).

(A)

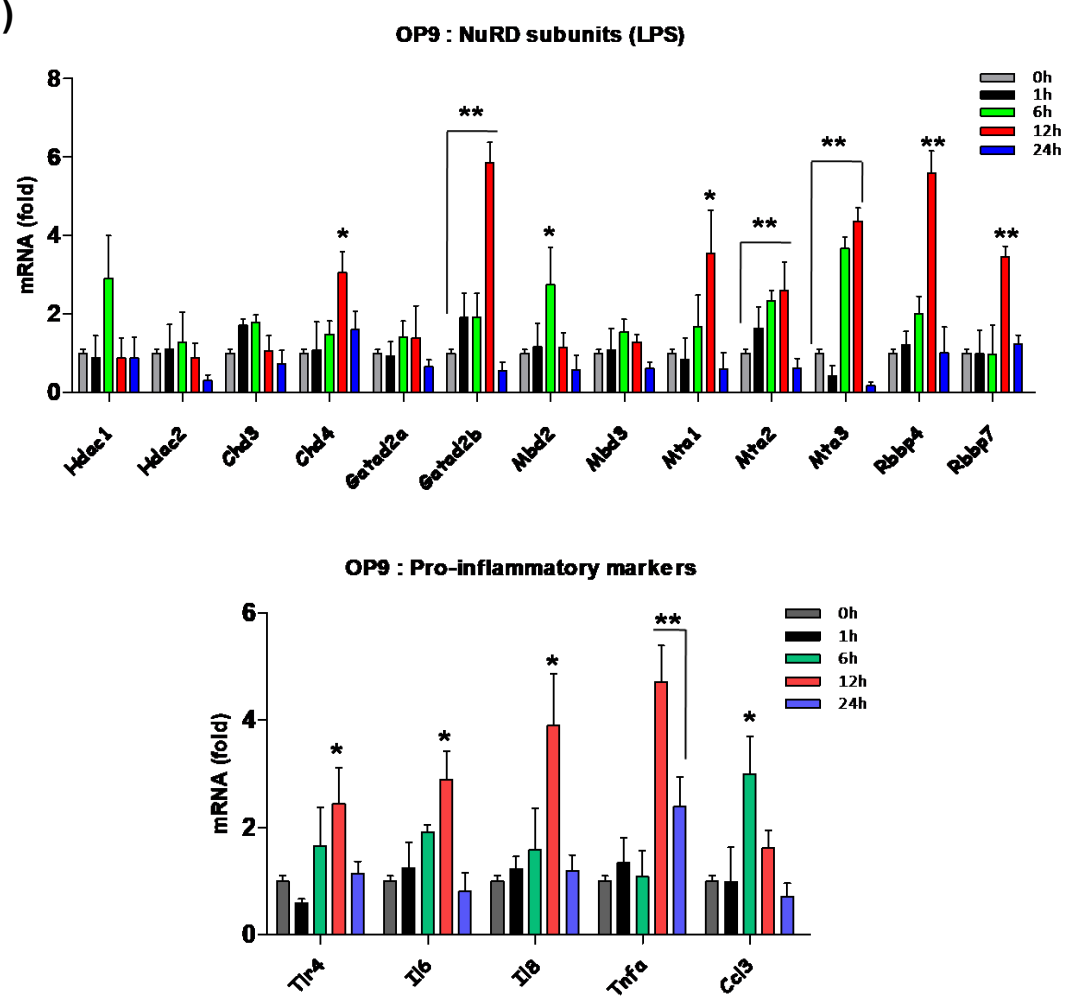
OP9 : NuRD subunits (LPS)
mRNA (fold)
0h
1h
6h
12h
24h
Hdac1
Hdac2
Chd3
Chd4
Gatad2a
Gatad2b
Mbd2
Mbd3
Mta1
Mta2
Mta3
Rbbp4
Rbbp7
OP9 : Pro-inflammatory markers
mRNA (fold)
Tlr4
Il6
Il8
Tnfa
Ccl3

(B)

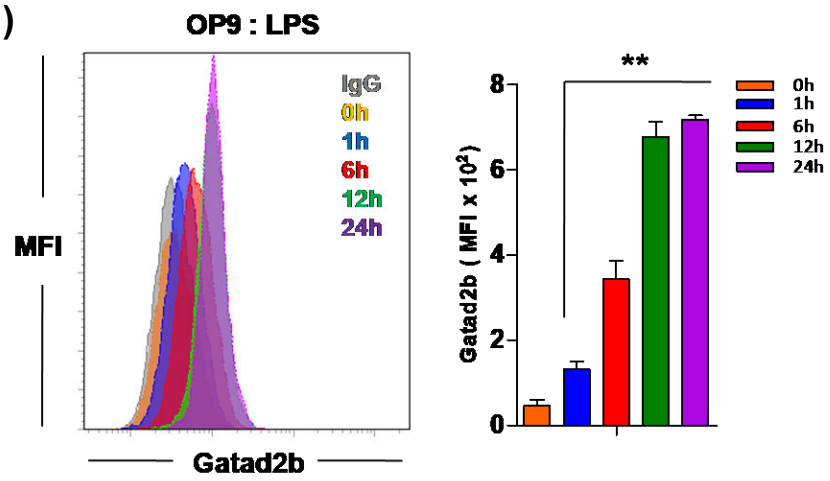
OP9 : LPS
IgG
0h
1h
6h
12h
24h
MFI
Gatad2b
Gatad2b (MFI x 10²)

(C)

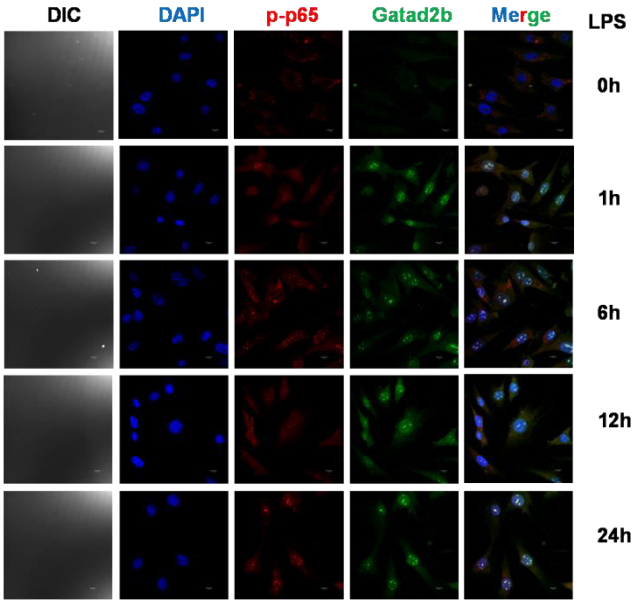
DIC
DAPI
p-p65
Gatad2b
Merge
LPS
0h
1h
6h
12h
24h

(D)

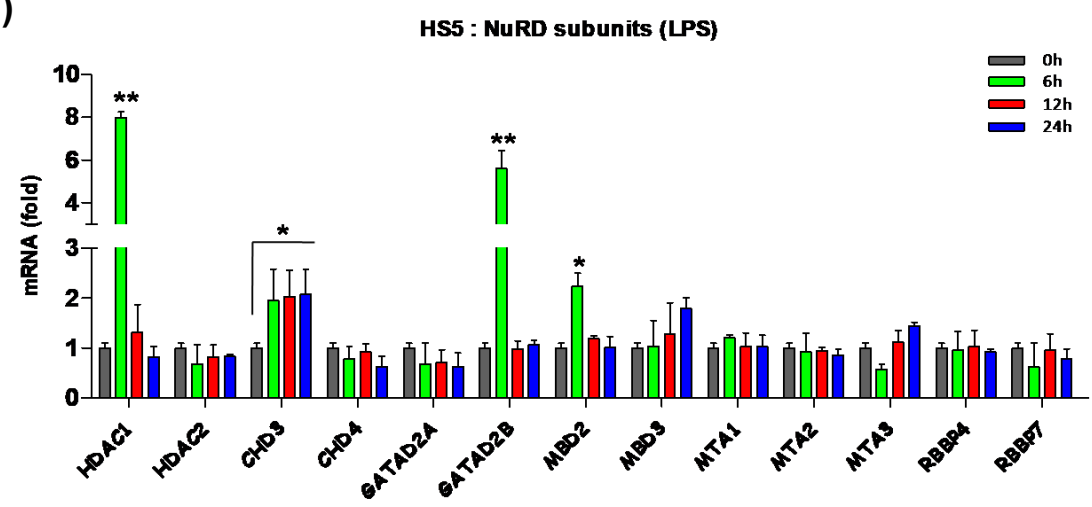
HS5 : NuRD subunits (LPS)
mRNA (fold)
0h
6h
12h
24h
HDAC1
HDAC2
CHD3
CHD4
GATAD2A
GATAD2B
MBD2
MBD3
MTA1
MTA2
MTA3
RBBP4
RBBP7

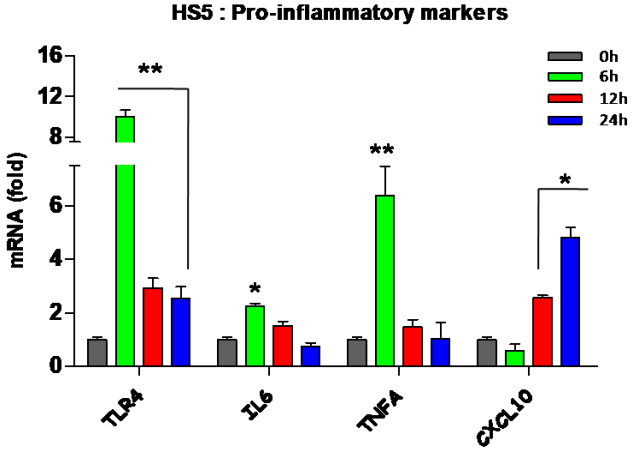
HS5 : Pro-inflammatory markers
mRNA (fold)
0h
6h
12h
24h
TLR4
IL6
TNFA
CXCL10

(E)

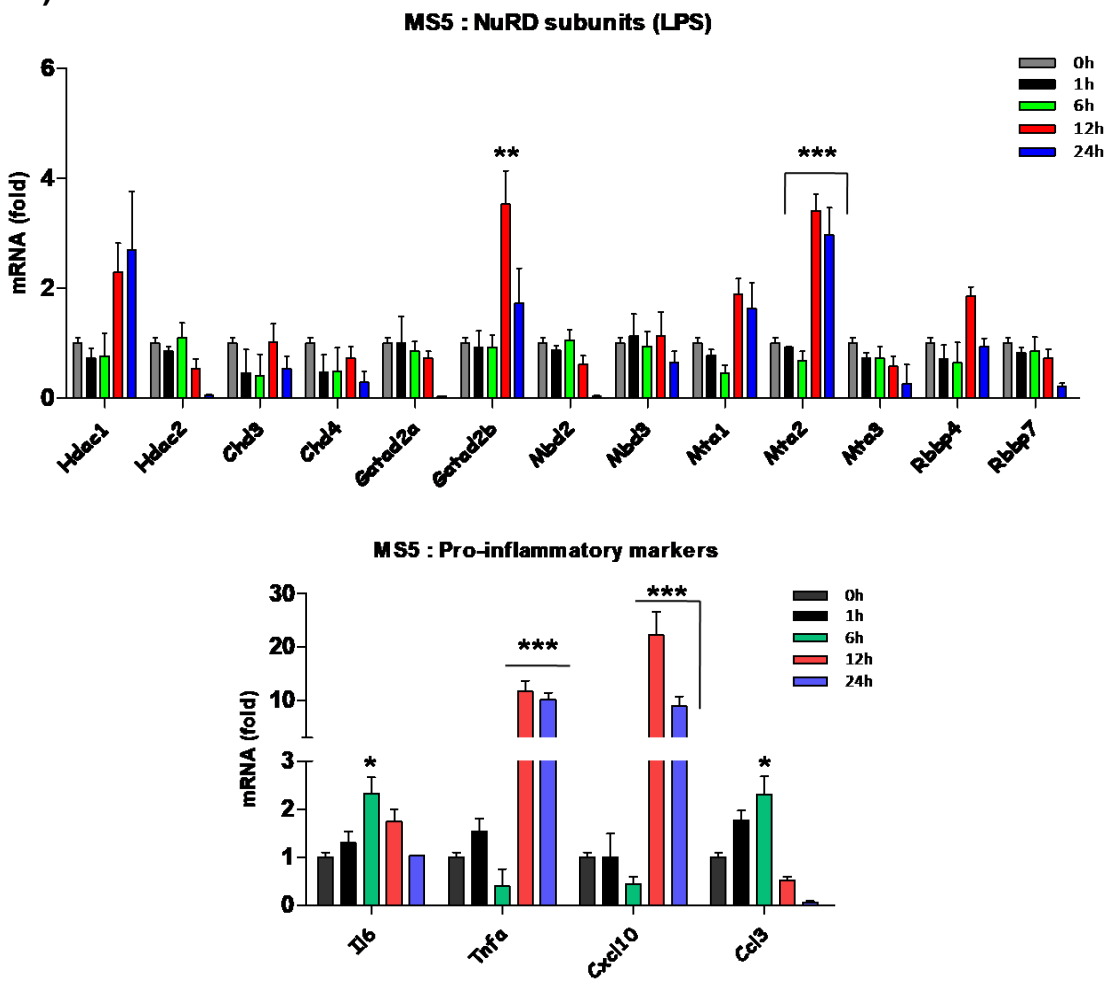
MS5 : NuRD subunits (LPS)
mRNA (fold)
0h
1h
6h
12h
24h
**
***
Hdac1
Hdac2
Chd3
Chd4
Gatad2a
Gatad2b
Mbd2
Mbd3
Mta1
Mta2
Mta3
Rbbp4
Rbbp7
MS5 : Pro-inflammatory markers
mRNA (fold)
*
***
Il6
Tnfa
Cxcl10
Ccl3

(F)

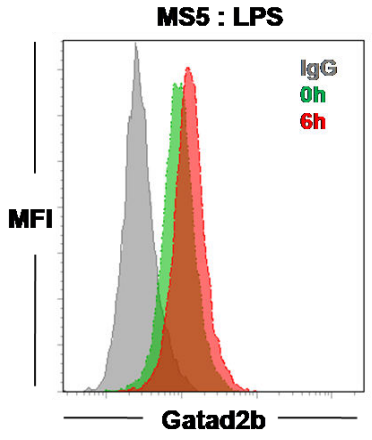
MS5 : LPS
IgG
0h
6h
MFI
Gatad2b

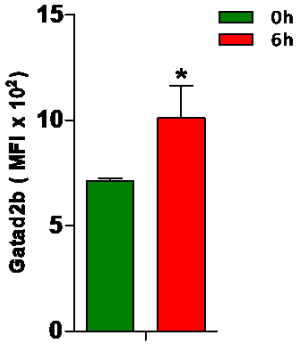
0h
6h
Gatad2b (MFI x 10²)
*

(G)

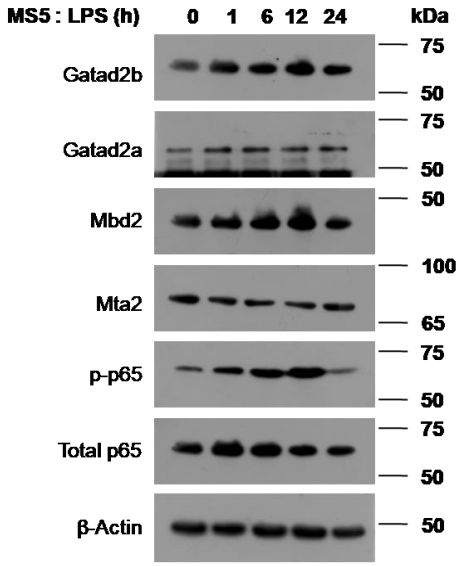
MS5 : LPS (h)
0 1 6 12 24
kDa
Gatad2b
Gatad2a
Mbd2
Mta2
p-p65
Total p65
β-Actin
75
50
100
65

(H)

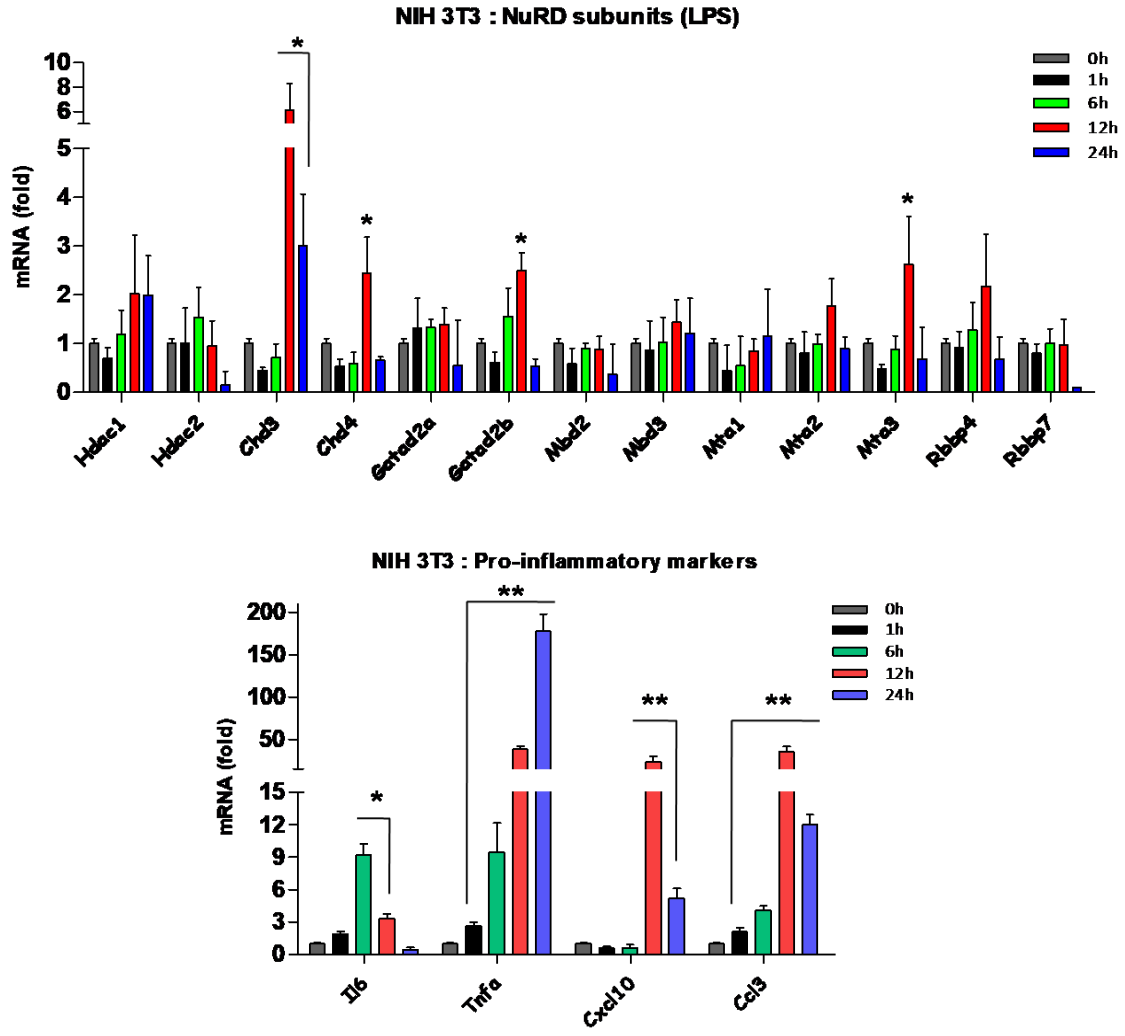

Fig. 33 : Response of different NuRD subunits upon LPS stimulation. RT-qPCR showing expression (normalized with respect to 0h as 1-fold) of NuRD components and pro-inflammatory markers upon treatment with LPS at different time points in **(A)** OP9, **(D)** HS-5, **(E)** MS-5 and **(H)** NIH-3T3 cell lines. Flow cytometry histogram analysis showing mean fluorescence intensity (MFI) of Gatad2b in LPS stimulated **(B)** OP9 cells and **(F)** MS-5 cells. **(C)** Immunofluorescence image analysis of Phospho-P65 and Gatad2b in OP9 cells treated with LPS at different time points. **(G)** Immunoblot analysis of NuRD proteins in MS-5 cells cultured in presence of LPS at different time points. RT-qPCR values were normalized to *Gapdh* (mouse) or *GAPDH* (human). Data represent three to five independent experiments including two to three biological replicates. Statistics were calculated with Student's *t*-test; error bars represent means ± s.d. if not specified otherwise. **P* < 0.05 was considered to be statistically significant.

Gatad2b induction is not restricted to TLR4-dependent pro-inflammatory signals only

So far our data demonstrate that *Gatad2b* is a LPS-responsive component of NuRD. In addition to gram-negative bacteria derived LPS there are various other PAMPs, DAMPs and pro-inflammatory cytokine responses which mimic viral infection, parasitic infections, helminthic infections, tissue injury, stress related hypoxia and tumor burden as well as malignant transformation. All of these factors are accountable for inducing immune response. So next we wanted to explore whether Gatad2b induction is TLR4 specific or it is a common inflammation-responsive epigenetic factor. For this study we treated OP9 and MS-5 cell lines with various other pro-inflammatory cytokines like (1) IFNβ which activates Type I interferon signaling pathway; (2) IFNγ which drives Type II interferon signaling pathway and (3) TNFα which acts through NFkB in addition to LPS. Gene expression analysis confirmed the induction of *Gatad2b* in both OP9 (Fig. 34A) as well as MS-5 (Fig. 34B) along with other pro-inflammatory markers while its mutually exclusive component *Gatad2a* remained unchanged.

(A)

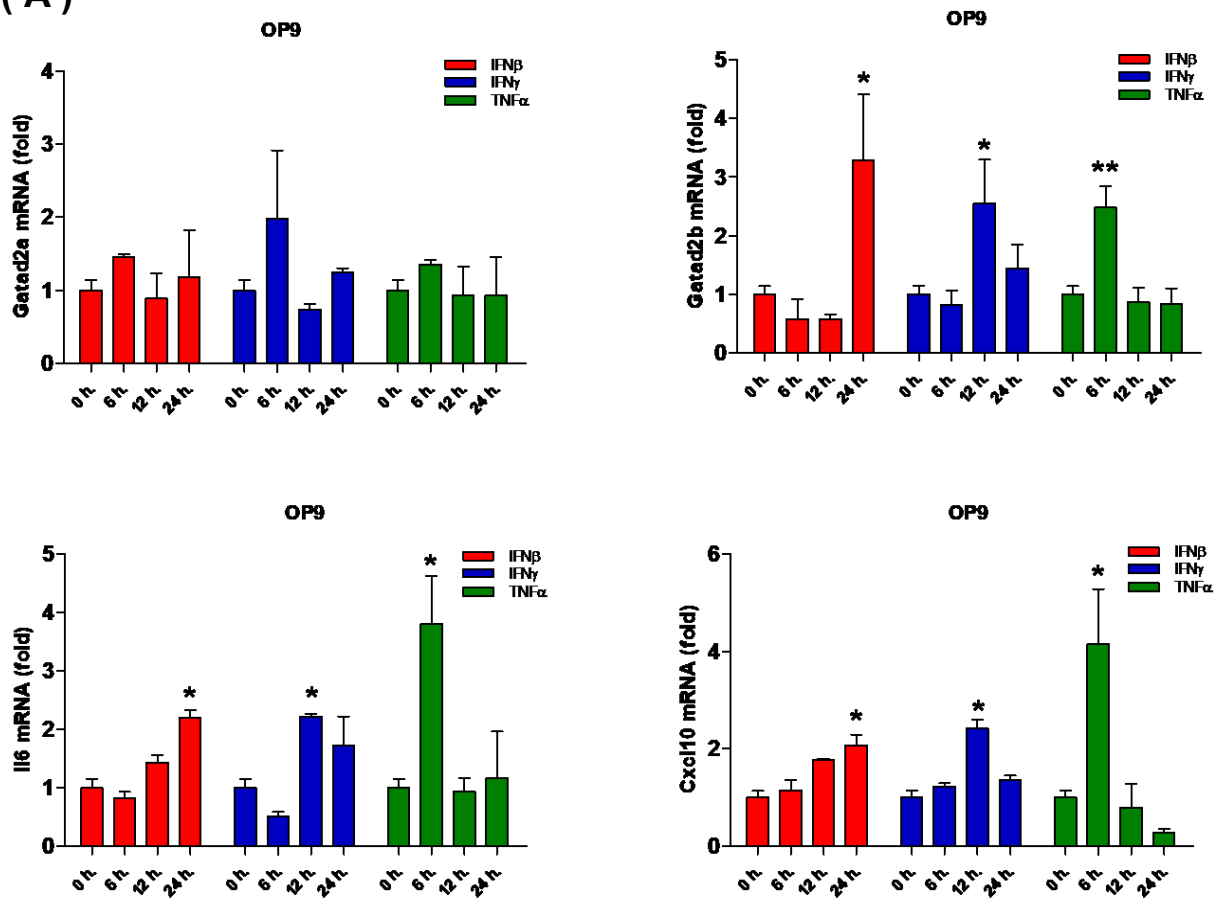

(B)

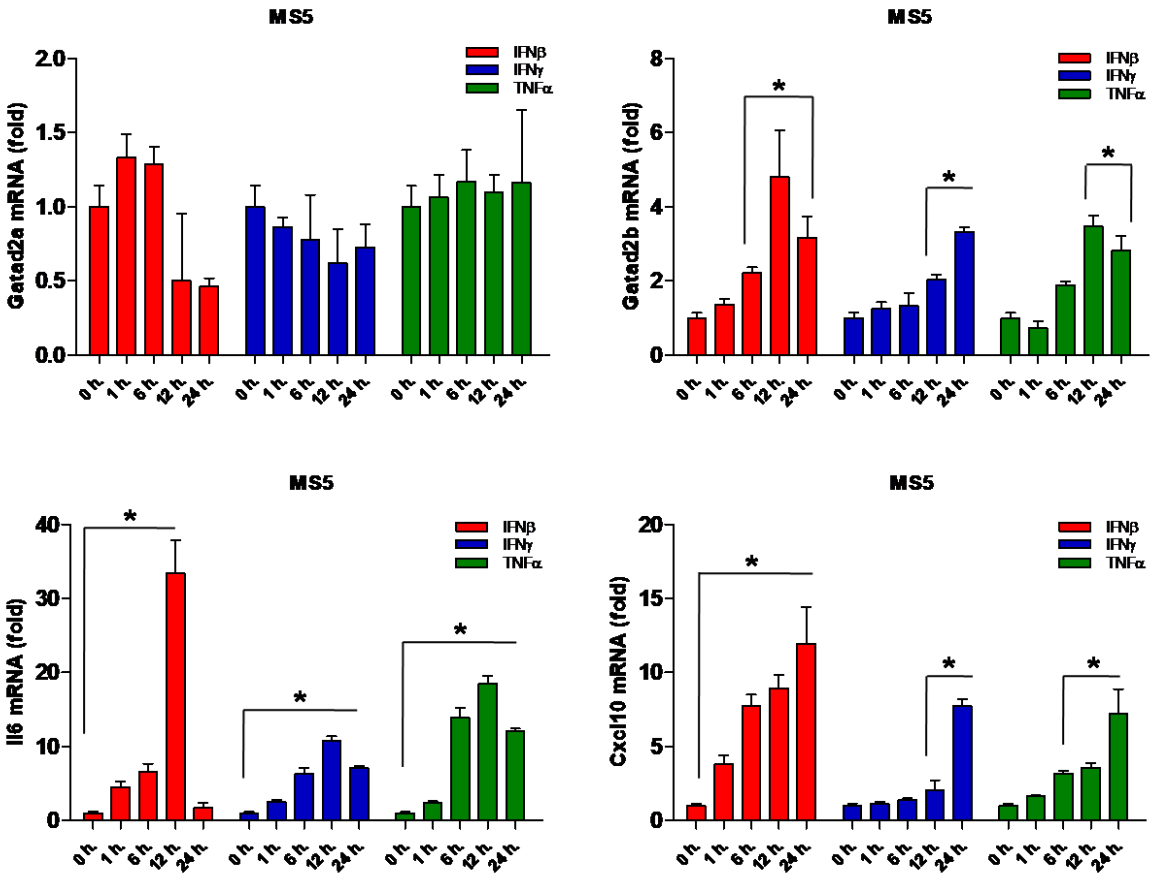

Fig. 34 : Response of NuRD subunits downstream of TLR4-independent pro-inflammatory stimuli. RT-qPCR showing expression (normalized with respect to 0h as 1-fold) of NuRD components and pro-inflammatory markers at different time points upon treatment with IFNβ, IFNγ and TNFα in **(A)** OP9 and **(B)** MS-5 cell lines. RT-qPCR values were normalized to *Gapdh* (mouse). Data represent three to five independent experiments including two to three biological replicates. Statistics were calculated with Student's *t*-test; error bars represent means ± s.d. if not specified otherwise. **P* < 0.05 was considered to be statistically significant.

Generation of *Gatad2b* deficient stable lines

To get a better insight about the role of *Gatad2b* during the immune-responsiveness of MSCs, we generated stable knockdown OP9, MS-5 and NIH-3T3 lines lacking *Gatad2b*. OP9 cells were transduced at MOI of 10 and the other twos at a MOI of 5 using lentiviral particles expressing short hairpin RNAs against Gatad2b gene (*sh-Gatad2b 1, sh-Gatad2b 2*) and a non-effective scrambled shRNA cassette (*sh-Control*) expressing GFP. 48 hours post transduction GFP expression of OP9 (Fig. 35A), MS5 (Fig. 35C) and NIH-3T3 (Fig. 35F) was checked and the transduced cells were selected by culturing in presence of 1ug/ml of puromycin for another 48 hours to make stable lines deficient of *Gatad2b*. The level of knockdown was confirmed by flowcytometry analysis and immunoblotting. *sh-Gatad2b (1)*

resulted in better knock-down compared to *sh-Gatad2b (2)* in OP9 (Fig. 35B), MS5 (Fig. 35D, 35E) and NIH-3T3 (Fig. 35G).

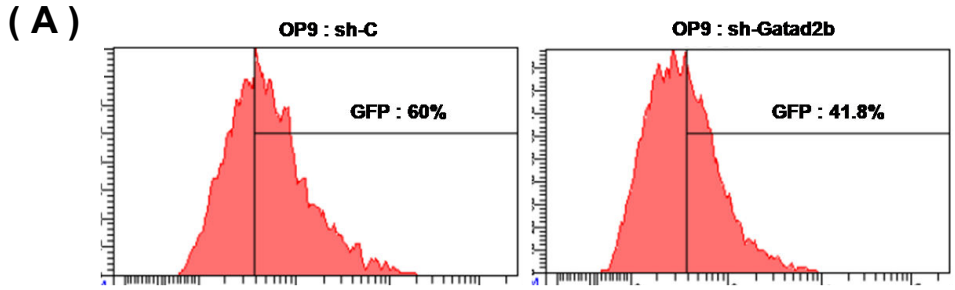

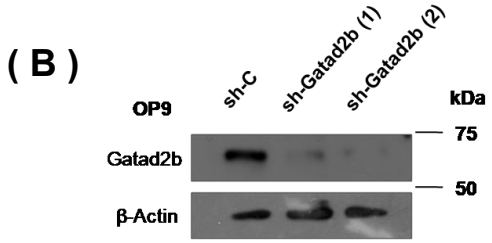

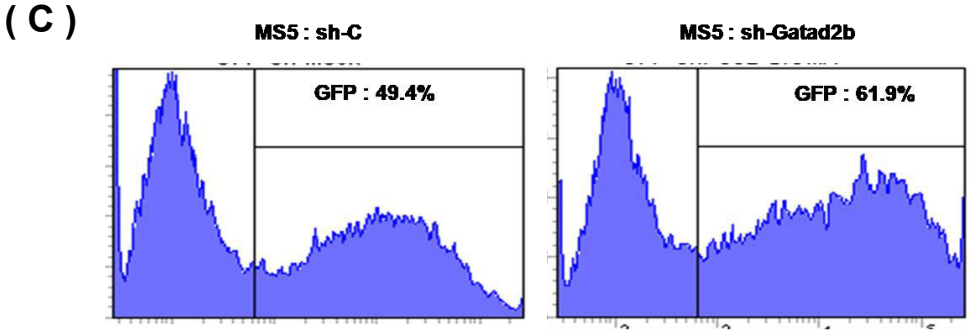

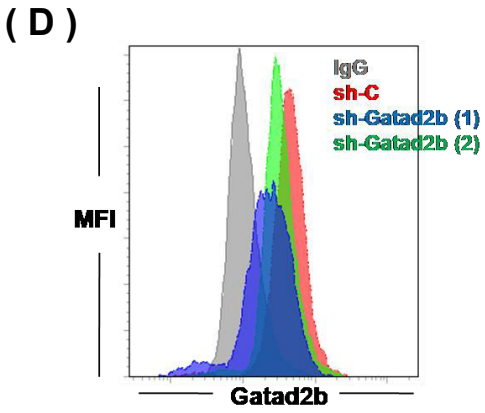

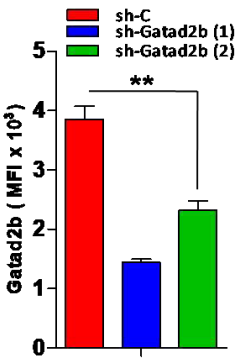

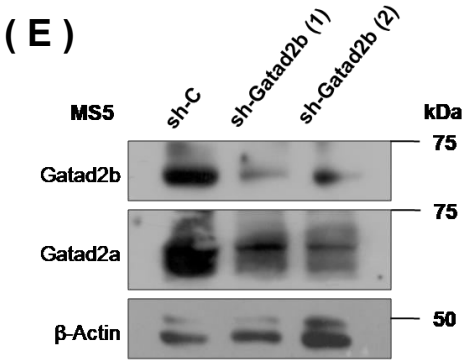

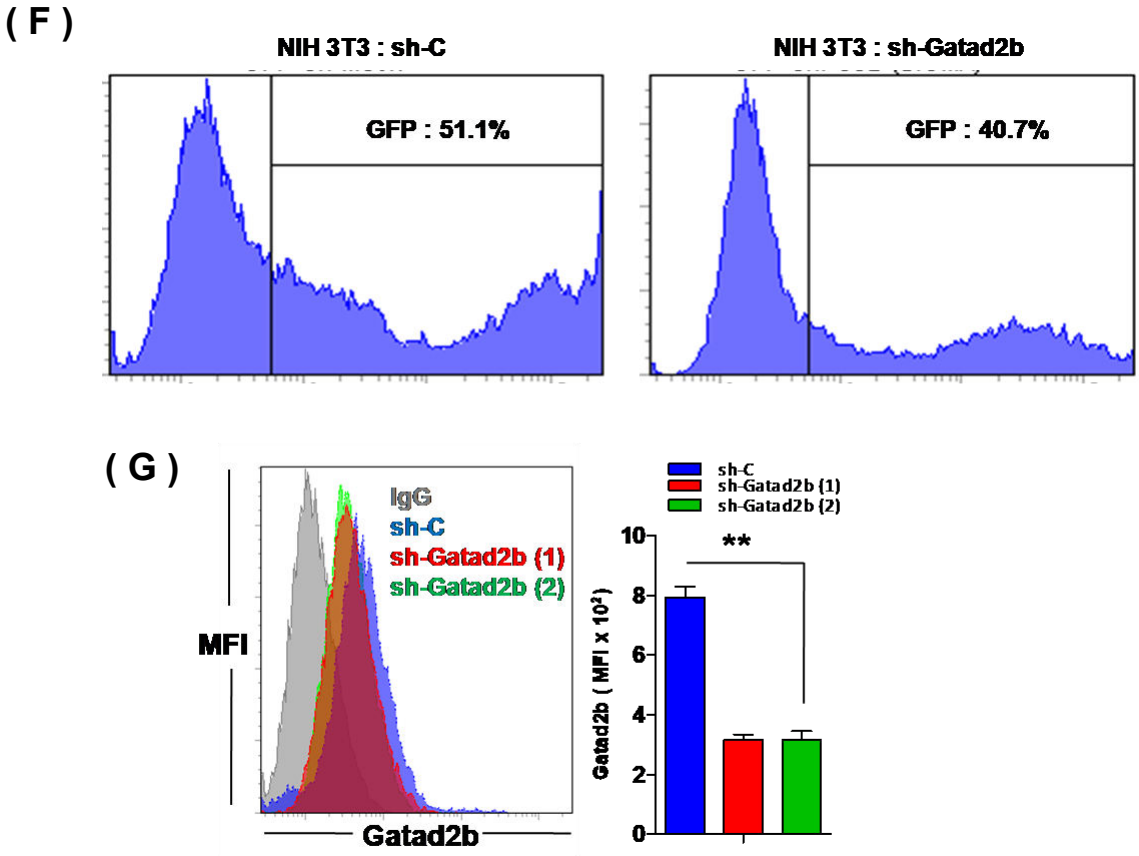

Fig. 35 : Generation of Gatad2b deficient lines. Flow cytometry histogram and immunoblot analysis showing GFP% and level of Gatad2b knockdown in **(A-B)** OP9, **(C-E)** MS5 and **(F-G)** NIH 3T3 cell line. Atleast two biological replicates were included in the study, two to three independent experiments were performed. Statistics were calculated with Student's *t*-test; error bars represent means ± s.d. if not specified otherwise. **P* < 0.05 was considered to be statistically significant.

Gatad2b is required for MSC associated immune-responsivenes

Since *Gatad2b* was induced by LPS and other pro-inflammatory stimulus, we next explored whether it plays any role in mesenchymal stromal inflammatory response. Selective shRNA-containing lentivirus mediated knockdown of *Gatad2b* in MSC lines showed an overall compromised immune responsive status during LPS treatment. Gene expression analysis showed abrogated *Tlr4* response as well as reduced response to LPS-driven induction of NF-kB target genes like *Il1b*, *Il6*, *Cxcl8*, *Cxcl10*, *Ccl3*, *Tnf-α* in a time dependent manner when cells lacking *Gatad2b* (Fig 36A, 36B, 36C). 23-plex chemokine assay using conditioned media from *sh-Control and sh-Gatad2b* MS-5 confirms the same for the secretory interlukins and chemokines during steady state as well as LPS stimulated condition suggesting a less immune-responsive or more immune-suppressive stroma (Fig. 36D). Flow cytometry analysis illustrated reduced Tlr4 protein expression in *Gatad2b* knock

down MS-5 cells during LPS treated condition while total P65 and IRAK1 remaining unaltered (Fig. 36E). Consistent with these findings when we overexpressed *Gatad2b* by lipofactamine based transient transfection method in wild type MS-5 line, differential gene expression analysis showed increased expression of *Tlr4* and NF-kB target genes like *Il1b*, *Il6*, *Cxcl10* (Fig. 36F). Altogether these findings confirmed the possibility that *Gatad2b* might be a potent regulator of NF-kB signaling avtivation in LPS-stimulated mesenchymal stromal cells.

(A)

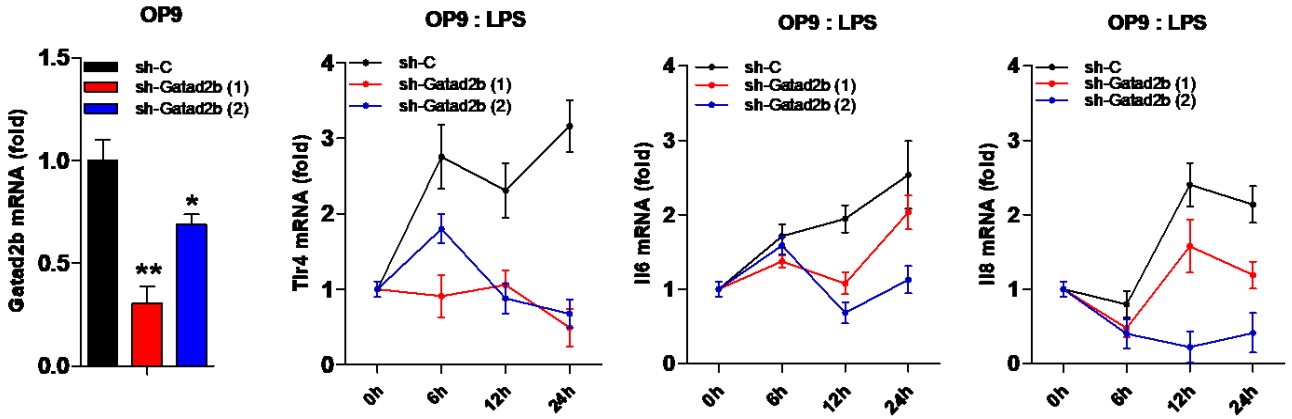

(B)

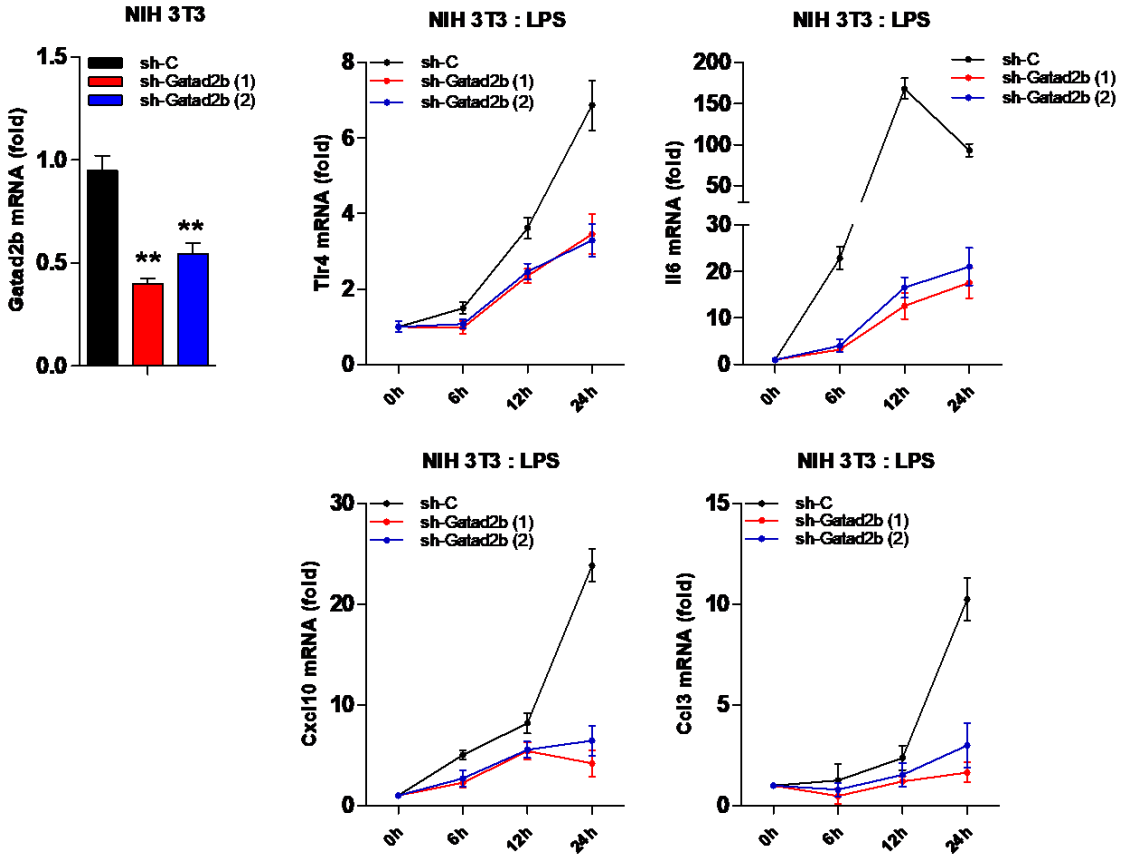

(C)

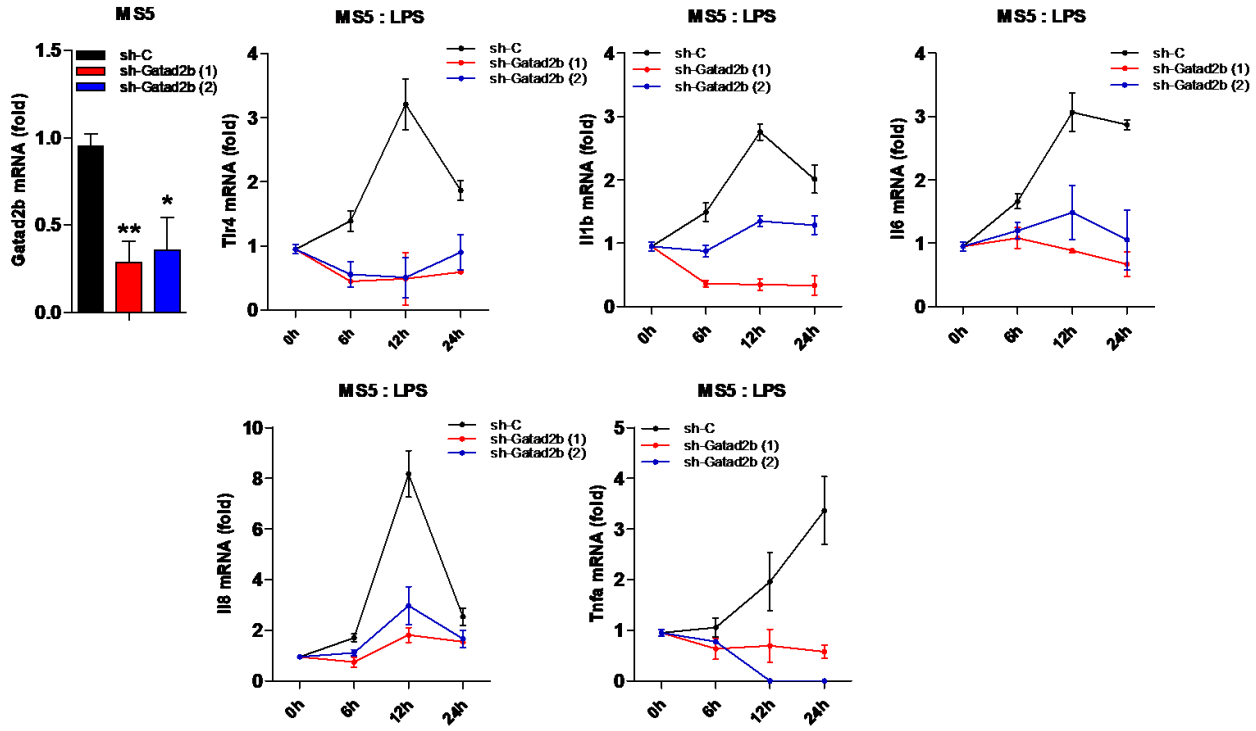
MS5
Gatad2b mRNA (fold)
sh-C
sh-Gatad2b (1)
sh-Gatad2b (2)
**
*
MS5 : LPS
Tlr4 mRNA (fold)
Il1b mRNA (fold)
Il6 mRNA (fold)
Il8 mRNA (fold)
Tnfa mRNA (fold)
0h
6h
12h
24h

(D)

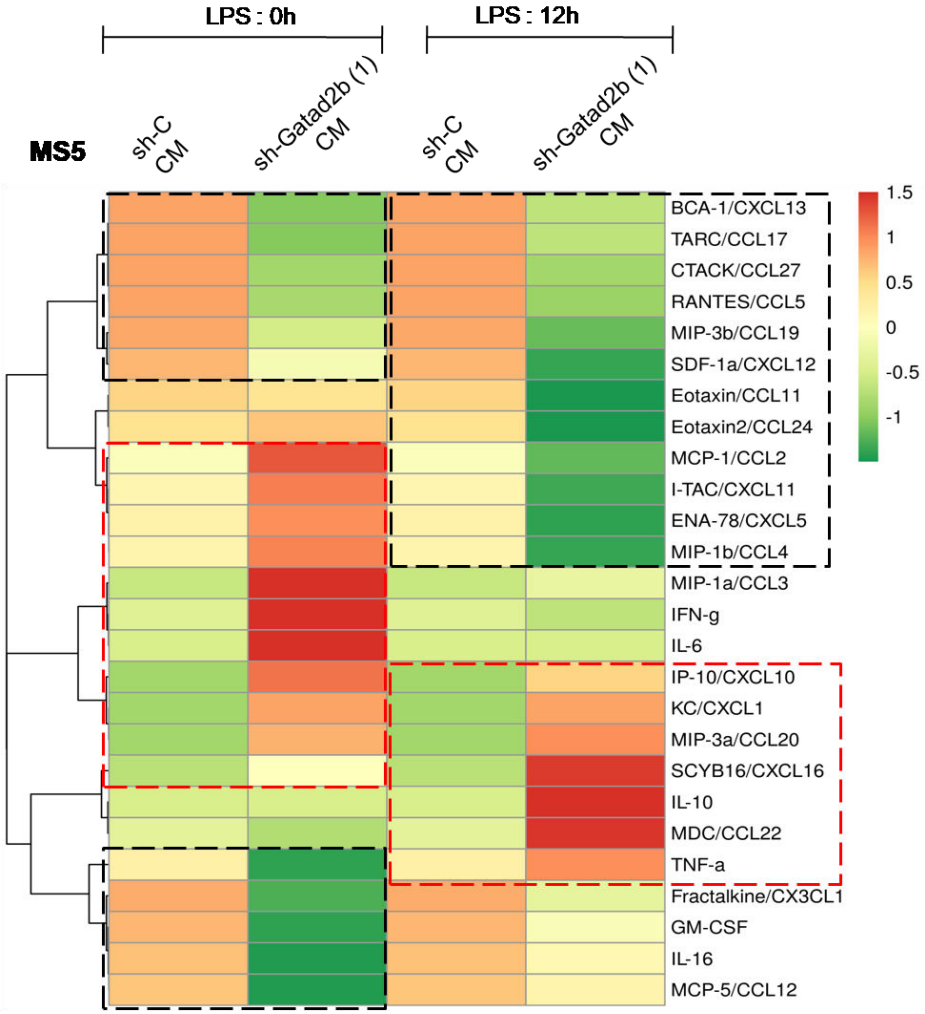
LPS : 0h
LPS : 12h
MS5
sh-C CM
sh-Gatad2b (1) CM
BCA-1/CXCL13
TARC/CCL17
CTACK/CCL27
RANTES/CCL5
MIP-3b/CCL19
SDF-1a/CXCL12
Eotaxin/CCL11
Eotaxin2/CCL24
MCP-1/CCL2
I-TAC/CXCL11
ENA-78/CXCL5
MIP-1b/CCL4
MIP-1a/CCL3
IFN-g
IL-6
IP-10/CXCL10
KC/CXCL1
MIP-3a/CCL20
SCYB16/CXCL16
IL-10
MDC/CCL22
TNF-a
Fractalkine/CX3CL1
GM-CSF
IL-16
MCP-5/CCL12
1.5
1
0.5
0
-0.5
-1

(E)

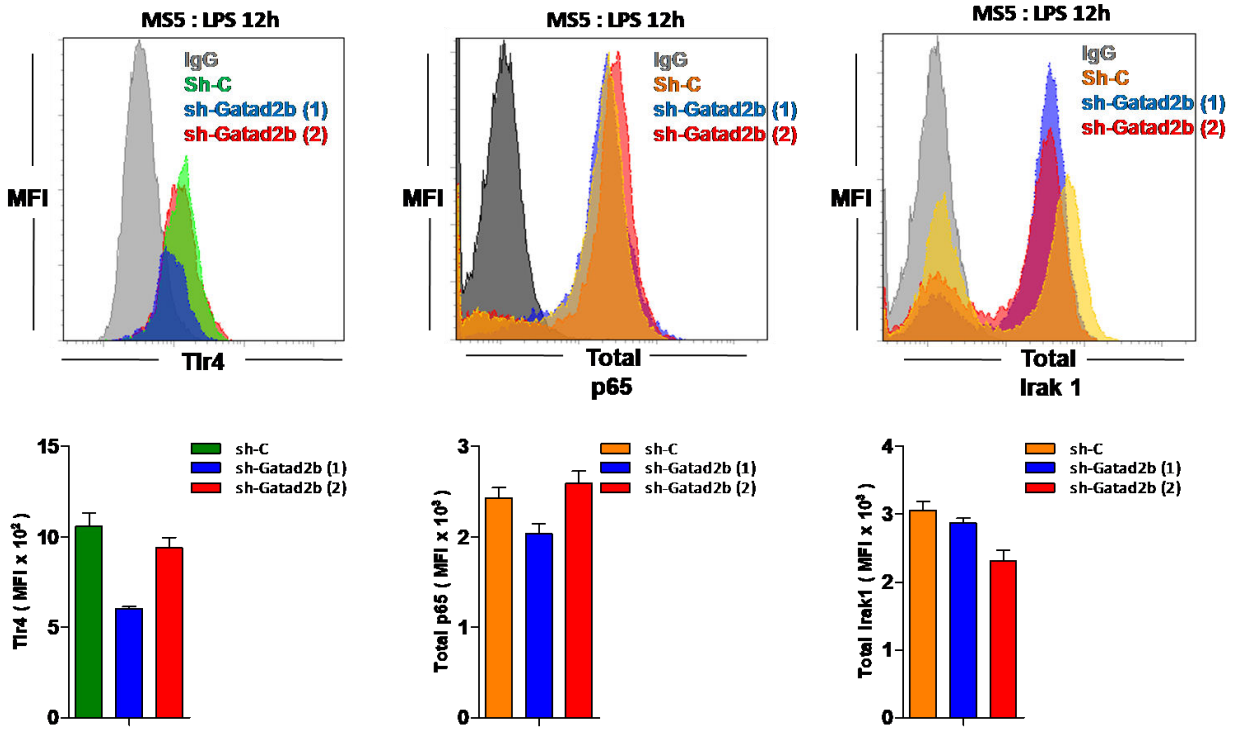
MS5 : LPS 12h
IgG
Sh-C
sh-Gatad2b (1)
sh-Gatad2b (2)
MFI
Tlr4
Total p65
Total Irak 1
Tlr4 (MFI x 10³)
Total p65 (MFI x 10³)
Total Irak1 (MFI x 10³)

(F)

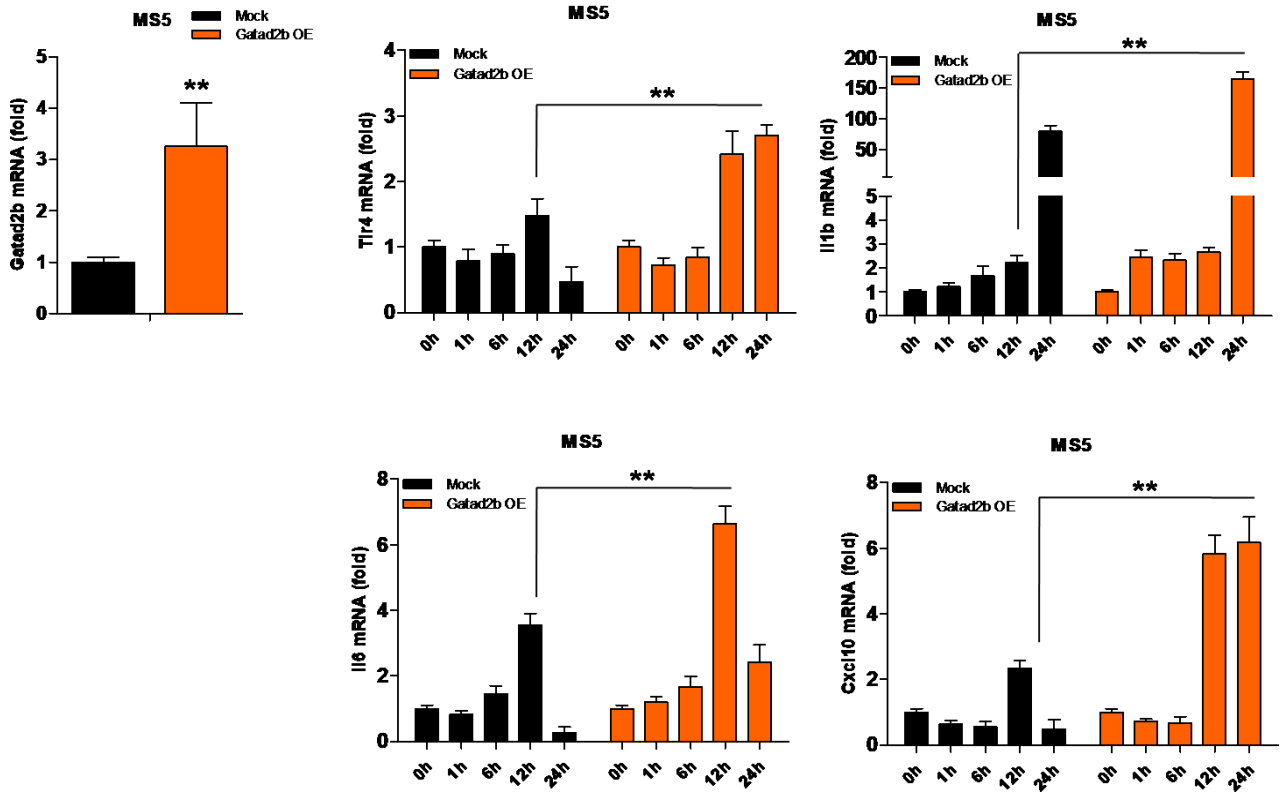
MS5
Mock
Gatad2b OE
Gatad2b mRNA (fold)
Tlr4 mRNA (fold)
Il1b mRNA (fold)
Il6 mRNA (fold)
Cxcl10 mRNA (fold)
**
0h
1h
6h
12h
24h

Fig. 36 : Gatad2b deficient MSCs are less immune responsive. RT-qPCR showing expression (normalized with respect to 0h as 1-fold) of *Tlr4* along with other pro-inflammatory markers in control or *Gatad2b*-deficient **(A)** OP9, **(B)** NIH 3T3 and **(C)** MS5 cells treated with LPS at different time points. **(D)** 23-plex chemokine assay followed by heatmap analysis showing differentially expressed cytokine/chemokine level in control and Gatad2b-deficient MS5 cells in resting as well as LPS induced condition. **(E)** Flow cytometry histogram analysis showing mean fluorescence intensity (MFI) of Tlr4 (left), Total p65 (middle) and Total Irak1 (right) in control or *Gatad2b*-deficient MS5 cells treated with LPS. **(F)** RT-qPCR illustrating the expression (normalized with respect to 0h as 1-fold) of *Tlr4* as well as other pro-inflammatory markers like *Il1b*, *Il6*, *Cxcl10* in control and *Gatad2b*-overexpressed MS5 cells. RT-qPCR values were normalized to *Gapdh* (mouse). Data represent three independent experiments including two to three biological replicates. Statistics were calculated with Student's *t*-test; error bars represent means ± s.d. if not specified otherwise. **P* < 0.05 was considered to be statistically significant.

Gatad2b deficiency alters the transcriptomic landscape of inflammatory pathway genes in MSCs

It was important to understand the effect of *Gatad2b* deficiency on a global level within the cells. Therefore when we compared between *shControl* and *shGatad2b* OP9 lines, differential gene expression analysis of the RNA sequencing data revealed a significant downregulated profile for the pro-inflammatory genes, their associated receptors and transcription factors positively regulating the pro-inflammatory pathways (Fig. 37A). GO and pathway analysis showed various inflammation promoting pathways to be compromised when cells have inadequate level of *Gatad2b* (Fig. 37B, 37C). Then we analysed the same in *shControl* and *shGatad2b* MS5 cells in both untreated and LPS treated condition. Here also an overall downregulated profile was observed for all the inflammation associated genes (Fig. 37D).

(A)

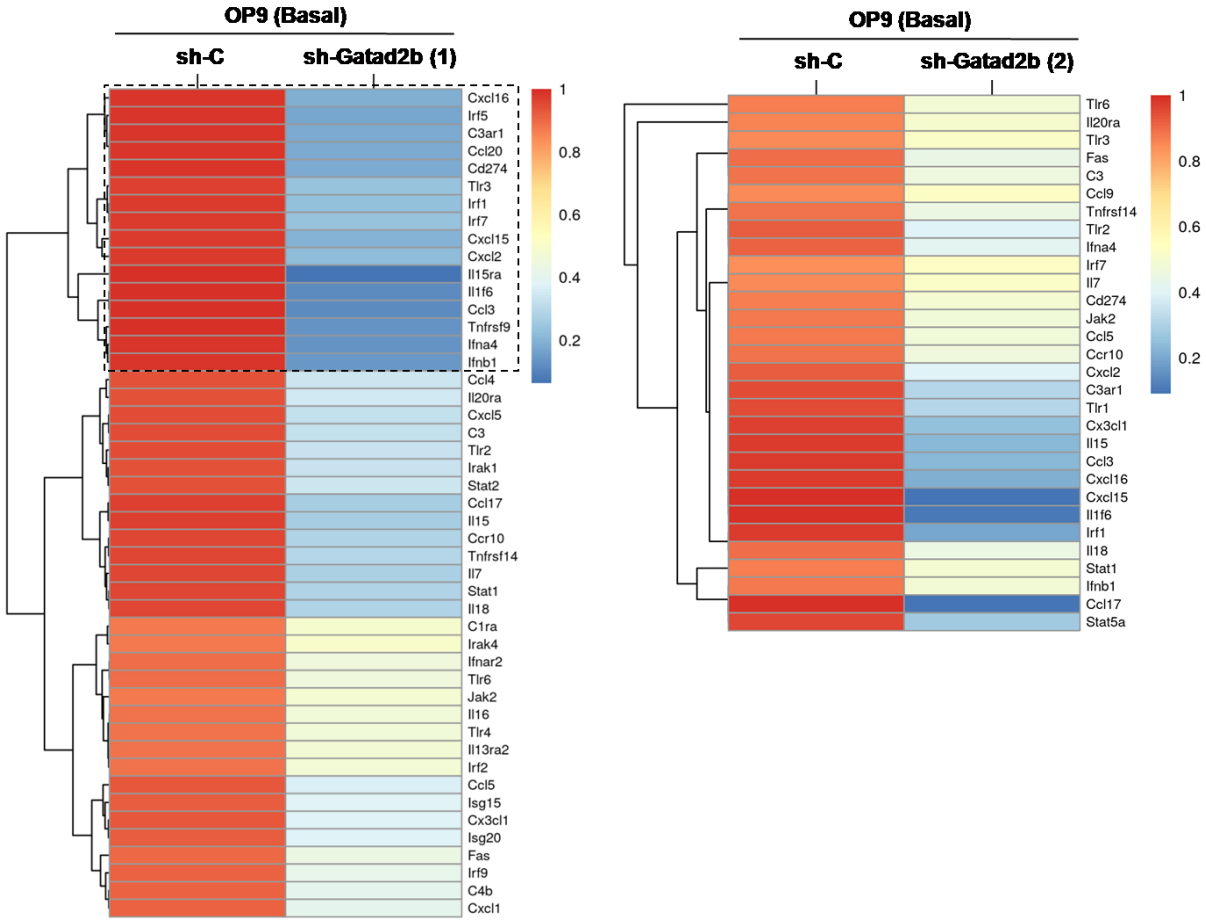
OP9 (Basal)
sh-C
sh-Gatad2b (1)
Cxcl16
Irf5
C3ar1
Ccl20
Cd274
Tlr3
Irf1
Irf7
Cxcl15
Cxcl2
Il15ra
Il1f6
Ccl3
Tnfrsf9
Ifna4
Ifnb1
Ccl4
Il20ra
Cxcl5
C3
Tlr2
Irak1
Stat2
Ccl17
Il15
Ccr10
Tnfrsf14
Il7
Stat1
Il18
C1ra
Irak4
Ifnar2
Tlr6
Jak2
Il16
Tlr4
Il13ra2
Irf2
Ccl5
Isg15
Cx3cl1
Isg20
Fas
Irf9
C4b
Cxcl1
1
0.8
0.6
0.4
0.2
OP9 (Basal)
sh-C
sh-Gatad2b (2)
Tlr6
Il20ra
Tlr3
Fas
C3
Ccl9
Tnfrsf14
Tlr2
Ifna4
Irf7
Il7
Cd274
Jak2
Ccl5
Ccr10
Cxcl2
C3ar1
Tlr1
Cx3cl1
Il15
Ccl3
Cxcl16
Cxcl15
Il1f6
Irf1
Il18
Stat1
Ifnb1
Ccl17
Stat5a
1
0.8
0.6
0.4
0.2

(B)

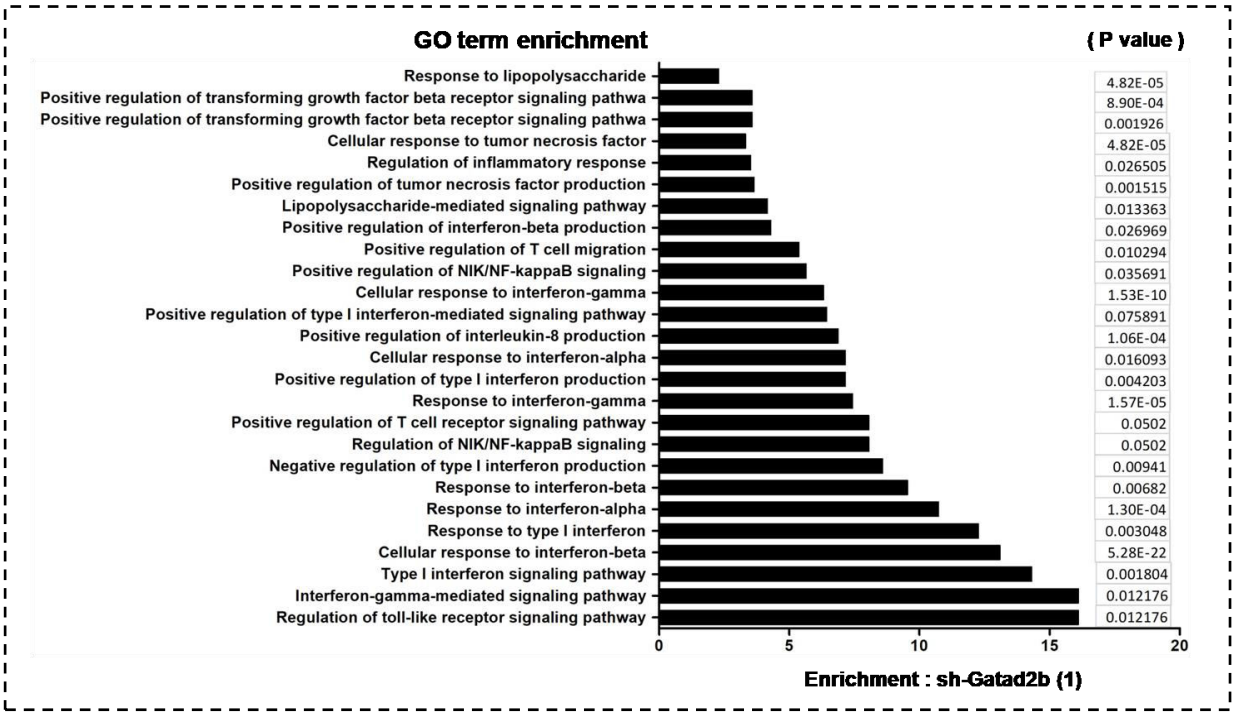
GO term enrichment
(P value)
Response to lipopolysaccharide 4.82E-05
Positive regulation of transforming growth factor beta receptor signaling pathwa 8.90E-04
Positive regulation of transforming growth factor beta receptor signaling pathwa 0.001926
Cellular response to tumor necrosis factor 4.82E-05
Regulation of inflammatory response 0.026505
Positive regulation of tumor necrosis factor production 0.001515
Lipopolysaccharide-mediated signaling pathway 0.013363
Positive regulation of interferon-beta production 0.026969
Positive regulation of T cell migration 0.010294
Positive regulation of NIK/NF-kappaB signaling 0.035691
Cellular response to interferon-gamma 1.53E-10
Positive regulation of type I interferon-mediated signaling pathway 0.075891
Positive regulation of interleukin-8 production 1.06E-04
Cellular response to interferon-alpha 0.016093
Positive regulation of type I interferon production 0.004203
Response to interferon-gamma 1.57E-05
Positive regulation of T cell receptor signaling pathway 0.0502
Regulation of NIK/NF-kappaB signaling 0.0502
Negative regulation of type I interferon production 0.00941
Response to interferon-beta 0.00682
Response to interferon-alpha 1.30E-04
Response to type I interferon 0.003048
Cellular response to interferon-beta 5.28E-22
Type I interferon signaling pathway 0.001804
Interferon-gamma-mediated signaling pathway 0.012176
Regulation of toll-like receptor signaling pathway 0.012176
0
5
10
15
20
Enrichment : sh-Gatad2b (1)

(C)

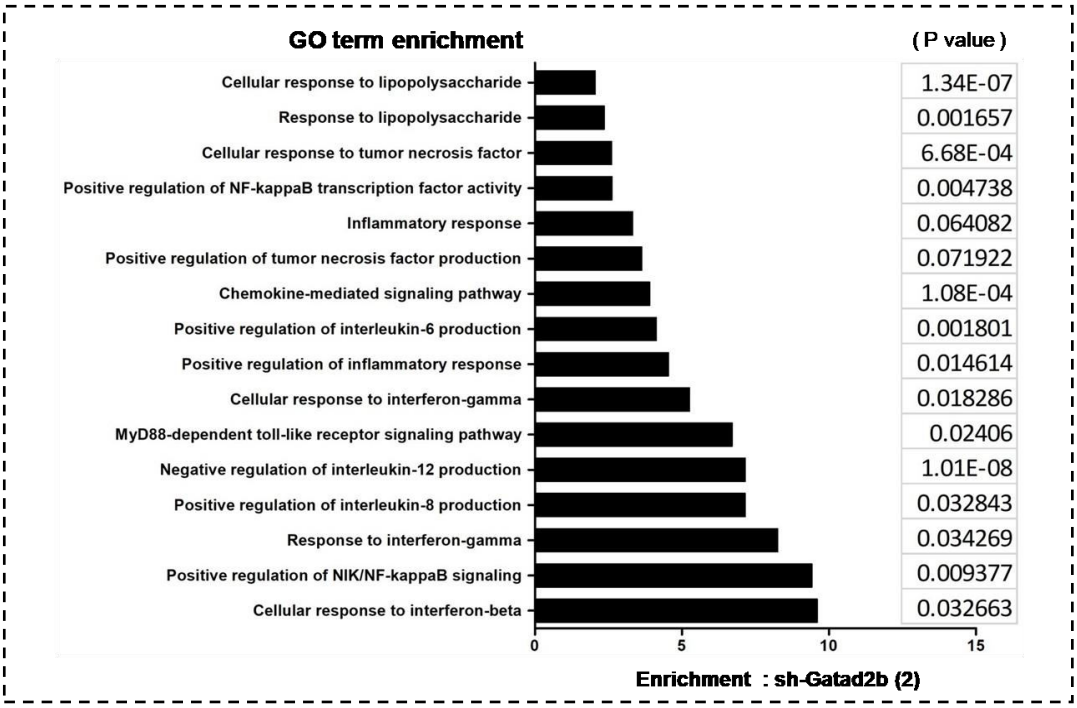

(D)

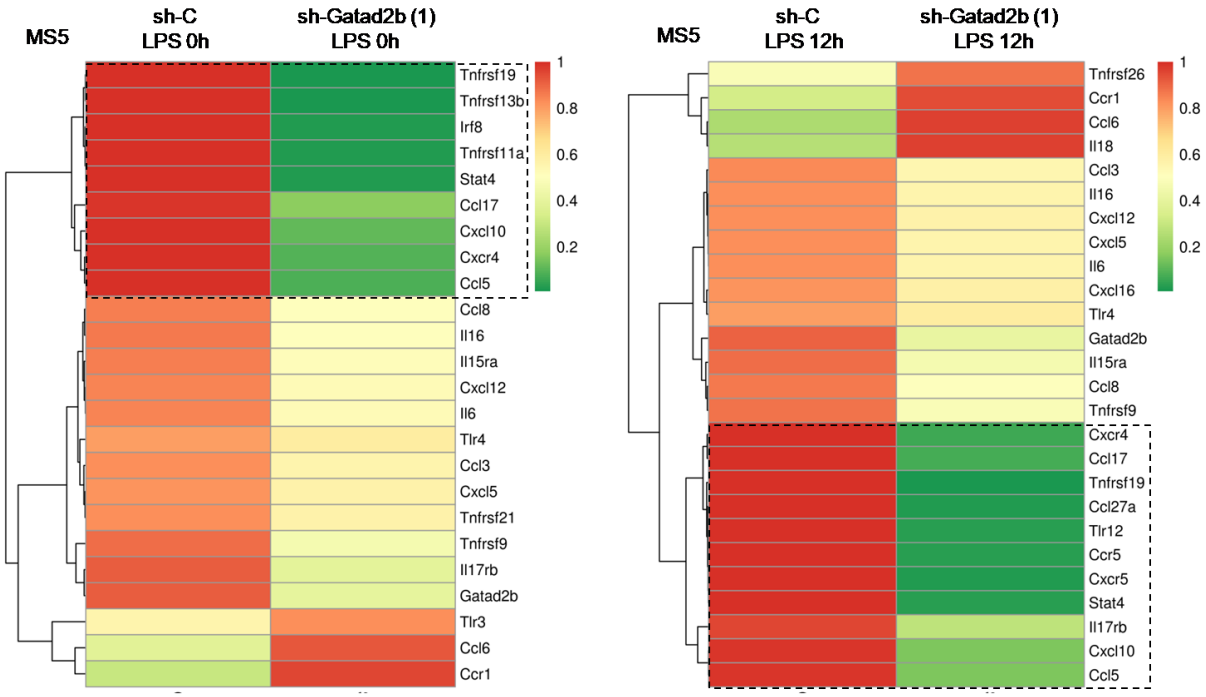

Fig. 37 : Loss of Gatad2b and its effect on transcriptome level. (A) RNA seq heatmap analysis (average of two replicates) showing differential expression of immunological pathway related genes in *Gatad2b* knockdown OP9 cells (Basal). **(B-C)** GO term enrichment analysis of the immune-related genes in *Gatad2b* deficient OP9 cells. **(D)** RNA seq followed by heatmap analysis (average of two replicates) of the inflammatory pathway genes in control and *Gatad2b* deficient MS5 cells during resting as well as LPS stimulated condition. *$P < 0.05$ was considered to be statistically significant.

Gatad2b and NFkB share a positive feed forward loop to regulate the expression of each other

In absence of *Gatad2b* the NFkb signaling pathway was getting impaired by the downregulation of Tlr4 leading to insufficient formation of phospho NFkB. But it was till now unknown what induces *Gatad2b* during LPS stimulation. When we pharmacologically inhibited the NFkB signaling pathway by using BAY11-7082 and stimulated wild type MS5 in presence of this NFkB pathway inhibitor we found *Gatad2b* to be downregulated along with the pro-inflammatory NFkB responsive genes (Fig. 38A). Gatad2b induction was also hampered in protein level during LPS stimulation when compared between DMSO- and BAY11-treated cells (Fig. 38B). Since the pharmacological inhibition often leads to non-specific targeting, next we knocked down *p65 (RelA)* which is a catalytic subunit of fully functional NFkB complex and differential gene expression data showed reduced level of *Gatad2b* which in turn resulted in *Tlr4* downregulation and eventually insufficient expression of the pro-inflammatory genes (Fig. 38C)

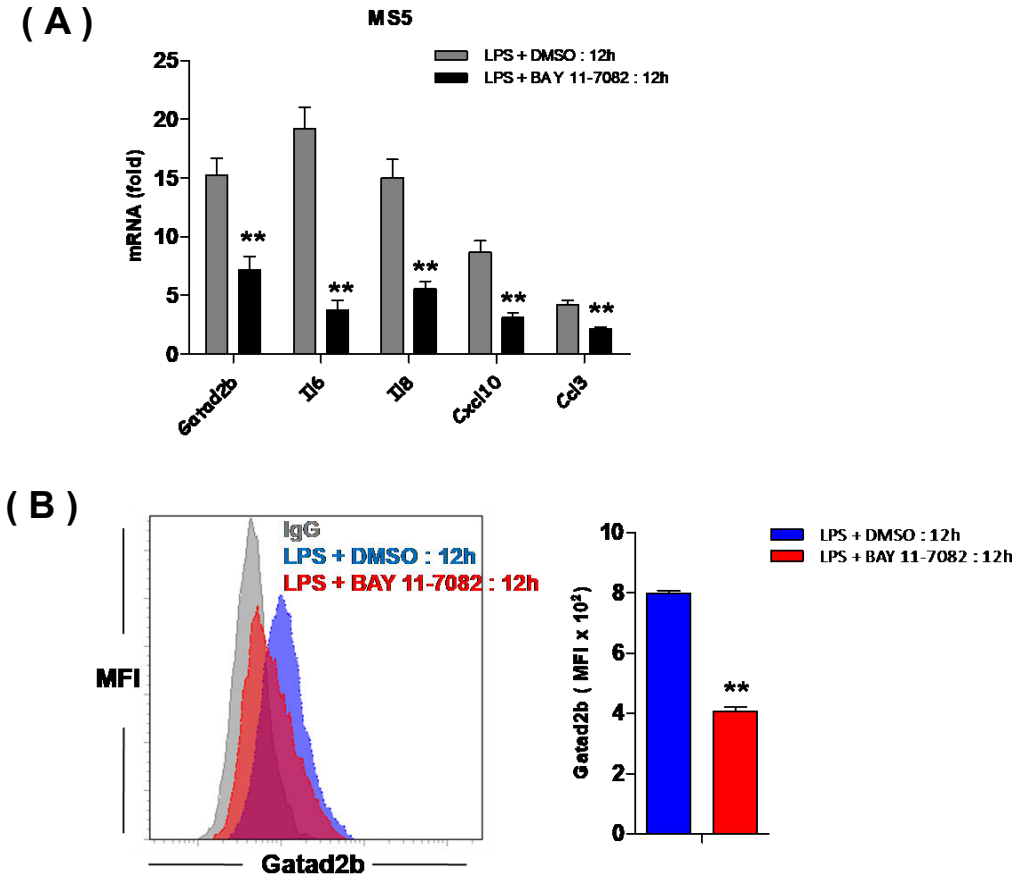

(C)

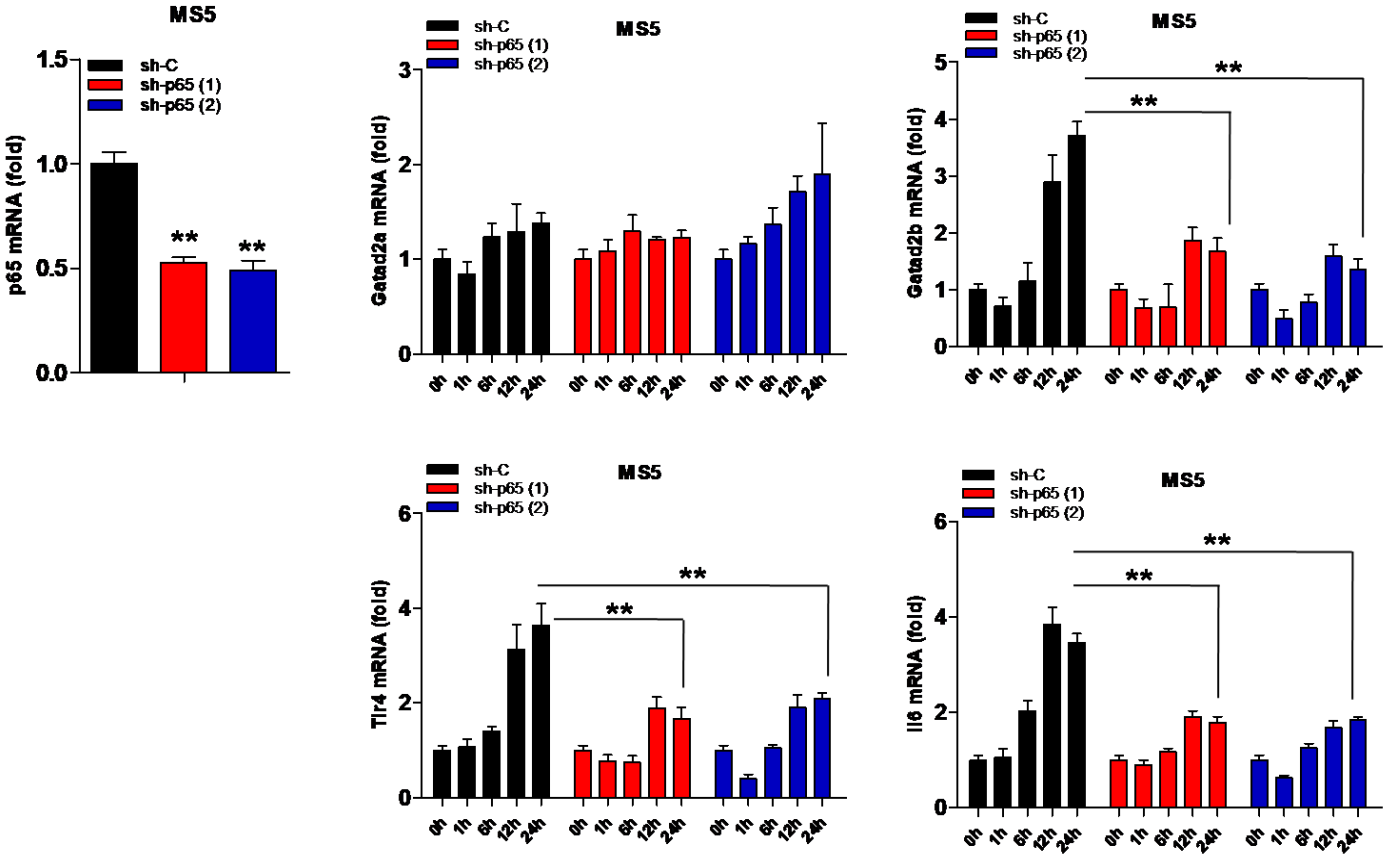

Fig 38 : Induction of Gatad2b is NFkB dependent. (A) RT-qPCR expression (normalized with respect to 0h as 1-fold) of *Gatad2b* along with pro-inflammatory markers *Il6, Il8, Cxcl10, Ccl3* and **(B)** Flow cytometry histogram analysis showing MFI of Gatad2b in MS5 cells cultured in presence of LPS and/or BAY11-7082 for 12h. (**C)** RT-qPCR expression *(left)* in MS5 cells expressing *sh-P65(1)* and *sh-p65(2)*. RT-qPCR expression analysis of *Gatad2b (upper right)*, *Tlr4 (lower middle)* and *Il6* (lower right) in control or *p65*-deficient MS5 cells treated with LPS at different time points. mean ± s.d. are specified by the error bars. Data represent three independent experiments including two to three biological replicates. Statistics were calculated with Student's *t*-test; error bars represent means ± s.d. if not specified otherwise. **P* < 0.05 was considered to be statistically significant.

NuRD subunits that bind directly to Gatad2b and their role during MSC-mediated inflammatory response

Being a part of NuRD complex Gatad2b acts as transcriptional repressor. Mbd2 and Mbd3 are the two subunits of NuRD which directly bind to Gatad2b and facilitate the repression activity by depositing onto certain gene promoters. But here in our study *Gatad2b* was playing a positive regulatory role during the inflammatory response. So it became obvious that we also study if there is any role of its binding partners namely *Mbd2* and *Mbd3* during the activation of inflammatory pathways. Using MS-5 cell line we knocked down Mbd2 and stimulated the cells with LPS. But there was no significant and consistent change in *Tlr4* as well as NFkB downstream genes in terms of their expression in a time-dependent manner (Fig. 39A). To knock down *Mbd3* we used two different sh-RNA constructs among which one did not show any change during LPS treatment while the other resulted in an upregulation of the *Tlr4* and the downstream inflammatory response genes (Fig. 39B) consistent with its repressive nature. These data indicated that the role of Gatad2b in the context of regulating inflammation in MSCs might be Mbd- as well as NuRD-independent.

(A)

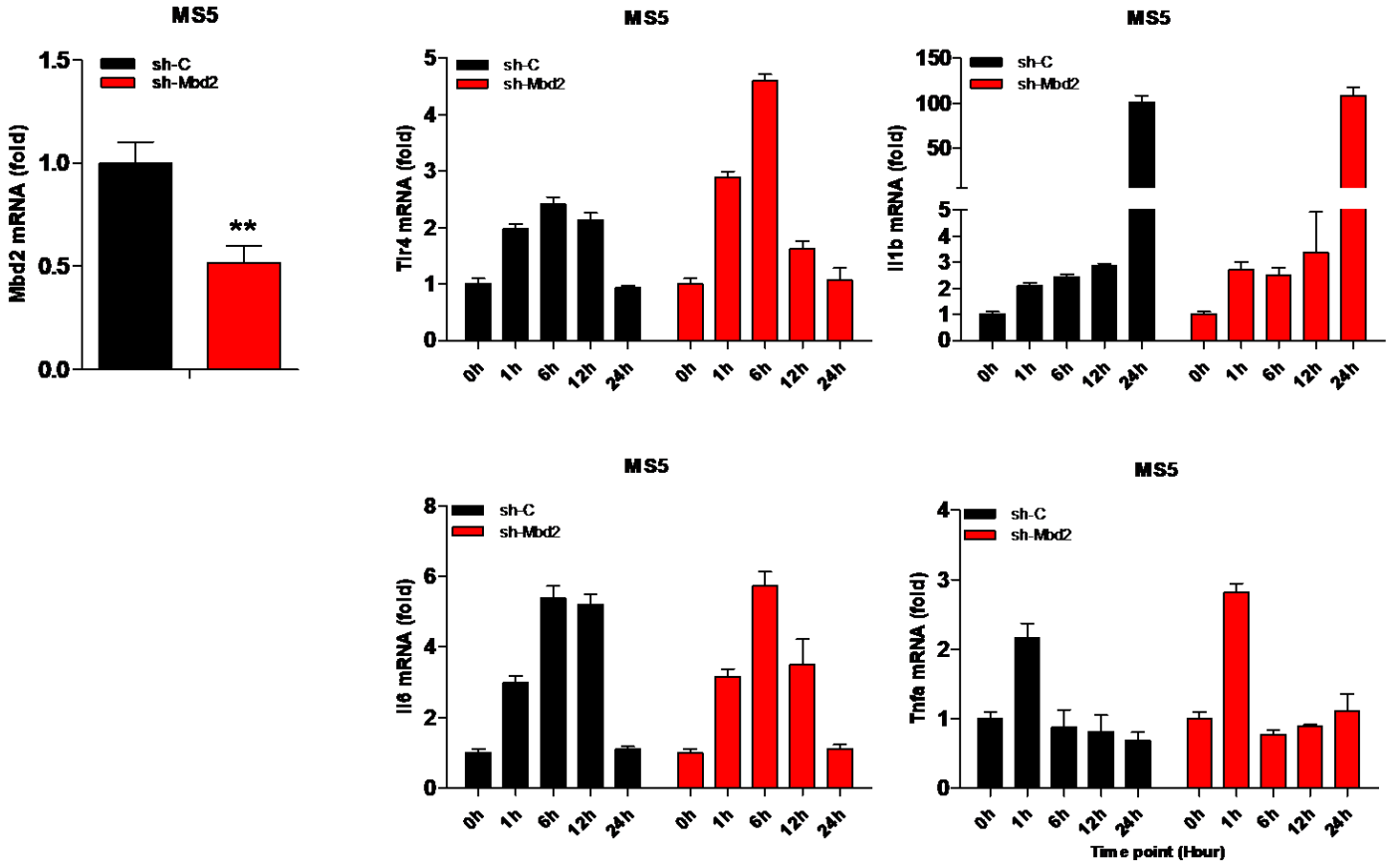

(B)

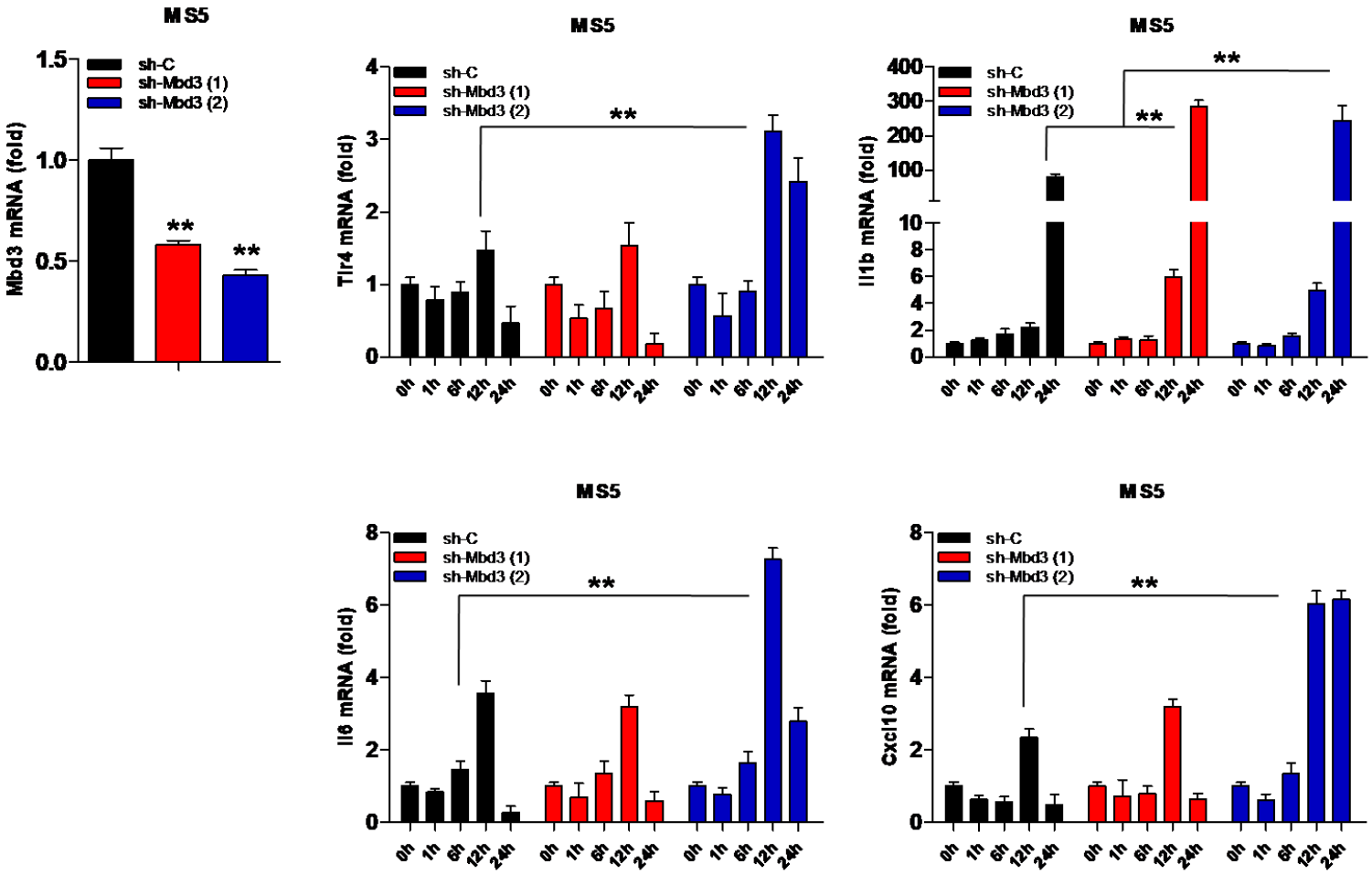

Fig 39 : Mbd2 and Mbd3, Gatad2b interacting subunits of NuRD complex and MSC driven inflammatory response. (**A)** RT-qPCR expression *(left)* in MS5 cells expressing *sh-Mbd2*. RT-qPCR expression analysis of *Tlr4*, *Il1b (upper middle and right)* and *Il6, Tnfa (lower middle and right)* in control or *Mbd2*-deficient MS5 cells treated with LPS at different time points. **(B)** RT-qPCR expression *(left)* in MS5 cells expressing *sh-Mbd3(1)* and *sh-Mbd3 (2)*. RT-qPCR expression analysis of *Tlr4*, *Il1b (upper middle and right)* and *Il6, Tnfa (lower middle and right)* in control or *Mbd3*-deficient MS5 cells treated with LPS at different time points. mean ± s.d. are specified by the error bars. Data represent three independent experiments including two to three biological replicates. Statistics were calculated with Student's *t*-test; error bars represent means ± s.d. if not specified otherwise. **P* < 0.05 was considered to be statistically significant.

Stroma intrinsic Gatad2b and its paracrine role in regulating the immune cells

Previously it was shown upon a 23-plex chemokine assay that absence of Gatad2b resulted the MSC secretome to be less immune responsive by the downregulation of all the major pro-inflammatory cytokines or more immune-suppressive. The secretome of MSCs do play an important role in regulating the activity of various immune cells by its paracrine effect. Therefore we wanted to see if Gatad2b deficiency is really causing the MSC secretome to be altered in terms of its immune potential. To assess whether this immune-plasticity reflects functionally in terms of regulating immune cells we performed an *in vitro* co-culture assay using RAW 264.7 murine macrophage cell line and MSC-derived cell free conditioned medium (MSC-CM) in presence or absence of exogenous M1/M2 stimuli and it was found that MSC-CM derived from *Gatad2b* deficient stroma polarised macrophages more towards M2 (Anti-inflamatory) and less towards M1 (Pro-inflammatory) compared to the MSC-CM derived from control stroma (Fig. 40A and 40B). This immunomodulating potential of MSC-CM upon MSC-intrinsic *Gatad2b* loss of function was also demonstrated in an in *vivo* system using female balb/c mice of 8-12 weeks. Murine breast carcinoma cell line 4T1 was injected orthotopically to induce the formation of tumor and MSC-CM from both control as well as *Gatad2b* knockdown stroma were injected intra-tumorally taking two different groups of mice. Within 18 hours of injection the mice were euthenised, tumors were isolated and single cells derived from the tumor mass were analysed for immune cells infiltration. Multicolor flowcytometry analysis showed tumors injected with *shGatad2b* MSC-CM had more percentage of immune-suppressive cells like CD206+ TAMs (Tumor-associated macrophage; resembles the M2 phenotype) and CD11b+ Ly6G+ MDSCs (Myeloid-derived suppressor cells). These findings further establish the functional role of stroma-intrinsic Gatad2b during MSC mediated inflammatory response (Fig. 40C).

(A)

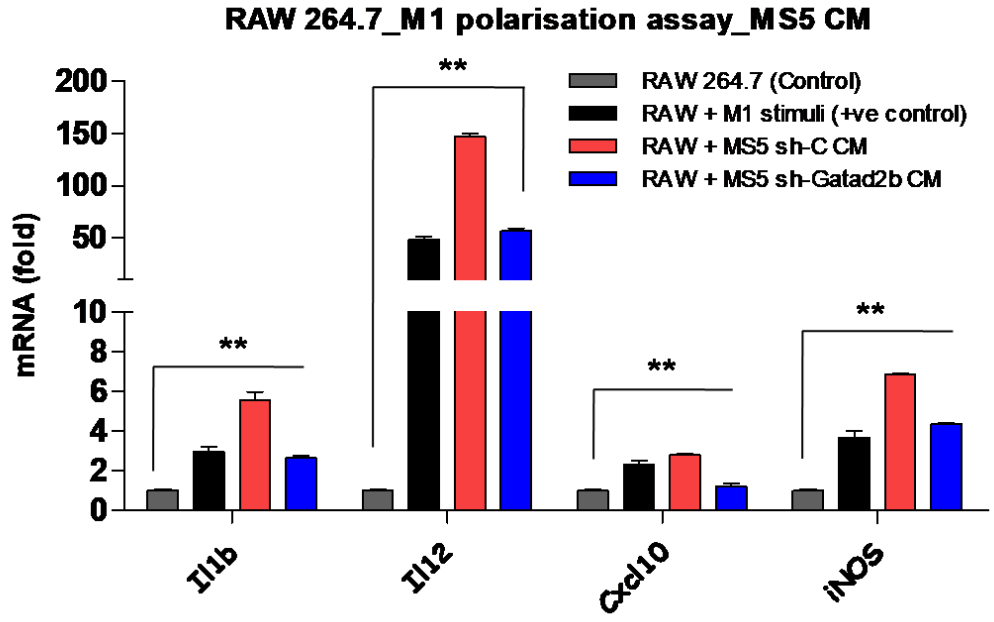
RAW 264.7_M1 polarisation assay_MS5 CM
RAW 264.7 (Control)
RAW + M1 stimuli (+ve control)
RAW + MS5 sh-C CM
RAW + MS5 sh-Gatad2b CM
mRNA (fold)
200
150
100
50
10
8
6
4
2
0
**
**
**
**
Il1b
Il12
Cxcl10
iNOS

(B)

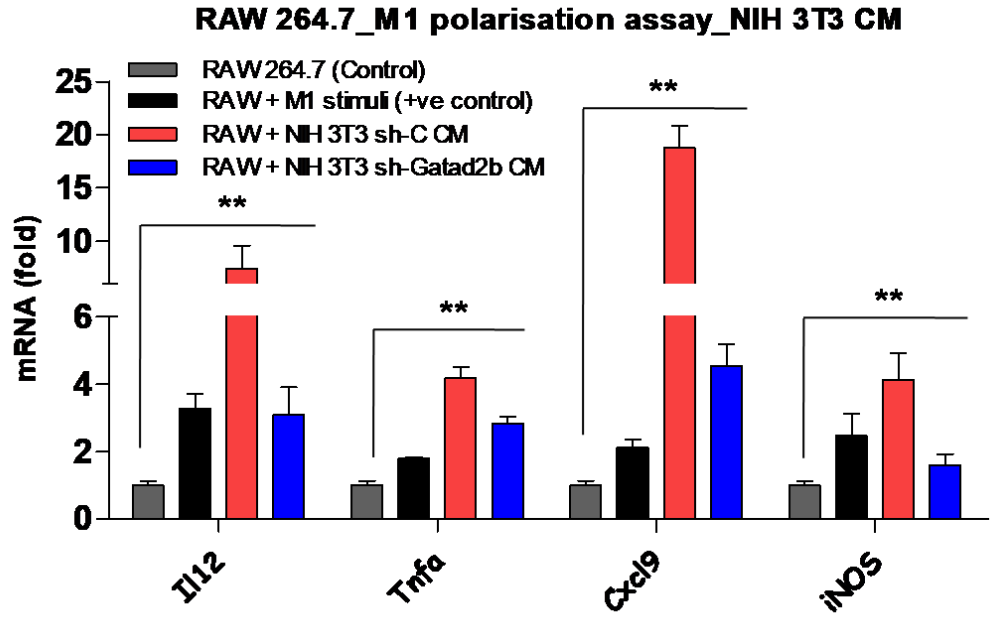
RAW 264.7_M1 polarisation assay_NIH 3T3 CM
RAW 264.7 (Control)
RAW + M1 stimuli (+ve control)
RAW + NIH 3T3 sh-C CM
RAW + NIH 3T3 sh-Gatad2b CM
mRNA (fold)
25
20
15
10
6
4
2
0
**
**
**
**
Il12
Tnfa
Cxcl9
iNOS

(C)

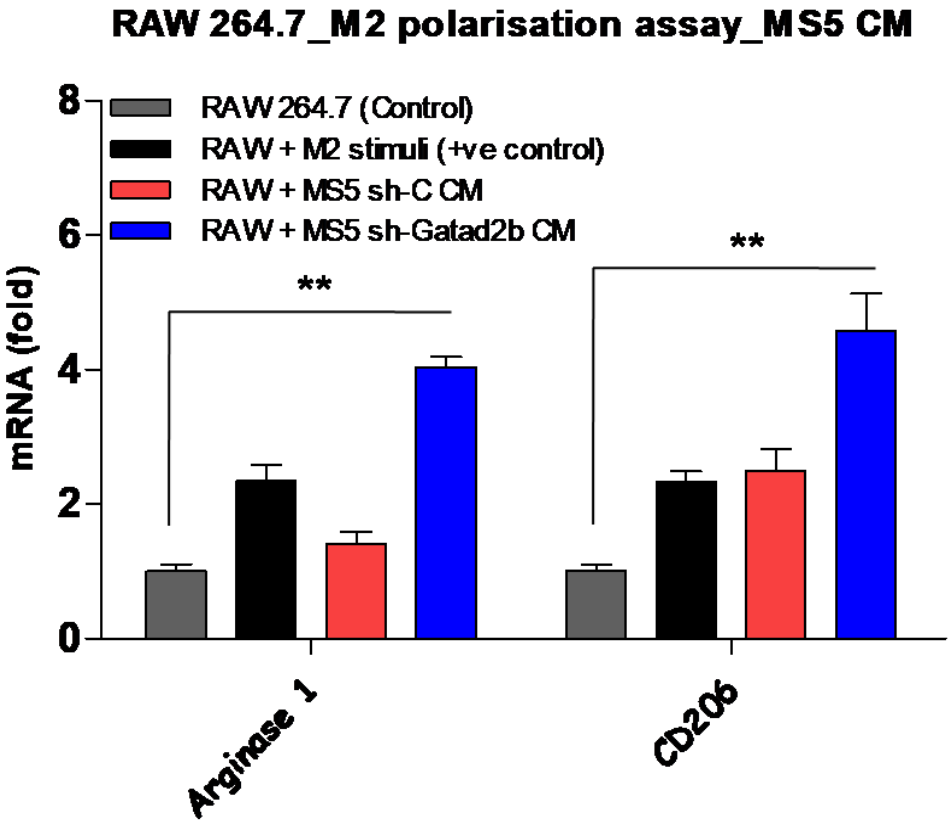
RAW 264.7_M2 polarisation assay_MS5 CM
RAW 264.7 (Control)
RAW + M2 stimuli (+ve control)
RAW + MS5 sh-C CM
RAW + MS5 sh-Gatad2b CM
mRNA (fold)
0
2
4
6
8
**
**
Arginase 1
CD206

(D)

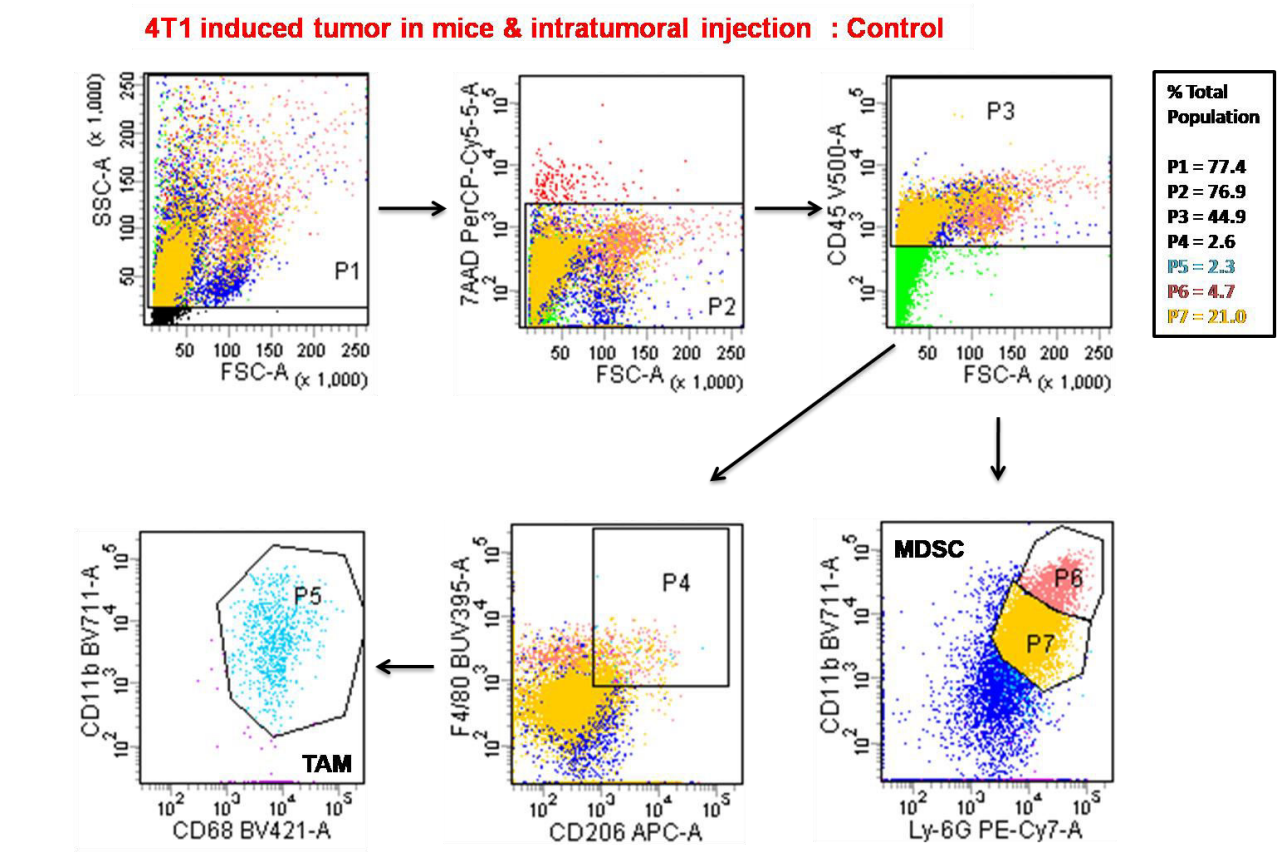
4T1 induced tumor in mice & intratumoral injection : Control
SSC-A (x 1,000)
FSC-A (x 1,000)
P1
7AAD PerCP-Cy5-5-A
P2
CD45 V500-A
P3
% Total Population
P1 = 77.4
P2 = 76.9
P3 = 44.9
P4 = 2.6
P5 = 2.3
P6 = 4.7
P7 = 21.0
CD11b BV711-A
CD68 BV421-A
TAM
F4/80 BUV395-A
CD206 APC-A
P4
P5
MDSC
P6
P7
Ly-6G PE-Cy7-A

4T1 induced tumor in mice & intratumoral injection : sh-C MS5-CM

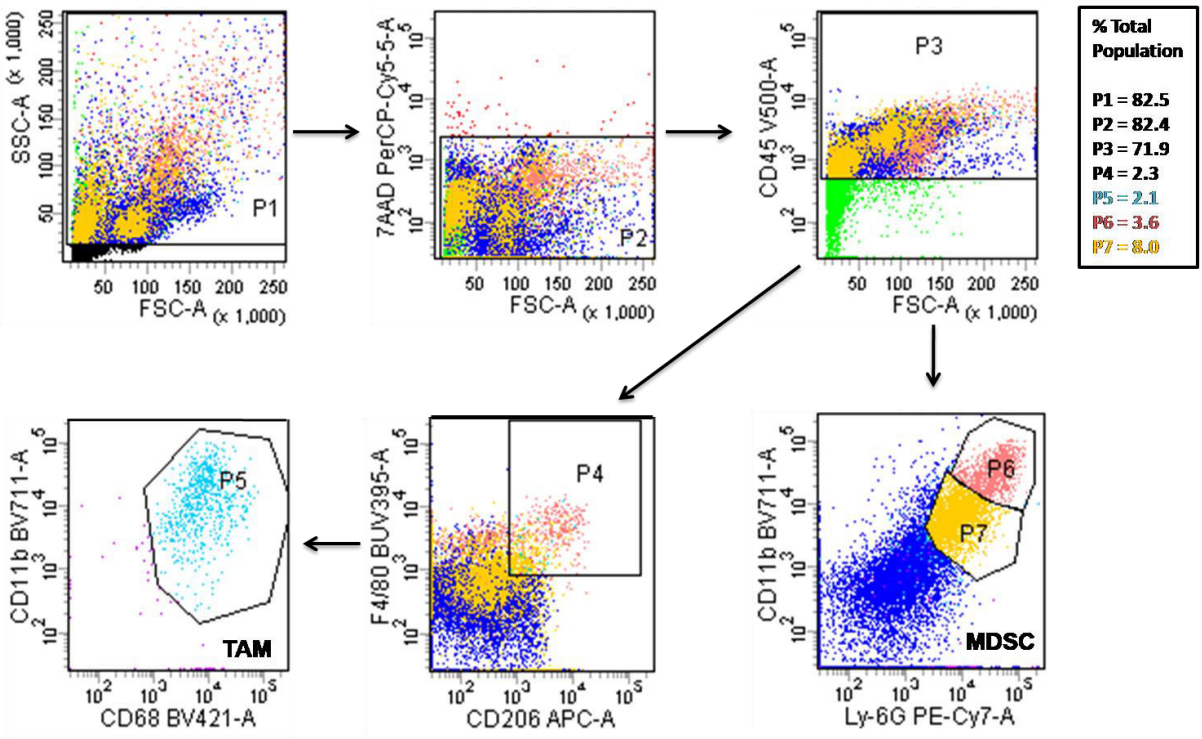

4T1 induced tumor in mice & intratumoral injection : sh-Gatad2b MS5-CM

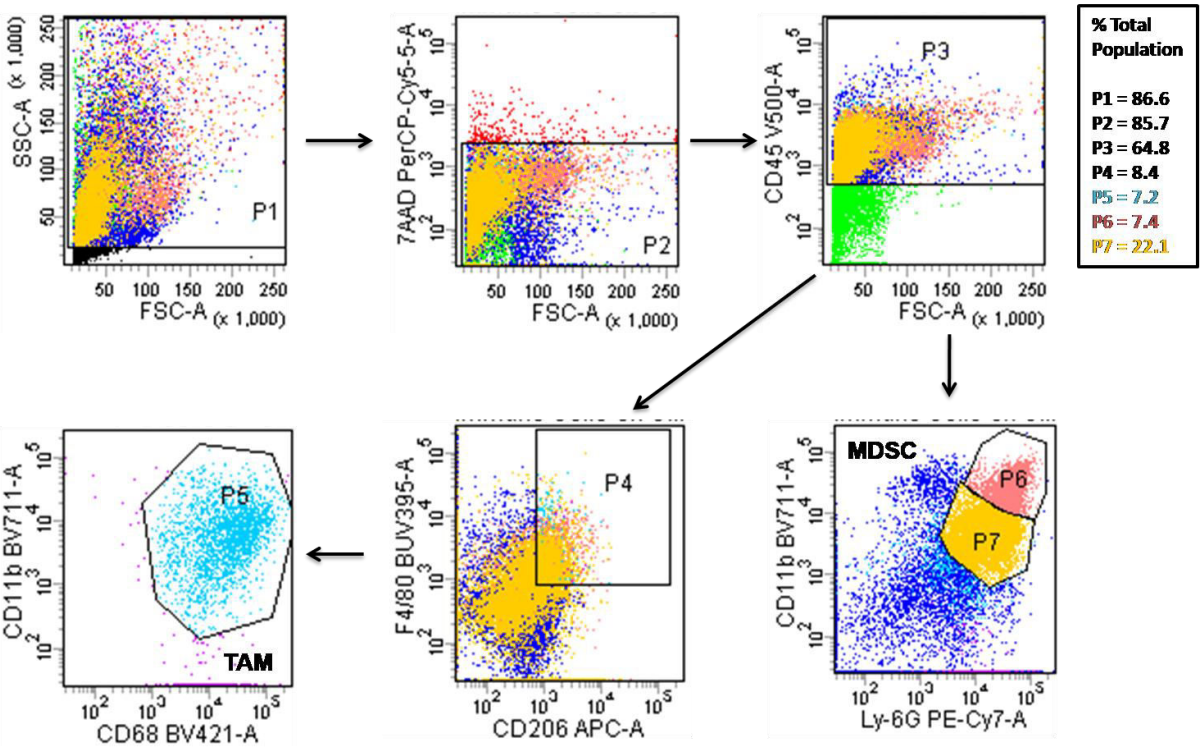

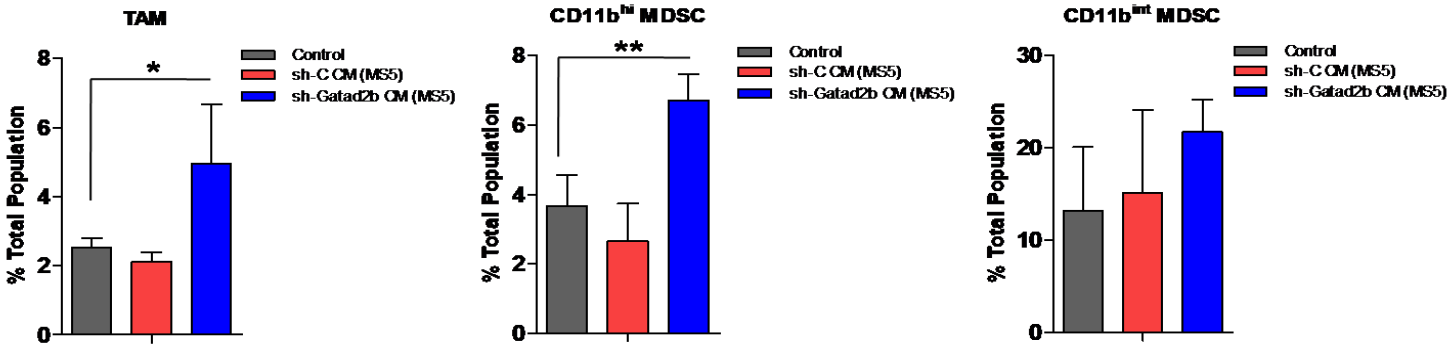

Fig 40 : Loss of Gatad2b in MSCs and its paracrine effect on immune cells. (**A)** RT-qPCR showing expression of M1 macrophage markers like *Il1b, Il12, Cxcl10, iNos* in RAW 264.7 cells when co-cultured in presence of conditioned media derived from *sh-C* or *sh-Gatad2b* MS5 **(B)** RT-qPCR showing expression of M1 macrophage markers like *Il12, Tnfa, Cxcl9, iNos* in RAW 264.7 cells when co-cultured in presence of conditioned media derived from *sh-C* or *sh-Gatad2b* NIH 3T3 **(C)** RT-qPCR showing expression of M2 macrophage markers like *Arginase 1, Cd206* in RAW 264.7 cells when co-cultured in presence of conditioned media derived from *sh-C* or *sh-Gatad2b* MS5 **(D)** Multicolor flow cytometry of a 4T1 cell derived syngeneic tumor injected with conditioned medium derived from *sh-C* and *sh-Gatad2b* MS5 *:* dot plot analysis showing %population of MDSCs and TAMs. mean ± s.d. are specified by the error bars. Data represent three to five independent experiments including two to three biological replicates. Statistics were calculated with Student's *t*-test; error bars represent means ± s.d. if not specified otherwise. **P* < 0.05 was considered to be statistically significant.

Response of Gatad2b during BMP2 signaling

Previously our data showed that in variety of *in vitro* cellular model of stromal inflammation the optimal *Gatad2b* response was in between 6 hours to 12 hours and this time frame mimics the acute stage of inflammation. Physiologically acute inflammation promotes osteogenesis. But it was a matter of study whether our in vitro cellular inflammation model also dictates the same. So we checked for the expression of the osteogenic markers during the early stages of LPS treatment *in vitro* using OP9 cell line and interestingly *Osx*, *Ocn*, *Alpl*, *Bsp1* were shown to be upregulated upon induction of inflammation (Fig. 41A). As Gatad2b was shown to regulate the acute phase of inflammation and acute inflammation in turn to induce the expression of osteogenic markers, next our aim was to investigate if there was any response of Gatad2b during the induction of these osteogenic markers. Bone morphogenetic proteins (BMPs) have been implicated in playing a crucial role in development and bone formation. OP9 cells are capable of undergoing osteogenesis and therefore we treated OP9 cells with BMP-2 and checked for the expression of *Gatad2b* along with other NuRD subunits. BMP-2 stimulation induced Gatad2b in concert with expression of

key osteogenic marker *Alpl* and osteoblast specific transcription factors *Runx2* and *Osx* (*Sp7*) (Fig. 41B). Complementary to the observation in OP9 cells, treatment with BMP4/7 heteromer in HS-5 and primary human normal bone marrow derived MSCS showed similar results (Fig. 41F, 41H). Transcriptional upregulation in these genes translated to the protein level as well. Induction in intracellular Gatad2b protein level was observed upon flow cytometry analysis in both OP9 and HS-5 (Fig. 41C, 41G). Additionally, confocal imaging and immunoblot using nuclear fraction from BMP-2 stimulated OP9 cells demonstrated Gatad2b induction as well as nuclear translocation in consistent with the induction of BMP-2 signaling component phospho-Smad 1/5/8 (Fig. 41D, 41E).

(A)

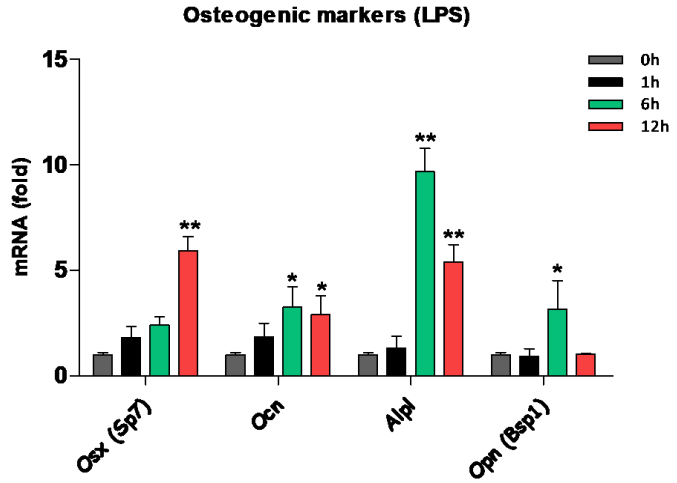

(B)

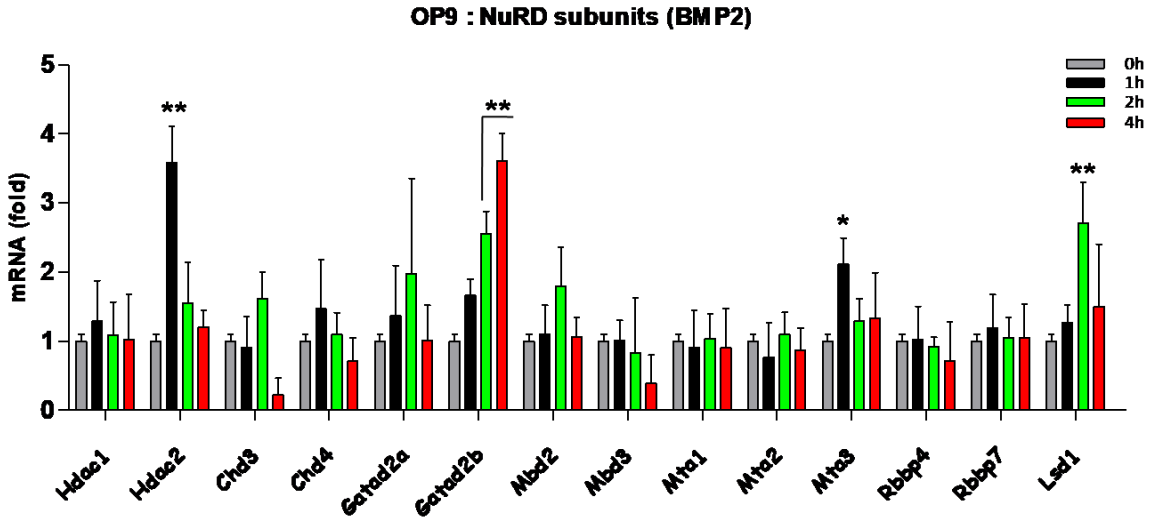

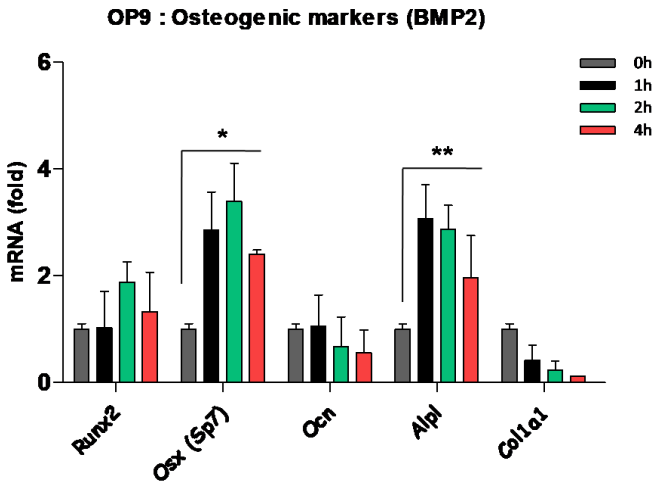
OP9 : Osteogenic markers (BMP2)
mRNA (fold)
0h
1h
2h
4h
*
**
Runx2
Osx (Sp7)
Ocn
Alpl
Col1a1

(C)

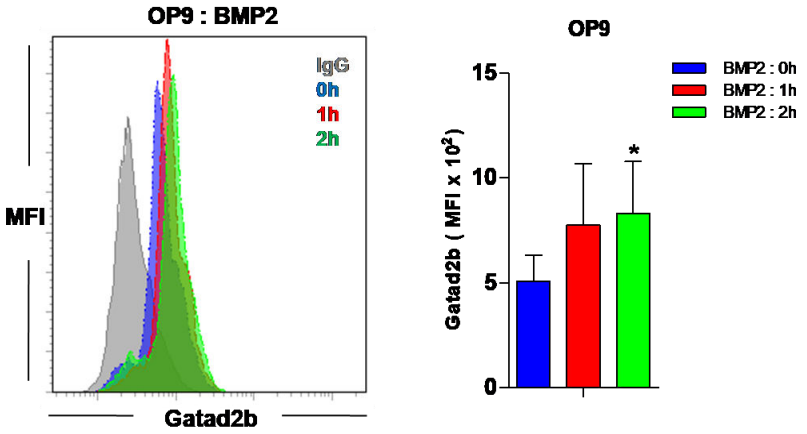
OP9 : BMP2
IgG
0h
1h
2h
MFI
Gatad2b
OP9
BMP2 : 0h
BMP2 : 1h
BMP2 : 2h
Gatad2b (MFI x 10²)
*

(D)

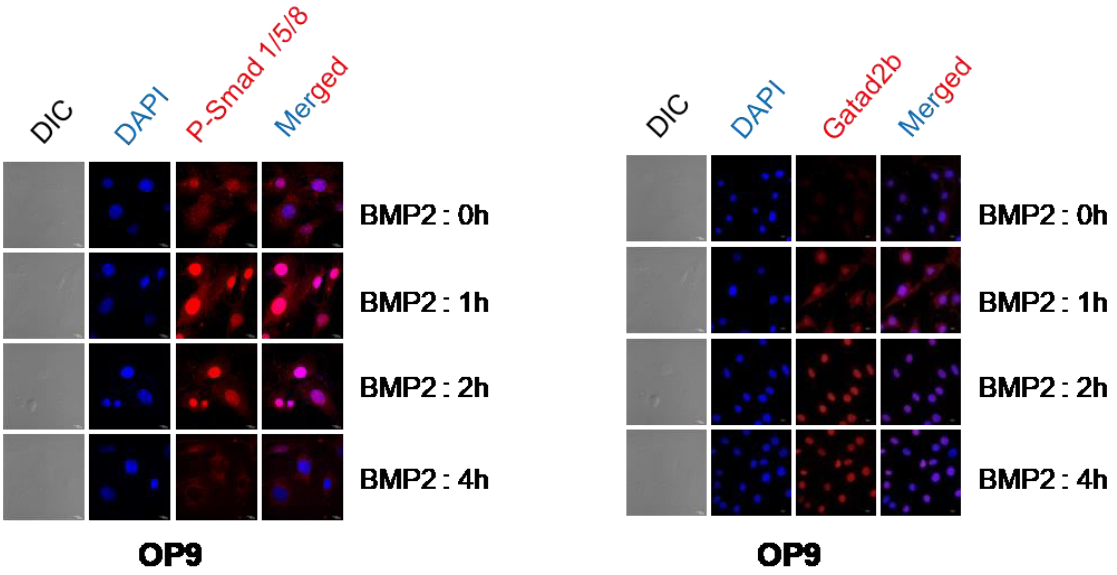
DIC
DAPI
P-Smad 1/5/8
Merged
BMP2 : 0h
BMP2 : 1h
BMP2 : 2h
BMP2 : 4h
OP9
DIC
DAPI
Gatad2b
Merged
BMP2 : 0h
BMP2 : 1h
BMP2 : 2h
BMP2 : 4h
OP9

(E)

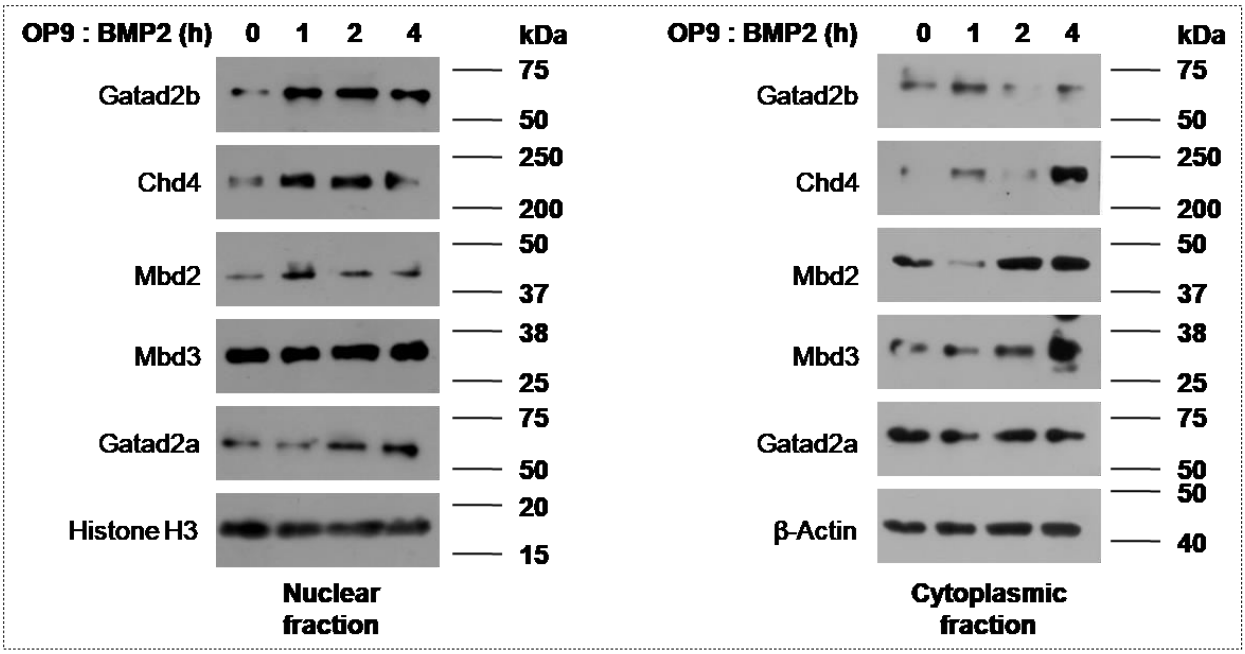
OP9 : BMP2 (h) 0 1 2 4
kDa
Gatad2b
Chd4
Mbd2
Mbd3
Gatad2a
Histone H3
75
50
250
200
50
37
38
25
75
50
20
15
Nuclear fraction
OP9 : BMP2 (h) 0 1 2 4
kDa
Gatad2b
Chd4
Mbd2
Mbd3
Gatad2a
β-Actin
75
50
250
200
50
37
38
25
75
50
50
40
Cytoplasmic fraction

(F)

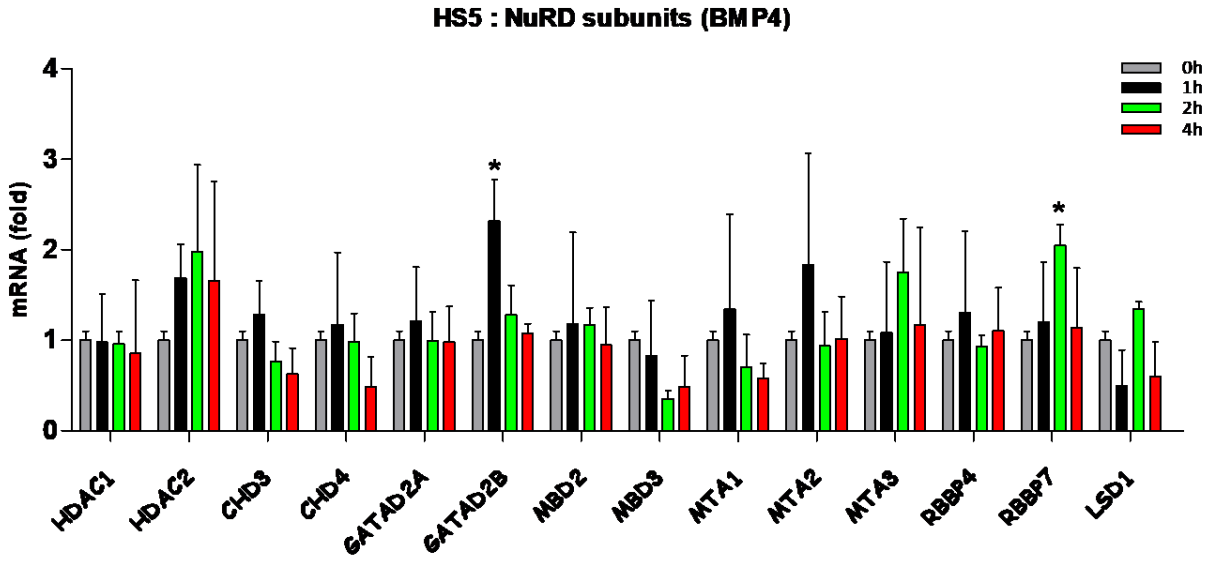
HS5 : NuRD subunits (BMP4)
mRNA (fold)
0h
1h
2h
4h
HDAC1
HDAC2
CHD3
CHD4
GATAD2A
GATAD2B
MBD2
MBD3
MTA1
MTA2
MTA3
RBBP4
RBBP7
LSD1

(G)

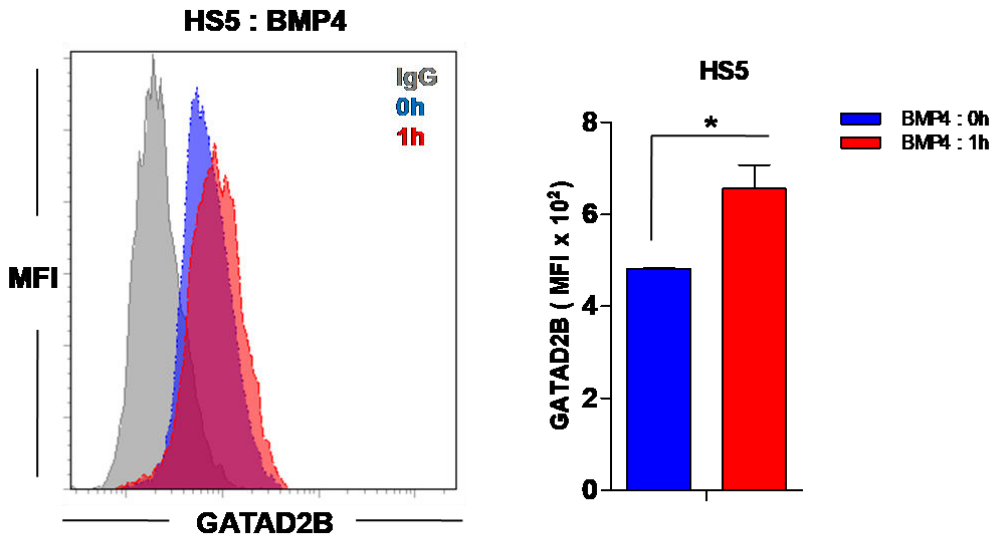
HS5 : BMP4
IgG
0h
1h
MFI
GATAD2B
HS5
BMP4 : 0h
BMP4 : 1h
GATAD2B (MFI x 10²)

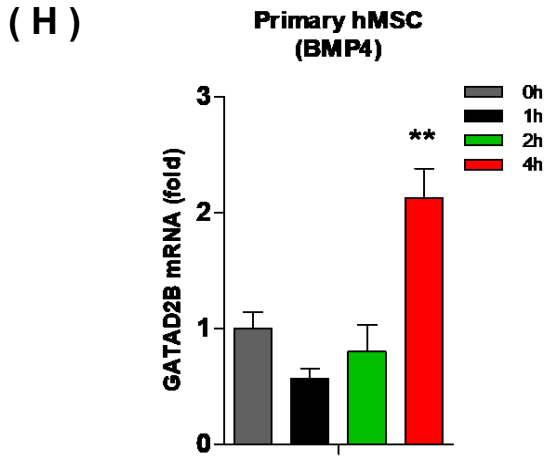

Fig. 41 : Response of different NuRD subunits during BMP-2 signaling. (A) RT-qPCR showing expression (normalized with respect to 0h as 1-fold) of osteogenic markers during treatment of OP9 cells with LPS over a time period of 12h. **(B)** RT-qPCR illustrating expression (normalized with respect to 0h as 1-fold) of different NuRD subunits along with osteogenic markers upon BMP-2 stimulation in OP9 cells at different time points. **(C)** Flow cytometry histogram analysis showing mean fluorescence intensity (MFI) of Gatad2b in BMP-2 stimulated OP9 cells **(D)** Immunofluorescence image analysis of Phospho-Smad 1/5/8 and Gatad2b in OP9 cells treated with BMP-2 at different time points. **(E)** Immunoblot analysis of NuRD components in both nuclear and cytoplasmic fraction derived from OP9 cells cultured in presence of BMP-2 at different time points. **(F)** RT-qPCR showing the response (normalized with respect to 0h as 1-fold) of NuRD subunits in HS-5 cells upon stimulation with BMP-4/7. **(G)** Flow cytometry histogram analysis showing MFI of GATAD2B in BMP-4/7 stimulated HS-5 cells. **(H)** RT-qPCR showing expression of *GATAD2B* (normalized with respect to 0h as 1-fold) in primary human MSCs stimulated with BMP-4/7 in a time-dependent manner. RT-qPCR values were normalized to *Gapdh* (mouse) or *GAPDH* (human). Data represent three to five independent experiments including two to three biological replicates. Statistics were calculated with Student's *t*-test; error bars represent means ± s.d. if not specified otherwise. **P* < 0.05 was considered to be statistically significant.

Gatad2b also responds to osteogenic cues

Consistent with the previous results long term differentiation over a period of 21 days in presence of osteogenic differentiation media showed Gatad2b induction as well in both OP9 and HS-5 (Fig. 42A and 42D). ALPL staining at different time points during the process confirmed the status of osteogenic differentiation (Fig. 42B). In addition, immunoblot also showed a pattern of induction in Gatad2b protein level of OP9 during the differentiation process (Fig. 42C). Co-immunoprecipitation studies further suggested that Gatad2b interacts with canonical transcriptional regulators of osteoblast differentiation during BMP-2 stimulation (Fig. 42E). Altogether these results highlight that both short term and long-term osteogenic cues induce expression of Gatad2b in mesenchymal stromal cells.

(A)

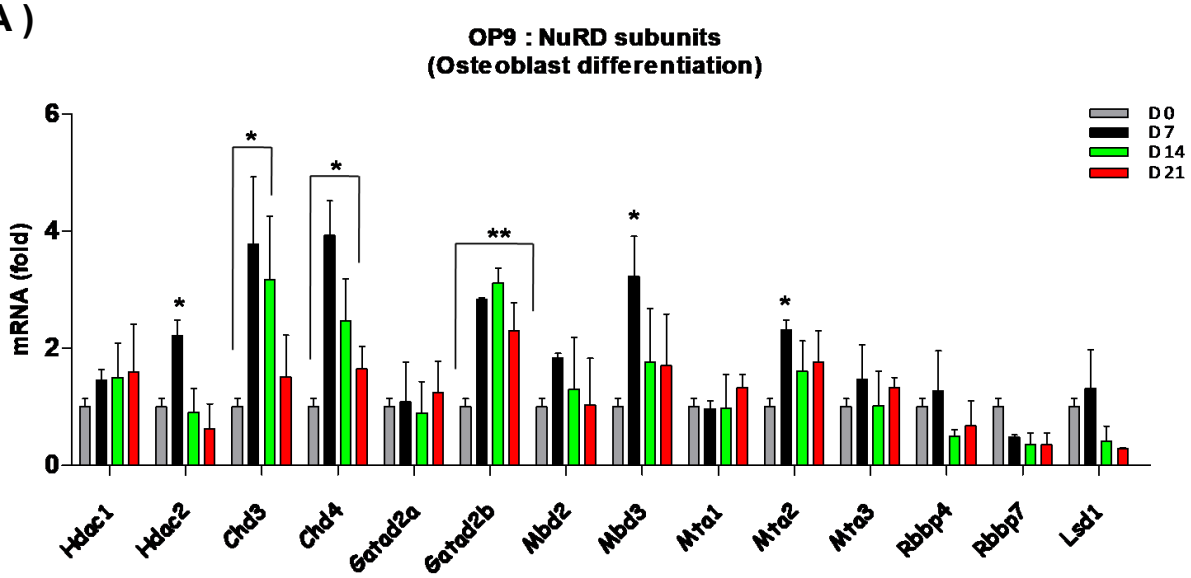
OP9 : NuRD subunits
(Osteoblast differentiation)
mRNA (fold)
D0
D7
D14
D21
Hdac1
Hdac2
Chd3
Chd4
Gatad2a
Gatad2b
Mbd2
Mbd3
Mta1
Mta2
Mta3
Rbbp4
Rbbp7
Lsd1

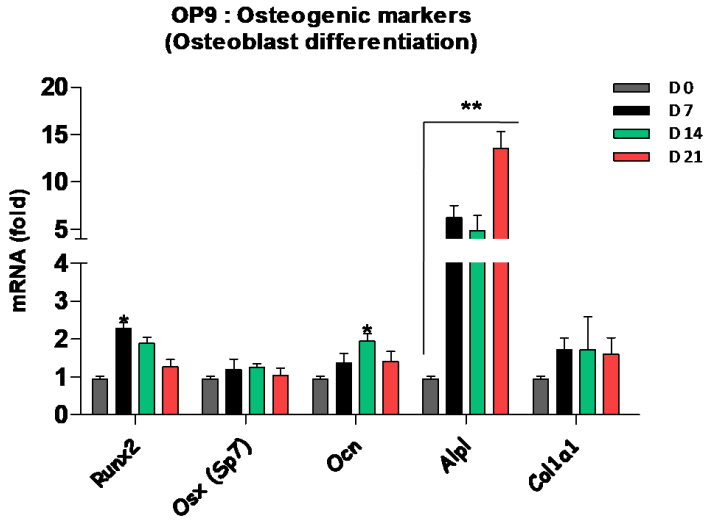
OP9 : Osteogenic markers
(Osteoblast differentiation)
mRNA (fold)
D0
D7
D14
D21
Runx2
Osx (Sp7)
Ocn
Alpl
Col1a1

(B)

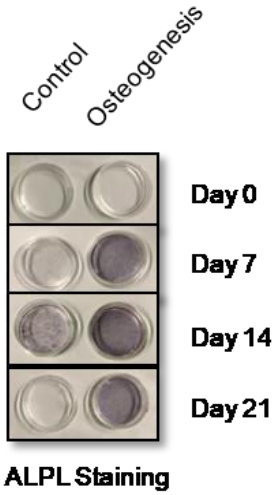
Control
Osteogenesis
Day 0
Day 7
Day 14
Day 21
ALPL Staining

(C)

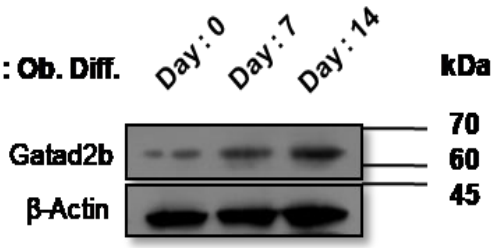
OP9 : Ob. Diff.
Day : 0
Day : 7
Day : 14
kDa
Gatad2b
β-Actin
70
60
45

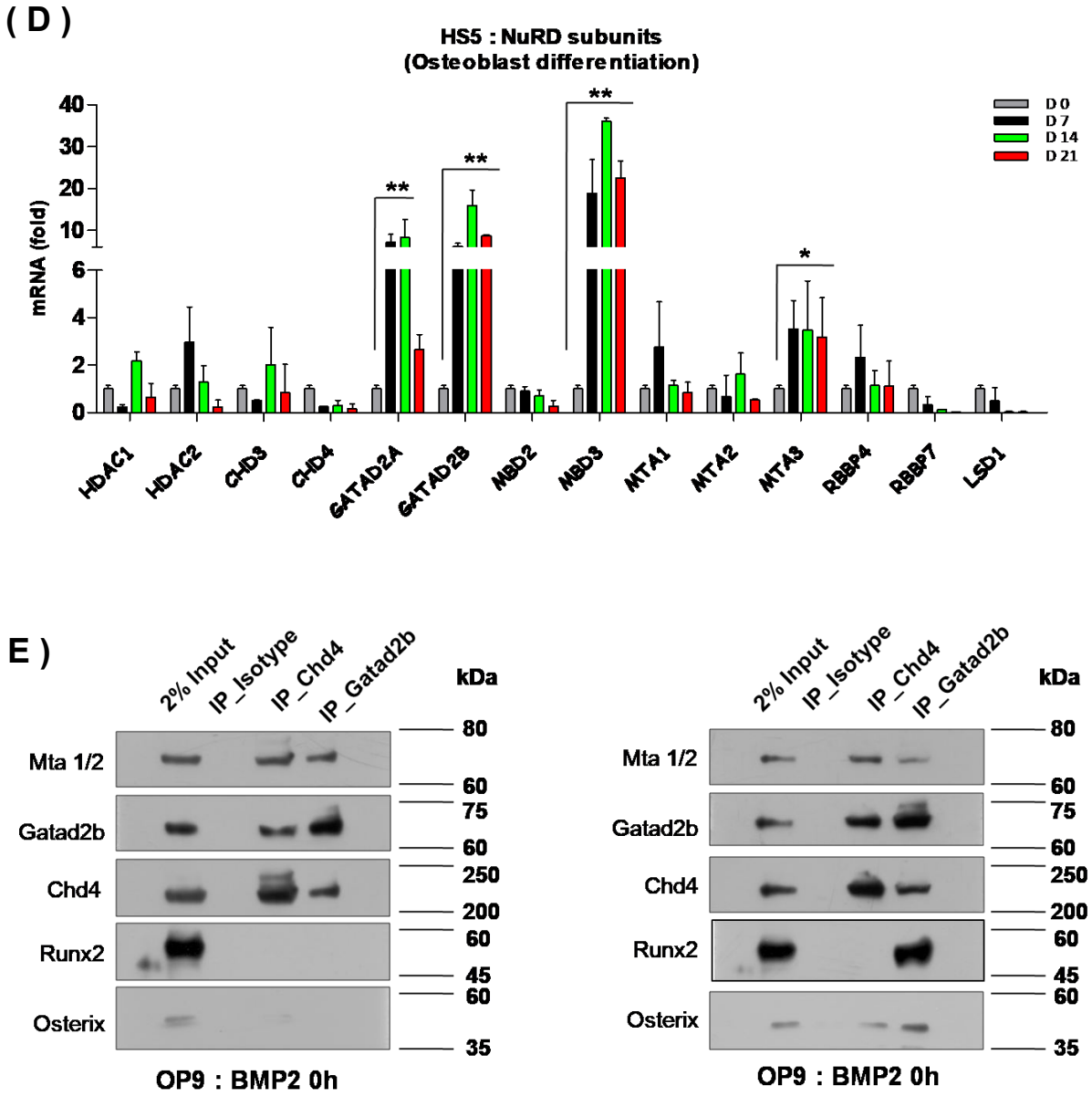

Fig 42 : Response of NuRD complex upon long term osteogenic differentiation in vitro. **(A)** RT-qPCR showing expression (normalized with respect to D0 as 1-fold) of NuRD components along with ostegenic markers at different time points during osteogenic differentiation in OP9 cells. **(B)** Alkaline phosphatase staining by NBT/BCIP reagent showing the intensity of osteogenic differentiation at different time points in OP9 cells over a period of 21 days. **(C)** Immunoblot showing the induction of Gatad2b in protein level during the osteogenic differentiation of OP9 cells. **(D)** RT-qPCR showing expression (normalized with respect to D0 as 1-fold) of NuRD components at different time points during osteogenic differentiation in HS-5 cells. **(E)** Co-immunoprecipitation with Chd4 and Gatad2b followed by immunoblot analysis with key osteogenic transcription factors Runx2 and Osterix in control as well as BMP-2 stimulated OP9 cells. mean ± s.d. are specified by the error bars. Data represent three to five independent experiments including two to three biological replicates. Statistics were calculated with Student's *t*-test; error bars represent means ± s.d. if not specified otherwise. **P* < 0.05 was considered to be statistically significant.

Characterisation of primary human MSCs derived from MDS patients bone marrow in terms of BMP-2 signaling, osteogenic differentiation and *GATAD2B* expression

Reduced self-renewal or tri-lineage commitment (Osteoblast, Adipocytes and Chondrocytes) potential of bone-marrow resident stromal cells is one of the major reasons of many bone related disorders and hematological malignancies. Myelodysplastic syndrome (MDS) is a pre-leukemic disease where patients have impaired stromal functions. Primary MSCs derived from bone marrow of MDS patients were expanded in vitro and characterised in terms of their osteogenic potential and BMP4 response. MDS derived human MSCs showed reduced endogenous expression of the osteogenic marker *ALPL* and osteoblast specific transcription factors *RUNX2*, *OSTERIX* along with reduced *GATAD2B* expression (Fig. 43A). These MSCs also had less BMP4 response potential as shown by reduced expression of phospho-SMAD 1/5/8 upon confocal imaging (Fig. 43B). Osteoblast differentiation potential was also less compared to NBM (Normal Bone Marrow)-derived MSCs as shown by ALPL staining with NBT/BCIP reagent (Fig. 43C). This indicates a positive correlation of *GATAD2B* with impairment of BMP signaling and osteogenesis potential.

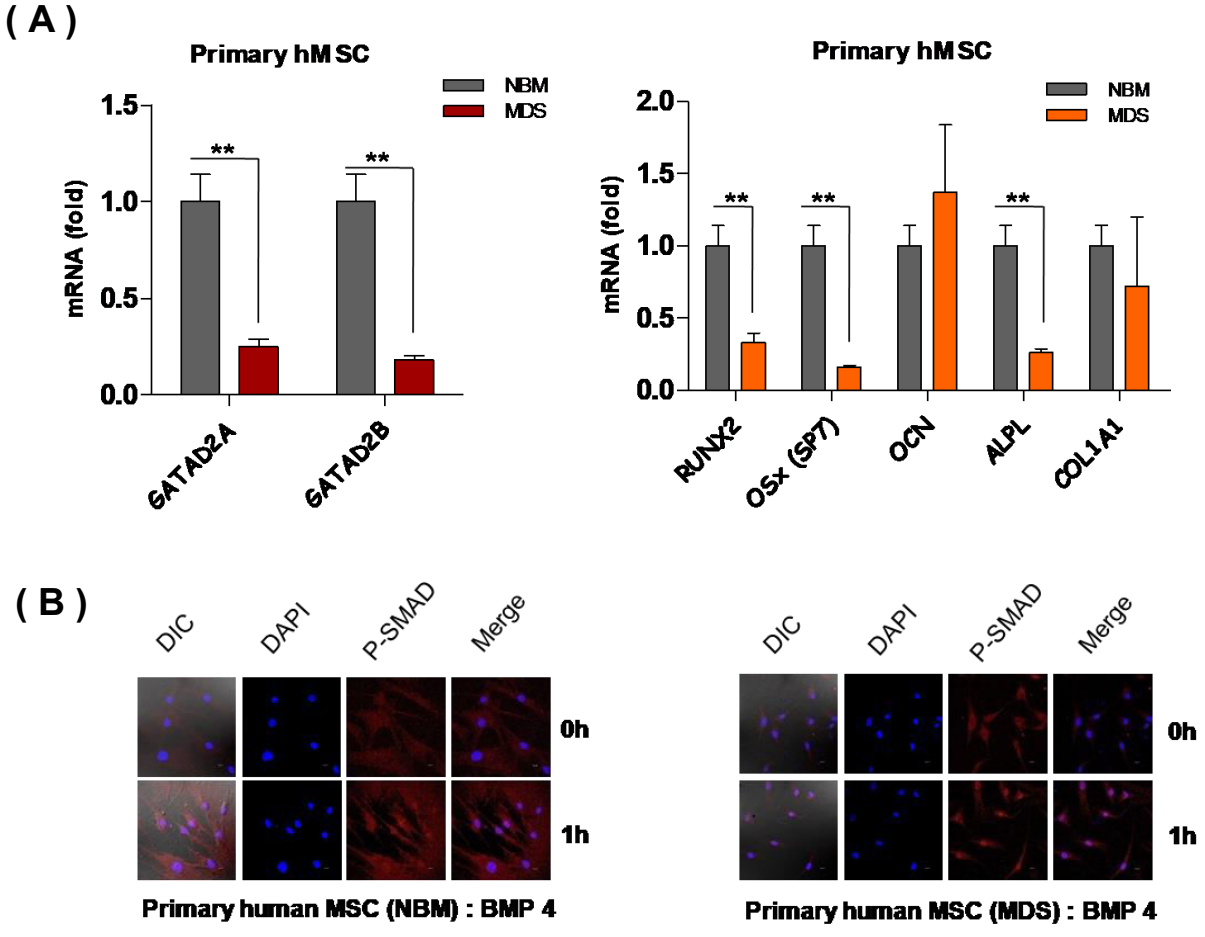

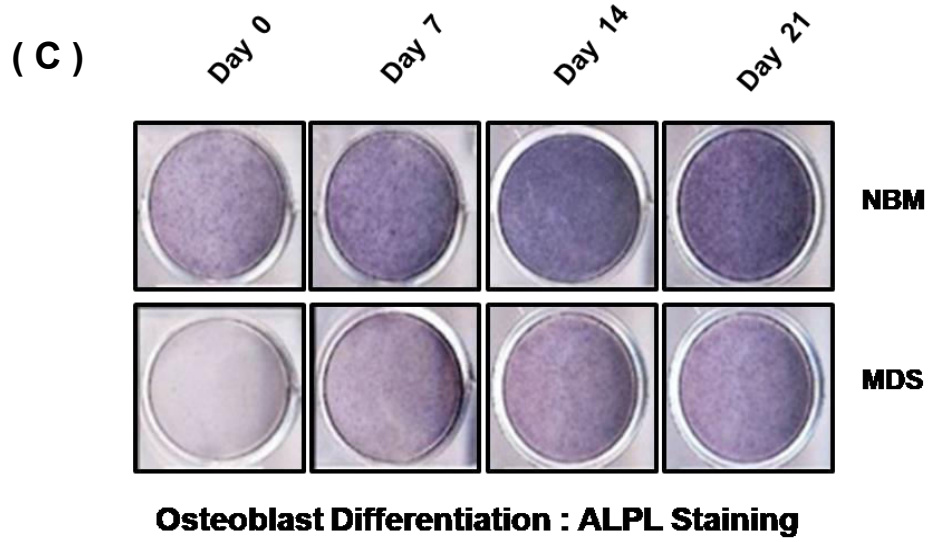

Fig 43 : Bone marrow derived primary human MSCs from MDS patients show impaired osteogenicity. (A) RT-qPCR showing the endogenous expression level of *GATAD2A/GATAD2B* along with key osteogenic markers in MDS patients derived primary human MSCs (normalised with respect to normal bone marrow derived MSCs as 1 fold) **(B)** Immunofluorescence image analysis of p-SMAD 1/5/8 in NBM-hMSCs and MDS-hMSCs during BMP-4/7 stimulation. **(C)** Alkaline phosphatase staining of NBM-hMSCs and MDS-hMSCs at different time points during in vitro osteogenic differentiation over a period of 21 days. mean ± s.d. are specified by the error bars. Data represent three independent experiments including two to three biological replicates. Statistics were calculated with Student's *t*-test; error bars represent means ± s.d. if not specified otherwise. **P* < 0.05 was considered to be statistically significant.

Gatad2b deficient cells show reduced response to BMPs and osteogenic stimuli

To appreciate the importance of *Gatad2b* in osteogenic commitment of MSCs, Gatad2b deficient OP9 cells were subjected to BMP-2 treatment. Herein, we find that cells lacking *Gatad2b*, showed reduced response to BMP-2 mediated induction of osteogenic genes *Alpl, Osx*, *Runx2,Osteocalcin (Ocn), Col1a1* (Fig. 44B) in addition to the same findings even in resting state (Fig. 44A). Among the Smads only *Smad1* displayed an impaired BMP-2 response pattern in OP9 cells lacking *Gatad2b* (Fig. 44C). Activation of BMP-2 signaling pathway was also hampered as shown by confocal imaging which indicated reduced level of phospho-Smad 1/5/8 in absence of *Gatad2b* (Fig. 44D). Gatad2b deficiency also resulted in impaired osteoblast differentiation as shown by reduced level of osteogenic markers expression over different time intervals (Fig. 44E) and less amount of ALPL staining (Fig. 44F) compared to control.

(A)

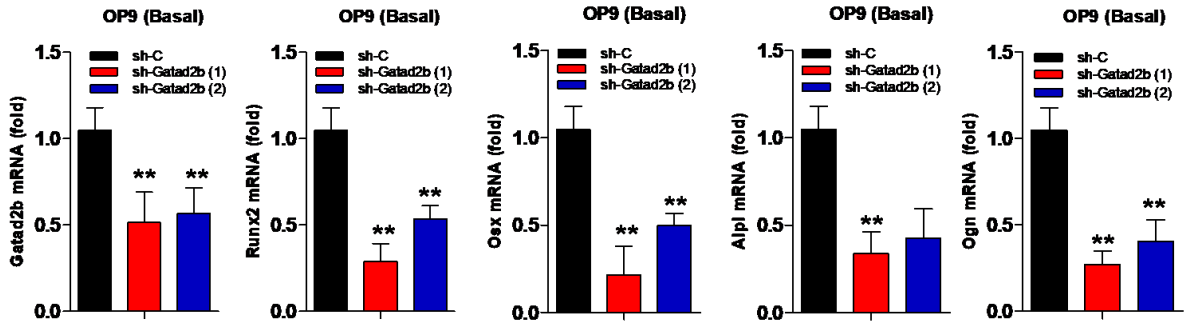
OP9 (Basal)
Gatad2b mRNA (fold)
Runx2 mRNA (fold)
Osx mRNA (fold)
Alpl mRNA (fold)
Ogn mRNA (fold)
sh-C
sh-Gatad2b (1)
sh-Gatad2b (2)
1.5
1.0
0.5
0.0
**

(B)

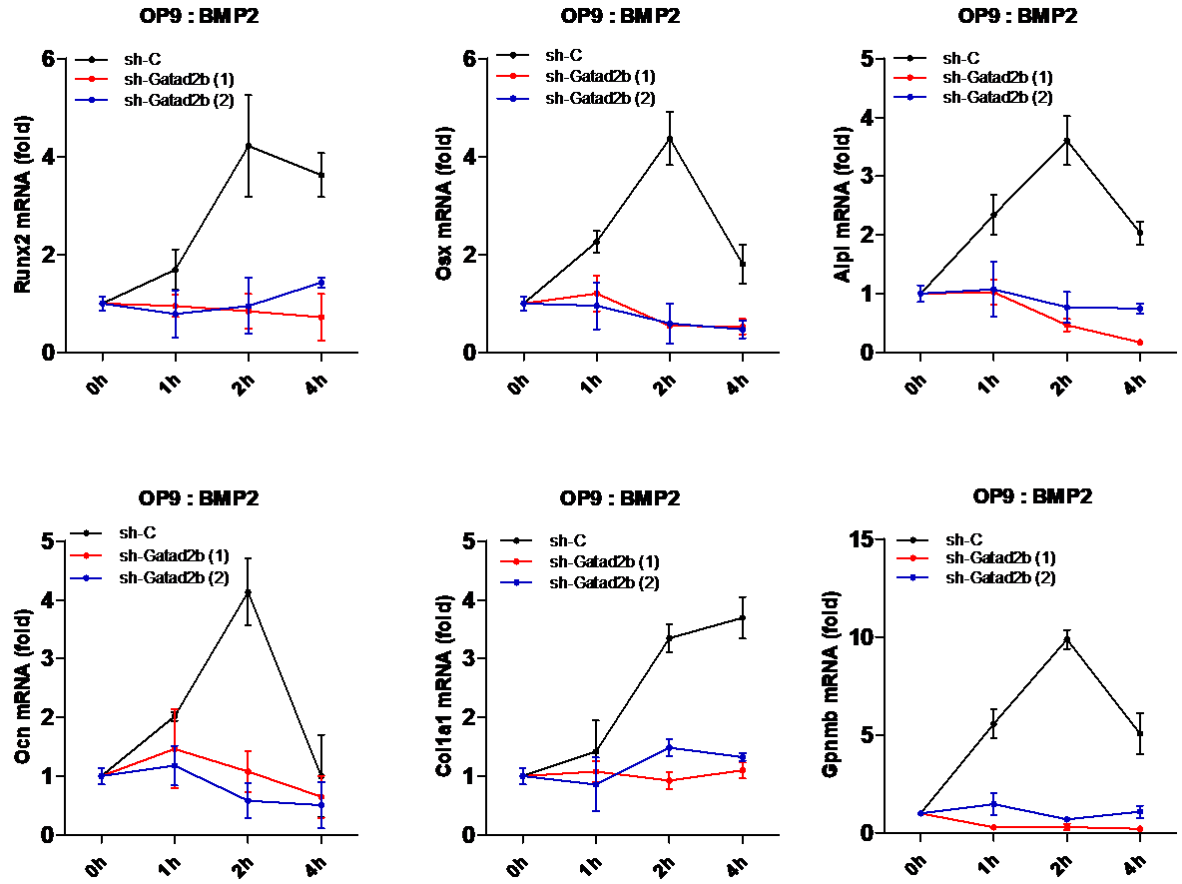
OP9 : BMP2
Runx2 mRNA (fold)
Osx mRNA (fold)
Alpl mRNA (fold)
Ocn mRNA (fold)
Col1a1 mRNA (fold)
Gpnmb mRNA (fold)
sh-C
sh-Gatad2b (1)
sh-Gatad2b (2)
0h
1h
2h
4h

(C)

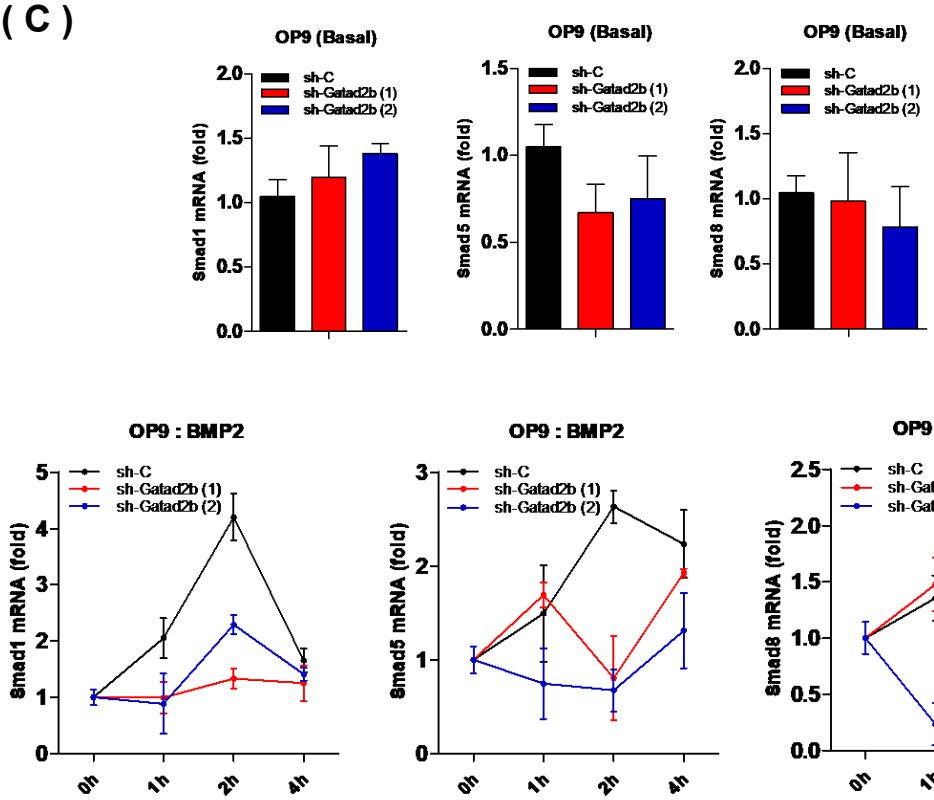
OP9 (Basal)
Smad1 mRNA (fold)
Smad5 mRNA (fold)
Smad8 mRNA (fold)
sh-C
sh-Gatad2b (1)
sh-Gatad2b (2)
OP9 : BMP2
0h
1h
2h
4h

(D)

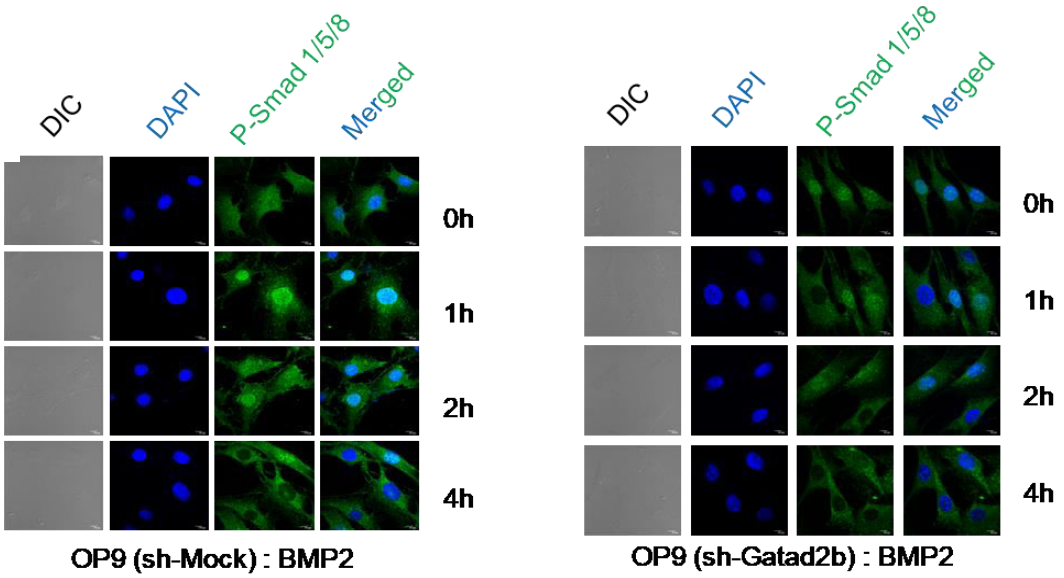
DIC
DAPI
P-Smad 1/5/8
Merged
0h
1h
2h
4h
OP9 (sh-Mock) : BMP2
OP9 (sh-Gatad2b) : BMP2

(E)

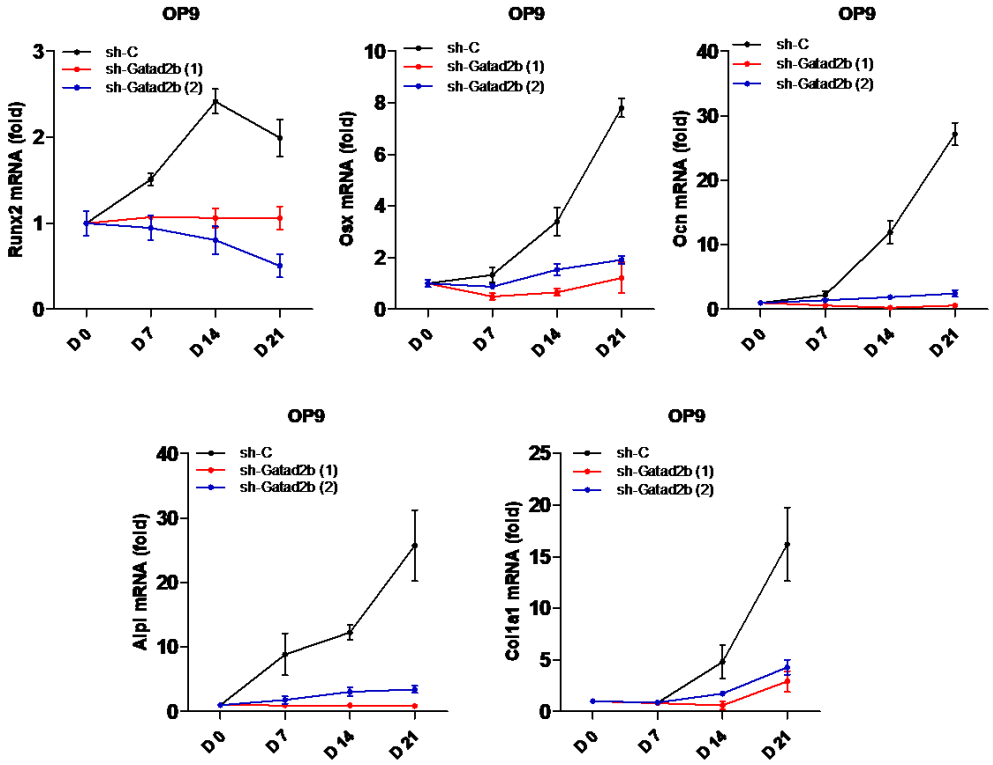

(F)

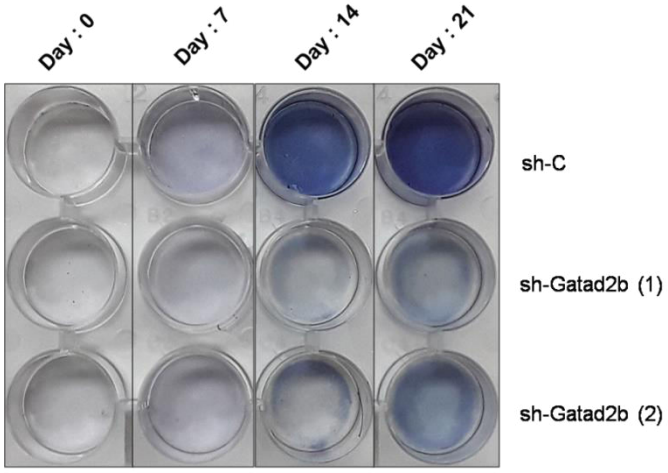

OP9 : Osteoblast Differentiation (Alpl Staining)

Fig 44 : Gatad2b deficient MSCs exhibit an impaired osteogenic potential. RT-qPCR showing the expression of key osteogenic markers in Gatad2b deficient OP9 cells during **(A)** steady state **(B)** BMP-2 response and **(E)** In vitro osteogenic differentiation **(C)** RT-qPCR showing the expression of *Smad 1*, *Smad 5* and *Smad 8* in steady state *(upper panel)* as well as during BMP-2 stimulation *(lower panel)* **(D)** Immunofluorescence image analysis demonstrating p-Smad 1/5/8 expression in *sh-Control* and *sh-Gatad2b* OP9 cells at different time points of BMP-2 stimulation **(F)** Alkaline phosphatase staining showing in vitro osteogenic differentiation potential of *sh-Control*, *sh-Gatad2b(1)* and *sh-Gatad2b(2)* OP9 cells at different time points. mean ± s.d. are specified by the error bars. Data represent three independent experiments including two to three biological replicates. Statistics were calculated with Student's *t*-test; error bars represent means ± s.d. if not specified otherwise. **P* < 0.05 was considered to be statistically significant.

DISCUSSION

From the recent development in research in MSC biology, it is evident that MSCs share a reciprocal relationship with inflammation. A properly functional MSC will 'switch off' the inflammatory response by virtue of its immunosuppressive potential to prevent disease progression. Molecular and functional integrity of MSCs is the key to maintain an immune homeostasis. The crosstalk between MSCs and inflammation is considered to be critical in the therapeutic efficacy of these cells. In fact, it has been suggested that the immunomodulatory ability of MSCs in response to inflammatory cytokines should be used in the standardization of MSC products. It is conceivable that among the diseases that have been treated with MSCs, the inflammatory tissue microenvironment varies and therefore so too does the influence on MSCs, to the extent that the fate of the MSCs administered differs and results in different outcomes.

Since a minimal amount of inflammation is needed to enable immunosuppression by MSCs, it is likely that conventional clinical anti-inflammation therapies could alter the inflammatory cytokine profile in the tissue microenvironment and thus modulate the effect of MSCs. There are several studies ongoing to investigate the mechanisms underlying failures in MSC-based therapy in the presence of immunosuppressants. Immunosuppresant drugs are given to treat immune-medated diseases which act by modulating the surrounding tissue microenvironement. But administration of these drugs can have a 'back-fire' impact on tissue resident or co-administered MSCs. Among the commonly used immunosuppressants, cyclosporin A prevents the activation of T cells and is frequently used to prevent the rejection of transplanted organs and to treat autoimmune conditions. In experiments, MSCs induce tolerance in mice that had received organ transplants, as expected, but this effect was reversed by cyclosporin A (**155**). Similarly, dexamethasone, another widely used immunosuppressant, also reverts MSC-mediated immunosuppression both *in vitro* and *in vivo*. Certain molecular studies have shown that dexamethasone blocks both iNOS expression in mouse MSCs and IDO expression in human MSCs and thus allows inflammation to proceed unchecked. Moreover, during the treatment of advanced liver fibrosis in mice, concurrent administration of steroids reversed MSC-mediated immunosuppression and eliminated their therapeutic effects (**156**). Together it can be concluded that MSC based treatments of inflammatory disorders use their immunosuppressive properties while a potential promising approach for anti tumor therapy will be to reprogramme MSCs from an immunosuppressive to an immunostimulatory

phenotype (**115**). So, instead of modulating the tissue microenvironment if we take an approach to modify the MSCs intrinsically followed by the administration of engineered MSCs, the outcome of the therapeutics will be much more promising and in doing so, nothing can be better than an epigenetic reprogramming as it involves transient modifications of DNA and histones which is expected to remain stable over many cell divisions. So heritable phenotype changes, often imprinted as 'epigenetic memory', without altering the genotype is the key secret behind the success of epigenetic therapies.

Our findings presented here have identified a new regulatory layer of NF-κB signaling during MSC-mediated inflammation and indicate that Gatad2b represents as an epigenetic player and modifier to the NF-κB signaling network as well as having a role in maintaining the homeostasis of inflammatory responses. Epigenetic reprogramming involving Gatad2b can be a promising therapeutic approach as its efficacy will depend solely on the genetically engineered MSCs and therefore the therapeutics won't have to rely upon the local tissue microenvironment which often creates a major challenge during the treatment of many diseased conditions, specially cancer and cancer-associated inflammation.

When our systems encounter any pathogen attack or endogenous damage or self-alteration an immune response develop which leads to the activation of a subset of immune cells. After coming back to the normal homeostatic condition these immune cells causing pro-inflammatory response are tuned off and the overall immune landscape gets back to the equilibrium. This switch on and switch off mechanism of immune cells are mediated by a diverse amount of soluble factors called cytokines and chemokines as well as cell to cell contact which are highly dependent upon the local microenvironment. Tissue-resident MSCs and their secretome do play a determining role for which subset of immune cells to be activated depending upon the type and stage of inflammation. During the initial stage of an immune response the abundance of pro-inflammatory type of immune cells are observed whereas during the resolution stage the anti-inflammatory ones prevail. If this balance is disrupted then it leads to chronic inflammation which defines the onset of various diseased conditions (**99,103,108**). Tageting a specific type of immune cell to attenuate a hyper-activated or to induce an insufficiently activated immune system during the treatment of inflammation associated disorders is very difficult since there are many types of pro-inflammatory or anti-inflammatory immune cells and targeting a specific one might not change the overall immune status of the diseased condition. Instead targeting the inflammatory mileu can be a better option for modulating the immune cells as it will cause a systemic impact within the damaged or infected tissue. Since MSCs are a major component and master regulator within the niche for controling many other types of immune and non-

immune cells (**92,95**), our aim was to find an MSC-intrinsic epigenetic modulator which in-turn can regulate the immune cell plasticity to counter-balance the inflammatory potential of the local tissue microenvironment.

As discussed earlier, the usage of HDAC inhibitors during the many ongoing clinical trials insisted us to target NuRD complex for the study of epigenetic regulators in MSC-mediated immune response. In our study, we mainly focused on the NFkB signaling dependent inflammatory response as it is a molecule through which many types of inflammatory pathways cross-talk with each other and because NFkB signaling is a part of the innate immune response which is broad-spectrum in terms targeting immune cells. LPS binds to TLR4 and activates a signaling cascade which involves IRAK1/4, IKKs, RelA/P65. Phosphorylated P65 (Active NFkB) translocates into the nucleus to induce the expression of downstream pro-inflammatory cytokines, chemokines and other transcriptional regulators (**175**). To check whether any of the NuRD subunits responds during an inflammatory response we used multiple in vitro cellular model of inflammation using MSC lines. Upon treating with LPS in a time-dependent manner we observed an induction in Gatad2b response. Since other interferons and cytokines also play a major role in promoting inflammation we therefore checked the response of Gatad2b upon IFNβ (Type I interferon), IFNγ (Type II interferon) as well as TNFα (TNFR mediated NFkB signaling) treatment and Gatad2b was found to be upregulated again. To check whether this response of Gatad2b was redundant or it was really regulating the inflammatory response we generated *Gatad2b*-deficient stable MSC lines and compared the inflammatory response with control MSCs.Differential gene expression analysis and chemokine assay showed majority of the pro-inflammatory markers to be downregulated basally as well as during LPS treatment over different time points in cells which had less amount of Gatad2b. Additionally, Tlr4 was also found to be attenuated in terms of their gene expression level as well as protein level in both resting and LPS-stimulated condition. This regulatory effect was further confirmed by transcriptome analysis by RNA sequencing method and the overall pro-inflammatory gene signature was found to be abrogated in cells lacking *Gatad2b*. Hence, it can be concluded that *Gatad2b* is a positive regulator of TLR4-driven pro-inflammatory response.

Our next question was if Gatad2b was really positively regulating the *Tlr4* and subsequently the NFkB downstream pro-inflammatory cytkines and chemokines, its absence will lead to impaired activation of NFkB pathway during the LPS treatment due to the reduced level of phospho-P65. The other TLR4 signaling pathway molecules could also be downregulated and/or inactive. To test this hypothesis we checked the intracellular protein level of total Irak1, total p65/RelA upon flow cytometry analysis but no change was found either in steady

state or in LPS-treated condition. When we checked for their phosphorylation level, immunoblot analysis showed a lower amount of phospho-p65 with time dependent LPS stimulation indicating that NFkB pathway activation was severely hampered in *Gatad2b* knock down stromal lines. In consistency with these findings when we overexpressed *Gatad2b* in wild type MSC lines, *Tlr4* and subsequently the other pro-inflammatory markers were found to be upregulated. Activation of NFkB can be considered as a double-edged sword as NFkB activity is required for inducing innate and adaptive immune response while uncontrolled and constitutive activation results into overexpression of the pro-inflammatory genes which lead to various inflammatory and autoimmune diseases. High NFkB activity has also been reported in many types of tumor cell lines and cancers (**175**). So, our findings suggest that the endogenous level of *Gatad2b* can be a decisive epigenetic regulatory factor to fine-tune the activity of NFkB.

Recent studies on NFkB signaling suggest that even the interferons can activate the classical NFkB pathway in a STAT3-dependent manner. Activation of NFkB through the canonical pathway requires the nuclear translocation of the p50:p65 (RelA) heterodimer. In absence of NFkB inducers this heterodimer remains inactive in the cytosol by the virtue of its binding to inhibitory IkB proteins. During activation IkB kinases (IKKs) phosphorylates IkB eventually resulting into its degradation. This makes the p50:p65 heterodimer free from IkB proteins which is followed by p65 phosphorylation and nuclear translocation of the active p50:p65 heterodimer. This signaling cascade can also be initiated by interferons. Upon binding to their cognitive receptors interferons recruit STAT3 at their cytoplasmic domain which acts as a docking site for PI3K/AKT. This signaling network of STAT3-PI3K/AKT finally leads to the degradation of IkB and nuclear translocation of active NFkB complex (p50:p65) (**176,177**). Additionally TNFa was already reported to act through NFkB signaling pathway. So, in consistency with these findings when we stimulated cells with interferons a profound response of Gatad2b was observed further confirming its involvement as a positive regulator of NFkB not only in a TLR4-restricted mechanism but also during cytokine induced NFkB activation.

Next, we inhibited the NFkB signaling downstrream of TLR4 activation using a pharmacological inhibitor BAY11-7082 which abrogated the expression of the pro-inflammatory markers along with Gatad2b. Since p65 (RelA) is the catalytic subunit of the active NFkB complex during the classical pathway activation, our approach involved using shRNA mediated knock down of p65 to check if there was any co-dependency between *p65* (*RelA*) and *Gatad2b* in terms of regulating the expression of each other. Eventually upon differential gene expression analysis it was observed that absence of *RelA* inhibited the

induction of Gatad2b which further attenuated the level of *Tlr4* and its downstream pro-inflammatory cytokines and chemokines.

If we look into the structural details of NuRD, Chd3/Chd4 are the two ATPase subunits which confer the chromating remodeling activity and Hdac1/Hdac2 are the deacetylase activity containing subunits which drive the repressive function of NuRD. Gatad2a/Gatad2b are the structural components of NuRD and these two can co-exist within a fully functional NuRD complex. Although these are mutually exclusive as a component of NuRD (**178**). Gatad2b can directly bind to histone tails but recruitment to genomic locations is dependent on Mbd proteins namely Mbd2 and Mbd3. Mbd2 can bind to methylated CpG islands of gene promoters and recruits Mbd3/NuRD to maintain a repressive epigenetic signature. However, Mbd3 is not capable of binding to methylated DNA; rather its recruitment onto genomic loci is dependent on Mbd2 and other transcription factors. A recent comparative study exploring the genome wide positioning of Mbd2 and Mbd3 revealed that MBD2–NuRD, in contrast to MBD3–NuRD, converts open chromatin with euchromatic histone modifications into tightly compacted chromatin with repressive histone marks. Genome-wide, a strong enrichment for MBD2 at methylated CpG sequences is found, whereas CpGs bound by MBD3 are devoid of methylation. MBD2-bound genes are generally lower expressed as compared with MBD3-bound genes. When depleting cells for MBD2, the MBD2- bound genes increase their activity, whereas MBD2 plus MBD3-bound genes reduce their activity. Most strikingly, MBD3 is enriched at active promoters, whereas MBD2 is bound at methylated promoters and enriched at exon sequences of active genes. MBD2 and MBD3 contain a conserved MBD motif. The MBD domain of MBD2 but not MBD3 binds methylated DNA. MBD2 also contains a glycine and arginine (GR) rich region and a transcriptional repression domain (TRD) involved in recruiting HDAC. MBD3 contains a glutamate (G) repeat region near the C-terminus. Analysis of Mbd2- and Mbd3-knockout mice confirmed the functional difference between the two MBD protein family members — Mbd3-knockout mice are embryonic lethal, whereas Mbd2-knockout mice are viable and have only mild defects (**179,180**).

As a component of NuRD, Gatad2b is considered to be a transcriptional repressor and its repressive activity is highly dependent upon its recruitment onto genomic loci via Mbd2 and Mbd3. However, NuRD-independent role of Gatad2b as a transcriptional regulator have also been reported and requires further studies. Gatad2a and Gatad2b contain two conserved regions. The amino-terminal conserved region directly interacts with Mbd2 or Mbd3, and the C-terminal conserved region can interact with histone tails and is important for targeting to specific genomic loci (**178,180**).

So far our data suggested a possible role of Gatad2b as a positive regulator of Tlr4 and NFkb siganaling pathway genes. This function must be independent of Mbd2/3 and subsequently independent of NuRD also as being a component of NuRD it is most likely not possible for Gatad2b to act as a positive regulator of gene transcription. In order to check for the functional overlap of Mbd2/3 with *Gatad2b* in our cellular model of inflammation, we again followed a shRNA based knock-down strategy against both *Mbd2* and *Mbd3*. Interestingly a non-parallel phenotype was shown as *Mbd2* knock-down did not lead to any changes in *Tlr4* and other NFkB downstrem gene expression while *Mbd3* knock-down resulted in upregulation of TLR4-mediated NFkB signaling molecules. Altogether these data indicate a possible NuRD-independent role of Gatad2b during the regulation of MSC associated inflammation. More extensive genomics and proteomics approaches are required to confirm this.

Considering the previous findings of our study, we can conclude that *Gatad2b* deficiency in MSCs results into a less immune-responsive or more immune-suppressive stroma as various genomics and proteomics approach confirmed that there was an overall attenuation of the pro-inflammatory pathway genes. This change in immune potential must reflect in terms of regulating immune cells also as MSC derived paracrine molecules control the functional diversity of immune system. Under normal homeostatic conditions, MSCs are considered as anti-inflammatory or immune-suppressive and known as MSC2 whereas during insufficient immune response these MSCs show a great potential of immune plasticity and switch themselves into MSC1 which are considered as pro-inflammatory or immune-stimulant. MSC1 are likely to activate certain subsets of immune cells which are pro-inflammatory in nature and induce immune response like M1 macrophage, Th1 subset of T cells and so on. MSC2 induces the formation of immune-suppressive and anti-inflammatory M2 macrophage, tumor-associated macrphage (TAM), Treg cells, myeloid-derived suppressor cells (MDSCs). To test the immune-regulating potential of MSC-intrinsic *Gatad2b* in vitro, we co-cultured a murine macropahge cell line RAW 264.7 with MSC-CM derived from both *sh-Control* and sh-*Gatad2b* MSCs and checked for M1/M2 polarisation potential of macropahges. Conditioned media derived from Gatad2b-deficient MSC line resulted in less M1 and more M2 differentiation of murine macropahge cells reflecting its immune-suppressive nature. Due to the non-availablility of any mice model of inflammatory diseases in our facility, we did induce an orthotopic tumor using a syngeneic murine breast carcinoma cell line 4T1 and MSC-CM from both *sh-Control* as well as *sh-Gatad2b* was injected intratumorally to check for the types of immune cells that infiltrate within the tumor microenvironment (TME). An increased infiltration of immune-suppressive cell populations was observed as tumors injected with MSC-CM derived from *sh-Gatad2b* MSCs showed a

higher percentage of TAMs and MDSCs suggesting the physiological relevance of the *in vitro* findings.

One of the most commonly encountered physiological health issues resulting from chronic inflammation is bone related disorders. A decrease in bone density, bone formation capacity and an increased bone resorption potential are observed in patients having chronic inflammatory disorders. Although during tissue repair processes an inflammatory stimuli is required for the initiation of osteogenesis but indefinite switch-on mode in the form of chronic inflammation is detrimental for any tissue formation and integrity (**99**). In our study we observed Gtatad2b to respond during the early stage of inflammatory stimuli (between 6h to 12h) which mimics the acute stage of inflammation physiologically. Additionally during the acute phase of LPS treatment osteoblast markers showed an induction in thier gene expression in our *in vitro* cellular model. Since acute inflammation promotes osteogenesis therefore our aim was to find out if there was any response and role of *Gatad2b* downstream of osteogenic cues. Both short-term (BMP-2) and long-term (osteogenic differentiation over 21 days) osteogenic stimuli induced Gatad2b along with induction of the BMP-2/Smad signaling molecules and its downstream osteogenic markers in OP9, HS-5 cell lines as well as in primary human MSCs. Genetic aberrations of *Gatad2b* resulted in impairment of BMP-2/Smad signaling pathway in the form of reduced level of phospho-Smad 1/5/8 level and showed decreased amount of osteogenesis upon Alpl staining by NBT/BCIP reagent ober a 21 day span further confirming its functional role during osteogenesis. In addition, primary human MSCs derived from the bone marrow of MDS patients showed a positive correlation between Gatad2b expression and osteogenic potential.

So considering all our findings it can be concluded that MSC-intrinsic Gatad2b has a pivotal role in stromal immune responses which in turn can also regulate certain inflammation-driven physiological conditions and therefore can be considered as a novel epigenetic marker during MSC mediated inflammatory response.

REFERENCES

1. Charbord, P. (2010) Bone marrow mesenchymal stem cells: historical overview and concepts. *Hum Gene Ther* 21, 1045-1056
2. Friedenstein, A. J., Petrakova, K. V., Kurolesova, A. I., and Frolova, G. P. (1968) Heterotopic of bone marrow. Analysis of precursor cells for osteogenic and hematopoietic tissues. *Transplantation* 6, 230-247
3. Bianco, P., Robey, P. G., and Simmons, P. J. (2008) Mesenchymal stem cells: revisiting history, concepts, and assays. *Cell stem cell* 2, 313-319
4. Pittenger, M. F., Discher, D. E., Peault, B. M., Phinney, D. G., Hare, J. M., and Caplan, A. I. (2019) Mesenchymal stem cell perspective: cell biology to clinical progress. *NPJ Regen Med* 4, 22
5. Morrison, S. J., and Scadden, D. T. (2014) The bone marrow niche for haematopoietic stem cells. *Nature* 505, 327-334
6. Ullah, I., Subbarao, R. B., and Rho, G. J. (2015) Human mesenchymal stem cells - current trends and future prospective. *Biosci Rep* 35
7. Hass, R., Kasper, C., Bohm, S., and Jacobs, R. (2011) Different populations and sources of human mesenchymal stem cells (MSC): A comparison of adult and neonatal tissue-derived MSC. *Cell Commun Signal* 9, 12
8. Chen, Q., Shou, P., Zheng, C., Jiang, M., Cao, G., Yang, Q., Cao, J., Xie, N., Velletri, T., Zhang, X., Xu, C., Zhang, L., Yang, H., Hou, J., Wang, Y., and Shi, Y. (2016) Fate decision of mesenchymal stem cells: adipocytes or osteoblasts? *Cell death and differentiation* 23, 1128-1139
9. Florencio-Silva, R., Sasso, G. R., Sasso-Cerri, E., Simoes, M. J., and Cerri, P. S. (2015) Biology of Bone Tissue: Structure, Function, and Factors That Influence Bone Cells. *Biomed Res Int* 2015, 421746
10. Perez-Campo, F. M., and Riancho, J. A. (2015) Epigenetic Mechanisms Regulating Mesenchymal Stem Cell Differentiation. *Curr Genomics* 16, 368-383
11. Teven, C. M., Liu, X., Hu, N., Tang, N., Kim, S. H., Huang, E., Yang, K., Li, M., Gao, J. L., Liu, H., Natale, R. B., Luther, G., Luo, Q., Wang, L., Rames, R., Bi, Y., Luo, J., Luu, H. H., Haydon, R. C., Reid, R. R., and He, T. C. (2011) Epigenetic regulation of mesenchymal stem cells: a focus on osteogenic and adipogenic differentiation. *Stem Cells Int* 2011, 201371
12. Avgustinova, A., and Benitah, S. A. (2016) Epigenetic control of adult stem cell function. *Nat Rev Mol Cell Biol* 17, 643-658
13. Siddiqi, S., Mills, J., and Matushansky, I. (2010) Epigenetic remodeling of chromatin architecture: exploring tumor differentiation therapies in mesenchymal stem cells and sarcomas. *Curr Stem Cell Res Ther* 5, 63-73
14. Ozkul, Y., and Galderisi, U. (2016) The Impact of Epigenetics on Mesenchymal Stem Cell Biology. *J Cell Physiol* 231, 2393-2401
15. Bentivegna, A., Roversi, G., Riva, G., Paoletta, L., Redaelli, S., Miloso, M., Tredici, G., and Dalpra, L. (2016) The Effect of Culture on Human Bone Marrow Mesenchymal Stem Cells: Focus on DNA Methylation Profiles. *Stem Cells Int* 2016, 5656701
16. Baylin, S. B., and Jones, P. A. (2016) Epigenetic Determinants of Cancer. *Cold Spring Harb Perspect Biol* 8
17. Hodges, C., Kirkland, J. G., and Crabtree, G. R. (2016) The Many Roles of BAF (mSWI/SNF) and PBAF Complexes in Cancer. *Cold Spring Harb Perspect Med* 6
18. Hargreaves, D. C., and Crabtree, G. R. (2011) ATP-dependent chromatin remodeling: genetics, genomics and mechanisms. *Cell research* 21, 396-420
19. Vignali, M., Hassan, A. H., Neely, K. E., and Workman, J. L. (2000) ATP-dependent chromatin-remodeling complexes. *Mol Cell Biol* 20, 1899-1910
20. Hota, S. K., and Bruneau, B. G. (2016) ATP-dependent chromatin remodeling during mammalian development. *Development* 143, 2882-2897
21. Clapier, C. R., Iwasa, J., Cairns, B. R., and Peterson, C. L. (2017) Mechanisms of action and regulation of ATP-dependent chromatin-remodelling complexes. *Nat Rev Mol Cell Biol* 18, 407-422

22. Yoo, A. S., and Crabtree, G. R. (2009) ATP-dependent chromatin remodeling in neural development. *Curr Opin Neurobiol* 19, 120-126
23. Chen, T., and Dent, S. Y. (2014) Chromatin modifiers and remodellers: regulators of cellular differentiation. *Nat Rev Genet* 15, 93-106
24. Gaspar-Maia, A., Alajem, A., Meshorer, E., and Ramalho-Santos, M. (2011) Open chromatin in pluripotency and reprogramming. *Nat Rev Mol Cell Biol* 12, 36-47
25. El Hadidy, N., and Uversky, V. N. (2019) Intrinsic Disorder of the BAF Complex: Roles in Chromatin Remodeling and Disease Development. *Int J Mol Sci* 20
26. Alfert, A., Moreno, N., and Kerl, K. (2019) The BAF complex in development and disease. *Epigenetics Chromatin* 12, 19
27. Young, D. W., Pratap, J., Javed, A., Weiner, B., Ohkawa, Y., van Wijnen, A., Montecino, M., Stein, G. S., Stein, J. L., Imbalzano, A. N., and Lian, J. B. (2005) SWI/SNF chromatin remodeling complex is obligatory for BMP2-induced, Runx2-dependent skeletal gene expression that controls osteoblast differentiation. *J Cell Biochem* 94, 720-730
28. Nguyen, K. H., Xu, F., Flowers, S., Williams, E. A., Fritton, J. C., and Moran, E. (2015) SWI/SNF-Mediated Lineage Determination in Mesenchymal Stem Cells Confers Resistance to Osteoporosis. *Stem cells* 33, 3028-3038
29. Villagra, A., Cruzat, F., Carvallo, L., Paredes, R., Olate, J., van Wijnen, A. J., Stein, G. S., Lian, J. B., Stein, J. L., Imbalzano, A. N., and Montecino, M. (2006) Chromatin remodeling and transcriptional activity of the bone-specific osteocalcin gene require CCAAT/enhancer-binding protein beta-dependent recruitment of SWI/SNF activity. *The Journal of biological chemistry* 281, 22695-22706
30. Flowers, S., Nagl, N. G., Jr., Beck, G. R., Jr., and Moran, E. (2009) Antagonistic roles for BRM and BRG1 SWI/SNF complexes in differentiation. *The Journal of biological chemistry* 284, 10067-10075
31. Grandy, R., Sepulveda, H., Aguilar, R., Pihan, P., Henriquez, B., Olate, J., and Montecino, M. (2011) The Ric-8B gene is highly expressed in proliferating preosteoblastic cells and downregulated during osteoblast differentiation in a SWI/SNF- and C/EBPbeta-mediated manner. *Mol Cell Biol* 31, 2997-3008
32. Sinha, S., Biswas, M., Chatterjee, S. S., Kumar, S., and Sengupta, A. (2020) Pbrm1 Steers Mesenchymal Stromal Cell Osteolineage Differentiation by Integrating PBAF-Dependent Chromatin Remodeling and BMP/TGF-beta Signaling. *Cell Rep* 31, 107570
33. Nagl, N. G., Jr., Patsialou, A., Haines, D. S., Dallas, P. B., Beck, G. R., Jr., and Moran, E. (2005) The p270 (ARID1A/SMARCF1) subunit of mammalian SWI/SNF-related complexes is essential for normal cell cycle arrest. *Cancer Res* 65, 9236-9244
34. van de Peppel, J., Strini, T., Tilburg, J., Westerhoff, H., van Wijnen, A. J., and van Leeuwen, J. P. (2017) Identification of Three Early Phases of Cell-Fate Determination during Osteogenic and Adipogenic Differentiation by Transcription Factor Dynamics. *Stem Cell Reports* 8, 947-960
35. Salma, N., Xiao, H., Mueller, E., and Imbalzano, A. N. (2004) Temporal recruitment of transcription factors and SWI/SNF chromatin-remodeling enzymes during adipogenic induction of the peroxisome proliferator-activated receptor gamma nuclear hormone receptor. *Mol Cell Biol* 24, 4651-4663
36. Agrawal Singh, S., Lerdrup, M., Gomes, A. R., van de Werken, H. J., Vilstrup Johansen, J., Andersson, R., Sandelin, A., Helin, K., and Hansen, K. (2019) PLZF targets developmental enhancers for activation during osteogenic differentiation of human mesenchymal stem cells. *Elife* 8
37. Meyer, M. B., Benkusky, N. A., Sen, B., Rubin, J., and Pike, J. W. (2016) Epigenetic Plasticity Drives Adipogenic and Osteogenic Differentiation of Marrow-derived Mesenchymal Stem Cells. *The Journal of biological chemistry* 291, 17829-17847
38. Olave, I. A., Reck-Peterson, S. L., and Crabtree, G. R. (2002) Nuclear actin and actin-related proteins in chromatin remodeling. *Annu Rev Biochem* 71, 755-781
39. Kapoor, P., and Shen, X. (2014) Mechanisms of nuclear actin in chromatin-remodeling complexes. *Trends Cell Biol* 24, 238-246
40. Sen, B., Xie, Z., Uzer, G., Thompson, W. R., Styner, M., Wu, X., and Rubin, J. (2015) Intranuclear Actin Regulates Osteogenesis. *Stem cells* 33, 3065-3076
41. Giancotti, V., Bergamin, N., Cataldi, P., and Rizzi, C. (2018) Epigenetic Contribution of High-Mobility Group A Proteins to Stem Cell Properties. *Int J Cell Biol* 2018, 3698078
42. Mashtalir, N., D'Avino, A. R., Michel, B. C., Luo, J., Pan, J., Otto, J. E., Zullow, H. J., McKenzie, Z. M., Kubiak, R. L., St Pierre, R., Valencia, A. M., Poynter, S. J., Cassel, S. H.,

Ranish, J. A., and Kadoch, C. (2018) Modular Organization and Assembly of SWI/SNF Family Chromatin Remodeling Complexes. *Cell* 175, 1272-1288 e1220
43. He, L., Tian, X., Zhang, H., Hu, T., Huang, X., Zhang, L., Wang, Z., and Zhou, B. (2014) BAF200 is required for heart morphogenesis and coronary artery development. *PloS one* 9, e109493
44. Kaeser, M. D., Aslanian, A., Dong, M. Q., Yates, J. R., 3rd, and Emerson, B. M. (2008) BRD7, a novel PBAF-specific SWI/SNF subunit, is required for target gene activation and repression in embryonic stem cells. *The Journal of biological chemistry* 283, 32254-32263
45. Yan, Z., Cui, K., Murray, D. M., Ling, C., Xue, Y., Gerstein, A., Parsons, R., Zhao, K., and Wang, W. (2005) PBAF chromatin-remodeling complex requires a novel specificity subunit, BAF200, to regulate expression of selective interferon-responsive genes. *Genes Dev* 19, 1662-1667
46. Wang, Z., Zhai, W., Richardson, J. A., Olson, E. N., Meneses, J. J., Firpo, M. T., Kang, C., Skarnes, W. C., and Tjian, R. (2004) Polybromo protein BAF180 functions in mammalian cardiac chamber maturation. *Genes Dev* 18, 3106-3116
47. Wang, W. (2003) The SWI/SNF family of ATP-dependent chromatin remodelers: similar mechanisms for diverse functions. *Curr Top Microbiol Immunol* 274, 143-169
48. Nie, Z., Xue, Y., Yang, D., Zhou, S., Deroo, B. J., Archer, T. K., and Wang, W. (2000) A specificity and targeting subunit of a human SWI/SNF family-related chromatin-remodeling complex. *Mol Cell Biol* 20, 8879-8888
49. Xu, F., Flowers, S., and Moran, E. (2012) Essential role of ARID2 protein-containing SWI/SNF complex in tissue-specific gene expression. *The Journal of biological chemistry* 287, 5033-5041
50. Marfella, C. G., and Imbalzano, A. N. (2007) The Chd family of chromatin remodelers. *Mutation research* 618, 30-40
51. Sun, F., Yang, Q., Weng, W., Zhang, Y., Yu, Y., Hong, A., Ji, Y., and Pan, Q. (2013) Chd4 and associated proteins function as corepressors of Sox9 expression during BMP-2-induced chondrogenesis. *J Bone Miner Res* 28, 1950-1961
52. Baumgart, S. J., Najafova, Z., Hossan, T., Xie, W., Nagarajan, S., Kari, V., Ditzel, N., Kassem, M., and Johnsen, S. A. (2017) CHD1 regulates cell fate determination by activation of differentiation-induced genes. *Nucleic Acids Res* 45, 7722-7735
53. Lee, H. W., Suh, J. H., Kim, A. Y., Lee, Y. S., Park, S. Y., and Kim, J. B. (2006) Histone deacetylase 1-mediated histone modification regulates osteoblast differentiation. *Mol Endocrinol* 20, 2432-2443
54. Kumar, A., Salimath, B. P., Schieker, M., Stark, G. B., and Finkenzeller, G. (2011) Inhibition of metastasis-associated gene 1 expression affects proliferation and osteogenic differentiation of immortalized human mesenchymal stem cells. *Cell Prolif* 44, 128-138
55. Zhou, C., Zou, J., Zou, S., and Li, X. (2016) INO80 is Required for Osteogenic Differentiation of Human Mesenchymal Stem Cells. *Scientific reports* 6, 35924
56. Breiling, A., and Lyko, F. (2015) Epigenetic regulatory functions of DNA modifications: 5-methylcytosine and beyond. *Epigenetics Chromatin* 8, 24
57. Bork, S., Pfister, S., Witt, H., Horn, P., Korn, B., Ho, A. D., and Wagner, W. (2010) DNA methylation pattern changes upon long-term culture and aging of human mesenchymal stromal cells. *Aging Cell* 9, 54-63
58. Cakouros, D., Hemming, S., Gronthos, K., Liu, R., Zannettino, A., Shi, S., and Gronthos, S. (2019) Specific functions of TET1 and TET2 in regulating mesenchymal cell lineage determination. *Epigenetics Chromatin* 12, 3
59. Shen, W. C., Lai, Y. C., Li, L. H., Liao, K., Lai, H. C., Kao, S. Y., Wang, J., Chuong, C. M., and Hung, S. C. (2019) Methylation and PTEN activation in dental pulp mesenchymal stem cells promotes osteogenesis and reduces oncogenesis. *Nature communications* 10, 2226
60. Thaler, R., Agsten, M., Spitzer, S., Paschalis, E. P., Karlic, H., Klaushofer, K., and Varga, F. (2011) Homocysteine suppresses the expression of the collagen cross-linker lysyl oxidase involving IL-6, Fli1, and epigenetic DNA methylation. *The Journal of biological chemistry* 286, 5578-5588
61. Zhou, C., Liu, Y., Li, X., Zou, J., and Zou, S. (2016) DNA N(6)-methyladenine demethylase ALKBH1 enhances osteogenic differentiation of human MSCs. *Bone research* 4, 16033
62. Tsuda, M., Takahashi, S., Takahashi, Y., and Asahara, H. (2003) Transcriptional co-activators CREB-binding protein and p300 regulate chondrocyte-specific gene expression via association with Sox9. *The Journal of biological chemistry* 278, 27224-27229

63. van Beekum, O., Brenkman, A. B., Grontved, L., Hamers, N., van den Broek, N. J., Berger, R., Mandrup, S., and Kalkhoven, E. (2008) The adipogenic acetyltransferase Tip60 targets activation function 1 of peroxisome proliferator-activated receptor gamma. *Endocrinology* 149, 1840-1849
64. Jing, H., Liao, L., Su, X., Shuai, Y., Zhang, X., Deng, Z., and Jin, Y. (2017) Declining histone acetyltransferase GCN5 represses BMSC-mediated angiogenesis during osteoporosis. *FASEB journal : official publication of the Federation of American Societies for Experimental Biology* 31, 4422-4433
65. Zhang, P., Liu, Y., Jin, C., Zhang, M., Lv, L., Zhang, X., Liu, H., and Zhou, Y. (2016) Histone H3K9 Acetyltransferase PCAF Is Essential for Osteogenic Differentiation Through Bone Morphogenetic Protein Signaling and May Be Involved in Osteoporosis. *Stem cells* 34, 2332-2341
66. Dudakovic, A., Samsonraj, R. M., Paradise, C. R., Galeano-Garces, C., Mol, M. O., Galeano-Garces, D., Zan, P., Galvan, M. L., Hevesi, M., Pichurin, O., Thaler, R., Begun, D. L., Kloen, P., Karperien, M., Larson, A. N., Westendorf, J. J., Cool, S. M., and van Wijnen, A. J. (2020) Inhibition of the epigenetic suppressor EZH2 primes osteogenic differentiation mediated by BMP2. *The Journal of biological chemistry* 295, 7877-7893
67. Hemming, S., Cakouros, D., Codrington, J., Vandyke, K., Arthur, A., Zannettino, A., and Gronthos, S. (2017) EZH2 deletion in early mesenchyme compromises postnatal bone microarchitecture and structural integrity and accelerates remodeling. *FASEB journal : official publication of the Federation of American Societies for Experimental Biology* 31, 1011-1027
68. Camilleri, E. T., Dudakovic, A., Riester, S. M., Galeano-Garces, C., Paradise, C. R., Bradley, E. W., McGee-Lawrence, M. E., Im, H. J., Karperien, M., Krych, A. J., Westendorf, J. J., Larson, A. N., and van Wijnen, A. J. (2018) Loss of histone methyltransferase Ezh2 stimulates an osteogenic transcriptional program in chondrocytes but does not affect cartilage development. *The Journal of biological chemistry* 293, 19001-19011
69. Dudakovic, A., Camilleri, E. T., Paradise, C. R., Samsonraj, R. M., Gluscevic, M., Paggi, C. A., Begun, D. L., Khani, F., Pichurin, O., Ahmed, F. S., Elsayed, R., Elsalanty, M., McGee-Lawrence, M. E., Karperien, M., Riester, S. M., Thaler, R., Westendorf, J. J., and van Wijnen, A. J. (2018) Enhancer of zeste homolog 2 (Ezh2) controls bone formation and cell cycle progression during osteogenesis in mice. *The Journal of biological chemistry* 293, 12894-12907
70. Dudakovic, A., Camilleri, E. T., Riester, S. M., Paradise, C. R., Gluscevic, M., O'Toole, T. M., Thaler, R., Evans, J. M., Yan, H., Subramaniam, M., Hawse, J. R., Stein, G. S., Montecino, M. A., McGee-Lawrence, M. E., Westendorf, J. J., and van Wijnen, A. J. (2016) Enhancer of Zeste Homolog 2 Inhibition Stimulates Bone Formation and Mitigates Bone Loss Caused by Ovariectomy in Skeletally Mature Mice. *The Journal of biological chemistry* 291, 24594-24606
71. Dudakovic, A., Camilleri, E. T., Xu, F., Riester, S. M., McGee-Lawrence, M. E., Bradley, E. W., Paradise, C. R., Lewallen, E. A., Thaler, R., Deyle, D. R., Larson, A. N., Lewallen, D. G., Dietz, A. B., Stein, G. S., Montecino, M. A., Westendorf, J. J., and van Wijnen, A. J. (2015) Epigenetic Control of Skeletal Development by the Histone Methyltransferase Ezh2. *The Journal of biological chemistry* 290, 27604-27617
72. Jung, Y., and Nolta, J. A. (2016) BMI1 Regulation of Self-Renewal and Multipotency in Human Mesenchymal Stem Cells. *Curr Stem Cell Res Ther* 11, 131-140
73. Hemming, S., Cakouros, D., Isenmann, S., Cooper, L., Menicanin, D., Zannettino, A., and Gronthos, S. (2014) EZH2 and KDM6A act as an epigenetic switch to regulate mesenchymal stem cell lineage specification. *Stem cells* 32, 802-815
74. Rojas, A., Aguilar, R., Henriquez, B., Lian, J. B., Stein, J. L., Stein, G. S., van Wijnen, A. J., van Zundert, B., Allende, M. L., and Montecino, M. (2015) Epigenetic Control of the Bone-master Runx2 Gene during Osteoblast-lineage Commitment by the Histone Demethylase JARID1B/KDM5B. *The Journal of biological chemistry* 290, 28329-28342
75. Ye, L., Fan, Z., Yu, B., Chang, J., Al Hezaimi, K., Zhou, X., Park, N. H., and Wang, C. Y. (2012) Histone demethylases KDM4B and KDM6B promotes osteogenic differentiation of human MSCs. *Cell stem cell* 11, 50-61
76. Sinha, K. M., Yasuda, H., Zhou, X., and deCrombrugghe, B. (2014) Osterix and NO66 histone demethylase control the chromatin of Osterix target genes during osteoblast differentiation. *J Bone Miner Res* 29, 855-865
77. Takada, I., Yogiashi, Y., and Kato, S. (2012) Signaling Crosstalk between PPARgamma and BMP2 in Mesenchymal Stem Cells. *PPAR Res* 2012, 607141

78. Takada, I., Kouzmenko, A. P., and Kato, S. (2009) Wnt and PPARgamma signaling in osteoblastogenesis and adipogenesis. *Nat Rev Rheumatol* 5, 442-447
79. Wang, L., Niu, N., Li, L., Shao, R., Ouyang, H., and Zou, W. (2018) H3K36 trimethylation mediated by SETD2 regulates the fate of bone marrow mesenchymal stem cells. *PLoS Biol* 16, e2006522
80. Yin, B., Yu, F., Wang, C., Li, B., Liu, M., and Ye, L. (2019) Epigenetic Control of Mesenchymal Stem Cell Fate Decision via Histone Methyltransferase Ash1l. *Stem cells* 37, 115-127
81. Yang, R., Yu, T., Kou, X., Gao, X., Chen, C., Liu, D., Zhou, Y., and Shi, S. (2018) Tet1 and Tet2 maintain mesenchymal stem cell homeostasis via demethylation of the P2rX7 promoter. *Nature communications* 9, 2143
82. Liu, S., Liu, D., Chen, C., Hamamura, K., Moshaverinia, A., Yang, R., Liu, Y., Jin, Y., and Shi, S. (2015) MSC Transplantation Improves Osteopenia via Epigenetic Regulation of Notch Signaling in Lupus. *Cell metabolism* 22, 606-618
83. Kornicka, K., Marycz, K., Maredziak, M., Tomaszewski, K. A., and Nicpon, J. (2017) The effects of the DNA methyltranfserases inhibitor 5-Azacitidine on ageing, oxidative stress and DNA methylation of adipose derived stem cells. *Journal of cellular and molecular medicine* 21, 387-401
84. Grandi, F. C., and Bhutani, N. (2020) Epigenetic Therapies for Osteoarthritis. *Trends Pharmacol Sci*
85. Im, G. I., and Choi, Y. J. (2013) Epigenetics in osteoarthritis and its implication for future therapeutics. *Expert Opin Biol Ther* 13, 713-721
86. Khan, N. M., and Haqqi, T. M. (2018) Epigenetics in osteoarthritis: Potential of HDAC inhibitors as therapeutics. *Pharmacol Res* 128, 73-79
87. Krosl, J., Mamo, A., Chagraoui, J., Wilhelm, B. T., Girard, S., Louis, I., Lessard, J., Perreault, C., and Sauvageau, G. (2010) A mutant allele of the Swi/Snf member BAF250a determines the pool size of fetal liver hemopoietic stem cell populations. *Blood* 116, 1678-1684
88. Li, R., Zhou, Y., Cao, Z., Liu, L., Wang, J., Chen, Z., Xing, W., Chen, S., Bai, J., Yuan, W., Cheng, T., Xu, M., Yang, F. C., and Zhao, Z. (2018) TET2 Loss Dysregulates the Behavior of Bone Marrow Mesenchymal Stromal Cells and Accelerates Tet2(-/-)-Driven Myeloid Malignancy Progression. *Stem Cell Reports* 10, 166-179
89. Derecka, M., Herman, J. S., Cauchy, P., Ramamoorthy, S., Lupar, E., Grun, D., and Grosschedl, R. (2020) EBF1-deficient bone marrow stroma elicits persistent changes in HSC potential. *Nature immunology* 21, 261-273
90. Pittenger, M. F., Mackay, A. M., Beck, S. C., Jaiswal, R. K., Douglas, R., Mosca, J. D., Moorman, M. A., Simonetti, D. W., Craig, S., and Marshak, D. R. (1999) Multilineage potential of adult human mesenchymal stem cells. *Science* 284, 143-147
91. Jiang, Y., Jahagirdar, B. N., Reinhardt, R. L., Schwartz, R. E., Keene, C. D., Ortiz-Gonzalez, X. R., Reyes, M., Lenvik, T., Lund, T., Blackstad, M., Du, J., Aldrich, S., Lisberg, A., Low, W. C., Largaespada, D. A., and Verfaillie, C. M. (2002) Pluripotency of mesenchymal stem cells derived from adult marrow. *Nature* 418, 41-49
92. Ma, S., Xie, N., Li, W., Yuan, B., Shi, Y., and Wang, Y. (2014) Immunobiology of mesenchymal stem cells. *Cell death and differentiation* 21, 216-225
93. Wang, Y., Chen, X., Cao, W., and Shi, Y. (2014) Plasticity of mesenchymal stem cells in immunomodulation: pathological and therapeutic implications. *Nature immunology* 15, 1009-1016
94. Uccelli, A., Moretta, L., and Pistoia, V. (2008) Mesenchymal stem cells in health and disease. *Nature reviews. Immunology* 8, 726-736
95. Shi, Y., Wang, Y., Li, Q., Liu, K., Hou, J., Shao, C., and Wang, Y. (2018) Immunoregulatory mechanisms of mesenchymal stem and stromal cells in inflammatory diseases. *Nature reviews. Nephrology* 14, 493-507
96. Prockop, D. J., and Oh, J. Y. (2012) Mesenchymal stem/stromal cells (MSCs): role as guardians of inflammation. *Molecular therapy : the journal of the American Society of Gene Therapy* 20, 14-20
97. Ranganath, S. H., Levy, O., Inamdar, M. S., and Karp, J. M. (2012) Harnessing the mesenchymal stem cell secretome for the treatment of cardiovascular disease. *Cell stem cell* 10, 244-258
98. Chen, L., Deng, H., Cui, H., Fang, J., Zuo, Z., Deng, J., Li, Y., Wang, X., and Zhao, L. (2018) Inflammatory responses and inflammation-associated diseases in organs. *Oncotarget* 9, 7204-7218

99. Eming, S. A., Krieg, T., and Davidson, J. M. (2007) Inflammation in wound repair: molecular and cellular mechanisms. *The Journal of investigative dermatology* 127, 514-525
100. Eggenhofer, E., Luk, F., Dahlke, M. H., and Hoogduijn, M. J. (2014) The life and fate of mesenchymal stem cells. *Frontiers in immunology* 5, 148
101. Li, M. O., and Flavell, R. A. (2008) Contextual regulation of inflammation: a duet by transforming growth factor-beta and interleukin-10. *Immunity* 28, 468-476
102. Li, Z., Kupcsik, L., Yao, S. J., Alini, M., and Stoddart, M. J. (2010) Mechanical load modulates chondrogenesis of human mesenchymal stem cells through the TGF-beta pathway. *Journal of cellular and molecular medicine* 14, 1338-1346
103. Crane, J. L., and Cao, X. (2014) Bone marrow mesenchymal stem cells and TGF-beta signaling in bone remodeling. *The Journal of clinical investigation* 124, 466-472
104. Bernardo, M. E., and Fibbe, W. E. (2013) Mesenchymal stromal cells: sensors and switchers of inflammation. *Cell stem cell* 13, 392-402
105. Waterman, R. S., Tomchuck, S. L., Henkle, S. L., and Betancourt, A. M. (2010) A new mesenchymal stem cell (MSC) paradigm: polarization into a pro-inflammatory MSC1 or an Immunosuppressive MSC2 phenotype. *PloS one* 5, e10088
106. Dumitru, C. A., Hemeda, H., Jakob, M., Lang, S., and Brandau, S. (2014) Stimulation of mesenchymal stromal cells (MSCs) via TLR3 reveals a novel mechanism of autocrine priming. *FASEB journal : official publication of the Federation of American Societies for Experimental Biology* 28, 3856-3866
107. Delarosa, O., Dalemans, W., and Lombardo, E. (2012) Toll-like receptors as modulators of mesenchymal stem cells. *Frontiers in immunology* 3, 182
108. Xu, X., Zheng, L., Yuan, Q., Zhen, G., Crane, J. L., Zhou, X., and Cao, X. (2018) Transforming growth factor-beta in stem cells and tissue homeostasis. *Bone research* 6, 2
109. Sheng, H., Wang, Y., Jin, Y., Zhang, Q., Zhang, Y., Wang, L., Shen, B., Yin, S., Liu, W., Cui, L., and Li, N. (2008) A critical role of IFNgamma in priming MSC-mediated suppression of T cell proliferation through up-regulation of B7-H1. *Cell research* 18, 846-857
110. Akiyama, K., Chen, C., Wang, D., Xu, X., Qu, C., Yamaza, T., Cai, T., Chen, W., Sun, L., and Shi, S. (2012) Mesenchymal-stem-cell-induced immunoregulation involves FAS-ligand-/FAS-mediated T cell apoptosis. *Cell stem cell* 10, 544-555
111. Chinnadurai, R., Copland, I. B., Patel, S. R., and Galipeau, J. (2014) IDO-independent suppression of T cell effector function by IFN-gamma-licensed human mesenchymal stromal cells. *Journal of immunology* 192, 1491-1501
112. Davies, L. C., Heldring, N., Kadri, N., and Le Blanc, K. (2017) Mesenchymal Stromal Cell Secretion of Programmed Death-1 Ligands Regulates T Cell Mediated Immunosuppression. *Stem cells* 35, 766-776
113. Augello, A., Tasso, R., Negrini, S. M., Amateis, A., Indiveri, F., Cancedda, R., and Pennesi, G. (2005) Bone marrow mesenchymal progenitor cells inhibit lymphocyte proliferation by activation of the programmed death 1 pathway. *European journal of immunology* 35, 1482-1490
114. Fregni, G., Quinodoz, M., Moller, E., Vuille, J., Galland, S., Fusco, C., Martin, P., Letovanec, I., Provero, P., Rivolta, C., Riggi, N., and Stamenkovic, I. (2018) Reciprocal modulation of mesenchymal stem cells and tumor cells promotes lung cancer metastasis. *EBioMedicine* 29, 128-145
115. Poggi, A., Varesano, S., and Zocchi, M. R. (2018) How to Hit Mesenchymal Stromal Cells and Make the Tumor Microenvironment Immunostimulant Rather Than Immunosuppressive. *Frontiers in immunology* 9, 262
116. Hong, I. S., Lee, H. Y., and Kang, K. S. (2014) Mesenchymal stem cells and cancer: friends or enemies? *Mutation research* 768, 98-106
117. Pure, E., and Lo, A. (2016) Can Targeting Stroma Pave the Way to Enhanced Antitumor Immunity and Immunotherapy of Solid Tumors? *Cancer immunology research* 4, 269-278
118. Sun, Z., Wang, S., and Zhao, R. C. (2014) The roles of mesenchymal stem cells in tumor inflammatory microenvironment. *Journal of hematology & oncology* 7, 14
119. Jing, Y., Han, Z., Liu, Y., Sun, K., Zhang, S., Jiang, G., Li, R., Gao, L., Zhao, X., Wu, D., Cai, X., Wu, M., and Wei, L. (2012) Mesenchymal stem cells in inflammation microenvironment accelerates hepatocellular carcinoma metastasis by inducing epithelial-mesenchymal transition. *PloS one* 7, e43272
120. Liu, Y., Han, Z. P., Zhang, S. S., Jing, Y. Y., Bu, X. X., Wang, C. Y., Sun, K., Jiang, G. C., Zhao, X., Li, R., Gao, L., Zhao, Q. D., Wu, M. C., and Wei, L. X. (2011) Effects of

inflammatory factors on mesenchymal stem cells and their role in the promotion of tumor angiogenesis in colon cancer. *The Journal of biological chemistry* 286, 25007-25015
121. Ren, G., Zhao, X., Wang, Y., Zhang, X., Chen, X., Xu, C., Yuan, Z. R., Roberts, A. I., Zhang, L., Zheng, B., Wen, T., Han, Y., Rabson, A. B., Tischfield, J. A., Shao, C., and Shi, Y. (2012) CCR2-dependent recruitment of macrophages by tumor-educated mesenchymal stromal cells promotes tumor development and is mimicked by TNFalpha. *Cell stem cell* 11, 812-824
122. Casado, J. G., Tarazona, R., and Sanchez-Margallo, F. M. (2013) NK and MSCs crosstalk: the sense of immunomodulation and their sensitivity. *Stem cell reviews and reports* 9, 184-189
123. Hu, C. D., Kosaka, Y., Marcus, P., Rashedi, I., and Keating, A. (2019) Differential Immunomodulatory Effects of Human Bone Marrow-Derived Mesenchymal Stromal Cells on Natural Killer Cells. *Stem cells and development* 28, 933-943
124. Krampera, M., Cosmi, L., Angeli, R., Pasini, A., Liotta, F., Andreini, A., Santarlasci, V., Mazzinghi, B., Pizzolo, G., Vinante, F., Romagnani, P., Maggi, E., Romagnani, S., and Annunziato, F. (2006) Role for interferon-gamma in the immunomodulatory activity of human bone marrow mesenchymal stem cells. *Stem cells* 24, 386-398
125. Rasmusson, I., Ringden, O., Sundberg, B., and Le Blanc, K. (2003) Mesenchymal stem cells inhibit the formation of cytotoxic T lymphocytes, but not activated cytotoxic T lymphocytes or natural killer cells. *Transplantation* 76, 1208-1213
126. Spaggiari, G. M., Capobianco, A., Abdelrazik, H., Becchetti, F., Mingari, M. C., and Moretta, L. (2008) Mesenchymal stem cells inhibit natural killer-cell proliferation, cytotoxicity, and cytokine production: role of indoleamine 2,3-dioxygenase and prostaglandin E2. *Blood* 111, 1327-1333
127. Poggi, A., Prevosto, C., Massaro, A. M., Negrini, S., Urbani, S., Pierri, I., Saccardi, R., Gobbi, M., and Zocchi, M. R. (2005) Interaction between human NK cells and bone marrow stromal cells induces NK cell triggering: role of NKp30 and NKG2D receptors. *Journal of immunology* 175, 6352-6360
128. Spaggiari, G. M., Capobianco, A., Becchetti, S., Mingari, M. C., and Moretta, L. (2006) Mesenchymal stem cell-natural killer cell interactions: evidence that activated NK cells are capable of killing MSCs, whereas MSCs can inhibit IL-2-induced NK-cell proliferation. *Blood* 107, 1484-1490
129. Beyth, S., Borovsky, Z., Mevorach, D., Liebergall, M., Gazit, Z., Aslan, H., Galun, E., and Rachmilewitz, J. (2005) Human mesenchymal stem cells alter antigen-presenting cell maturation and induce T-cell unresponsiveness. *Blood* 105, 2214-2219
130. Nauta, A. J., Kruisselbrink, A. B., Lurvink, E., Willemze, R., and Fibbe, W. E. (2006) Mesenchymal stem cells inhibit generation and function of both CD34+-derived and monocyte-derived dendritic cells. *Journal of immunology* 177, 2080-2087
131. Zhang, B., Liu, R., Shi, D., Liu, X., Chen, Y., Dou, X., Zhu, X., Lu, C., Liang, W., Liao, L., Zenke, M., and Zhao, R. C. (2009) Mesenchymal stem cells induce mature dendritic cells into a novel Jagged-2-dependent regulatory dendritic cell population. *Blood* 113, 46-57
132. Chabannes, D., Hill, M., Merieau, E., Rossignol, J., Brion, R., Soulillou, J. P., Anegon, I., and Cuturi, M. C. (2007) A role for heme oxygenase-1 in the immunosuppressive effect of adult rat and human mesenchymal stem cells. *Blood* 110, 3691-3694
133. De Miguel, M. P., Fuentes-Julian, S., Blazquez-Martinez, A., Pascual, C. Y., Aller, M. A., Arias, J., and Arnalich-Montiel, F. (2012) Immunosuppressive properties of mesenchymal stem cells: advances and applications. *Current molecular medicine* 12, 574-591
134. Nasef, A., Chapel, A., Mazurier, C., Bouchet, S., Lopez, M., Mathieu, N., Sensebe, L., Zhang, Y., Gorin, N. C., Thierry, D., and Fouillard, L. (2007) Identification of IL-10 and TGF-beta transcripts involved in the inhibition of T-lymphocyte proliferation during cell contact with human mesenchymal stem cells. *Gene expression* 13, 217-226
135. Najar, M., Fayyad-Kazan, H., Faour, W. H., Merimi, M., Sokal, E. M., Lombard, C. A., and Fahmi, H. (2019) Immunological modulation following bone marrow-derived mesenchymal stromal cells and Th17 lymphocyte co-cultures. *Inflammation research : official journal of the European Histamine Research Society ... [et al.]* 68, 203-213
136. Zimmermann, J. A., Hettiaratchi, M. H., and McDevitt, T. C. (2017) Enhanced Immunosuppression of T Cells by Sustained Presentation of Bioactive Interferon-gamma Within Three-Dimensional Mesenchymal Stem Cell Constructs. *Stem cells translational medicine* 6, 223-237
137. Francois, M., Romieu-Mourez, R., Li, M., and Galipeau, J. (2012) Human MSC suppression correlates with cytokine induction of indoleamine 2,3-dioxygenase and bystander M2

macrophage differentiation. *Molecular therapy : the journal of the American Society of Gene Therapy* 20, 187-195
138. Nemeth, K., Leelahavanichkul, A., Yuen, P. S., Mayer, B., Parmelee, A., Doi, K., Robey, P. G., Leelahavanichkul, K., Koller, B. H., Brown, J. M., Hu, X., Jelinek, I., Star, R. A., and Mezey, E. (2009) Bone marrow stromal cells attenuate sepsis via prostaglandin E(2)-dependent reprogramming of host macrophages to increase their interleukin-10 production. *Nature medicine* 15, 42-49
139. Philipp, D., Suhr, L., Wahlers, T., Choi, Y. H., and Paunel-Gorgulu, A. (2018) Preconditioning of bone marrow-derived mesenchymal stem cells highly strengthens their potential to promote IL-6-dependent M2b polarization. *Stem cell research & therapy* 9, 286
140. Yu, T., Liu, D., Zhang, T., Zhou, Y., Shi, S., and Yang, R. (2019) Inhibition of Tet1- and Tet2-mediated DNA demethylation promotes immunomodulation of periodontal ligament stem cells. *Cell death & disease* 10, 780
141. Azevedo, R. I., Minskaia, E., Fernandes-Platzgummer, A., Vieira, A. I. S., da Silva, C. L., Cabral, J. M. S., and Lacerda, J. F. (2020) Mesenchymal stromal cells induce regulatory T cells via epigenetic conversion of human conventional CD4 T cells in vitro. *Stem cells* 38, 1007-1019
142. Khosravi, M., Bidmeshkipour, A., Cohen, J. L., Moravej, A., Hojjat-Assari, S., Naserian, S., and Karimi, M. H. (2018) Induction of CD4(+)CD25(+)FOXP3(+) regulatory T cells by mesenchymal stem cells is associated with modulation of ubiquitination factors and TSDR demethylation. *Stem cell research & therapy* 9, 273
143. Yang, R., Qu, C., Zhou, Y., Konkel, J. E., Shi, S., Liu, Y., Chen, C., Liu, S., Liu, D., Chen, Y., Zandi, E., Chen, W., Zhou, Y., and Shi, S. (2015) Hydrogen Sulfide Promotes Tet1- and Tet2-Mediated Foxp3 Demethylation to Drive Regulatory T Cell Differentiation and Maintain Immune Homeostasis. *Immunity* 43, 251-263
144. Khosravi, M., Bidmeshkipour, A., Moravej, A., Hojjat-Assari, S., Naserian, S., and Karimi, M. H. (2018) Induction of CD4(+)CD25(+)Foxp3(+) regulatory T cells by mesenchymal stem cells is associated with RUNX complex factors. *Immunologic research* 66, 207-218
145. Loh, C., Park, S. H., Lee, A., Yuan, R., Ivashkiv, L. B., and Kalliolias, G. D. (2019) TNF-induced inflammatory genes escape repression in fibroblast-like synoviocytes: transcriptomic and epigenomic analysis. *Annals of the rheumatic diseases* 78, 1205-1214
146. Ai, R., Laragione, T., Hammaker, D., Boyle, D. L., Wildberg, A., Maeshima, K., Palescandolo, E., Krishna, V., Pocalyko, D., Whitaker, J. W., Bai, Y., Nagpal, S., Bachman, K. E., Ainsworth, R. I., Wang, M., Ding, B., Gulko, P. S., Wang, W., and Firestein, G. S. (2018) Comprehensive epigenetic landscape of rheumatoid arthritis fibroblast-like synoviocytes. *Nature communications* 9, 1921
147. De Witte, S. F. H., Peters, F. S., Merino, A., Korevaar, S. S., Van Meurs, J. B. J., O'Flynn, L., Elliman, S. J., Newsome, P. N., Boer, K., Baan, C. C., and Hoogduijn, M. J. (2018) Epigenetic changes in umbilical cord mesenchymal stromal cells upon stimulation and culture expansion. *Cytotherapy* 20, 919-929
148. Teklemariam, T., Purandare, B., Zhao, L., and Hantash, B. M. (2014) Inhibition of DNA methylation enhances HLA-G expression in human mesenchymal stem cells. *Biochemical and biophysical research communications* 452, 753-759
149. Rovira Gonzalez, Y. I., Lynch, P. J., Thompson, E. E., Stultz, B. G., and Hursh, D. A. (2016) In vitro cytokine licensing induces persistent permissive chromatin at the Indoleamine 2,3-dioxygenase promoter. *Cytotherapy* 18, 1114-1128
150. Lee, S., Kim, H. S., Roh, K. H., Lee, B. C., Shin, T. H., Yoo, J. M., Kim, Y. L., Yu, K. R., Kang, K. S., and Seo, K. W. (2015) DNA methyltransferase inhibition accelerates the immunomodulation and migration of human mesenchymal stem cells. *Scientific reports* 5, 8020
151. Kim, K. W., Kim, H. J., Kim, B. M., Kwon, Y. R., Kim, H. R., and Kim, Y. J. (2018) Epigenetic modification of mesenchymal stromal cells enhances their suppressive effects on the Th17 responses of cells from rheumatoid arthritis patients. *Stem cell research & therapy* 9, 208
152. Vella, S., Conaldi, P. G., Cova, E., Meloni, F., Liotta, R., Cuzzocrea, S., Martino, L., Bertani, A., Luca, A., and Vitulo, P. (2018) Lung resident mesenchymal cells isolated from patients with the Bronchiolitis Obliterans Syndrome display a deregulated epigenetic profile. *Scientific reports* 8, 11167
153. Lim, J., Lee, S., Ju, H., Kim, Y., Heo, J., Lee, H. Y., Choi, K. C., Son, J., Oh, Y. M., Kim, I. G., and Shin, D. M. (2017) Valproic acid enforces the priming effect of sphingosine-1 phosphate on human mesenchymal stem cells. *International journal of molecular medicine* 40, 739-747

154. Kim, S. H., In Choi, H., Choi, M. R., An, G. Y., Binas, B., Jung, K. H., and Chai, Y. G. (2020) Epigenetic regulation of IFITM1 expression in lipopolysaccharide-stimulated human mesenchymal stromal cells. *Stem cell research & therapy* 11, 16
155. Inoue, S., Popp, F. C., Koehl, G. E., Piso, P., Schlitt, H. J., Geissler, E. K., and Dahlke, M. H. (2006) Immunomodulatory effects of mesenchymal stem cells in a rat organ transplant model. *Transplantation* 81, 1589-1595
156. Chen, X., Gan, Y., Li, W., Su, J., Zhang, Y., Huang, Y., Roberts, A. I., Han, Y., Li, J., Wang, Y., and Shi, Y. (2014) The interaction between mesenchymal stem cells and steroids during inflammation. *Cell death & disease* 5, e1009

157. Ramirez-Carrozzi VR, Nazarian AA, Li CC, Gore SL, Sridharan R, Imbalzano AN, Smale ST. Selective and antagonistic functions of SWI/SNF and Mi-2beta nucleosome remodeling complexes during an inflammatory response. *Genes Dev*. 2006 Feb 1;20(3):282-96.

158. El-Nikhely N, Karger A, Sarode P, Singh I, Weigert A, Wietelmann A, Stiewe T, Dammann R, Fink L, Grimminger F, Barreto G, Seeger W, Pullamsetti SS, Rapp UR, Savai R. Metastasis-Associated Protein 2 Represses NF-κB to Reduce Lung Tumor Growth and Inflammation. Cancer Res. 2020 Oct 1;80(19):4199-4211. doi: 10.1158/0008-5472.CAN-20-1158. Epub 2020 Aug 14. *Erratum in: Cancer Res*. 2022 Feb 15;82(4):736.

159. M. Trizzino, A. Zucco, S. Deliard, F. Wang, E. Barbieri, F. Veglia, D. Gabrilovich, A. Gardini, EGR1 is a gatekeeper of inflammatory enhancers in human macrophages. *Sci. Adv.* 7, eaaz8836 (2021).

160. Oh KS, Gottschalk RA, Lounsbury NW, Sun J, Dorrington MG, Baek S, Sun G, Wang Z, Krauss KS, Milner JD, Dutta B, Hager GL, Sung MH, Fraser IDC. Dual Roles for Ikaros in Regulation of Macrophage Chromatin State and Inflammatory Gene Expression. *J Immunol*. 2018 Jul 15;201(2):757-771.

161. Suresh B. Pakala, Sirigiri Divijendra Natha Reddy, Tri M. Bui-Nguyen, Siddharth S. Rangparia,Anitha Bommana, Rakesh Kumar. MTA1 Coregulator Regulates LPS Response via MyD88-dependent Signaling. *Journal of Biological Chemistry*, Volume 285, Issue 43, 2010, Pages 32787-32792

162. Elizabeth E. Hull, McKale R. Montgomery, Kathryn J. Leyva, "HDAC Inhibitors as Epigenetic Regulators of the Immune System: Impacts on Cancer Therapy and Inflammatory Diseases", *BioMed Research International*, vol. 2016, Article ID 8797206, 15 pages, 2016.

163. Halili MA, Andrews MR, Sweet MJ, Fairlie DP. Histone deacetylase inhibitors in inflammatory disease. Curr Top Med Chem. 2009;9(3):309-19.

164. Pfefferli, C., Müller, F., Jaźwińska, A., & Wicky, C. (2014). Specific NuRD components are required for fin regeneration in zebrafish. *BMC biology*, *12*, 30.

165. Amarasekara DS, Kim S, Rho J. Regulation of Osteoblast Differentiation by Cytokine Networks. Int J Mol Sci. 2021 Mar 11;22(6):2851.

166. Chen, L., Deng, H., Cui, H., Fang, J., Zuo, Z., Deng, J., Li, Y., Wang, X., & Zhao, L. (2017). Inflammatory responses and inflammation-associated diseases in organs. *Oncotarget*, *9*(6), 7204–7218

167. David S. Pearlman, Pathophysiology of the inflammatory response, Journal of Allergy and Clinical Immunology, Volume 104, Issue 4, 1999, Pages s132-s137

168. Liu, J., & Cao, X. (2016). Cellular and molecular regulation of innate inflammatory responses. *Cellular & molecular immunology*, *13*(6), 711–721.

169. Mogensen T. H. (2009). Pathogen recognition and inflammatory signaling in innate immune defenses. *Clinical microbiology reviews*, *22*(2), 240–273.

170. Newton K, Dixit VM. Signaling in innate immunity and inflammation. Cold Spring Harb Perspect Biol. 2012 Mar 1;4(3):a006049.

171. Mark D. Turner, Belinda Nedjai, Tara Hurst, Daniel J. Pennington, Cytokines and chemokines: At the crossroads of cell signalling and inflammatory disease, Biochimica et Biophysica Acta (BBA) - Molecular Cell Research, Volume 1843, Issue 11, 2014, Pages 2563-2582.

172. Owen KL, Brockwell NK, Parker BS. JAK-STAT Signaling: A Double-Edged Sword of Immune Regulation and Cancer Progression. Cancers (Basel). 2019 Dec 12;11(12):2002.

173. Parveen N, Dhawan S. DNA Methylation Patterning and the Regulation of Beta Cell Homeostasis. Front Endocrinol (Lausanne). 2021 May 7;12:651258.

174. Sun W, Lv S, Li H, Cui W, Wang L. Enhancing the Anticancer Efficacy of Immunotherapy through Combination with Histone Modification Inhibitors. *Genes*. 2018; 9(12):633.

175. Taniguchi K, Karin M. NF-κB, inflammation, immunity and cancer: coming of age. Nat Rev Immunol. 2018 May;18(5):309-324.

176. Pfeffer LM. The role of nuclear factor κB in the interferon response. J Interferon Cytokine Res. 2011 Jul;31(7):553-9.

177. Piaszyk-Borychowska A, Széles L, Csermely A, Chiang HC, Wesoły J, Lee CK, Nagy L, Bluyssen HAR. Signal Integration of IFN-I and IFN-II With TLR4 Involves Sequential Recruitment of STAT1-Complexes and NFκB to Enhance Pro-inflammatory Transcription. Front Immunol. 2019 Jun 4;10:1253.

178. Lai, A., Wade, P. Cancer biology and NuRD: a multifaceted chromatin remodelling complex. *Nat Rev Cancer* **11,** 588–596 (2011).

179. Le Guezennec X, Vermeulen M, Brinkman AB, Hoeijmakers WA, Cohen A, Lasonder E, Stunnenberg HG. MBD2/NuRD and MBD3/NuRD, two distinct complexes with different biochemical and functional properties. Mol Cell Biol. 2006 Feb;26(3):843-51.

180. Brackertz M, Boeke J, Zhang R, Renkawitz R. Two highly related p66 proteins comprise a new family of potent transcriptional repressors interacting with MBD2 and MBD3. J Biol Chem. 2002 Oct 25;277(43):40958-66.

PUBLICATIONS

1. **Chakraborty S**, Sinha S, Sengupta A. Emerging trends in chromatin remodeler plasticity in mesenchymal stromal cell function. ***FASEB J. 2021***; 35:e21234.

2. Sinha S, **Chakraborty S**, Sengupta A. Establishment of a Long-Term Co-culture Assay for Mesenchymal Stromal Cells and Hematopoietic Stem/Progenitors. **STAR Protoc. 2020**; 1(3):100161.

3. Biswas M, Chatterjee SS, Boila LD, **Chakraborty S**, Banerjee D, Sengupta A. MBD3/NuRD loss participates with KDM6A program to promote DOCK5/8 expression and Rac GTPase activation in human acute myeloid leukemia. ***FASEB J. 2019***; 33(4):5268-5286.

4. Das N, Giri A, **Chakraborty S**, Bhattacharjee P. Association of single nucleotide polymorphism with arsenic-induced skin lesions and genetic damage in exposed population of West Bengal, India. ***Mutation Research - Genetic Toxicology and Environmental Mutagenesis 2016*;** 809:50-56.

5. **Chakraborty S**, ... , Sengupta A. Nucleosome remodeling in Mesenchymal stromal cells driven immune regulation. (*Manuscript under preparation*)

Received: 29 September 2020 | Revised: 10 November 2020 | Accepted: 13 November 2020

DOI: 10.1096/fj.202002232R

REVIEW

THE FASEB JOURNAL

Emerging trends in chromatin remodeler plasticity in mesenchymal stromal cell function

Sayan Chakraborty[1,2] | **Sayantani Sinha**[1,2] | **Amitava Sengupta**[1,2]

[1]Stem Cell & Leukemia Laboratory, Cancer Biology & Inflammatory Disorder Division, CSIR-Indian Institute of Chemical Biology, Kolkata, India

[2]Translational Research Unit of Excellence (TRUE), Kolkata, India

Correspondence
Amitava Sengupta, Stem Cell & Leukemia Laboratory, Cancer Biology & Inflammatory Disorder Division, CSIR-Indian Institute of Chemical Biology, 4, Raja S.C. Mullick Road, Jadavpur, Kolkata 700032, West Bengal, India.
Email: amitava.sengupta@iicb.res.in; amitava.iicb@gmail.com

Funding information
Council of Scientific & Industrial Research (CSIR), Grant/Award Number: MMP/HCP-0008; Department of Biotechnology (DBT), Grant/Award Number: BT/RLF/RE-ENTRY/06/2010 and BT/PR13023/MED/31/311/2015; SERB-Department of Science & Technology (DST), Grant/Award Number: SB/SO/HS-053/2013; Indian Council of Medical Research, Grant/Award Number: INDO/FRC/452/S-11/2019-20-lHD

Abstract

Emerging evidences highlight importance of epigenetic regulation and their integration with transcriptional and cell signaling machinery in determining tissue resident adult pluripotent mesenchymal stem/stromal cell (MSC) activity, lineage commitment, and multicellular development. Histone modifying enzymes and large multi-subunit chromatin remodeling complexes and their cell type-specific plasticity remain the central defining features of gene regulation and establishment of tissue identity. Modulation of transcription factor expression gradient ex vivo and concomitant flexibility of higher order chromatin architecture in response to signaling cues are exciting approaches to regulate MSC activity and tissue rejuvenation. Being an important constituent of the adult bone marrow microenvironment/niche, pathophysiological perturbation in MSC homeostasis also causes impaired hematopoietic stem/progenitor cell function in a non-cell autonomous mechanism. In addition, pluripotent MSCs can function as immune regulatory cells, and they reside at the crossroad of innate and adaptive immune response pathways. Research in the past few years suggest that MSCs/stromal fibroblasts significantly contribute to the establishment of immunosuppressive microenvironment in shaping antitumor immunity. Therefore, it is important to understand mesenchymal stromal epigenome and transcriptional regulation to leverage its applications in regenerative medicine, epigenetic memory-guided trained immunity, immune-metabolic rewiring, and precision immune reprogramming. In this review, we highlight the latest developments and prospects in chromatin biology in determining MSC function in the context of lineage commitment and immunomodulation.

KEYWORDS

cell differentiation, chromatin remodeling, epigenetics, gene regulation, hematopoiesis, inflammation, innate immunity, mesenchymal stem cells (MSCs), tumor microenvironment

Abbreviations: 5mc, 5-methyl cytosine; Alpl, alkaline phosphatase; BMP, bone morphogenetic protein; CAR cell, Cxcl12-abundant reticular cell; CHD, chromodomain helicase DNA binding; DAMP, *damage-associated molecular pattern*; ES cell, embryonic stem cell; HDAC, histone deacetylase; HLA, human leukocyte antigen; HMGA, high-mobility group protein A; HSPC, hematopoietic stem and progenitor cell; IFN, interferon; *IFITM1*, *interferon-induced transmembrane protein 1*; IRF, interferon-regulatory factor; iTreg, induced Treg; KDM, lysine demethylase; LPS, lipopolysaccharide; MSC, mesenchymal stromal cell; MSCF, mesenchymal stromal cell and fibroblast; N6mA, N6-methyladenine; NuRD, nucleosome remodeler deacetylase; *PAMP*, *pattern-associated molecular pattern*; PBAF, polybromo brahma-associated factor; PRC, polycomb repressive complex; PRR, pattern recognition receptor; S1P, sphingosine-1 phosphate; SWI/SNF, switch/sucrose non-fermentable; Tet, ten-eleven translocation; TGF-β, transforming growth factor-β; TIME, tumor immune microenvironment; TLR, toll like receptor; Treg cell, regulatory T cell; TSS, transcription start site.

Sayan Chakraborty and Sayantani Sinha have contributed equally.

1 | INTRODUCTION

Multipotency (*ability to differentiate into multiple mature cell types*) governed by asymmetric cell division, and self-renewal capacity (*ability to replenish the stem cell pool*) through symmetrical division are the central features of adult pluripotent stem cells that regulate tissue homeostasis, regeneration, and repair. One of the most widely studied multipotent stem cells is mesenchymal stem/stromal cell population (MSCs) which was initially discovered in the bone marrow stroma in 1960s and characterized as the "colony-forming unit fibroblast".[1,2] The existence of a stromal system with stromal stem cell as the major node was popularized about three decades ago.[3] MSCs in general are heterogeneous in nature, specific tissue-resident MSCs are able to differentiate into osteoblasts, adipocytes, and chondrocytes, and they overall constitute an integral component of tissue and immune-microenvironment.

Bone marrow-derived MSCs are the most commonly isolated and characterized source of cells constituting the bone marrow microenvironment or niche.[4-7] Other major sources of adult MSCs include adipose tissue, umbilical cord blood, synovial membrane, and dental pulp.[8] Unlike hematopoietic stem/progenitor cells (HSPCs), lack of expression of enough cell surface markers remains a challenge for a robust immunophenotypic identification of MSCs. In general, mammalian MSCs have been found to be negative for expression of CD45 and CD31, while they express mesodermal markers CD29, CD44, CD51, CD73, CD90, CD105, CD106, CD146, and CD166.[9] Ex vivo tri-lineage differentiation in presence of conditioned media are commonly used as surrogate assays for characterization of MSCs.[10] Bone initiated diseases like osteoporosis, osteopetrosis and osteopenia emerge due to deranged MSC lineage commitment, osteogenesis, and bone resorption.[11]

In the past few years growing body of evidence suggests molecular regulation for MSC lineage commitment and differentiation in response to signaling cues and immunomodulation. Recent studies indicate that epigenetic mechanisms that attune histone and DNA modifications could be critical for MSC lineage specification and homeostasis.[12,13] Although transcriptional control of MSC physiology has been widely studied, little is known about the epigenetic mechanisms underlining key aspects of MSC function. Epigenetic changes regulating gene expression is heritable and is reflected in cells that have undergone terminal differentiation.[14] Comparison of methylation architecture of embryonic stem (ES) cells and MSCs highlights MSCs have relatively limited differentiation potential and may frequently involve chromatin-based remodeling strategies to undergo lineage commitment.[13,15,16] Such epigenetic regulation provides plasticity to the cells, favoring context dependent adaptation, multicellular development, and regeneration.[17,18] Epigenetic changes being reversible also provides an opportunity for therapeutic tissue regeneration.[19] Therefore, MSC epigenetics remains an intriguing area of investigation holding promise for both fundamental and translational research. In this review, we summarize our current knowledge of epigenetic changes associated with MSC lineage commitment, non-cell autonomous regulation of hematopoiesis and immune modulation.

2 | NON-CELL AUTONOMOUS REGULATION OF HEMATOPOIESIS

Mammalian hematopoietic stem/progenitor cell (HSPC) function within bone marrow microenvironment is regulated by stromal niche-derived soluble factors/cytokines and cell-to-cell communication between HSPCs and MSCs.[5,20-22] Mice expressing mutant alleles of Swi/Snf component *Arid1a* (Baf250a) were suggested to control fetal liver HSC pool and primitive hematopoiesis in a stroma-dependent mechanism, highlighting non-cell autonomous chromatin regulation in hematopoiesis.[23] Interestingly, in our recent report, we have revealed that mesenchymal stromal loss of polybromo Swi/Snf subunit *Pbrm1* significantly impair HSPC long-term clonogenic potential.[24] In addition, nonhematopoietic loss of *Tet2* increases MSC osteoblast differentiation and augments HSPC supportive potential and myeloid transformation.[25,26] Conditional genetic inactivation of *Ebf1* in MSCs also alters bone marrow microenvironment architecture and diminishes HSC myeloid repopulation.[27] In a separate study, genetic lineage tracing experiments have identified preferential expression of Ebf3, another member of early B-cell factor family of transcription factor, in Cxcl12-abundant reticular cell or leptin receptor-expressing (CAR/LepR$^+$) self-renewing niche cells. Deficiency of *Ebf3* dramatically impairs marrow physiology and inhibits osteoblast differentiation and HSPC niche-supporting function.[28] Importantly, recent identification of engineering of defined transcription factor expression in nestin-expressing MSCs has shown immense promise in revitalizing MSC function and augmenting HSPC repopulation.[29] Collectively, these evidences underscore mesenchymal stroma-intrinsic chromatin regulation in maintaining niche integrity, HSPC function, and hematopoiesis.

3 | INFLAMMATION AND STROMAL IMMUNOMODULATION

Multipotency and immunomodulation are the key defining features of adult MSCs for maintaining tissue homeostasis upon injury and infection.[30-37] Inflammation refers to the responsiveness of our body's immune system against a wide array of *danger signals* like pathogens *(recognized by pattern recognition receptors, PRRs)*, tissue injury, toxic compounds,

or irradiation. In addition to the involvement of *pattern-associated molecular patterns (PAMPs)* secondary to microbial infection, endogenous physiological stress response pathways, *damage-associated molecular patterns (DAMPs),* and redox signaling also induce sterile inflammation. Overall inflammatory phenomenon is considered as a robust homeostatic mechanism safeguarding tissue integrity. While acute inflammation generates robust and short lasting symptoms, chronic inflammation impairs tissue homeostasis and associates with development of metabolic syndromes *(metaflammation)* and lifestyle disorders including cancer.[38,39]

Inflamed tissues secrete various pro-inflammatory cytokines (like IL-1, IL-6, TNF-α) to activate MSCs. Additionally, a broad range of chemokines including MCP-1, MIP-1α, MIP-1β, RANTES, CXCL12 etc and growth factors are also released enabling recruitment of MSCs from localized tissue microenvironment or from distal sites like bone marrow or adipose tissue to the site of inflammation. It has been shown that tissue resident MSCs significantly contribute to the inflammatory response pathways. First, MSC-derived secretome contains critical immunomodulatory effector molecules that sense the extent of inflammation for fine tuning immune response. Second, these multipotent MSCs can undergo differentiation and deposit extracellular matrix for tissue regeneration.[40] In addition, TGF-β plays an important role in limiting the inflammatory response, which promotes accumulation and proliferation of stromal fibroblasts and the deposition of an extracellular matrix that is required for proper tissue repair.[41-44]

3.1 | MSC polarization

Depending on the severity of inflammation MSCs can switch between a pro-inflammatory (MSC1) and anti-inflammatory or immunosuppressive (MSC2) phenotypes. Inflammatory tissue microenvironment determines MSC plasticity and immune response. MSCs are licensed to exert immunomodulatory effects (eg, activation of T lymphocytes) after stimulation with interferon-γ (IFN-γ) in the presence of TNF, IL-1α, or IL-1β. During the initial stage of acute inflammation, MSCs promote inflammation (through MSC1), while during hyper-activation of the immune system MSCs switch into a MSC2 phenotype.[33,35,45] It has been shown that polarization into MSC1 phenotype can be influenced by lipopolysaccharide (LPS)-dependent TLR4 activation, while double stranded RNA (dsRNA)-dependent activation of TLR3 induces MSC2.[46] Paradoxically, TLR3 stimulation of MSCs has also been shown to induce a pro-inflammatory response, suggesting nonredundant and spatiotemporal mechanisms.[47,48] In addition, anti-inflammatory cytokine like TGF-β can modulate the differentiation and regenerative capacities of MSCs. MSCs themselves can produce abundant TGF-β, which probably acts as a feedback control to partially sustain inflammation.[49] Apart from the soluble factors, presence of membrane bound immunoregulatory molecules (like PD-L1, FASL, B7-1, B7-2 etc) on MSCs play important role in immune effector responses.[50-52] In agreement with this phenomenon, it was reported that blocking PD-L1 and PD-L2 pathways significantly impairs immune-suppressive effects of MSCs.[53,54]

3.2 | Tumor-immune microenvironment

MSCs and stromal fibroblasts (MSCFs) are the crucial machinery in the regulation of tumor-immune microenvironment (TIME) ecosystem in cancer pathogenesis.[55-57] Given that MSCFs are characterized by a considerable degree of phenotypic and functional heterogeneity, their overall contribution to tumorigenesis (either tumor-promoting or antitumorigenic role) remains cell type and context dependent.[57-60] In general, MSCFs have been shown to confer pro-tumorigenic and metastatic properties by inducing expression of epithelial-mesenchymal transition (EMT) and hypoxia-related genes in primary tumors.[61] TGF-β and IL-6, secreted by MSCFs, induce EMT and create a tumor-angiogenic niche.[62,63] MSFCs also deposit extra-cellular matrix (ECM) components and remodel the TIME.[64] The activated TIME in turn reprograms tissue-resident and tumor-recruited MSFCs. Importantly, tumor-associated MSCFs are immunophenotypically and functionally distinct from the nontumor MSCs.[65] Presence of TNF-α and IFN-γ are the signature hallmarks of TIME mileu, which induce the MSFCs to produce TGF-β and VEGF. Synergistic effects of these two pro-inflammatory cytokines enhance the immunosuppressive nature of MSFCs that collectively helps in tumor dissemination.[66-68] Putting together, the chronic inflammatory nature of TIME imparts immunosuppressive property of MSCFs and facilitates tumor evolution by modulating the adaptive and innate immune system in several ways: (i) MSCFs can inhibit proliferation and cytotoxicity of NK cells by secreting PGE2 and IDO.[69-75] (ii) MSCFs impair dendritic cell (DC) maturation and function.[76-78] (iii) MSCFs affect $CD4^+$ T-cell activity by secreting PGE2, IDO, TGF-β, HGF, and iNOS.[79-83] iv) MSCFs, by the combined action of PGE2, IL-10, and TGF-β, help polarize macrophages into anti-inflammatory M2 population facilitating tumorigenesis.[84-86]

4 | ATP-DEPENDENT CHROMATIN REMODELERS IN MSC LINEAGE COMMITMENT

ATP-dependent chromatin remodeling complexes are large multi subunit protein complexes that utilize the energy from

ATP hydrolysis to disrupt or alter histone-DNA interactions, and further in synergy with cell type-specific transcriptional co-activators, regulate gene expression, transcriptional architecture, promote multicellular development, and establish tissue identity.[87-91] The mammalian system involves four subfamilies of ATP-dependent chromatin remodeling complexes namely switch/sucrose non-fermentable (SWI/SNF), nucleosome remodeler deacetylase (NuRD), INO80, and imitation switch (ISWI).[92] Particular chromatin outcome involving chromatin assembly, accessibility and editing is achieved by each specialized subfamily.[93] Except for ISWI, the other three nucleosome remodelers have been reported so far to regulate MSC lineage commitment (Table 1).

4.1 | SWI/SNF

SWI/SNF (Brahma-Associated Factor, BAF) plasticity associated with combinatorial subunit assembly was initially reported in the context of neural cell development and heterochromatin formation in ES cell differentiation.[94-96] Lineage differentiation by regulating expression of Nanog reveals specialized role of BAF complex subunits Brg1, Baf57, and Baf47.[97,98] Recent studies indicate that BAF complex has also emerged as an important regulator of MSC tri-lineage differentiation by interaction with tissue-specific transcription factors and crosstalk with cell signaling machinery.[24,98,99] Bone morphogenetic protein-2 (BMP-2) treatment of premyogenic cells C2C12, leads to an induction of various subunits of the SWI/SNF complex along with an induction of early responsive osteogenic gene alkaline phosphatase *(Alpl)*.[100] Several studies have demonstrated that ATPase subunit of SWI/SNF complex Brg1 is an important regulator of skeletal genes.[101] Dominant negative expression of *Brg1* was found to abrogate BMP-2-induced *Alpl* expression, suggesting that expression of skeletal genes requires functional SWI/SNF machinery.[100] Transcriptional activation of *osteocalcin* also involves active promoter recruitment of SWI/SNF along with C/EBPβ and Runx2.[102] Mammalian SWI/SNF complexes usually contain mutually exclusive ATPase subunits Brg1 and Brm.[87,103-105] Interestingly, antagonistic roles of Brg1 and Brm containing complexes have been implicated in MSC osteolineage commitment.[106] Brm expressing SWI/SNF complex represses osteogenic gene expression along with HDAC1. Depletion of Brm leads to constitutive osteolineage gene expression.[106] Nevertheless, the role of Brm in maintaining homeotic balance between osteogenesis and adipogenesis in the setting of MSC lineage commitment in vivo warrants further investigation.

Signaling pathways critical for MSC fate decisions, like Ric-8B, Wnt, PI3K/AKT, and Smad, was shown to be regulated by Brg1 and SWI/SNF.[24,107] Loss of classical BAF restricted subunit *Arid1a* leads to cell cycle arrest and downregulation of *Alpl* expression during osteogenesis.[24,108] BAF45A was identified as an important regulator of adipogenic differentiation of human MSCs.[109] In addition, MSC adipogenic differentiation requires C/EBPα mediated direct activation of adipogenic promoters, which involves SWI/SNF-dependent chromatin remodeling.[110] Recent reports have suggested that chromatin remodeling and de novo activation of enhancers is predominant during MSC adipogenic lineage specification.[111-113] However, using comprehensive epigenomic and transcriptomic analysis coupled with machine learning approaches, it was revealed that human MSC osteogenic commitment is associated with activation of pre-established enhancers.[113] Nuclear actin is an important component of the BAF complex.[114,115] Osteoblast differentiation program of MSCs associates with accumulation of nuclear actin entailing a transcriptional program for expression of osteogenic transcription factors Osterix and Osteocalcin. Nuclear actin favors export of repressor protein YAP from the nucleus, inducing *Runx2* expression.[116] In addition, high-mobility group protein A (HMGA) regulates histone DNA interactions and chromatin architecture. HMGA helps to maintain an open chromatin conformation in the progenitor cells favoring osteolineage and adipogenic differentiation. Depending on Wnt/β-catenin signaling HMGA activates expression of either *Runx2* or *C/EBP* and *PPARγ* to facilitate lineage commitment in a context-dependent fashion.[117]

In addition to the classical BAF, mammalian cells also contain an altered BAF complex known as polybromo-BAF (BAF), which involves Pbrm1, Arid2, and Brd7 subunits.[99,118-124] Emerging evidences suggest that PBAFs play important role in MSC fate determination.[24,125] In a recent finding, we have identified that loss of *Pbrm1* and PBAFs significantly impair both human and murine MSC osteolineage differentiation and osteogenesis.[24] We have demonstrated that loss of Pbrm1/PBAF impair Smad1/5/8 activation and BMP-early-responsive gene expression, which involves Pbrm1 bromodomain function and locus-specific chromatin remodeling, and transcriptional downregulation of *Bmp/Tgfβ* receptor genes.[24] Together, our findings essentially highlight epigenomic feedforward control of BMP/TGF-β signaling in mammalian MSC physiology.

4.2 | NuRD and INO80

Apart from SWI/SNF, other ATP-dependent chromatin remodelers found in the mammalian system are NuRD, INO80, and ISWI complexes.[92] The ATPase subunit of the NuRD complex includes chromodomain helicase DNA binding (CHD) protein. Among the nine members (CHD1-CHD9), CHD3 and CHD4 play the key ATPase subunits for NuRD activity.[126] It was reported that CHD4 along with HDAC1/2 interact with Cbx1 and Kap1 to regulate *Sox9*

TABLE 1 Epigenetic regulators of MSC lineage commitment

Epigenetic regulation	Target	Role	Reference
Chromatin remodeling			
BRG1	RUNX2, RIC8B, WNT & PI3K signaling pathways	Involved in multiple pathways of early and late response osteolineage gene expression	(100,188)
BRM	OCN	Negatively regulates expression of osteocalcin along with HDAC1	(106)
BAF250A	Primitive hematopoiesis	Regulates stroma-dependent and non-cell autonomous fetal liver HSC function	(23)
BAF180	ALPL, RUNX2, OSX & BMP receptors	Determines chromatin remodeling of key osteolineage and BMPR genes	(24)
BAF200	ALPL, RUNX2, OSX, BMP receptors, BMP4 & FGFR	Regulates expression of key osteogenic genes by binding to DNA regulatory elements	(119,124)
BAF45A	Unknown	Expression found in early adipogenic differentiation of MSCs	(109)
HMGA2	C/EBP & PPARγ	Maintains open chromatin conformation, lineage specification	(117)
Nuclear actin	RUNX2	Exports repressor protein YAP from the nucleus for gene regulation	(116)
CHD4	SOX9	Implicated in chondrogenesis	(127)
CHD1	RNA POL-II & H2A.Z	Transcriptional regulation at key osteogenic loci	(128)
MTA1	BSP, OCN	Negatively regulates osteolineage gene expression	(130)
INO80	WNT signaling	Interacts with WDR5 and regulates WNT signaling in osteogenesis	(131)
DNA methylation & acetylation			
TET1/2/3	5mC	Expression increases during osteogenesis, causing increased methylation of pluripotent genes	(25,26)
DNMT1	LOX gene	Methylates promoter region and determines bone matrix formation	(133,181)
DNMT3B	PTEN promoter	Associated with methylation of target promoter region	(136)
G9A	PTEN promoter	Implicated in promoter methylation by increasing H3K9me2 repressive mark	(136)
ALKBH1	N6mA	Regulates N6mA on ATF4 promoter region during osteogenesis	(139)
Histone methylation & demethylation			
SETDB1	H3K9	Regulates adipogenic commitment	(190,191)
EZH2	H3K27	Essential for MSC proliferation, osteogenic differentiation	(172-175,178,187)
BMI1	H3K27	Maintains transcriptional silencing at important developmental loci	(183)
SETD7	H3K4	Implicated in chondrogenesis	(190,191,195)
MLL1	H3K4	Involved in bone aging	(202)
KMT3B	H3K36	Associated with osteoblast gene expression and Soto syndrome	(202)
WHSC1	H3K36	Involved in bone development	(155)
PRMT4	H3R2, H3R17, H3R26, SOX9	Regulates chondrocyte proliferation and endochondral ossification via arginine methylation of SOX9	(203)
LSD1	H3K4, H3K9	Regulates NFAT1-dependent chondrogenesis and adipose tissue-derived osteogenesis	(192)
KDM4B	H3K9, H3K36	Positively regulates osteogenesis by regulating DLX gene expression	(189)

(Continues)

TABLE 1 (Continued)

Epigenetic regulation	Target	Role	Reference
KDM6A	H3K27	Regulates osteogenic differentiation along with RUNX2, PPARγ, C/EBP	(186)
KDM6B	H3K27	Promotes osteogenesis by regulating HOX gene expression	(189)
NO66	H3K4, H3K36	Determines stromal osteogenic commitment by regulating Osx expression	(211)
Histone acetylation, deacetylation & other chromatin regulation			
WDR5	H3K4, H3K8	Regulates bone formation during development	(131)
KAT6A	H3, H4	Participates in bone development, and associated with genitopatellar syndrome	(186)
KAT6B	H3, H4	Interacts with Runx2 and implicated in MSC lineage specification	(158)
P300	H3	Regulates osteoblast gene expression	(104,153,158)
CBP	H2A, H2B, H3	Associated with osteogenic gene expression and Rubinstein-Tybi syndrome	(104)
PCAF	H2B, H3	Determines osteoblast gene expression and implicated in osteoarthritis pathophysiology	(159)
SIRT1	H3, H4	Contributes to MSC self-renewal, cartilage, and bone maturation	
	(155,219)		
SIRT6	H3, H4, H3K9, H3K56	Regulates bone development and chondrocyte hypertrophy	(155,218)
HDACs	H2A, H2B, H3, H4	Implicated in MSC lineage commitment, bone homeostasis, and craniofacial development	(129,219)
EBF1	HSC adhesion and quiescence-regulatory genes present in MSCs	Regulates stromal architecture and hematopoiesis	(27)
EBF3	HSC niche-regulatory genes	Maintains stem cell niche architecture and HSC repopulation	(28)

expression during chondrogenesis.[127] Expression of CHD1 regulated genes are induced during osteoblast differentiation. Depletion of CHD1 stalls RNA Pol II, and H2A.Z occupancy is reduced at transcription start site (TSS) of target osteogenic loci.[128] Reduction in HDAC activity was also demonstrated during adipogenic differentiation of stromal cells.[129] MTA1, another important subunit of NuRD, was suggested to negatively regulate osteogenic commitment of human MSCs. Accordingly, depletion of MTA-1 was associated with an increase in calcium deposition and osteogenic gene expression.[130] Whether other related members MTA2 and MTA3 also have similar effects on MSC lineage commitment remains to be identified.

INO80 was also implicated in reprogramming and multicellular development. INO80 was found to interact with Trithorax member Wdr5 to regulate canonical WNT signaling during MSC differentiation. Silencing of IN080 or Wrd5 dramatically reduces expression of osteoblast marker genes, and impairs bone forming potential of the MSCs.[131] Whether this complex further regulates differentiation of MSCs into other lineage remain unidentified. Together, context- and tissue-specific expression footprints and dynamic nature of subunit assembly and stoichiometry highlights chromatin remodeler plasticity in the backdrop of mammalian MSC lineage specification.

5 | DNA METABOLISM IN MSC FATE DETERMINATION

5-methyl cytosine (5mC) represents one of the most frequently modified bases in mammalian tissue development.[132] Comparison of the CpG methylation levels between young and aged MSCs have revealed distinct footprints.[133] Some of these methylation marks have been found to overlap with occupancy of H3K9me3, H3K27me3, and polycomb repressive complex 2 (PRC2) at target loci, highlighting CpG methylation pattern as an important molecular marker of MSCs. In addition, MSC osteolineage commitment causes an increase in promoter methylation of the genes that regulate pluripotency and ERα signaling, while osteocalcin promoter shows reduced level of methylation.[12] Tet family of

DNA hydroxymethylases critically regulate metabolic output of 5mC leading to formation of 5hmC. All the three members of Tet family Tet1, Tet2, and Tet3 show enhanced activity during stromal cell differentiation. Loss of *Tet1/Tet2* impairs MSC osteoblast differentiation, and *Tet1/Tet2* deficient mice develop osteoporosis.[25] Absence of Tet1 and Tet2 also prevents *P2rx7* promoter demethylation leading to microRNA containing exosome accumulation. Accumulated microRNAs miR-297a-5p, miR-297b-5p, and miR-297c-5p disrupts Runx2 mediated MSC functioning.[134] Contrasting to these reports, while Tet1 has been found to recruit co repressor proteins Sin3a and histone methyl transferase Ezh2 to osteogenic loci, Tet2 has been found to regulate 5hmC levels of promoters of osteogenic and adipogenic lineage-specific genes.[25] The other family of DNA methylating enzyme (DNA methyltransferases) includes Dbmt1, Dnmt3a, and Dnmt3b. While Dnmt3a and Dnmt3b are de novo methyl transferases that methylate CpG dinucleotides, Dnmt1 functions as a maintenance methyl transferase. Inhibition of Dnmt upregulates expression of osteogenic genes suggesting DNA demethylation is associated with osteoblastic differentiation of MSCs.[135]

In addition, DNA methyl transferases Dnmt3b and G9a negatively regulate ectopic bone formation of dental pulp MSCs.[136] However, Dnmt3b expression is upregulated during early stages of fracture repair, and chondroblast-specific deletion impairs the repair process.[137] Porcine derived MSCs have increased transcript levels of Dnmt3a and Dnmt3b during differentiation.[138] Methylation of DNA to form N6-methyladenine (N6-mA) occurs in presence of 2-oxoglutarate- and $Fe2^{+}$-dependent dioxygenase. N6mA demethylase ALKBH1 plays essential role in MSC osteoblast differentiation.[139] Homolog of *Drosophila* methylase CG14906 and *C elegans* methylase Damt-1, Mettl4 was demonstrated to be a mammalian N^6-adenine methylase that functions in adipogenesis. Silencing of *Mettl4* causes altered adipocyte differentiation.[140] Treatment of MC3T3 cells with IL-6 and homocysteine increases expression of Dnmt1 with a concomitant promoter methylation of lysyl oxidase gene that negatively regulates bone matrix formation.[141]

Moreover, overexpression of Dnmt1 causes H19 lncRNA promoter hypermethylation and inhibition of Erk signaling pathway in disuse osteoporosis.[142] Oct4 and Nanog have been found to induce Dnmt1 expression by directly binding to its promoter and help to maintain MSC self-renewal.[143] Further studies suggested that miR-149 mediated osteogenesis was steered by methyltransferases.[144] Contrasting findings regarding the role of Dnmts were reported during adipogenesis. While inhibition of Dnmt in multipotent C3H10T1/2 cells and 3T3-L1 preadipocytes favored adipogenesis,[145,146] upregulation of canonical Wnt signaling was demonstrated upon Dnmt inhibition in 3T3-L1 and ST2 mesenchymal precursor cells hindering adipogenesis.[147] Genetic evidences suggested that deficiency of Dnmt1 and Dnmt3a impaired adipogenesis in 3T3-L1 cells.[148,149] Dnmt1 and Dnmt3a are also critical regulators of endothelial cell marker gene expression. Silencing of these methyl transferases favor MSC mediated angiogenesis promoting arterial-specific differentiation.[150] Moreover, knockdown of Gadd45a, the growth arrest and DNA damage inducible protein lead to hypermethylation of *Dlx5, Runx2, Bglap*, and *Osterix* promoters followed by suppressed gene expression and impaired osteogenic differentiation.[151] Therefore, it plays an essential role in locus-specific DNA demethylation. Collectively, these reports account for critical role of the enzymes regulating DNA metabolism in determining MSC lineage commitment.

6 | CHROMATIN-MODIFYING ENZYMES IN MESENCHYMAL STROMAL DIFFERENTIATION

Similar to DNA methylation, histone modifications including histone methylation and acetylation play important role in transcriptional regulation. While H3K27ac level associates with locus-specific transcriptional activation, H3K9me3 and H3K27me3 marks represent transcriptionally repressed chromatin states. It has been reported that osteocalcin gene promoter and coding region contain low levels of acetylated H3 and H4 during the proliferative phase of osteogenic differentiation. Mature osteoblasts with active osteocalcin gene expression correlate with an enriched H4 acetylation, connecting osteogenic differentiation and histone acetylation.[152] Growing bodies of evidences indicate that histone-modifying enzymes significantly contribute to MSC lineage specification. For example, histone acetyl transferase p300/CBP promotes chondrogenesis, while Tip60 which acetylates H3K25, promotes adipogenic differentiation.[153-155] The amino terminus of PPARγ2 is occupied by p300 and CBP in a ligand-independent manner, that allows recruitment of HATs decompacting the chromatin to allow the transcriptional machinery to access the gene promoter.[156] Recent report suggests that bone-specific osteocalcin gene regulation by p300 requires Runx2 independent of its histone acetylase activity.[157]

Histone acetyltransferases like Wdr5, Kat6a, and Kat6b regulates various aspects of bone development and lineage specification of MSCs. H3K9 histone acetylase Gcn5 represses angiogenesis in bone marrow derived MSCs during osteoporosis and PCAF promotes osteogenesis via BMP signaling.[158,159] Gcn5 mediated H3K9 acetylation at Wnt1, Wnt6, Wnt10a, and Wnt10b promoters facilitate MSC osteogenic gene expression. In addition, PCAF, another H3K9 acetyl transferase, promotes osteogenesis via BMP signaling. PCAF is recruited to the promoters of Bmp2, Bmp3, Bmpr1β, and Runx2 loci during osteogenic differentiation.[160]

HDACs generally repress transcription by counteracting the function of histone acetyl transferases. It has been shown that deletion of HDAC1 and HDAC2 in cultured mesenchymal precursor cells dampened lipid accumulation. Binding of HDAC1 to C/EBPα promoter during adipogenesis further strengthens its regulatory role in MSC lineage commitment. In contrast, HDAC6 positively regulates adipogenesis at the expense of osteogenesis in human adipose and dental derived MSCs.[161,162] Over expression of long non-coding RNA H19 leads to downregulation of HDAC4 and 5, necessary for adipogenesis. HDAC4 and HDAC5 deacetylated Runx2, allowing the protein to undergo Smurf-mediated degradation. HDAC6 together with glucocorticoid receptor mediates the effect of dexamethasone during MSC osteogenesis.[163] SIRT1, a member of the sirtuin family of histone deacetylase, binds to adipogenic transcription factor Pparγ inhibiting adipogenesis.[164,165] Lower levels of SIRT1 cause concomitant decrease in acetylated Pparγ and an increase in C/EBPα, favoring lipid accumulation.[166] Resveratrol mediated osteogenesis of human MSCs depends on Runx2 upregulation via SIRT1/FOXO3A axis.[167] Knockdown of SIRT1 in bone marrow derived MSCs downregulated Sox2 expression leading to deterioration of MSC self-renewal and differentiation.[168] Additionally, SIRT1 also regulates differentiation of MSCs by regulating β-catenin accumulation and transcriptional activation of MSC differentiation-specific genes.[169] Cartilage-specific differentiation of bone marrow derived MSCs require Sox9 and NF-κβ deacetylation by SIRT1. Studies in rat derived MSCs highlighted that SIRT6, another H3K9 deacetylase, stimulates osteogenic differentiation by inhibiting NF-κβ signaling.[170] However, histone deacetylase independent function of SIRT6 was also reported in BMP mediated MSC differentiation.[171]

The dynamic alteration of histone methylation during MSC lineage commitment is orchestrated by coordinated activity of histone methyl transferases and histone demethylases. Pharmacological inhibition of Ezh2, a H3K27 methyl transferase, facilitates marrow MSC osteolineage differentiation.[172,173] In addition, conditional deletion of *Ezh2* in mesenchyme, osteoblasts, and chondrocytes has been shown to manifest cell type-specific effects. While loss of *Ezh2* in the mesenchyme *(Ezh2$^{f/f}$; Prx1-Cre)* attenuates skeletal development, *Ezh2* deficiency in preosteoblasts favors osteogenic differentiation at the expense of adipogenesis.[174] Moreover, *Ezh2* loss in chondrocytes *(Ezh2$^{f/f}$; Col2α1-Cre)*, induces osteogenic gene expression with a reduced levels of H3K27me3 and postnatal bone phenotype.[175-178] In contrast, deletion of *Ezh2* in Nestin^{+} pubertal MSCs leads to low-bone density, suggesting cell type and context dependent epigenetic regulation of gene expression, cellular plasticity, and differentiation.[176] Genome-wide investigation of Ezh2 target genes showed a dramatic decrease in Ezh2 occupied loci after osteogenic differentiation with a concomitant decrease in the H3K27me3 mark. Phosphorylation of Ezh2 at Thr487 by activated Cdk1 promotes MSC osteogenic commitment.[179] In addition, lncRNA-ANCR associates with Ezh2 to downregulate Runx2 levels and impedes osteogenesis of MSCs.[180] Bmi1 is an important member of the PRC1 complex and is responsible for monoubiquitination of H2AK119, helping in stabilization of H3K27me3 mark.[181,182] It has been demonstrated that Bmi1 regulates bone marrow MSC osteogenic commitment and hematopoiesis.[183] On the contrary, H3K27me3 demethylase Kdm6a, which antagonizes PRC function,[184-186] positively regulate MSC osteolineage specification. It was demonstrated that knockdown of *Kdm6a* favor adipogenesis at the expense of osteogenesis.[187] Likewise, Kdm5b demethylates *Runx2* promoter region during osteoblast and myoblast differentiation.[188] Both H3K9me3 and H3K27me3 demethylases, KDM4B and KDM6B, respectively, are implicated to promote osteoblast differentiation and bone formation of human primary MSCs.[189] In addition, H3K9 methyl transferase Setdb1 undergoes phosphorylation in response to Wnt5a signaling, suppressing *Pparγ* expression and adipogenesis, while favoring osteogenesis.[190-192]

Loss of *Setdb1* causes long bone defects and reduction in trabecular bone in embryos and postnatal mice.[193,194] High-fat diet feeding mice and genetically predisposed obese mice have lower expression of Setdb1. Setdb2 that trimethylates H3K36, also positively regulates osteogenesis by inhibiting adipogenesis as conditional deletion of *Setd2* in mesenchyme promotes adipogenesis with reduced bone mass.[195] Inhibition of G9a, a H3K9 methyl transferase, converts MSCs to cardiac competent progenitor cells.[196] SET domain mutant Mll1 mice exhibited skeletal defect.[197,198] It was demonstrated that Mll3/Mll4 (methyltransferases of H3K4) interacts with PPARγ and facilitate adipogenesis.[199] Wolf-Hirschhorn syndrome candidate 1 (WHSC1), also known as NSD2, another H3K36 methyltransferase favors Runx2 and p300 interaction during osteogenesis.[200] H4 methyl transferase Suv40h2 also plays critical role in osteoblast formation and bone matrix development.[201] Additionally, deficiency of *Ash1l* methyl transferase in mice leads to development of arthritis with severe destruction of bone and cartilage. In agreement with this, C3H10T1/2 cells demonstrate reduced osteogenic and chondrogenic potential in absence of *Ash1l* with an increased adipogenic commitment.[202] Moreover, histone arginine methyltransferase PRMT4 (CARM1) also plays important role in regulating chondrocyte proliferation and endochondral ossification via arginine methylation of Sox9.[203]

Kdm2 enzymes catalyze removal of tri-methyl marks at H3K4, as well as mono- and di-methyl marks at H3K36. While Kdm2a is important for MSC proliferation,

Kdm2b regulates cell proliferation and senescence.[204] Co-recruitment of Kdm2b and BCOR complex was found in the promoter region of activating enhancer-binding protein 2α (AP-2α), during osteogenic differentiation.[205,206] Together these proteins lead to H3K4/36 methylation at epiregulin (EREG) promoter, causing transcriptional suppression. Induction of osteogenic genes like Osx and Dlx5 requires expression of EREG.[207] As opposed to Ezh2, Kdm6a positively regulates MSC osteolineage specification. Knockdown of Kdm6a favored adipogenesis at the expense of osteogenesis. Likewise, Kdm5b demethylates Runx2 promoter during osteoblast and myoblast differentiation. H3K9me3 demethylase KDM4B and H3K27me3 demethylase KDM6B are selectively induced in human MSC osteogenesis. In addition, Kdm4b functions as a co-factor of C/EBPβ to promote mitotic clonal expansion during differentiation of 3T3-L1 preadipocytes. Kdm4b facilitates C/EBPβ target gene expression by removing H3K9me3 marks.[208] Inhibition of Kdm4c by IDH1 mutation blocks differentiation of preadipocytes.[209] Kdm6b was also found to facilitate odontogenic differentiation of dental MSCs by removing the H3K27me3 mark from the BMP promoter. KDM5A was also implicated in MSC lineage specification.[210] Expression of Osx has been found to be regulated by H3K4 and H3K36me3 demethylase NO66.[211] Recently, LSD1 was shown to inhibit osteoblast differentiation of human MSCs. Conversely, deletion of LSD1 in osteoblast progenitor cells leads to increased bone mass.[212] In addition, Phf2 (or Jhdm1e) catalyses removal of di-methyl marks at H3K9. Deletion of *Phf2* in adipose tissue reduces white adipose tissue level by 50% without affecting brown adipose tissue level. Together with C/EBPα it promotes adipogenesis by demethylating H3K9me2 mark at specific adipogenic loci.[213,214]

Adult MSCs also play significant role in tissue homeostasis **(Figure 1)**. Decline in MSC function is linked with pathogenesis of osteoporosis and osteoarthritis. Deranged Tet/P2rX7/Runx2 signaling axis has emerged as potential target for osteopenia.[134] Transplantation of healthy MSCs in osteoporotic setting causes exosome mediated transfer of Fas proteins that recues Dnmt1 expression, reversing osteoporotic MSC phenotype.[215] Improvement of osteopenia and MSC fitness, using apoptotic bodies that transfer ubiquitin ligase RNF146 and miR-328-3p to activate Wnt/β signaling, suggests potential therapeutic modality for osteoporosis. Pargyline and JIB-04, small molecule inhibitors of Kdm1 and Kdm5a, respectively, have been found to rescue ovariectomy-induced bone loss by restoring H3K4 methylation level.[216] Ezh2 inhibitor DZNep enhances osteogenesis even during estrogen deficiency. In addition, ectopic expression of PRC1 member and H3K9me3 reader protein Cbx4 in bone joints has been proposed to ameliorate osteoarthritis-related bone loss and cartilage erosion.[217-219] Taken together, harnessing chromatin remodelers and epigenetic enzymes that regulate physiological processes of bone homeostasis posit potential therapeutic avenues for regenerative medicine.

7 | STROMAL EPIGENETIC REGULATION IN IMMUNITY

Evidences arising from context dependent experimental manipulation of chromatin modifying enzymes primarily suggest mesenchymal stromal epigenetic contribution in immune response and inflammation (Table 2). However, there is a real paucity of molecular and genetic analysis in support of MSC intrinsic epigenetic and transcriptional regulators implicated in immunomodulation. It has been reported that deficiency of *Tet1* and *Tet2* enhance periodontal ligament stem cell mediated T lymphocyte apoptosis ameliorating colitis. Loss of Tet1 and Tet2 led to a hypermethylated *Dkk-1* promoter, which induces Wnt/β-catenin signaling and Fas-ligand expression.[220] In addition, MSCs have been shown to convert conventional T lymphocytes into iTreg cells.[221] Posttranslational stability of Foxp3, through ubiquitin modifications, determines immunosuppressive function of iTreg cells. Cell-to-cell interaction between MSCs and Tregs followed by enhanced demethylation of the Foxp3-expressing Treg-specific demethylated region contribute to immunosuppression.[222] In addition, hydrogen sulfide promotes expression of Tet1 and Tet2 that mediate Foxp3 demethylation downstream of TGF-β and IL-2 signaling to promote Treg cell function and immune homeostasis.[223] Induction of Tregs mediated by MSCs is further associated with direct modifications of Runx1, Runx3, and Cbfβ.[224] Interestingly, epigenomic analysis of fibroblast-like synoviocytes, and MSCs isolated from autoimmune rheumatoid arthritis patients shows elevated H3K27 acetylation and increased chromatin accessibility, which is associated with active enhancers and promoters in the regulatory elements of NF-kB signaling and interferon-regulatory factors (IRFs).[225,226]

DNA methylation is only marginally affected by ex vivo priming of human umbilical cord blood-derived MSCs with pro-inflammatory cytokines. However, subsequent expansion of the MSC pool is associated with alterations in DNA methylation.[227] Human leukocyte antigen (HLA)-G contributes to the immunomodulatory properties of MSCs. Aberrant promoter methylation is associated with low levels of HLA-G expression in MSCs. Consistent with this pharmacological inhibition of DNMT activity de-represses expression of HLA-G1 and HLA-G3 in adipose and bone marrow-derived MSCs.[228] In addition, histone modifications have been reported to play a key role during IFN-γ priming of MSCs. Induction of *Ido1* expression followed by IFN-γ treatment associates with increased H3K9

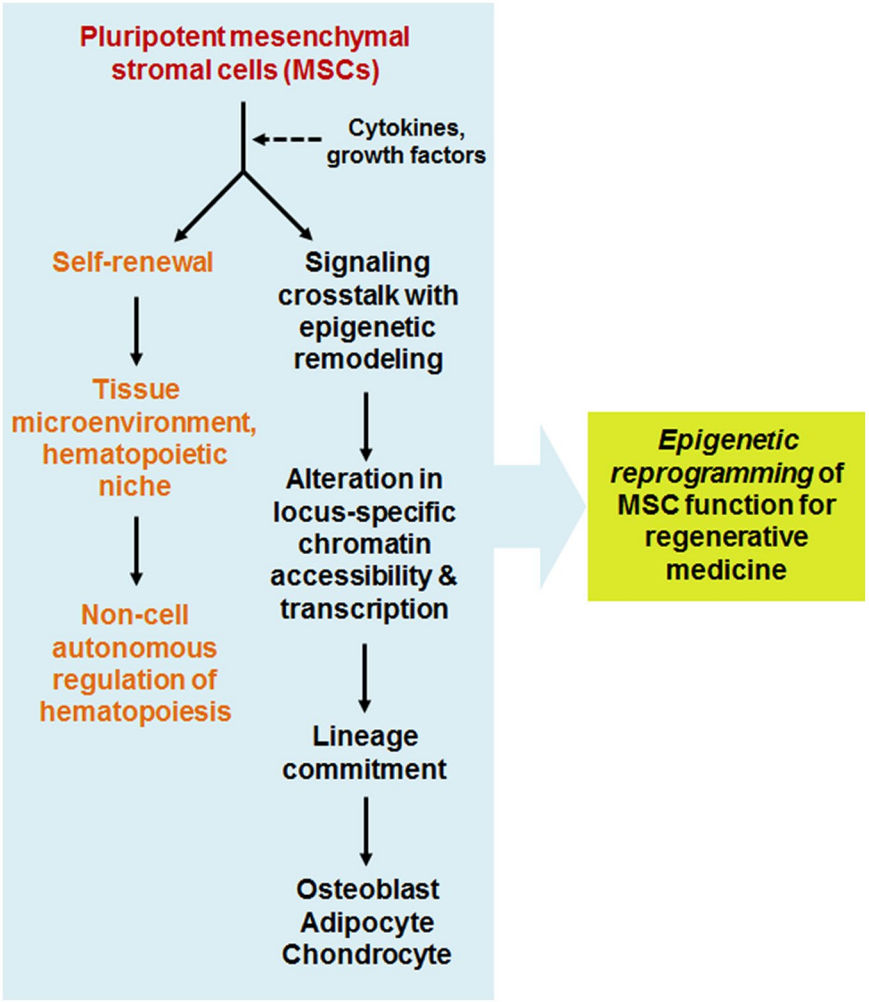

FIGURE 1 Schema represents adult MSC lineage commitment. Cell type-specific and context-dependent developmental signaling cues cooperate with chromatin remodeling machinery and orchestrate lineage priming and determine multicellular development. Bone marrow-derived MSCs also constitute an important constituent of hematopoietic microenvironment/niche, and therefore, therapeutic manipulation of stromal epigenetic regulators would rejuvenate hematopoietic stem/progenitor cell function and hematopoiesis in a non-cell autonomous fashion. Overall, targeted epigenetic reprogramming of MSCs posits immense potential in tissue regeneration and cell therapy

acetylation concomitant with a reduction in H3K9me3 at *Ido1* promoter. Importantly, this activated chromatin state was maintained as *epigenetic memory* even after the removal of the primary cytokine stimuli. Subsequent to re-exposure of previously primed MSCs demonstrated a robust and relatively faster induction in *Ido1* transcription, highlighting key aspects of transcriptional memory and immune training.[229,230] Given that, pluripotent MSCs reside at the crossroad of extended innate and adaptive immune response machinery, it would be important to discover and leverage key epigenetic nodes and transcriptional dependencies for trained central immunity in MSCs for precision medicine (Figure 2).

Systemic MSC transplantation has been proposed to rescue lupus autoimmune phenotype with a compromised tissue homeostasis. Deficiency of Fas in lupus mice restricts miR-29b release and downregulates *DNMT1* expression in the bone marrow MSCs, causing Notch signaling pathway activation with an impaired osteogenic differentiation. Transplanted MSCs facilitate release and transfer of exosomal Fas and restore DNMT1, highlighting MSC mediated epigenetic rejuvenation in immunity.[215] Independently it was shown that pharmacological inhibition of DNMT, using 5-azacytidine, hypomethylates promoters of key immunomodulatory factors like COX2, PTGES and chemokines CXCR2, CXCR4, reprogramming MSC immunomodulatory function. Hypomethylating agents were also shown to be effective for MSC mediated amelioration of disease phenotypes in experimental colitis model.[231] In addition, an optimal combination of hypomethylating agents and HDAC inhibition, by inducing expression of *IL-10* and *IDO* augment human MSC immunomodulatory potential in rheumatoid arthritis. Epigenetically harnessed human MSCs also show an increased immunosuppressive effect on T-cell proliferation and Th17 differentiation. Furthermore, co-culture of epigenetically primed MSCs with synovial fluid mononuclear cells from rheumatoid arthritis patients decreases IL-17$^+$/CD4$^+$ T-cell populations and downregulates IL-17 and IL-2 expression.[232] Inhibition of HDAC further impairs stromal TGF-β1 to attenuate lung fibrosis.[233] Sphingosine-1 phosphate (S1P) is commonly used as a priming factor for MSC mediated cell therapy applications. Interestingly, HDAC inhibition can cooperate with S1P to increase CXCR4 expression and augment MSC homing, self-renewal, and anti-inflammatory properties.[234] Additionally, LPS mediated activation

TABLE 2 Chromatin modifications in stromal immunomodulation

Epigenetic regulation	Target	Role	Reference
DNA methylation			
TET1/2	DKK-1 promoter	Associated with promoter methylation levels in stromal cells that in turn effects T-cell survival	(220)
	FOXP3	Determines TGF-β and IL-2-dependent FOXP3 expression and iTreg induction	(134,221-224)
DNMTs	HLA-G	Regulates expression of HLA-G1/G3 in human MSCs	(228)
	COX2, PTGES, CXCR2 & CXCR4 promoters	Pharmacological inhibition of DNMTs causes promoter hypomethylation and enhance human MSCs immunosuppression	(231)
	IL-10, IDO	Hypomethylating agents, in combination with HDAC inhibitors, increase gene expression and enhance MSC immunosuppressive potential	(232)
Histone modifications			
H3K27ac	NF-kB signaling regulatory elements & IRFs	Associates with active enhancers and promoters with an increased chromatin accessibility in the regulatory elements in synoviocytes and rheumatoid arthritis MSCs	(225,226)
	IFITM1 enhancer region	Activation of TLR4 signaling increases enhancer RNA expression and enriches for transcriptionally active chromatin mark.	(235)
H3K9ac, H3K9me3	IDO1 promoter	IFN-γ treatment associates with increased H3K9ac level concomitant with a reduction in H3K9me3 at the promoter region	(229)
HDACs	TGF-β1	Pharmacological inhibition of HDACs impairs stromal TGF-β1 in lung fibrosis	(233)
	CXCR4	HDAC inhibition cooperates with sphingosine-1 phosphate to increase CXCR4 expression in MSCs and promote MSC migration, self-renewal, and anti-inflammatory function	(234)

of TLR4 signaling in human MSCs induces enhancer RNA expression of *interferon-induced transmembrane protein 1 (IFITM1)* promoting cell trafficking.[235] Collectively these evidences advocate for epigenetic reprogramming of MSC function for immunomodulation and tissue homeostasis.

8 | CONCLUSION AND FUTURE PERSPECTIVE

Chromatin remodeling, epigenetic modifications, and transcriptional regulation have emerged as key aspects in orchestrating pluripotency, stem cell plasticity, cellular reprogramming, and multicellularity. Multipotent nature of adult tissue resident MSCs together with their immunomodulatory potential highlights applications in cellular therapy and regenerative medicine. Moreover, harnessing epigenetic basis of bone marrow MSC microenvironment physiology posits significant implications in the regulation of mammalian hematopoietic stem cell function and hematopoiesis. Similar to other somatic pluripotent cells MSCs also undergo physiological aging-associated senescence and a progressive decline in their regenerative ability. Epigenetic changes are reversible, which together with a recent surge in precise genome editing technologies brings an opportunity to amend epi-mutations and molecular derangements in the chromatin remodeling machinery. In addition, singe-cell-based systems-level epi/genomic and proteomic/mass cytometry interrogations would also help understand molecular and cellular heterogeneity in the MSC compartment. Therefore, identification of the key regulators of MSC function would allow therapeutic reprogramming and possibly reversal of tissue attrition. Together, fundamental and preclinical studies focusing on epigenetic regulation of MSC pluripotency and immunomodulation will have immense promise in regenerative and precision medicine.

MSCs are important regulators of the immune ecosystem. The crosstalk between MSCs and inflammatory response plays critical role in immune homeostasis. Presumably a basal inflammatory stimulus may be required to maintain MSC mediated immunosuppression in the setting of both endogenous tissue homeostasis as well as clinical grade

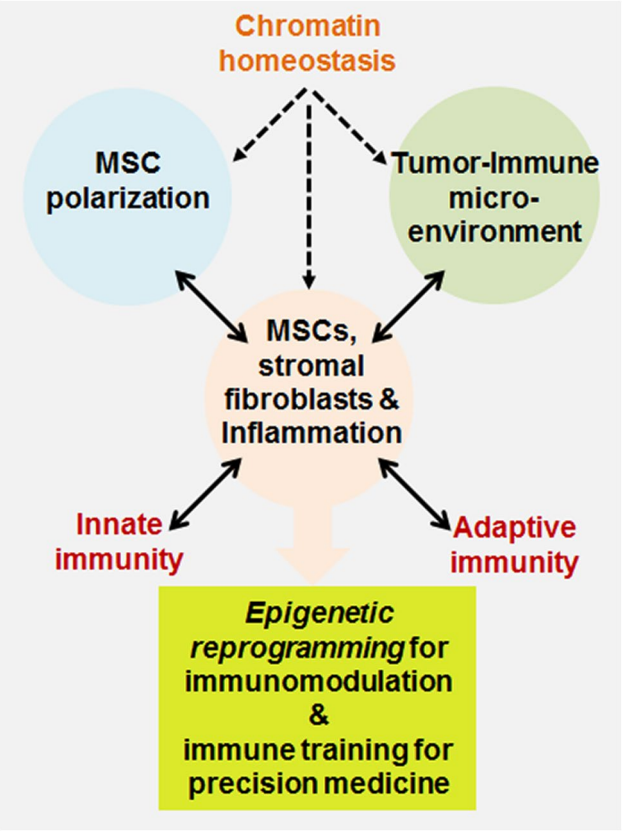

FIGURE 2 Graphical representation of MSC/stromal fibroblasts (MSCFs)-mediated inflammatory response in the context of immune regulation and tumor-immune microenvironment. MSCFs reside at the crossroad of innate and adaptive immune machinery. Identification, genetic and functional characterization of the key chromatin regulators within MSCFs would be instrumental in reprogramming immunosuppressive tumor-immune microenvironment and designing modalities of immune training for precision medicine

transplantation studies. Therefore, as one of the potential caveats it is likely that conventional and systemic anti-inflammatory regimens could alter the inflammatory milieu of tissue microenvironments countering MSC function. For example, among the commonly used immunosuppressive agents cyclosporin A prevents the activation of T lymphocytes and is frequently used to prevent transplant rejection and also to treat autoimmune disorders. However, it has been demonstrated that cyclosporin reverses MSC-induced tolerance in mice undergoing organ transplantations.[236] Similarly, dexamethasone, another widely used immunosuppressant, also revert MSC driven immunosuppression both in vitro and in vivo. Dexamethasone was shown to attenuate expression of iNOS and IDO in murine and human MSCs, respectively, and thus, sustains a hyper-inflammatory phenotype.[237] Moreover, concurrent steroid administration reverses MSC-mediated immunosuppression, and eliminates therapeutic benefits during the treatment of advanced liver fibrosis.[237] Several studies are currently ongoing to investigate the mechanisms underlying failures in MSC-based therapy in the presence of immunosuppressive agents. Systematic follow-up and retrospective analysis of the trials, coupled to a better molecular understanding of MSC epigenetics and immune-regulation, will allow us critically interrogate furtherance of MSC-based physiological reprogramming.

In sum, while MSC-based interventions for inflammatory disorders may rely on their immunosuppressive properties, cancer therapy in contrary should envisage reprogram tumor-associated stromal fibroblasts from an immunosuppressive to an immunostimulatory phenotype.[62] Nevertheless, deeper mechanistic investigations to identify chromatin and transcriptional regulation of MSC pluripotency and immunoregulatory function, and their interplay with stromal metabolome and metabolic rewiring, should define modalities conducive for tailored engineering and reprogramming of mesenchymal stromal function. Ongoing and future endeavors to leveraging heritable phenotype changes, often imprinted as *epigenetic memory*, without compromising the genotype should be one of the central goals for mesenchymal stroma-based epigenetic therapies. To conclude, considering that pluripotent MSCs may represent an important cell type belonging to an extended family of innate immune machinery, future studies must highlight and harness context-specific chromatin homeostasis and transcriptional dependencies for epigenetic memory-guided innate immune training, personalized medicine, and targeted therapy.

ACKNOWLEDGMENTS

This study is supported by funding from Council of Scientific & Industrial Research (CSIR) (MMP/HCP-0008 to AS), Department of Biotechnology (DBT) (BT/RLF/RE-ENTRY/06/2010), Ramalingaswami Fellowship (to AS), DBT (BT/PR13023/MED/31/311/2015) (to AS), and SERB-Department of Science & Technology (DST) (SB/SO/HS-053/2013) Govt. of India (to AS). AS is a recipient of Indian Council of Medical Research-Department of Health Research (ICMR-DHR) International Fellowship for Indian Biomedical Scientists (INDO/FRC/452/S-11/2019-20-lHD). SC and SS acknowledge support for graduate research fellowships from UGC and CSIR, respectively. We regret for not citing several other original references due to space constraints.

CONFLICT OF INTEREST

The authors declare no conflicts of interest in regards to this manuscript.

AUTHOR CONTRIBUTIONS

Manuscript design, writing and editing: S. Chakraborty, S. Sinha, A. Sengupta; Curation of data sets: mesenchymal stromal immune regulation: S. Chakraborty; MSC lineage commitment: S. Sinha; Conception, figure illustration and overall direction: A. Sengupta.

ORCID

Amitava Sengupta https://orcid.org/0000-0002-2804-1774

REFERENCES

1. Charbord P. Bone marrow mesenchymal stem cells: historical overview and concepts. *Hum Gene Ther*. 2010;21:1045-1056.
2. Friedenstein AJ, Petrakova KV, Kurolesova AI, Frolova GP. Heterotopic of bone marrow. Analysis of precursor cells for osteogenic and hematopoietic tissues. *Transplantation*. 1968;6:230-247.
3. Bianco P, Robey PG, Simmons PJ. Mesenchymal stem cells: revisiting history, concepts, and assays. *Cell Stem Cell*. 2008;2:313-319.
4. Pittenger MF, Discher DE, Peault BM, Phinney DG, Hare JM, Caplan AI. Mesenchymal stem cell perspective: cell biology to clinical progress. *NPJ Regen Med*. 2019;4:22.
5. Morrison SJ, Scadden DT. The bone marrow niche for haematopoietic stem cells. *Nature*. 2014;505:327-334.
6. Fielding C, Mendez-Ferrer S. Neuronal regulation of bone marrow stem cell niches. *F1000Research*. 2020;9:614. https://doi.org/10.12688/f1000research.22554.1
7. Yu VW, Scadden DT. Hematopoietic stem cell and its bone marrow niche. *Curr Top Dev Biol*. 2016;118:21-44.
8. Ullah I, Subbarao RB, Rho GJ. Human mesenchymal stem cells—current trends and future prospective. *Biosci Rep*. 2015;35.
9. Hass R, Kasper C, Bohm S, Jacobs R. Different populations and sources of human mesenchymal stem cells (MSC): a comparison of adult and neonatal tissue-derived MSC. *Cell Commun Signal*. 2011;9:12.
10. Chen Q, Shou P, Zheng C, et al. Fate decision of mesenchymal stem cells: adipocytes or osteoblasts? *Cell Death Differ*. 2016;23:1128-1139.
11. Florencio-Silva R, Sasso GR, Sasso-Cerri E, Simoes MJ, Cerri PS. Biology of bone tissue: Structure, function, and factors that influence bone cells. *Biomed Res Int*. 2015;2015:421746.
12. Perez-Campo FM, Riancho JA. Epigenetic mechanisms regulating mesenchymal stem cell differentiation. *Curr Genomics*. 2015;16:368-383.
13. Teven CM, Liu X, Hu N, et al. Epigenetic regulation of mesenchymal stem cells: a focus on osteogenic and adipogenic differentiation. *Stem Cells Int*. 2011;2011:201371.
14. Avgustinova A, Benitah SA. Epigenetic control of adult stem cell function. *Nat Rev Mol Cell Biol*. 2016;17:643-658.
15. Siddiqi S, Mills J, Matushansky I. Epigenetic remodeling of chromatin architecture: exploring tumor differentiation therapies in mesenchymal stem cells and sarcomas. *Curr Stem Cell Res Ther*. 2010;5:63-73.
16. Dixon JR, Jung I, Selvaraj S, et al. Chromatin architecture reorganization during stem cell differentiation. *Nature*. 2015;518:331-336.
17. Ozkul Y, Galderisi U. The impact of epigenetics on mesenchymal stem cell biology. *J Cell Physiol*. 2016;231:2393-2401.
18. Bentivegna A, Roversi G, Riva G, et al. The effect of culture on human bone marrow mesenchymal stem cells: Focus on DNA methylation profiles. *Stem Cells Int*. 2016;2016:5656701.
19. Baylin SB, Jones PA. Epigenetic determinants of cancer. *Cold Spring Harb Perspect Biol*. 2016;8.
20. Gonzalez-Nieto D, Li L, Kohler A, et al. Connexin-43 in the osteogenic BM niche regulates its cellular composition and the bidirectional traffic of hematopoietic stem cells and progenitors. *Blood*. 2012;119:5144-5154.
21. Chang KH, Sengupta A, Nayak RC, et al. p62 is required for stem cell/progenitor retention through inhibition of IKK/NF-kappaB/Ccl4 signaling at the bone marrow macrophage-osteoblast niche. *Cell Rep*. 2014;9:2084-2097.
22. Sengupta A, Duran A, Ishikawa E, et al. Atypical protein kinase C (aPKCzeta and aPKClambda) is dispensable for mammalian hematopoietic stem cell activity and blood formation. *Proc Natl Acad Sci USA*. 2011;108:9957-9962.
23. Krosl J, Mamo A, Chagraoui J, et al. A mutant allele of the Swi/Snf member BAF250a determines the pool size of fetal liver hemopoietic stem cell populations. *Blood*. 2010;116:1678-1684.
24. Sinha S, Biswas M, Chatterjee SS, Kumar S, Sengupta A. Pbrm1 steers mesenchymal stromal cell osteolineage differentiation by integrating PBAF-dependent chromatin remodeling and BMP/TGF-beta signaling. *Cell Rep*. 2020;31:107570.
25. Cakouros D, Hemming S, Gronthos K, et al. Specific functions of TET1 and TET2 in regulating mesenchymal cell lineage determination. *Epigenetics & chromatin*. 2019;12:3.
26. Li R, Zhou Y, Cao Z, et al. TET2 loss dysregulates the behavior of bone marrow mesenchymal stromal cells and accelerates Tet2(-/-)-driven myeloid malignancy progression. *Stem Cell Reports*. 2018;10:166-179.
27. Derecka M, Herman JS, Cauchy P, et al. EBF1-deficient bone marrow stroma elicits persistent changes in HSC potential. *Nat Immunol*. 2020;21:261-273.
28. Seike M, Omatsu Y, Watanabe H, Kondoh G, Nagasawa T. Stem cell niche-specific Ebf3 maintains the bone marrow cavity. *Genes Dev*. 2018;32:359-372.
29. Nakahara F, Borger DK, Wei Q, et al. Engineering a haematopoietic stem cell niche by revitalizing mesenchymal stromal cells. *Nat Cell Biol*. 2019;21:560-567.
30. Pittenger MF, Mackay AM, Beck SC, et al. Multilineage potential of adult human mesenchymal stem cells. *Science*. 1999;284:143-147.
31. Jiang Y, Jahagirdar BN, Reinhardt RL, et al. Pluripotency of mesenchymal stem cells derived from adult marrow. *Nature*. 2002;418:41-49.
32. Ma S, Xie N, Li W, Yuan B, Shi Y, Wang Y. Immunobiology of mesenchymal stem cells. *Cell Death Differ*. 2014;21:216-225.
33. Wang Y, Chen X, Cao W, Shi Y. Plasticity of mesenchymal stem cells in immunomodulation: pathological and therapeutic implications. *Nat Immunol*. 2014;15:1009-1016.
34. Uccelli A, Moretta L, Pistoia V. Mesenchymal stem cells in health and disease. *Nat Rev Immunol*. 2008;8:726-736.
35. Shi Y, Wang Y, Li Q, et al. Immunoregulatory mechanisms of mesenchymal stem and stromal cells in inflammatory diseases. *Nat Rev Nephrol*. 2018;14:493-507.
36. Prockop DJ, Oh JY. Mesenchymal stem/stromal cells (MSCs): role as guardians of inflammation. *Mol Ther*. 2012;20:14-20.
37. Ranganath SH, Levy O, Inamdar MS, Karp JM. Harnessing the mesenchymal stem cell secretome for the treatment of cardiovascular disease. *Cell Stem Cell*. 2012;10:244-258.
38. Chen L, Deng H, Cui H, et al. Inflammatory responses and inflammation-associated diseases in organs. *Oncotarget*. 2018;9:7204-7218.
39. Eming SA, Krieg T, Davidson JM. Inflammation in wound repair: molecular and cellular mechanisms. *J Invest Dermatol*. 2007;127:514-525.

40. Eggenhofer E, Luk F, Dahlke MH, Hoogduijn MJ. The life and fate of mesenchymal stem cells. *Front Immunol*. 2014;5:148.
41. Li MO, Flavell RA. Contextual regulation of inflammation: a duet by transforming growth factor-beta and interleukin-10. *Immunity*. 2008;28:468-476.
42. Li Z, Kupcsik L, Yao SJ, Alini M, Stoddart MJ. Mechanical load modulates chondrogenesis of human mesenchymal stem cells through the TGF-beta pathway. *J Cell Mol Med*. 2010;14:1338-1346.
43. Crane JL, Cao X. Bone marrow mesenchymal stem cells and TGF-beta signaling in bone remodeling. *J Clin Invest*. 2014;124:466-472.
44. Mariathasan S, Turley SJ, Nickles D, et al. TGFbeta attenuates tumour response to PD-L1 blockade by contributing to exclusion of T cells. *Nature*. 2018;554:544-548.
45. Bernardo ME, Fibbe WE. Mesenchymal stromal cells: sensors and switchers of inflammation. *Cell Stem Cell*. 2013;13:392-402.
46. Waterman RS, Tomchuck SL, Henkle SL, Betancourt AM. A new mesenchymal stem cell (MSC) paradigm: polarization into a pro-inflammatory MSC1 or an Immunosuppressive MSC2 phenotype. *PLoS One*. 2010;5:e10088.
47. Dumitru CA, Hemeda H, Jakob M, Lang S, Brandau S. Stimulation of mesenchymal stromal cells (MSCs) via TLR3 reveals a novel mechanism of autocrine priming. *FASEB J*. 2014;28:3856-3866.
48. Delarosa O, Dalemans W, Lombardo E. Toll-like receptors as modulators of mesenchymal stem cells. *Front Immunol*. 2012;3:182.
49. Xu X, Zheng L, Yuan Q, et al. Transforming growth factor-beta in stem cells and tissue homeostasis. *Bone Res*. 2018;6:2.
50. Sheng H, Wang Y, Jin Y, et al. A critical role of IFNgamma in priming MSC-mediated suppression of T cell proliferation through up-regulation of B7–H1. *Cell Res*. 2008;18:846-857.
51. Akiyama K, Chen C, Wang D, et al. Mesenchymal-stem-cell-induced immunoregulation involves FAS-ligand-/FAS-mediated T cell apoptosis. *Cell Stem Cell*. 2012;10:544-555.
52. Chinnadurai R, Copland IB, Patel SR, Galipeau J. IDO-independent suppression of T cell effector function by IFN-gamma-licensed human mesenchymal stromal cells. *J Immunol*. 2014;192:1491-1501.
53. Davies LC, Heldring N, Kadri N, Le Blanc K. Mesenchymal stromal cell secretion of programmed death-1 ligands regulates T cell mediated immunosuppression. *Stem Cells*. 2017;35:766-776.
54. Augello A, Tasso R, Negrini SM, et al. Bone marrow mesenchymal progenitor cells inhibit lymphocyte proliferation by activation of the programmed death 1 pathway. *Eur J Immunol*. 2005;35:1482-1490.
55. Turley SJ, Cremasco V, Astarita JL. Immunological hallmarks of stromal cells in the tumour microenvironment. *Nat Rev Immunol*. 2015;15:669-682.
56. Zhang XH, Jin X, Malladi S, et al. Selection of bone metastasis seeds by mesenchymal signals in the primary tumor stroma. *Cell*. 2013;154:1060-1073.
57. Karnoub AE, Dash AB, Vo AP, et al. Mesenchymal stem cells within tumour stroma promote breast cancer metastasis. *Nature*. 2007;449:557-563.
58. Djurec M, Grana O, Lee A, et al. Saa3 is a key mediator of the protumorigenic properties of cancer-associated fibroblasts in pancreatic tumors. *Proc Natl Acad Sci USA*. 2018;115:E1147-E1156.
59. Linares JF, Cordes T, Duran A, et al. ATF4-induced metabolic reprograming is a synthetic vulnerability of the p62-deficient tumor stroma. *Cell Metab*. 2017;26(817–829):e816.
60. Li HJ, Reinhardt F, Herschman HR, Weinberg RA. Cancer-stimulated mesenchymal stem cells create a carcinoma stem cell niche via prostaglandin E2 signaling. *Cancer Discov*. 2012;2:840-855.
61. Fregni G, Quinodoz M, Moller E, et al. Reciprocal modulation of mesenchymal stem cells and tumor cells promotes lung cancer metastasis. *EBioMedicine*. 2018;29:128-145.
62. Poggi A, Varesano S, Zocchi MR. How to hit mesenchymal stromal cells and make the tumor microenvironment immunostimulant rather than immunosuppressive. *Front Immunol*. 2018;9:262.
63. Hong IS, Lee HY, Kang KS. Mesenchymal stem cells and cancer: friends or enemies? *Mutat Res*. 2014;768:98-106.
64. Pure E, Lo A. Can targeting stroma pave the way to enhanced antitumor immunity and immunotherapy of solid tumors? *Cancer Immunol Res*. 2016;4:269-278.
65. Sun Z, Wang S, Zhao RC. The roles of mesenchymal stem cells in tumor inflammatory microenvironment. *J Hematol Oncol*. 2014;7:14.
66. Jing Y, Han Z, Liu Y, et al. Mesenchymal stem cells in inflammation microenvironment accelerates hepatocellular carcinoma metastasis by inducing epithelial-mesenchymal transition. *PLoS One*. 2012;7:e43272.
67. Liu Y, Han ZP, Zhang SS, et al. Effects of inflammatory factors on mesenchymal stem cells and their role in the promotion of tumor angiogenesis in colon cancer. *J Biol Chem*. 2011;286:25007-25015.
68. Ren G, Zhao X, Wang Y, et al. CCR2-dependent recruitment of macrophages by tumor-educated mesenchymal stromal cells promotes tumor development and is mimicked by TNFalpha. *Cell Stem Cell*. 2012;11:812-824.
69. Casado JG, Tarazona R, Sanchez-Margallo FM. NK and MSCs crosstalk: the sense of immunomodulation and their sensitivity. *Stem Cell Rev Rep*. 2013;9:184-189.
70. Hu CD, Kosaka Y, Marcus P, Rashedi I, Keating A. Differential immunomodulatory effects of human bone marrow-derived mesenchymal stromal cells on natural killer cells. *Stem Cells Dev*. 2019;28:933-943.
71. Krampera M, Cosmi L, Angeli R, et al. Role for interferon-gamma in the immunomodulatory activity of human bone marrow mesenchymal stem cells. *Stem Cells*. 2006;24:386-398.
72. Rasmusson I, Ringden O, Sundberg B, Le Blanc K. Mesenchymal stem cells inhibit the formation of cytotoxic T lymphocytes, but not activated cytotoxic T lymphocytes or natural killer cells. *Transplantation*. 2003;76:1208-1213.
73. Spaggiari GM, Capobianco A, Abdelrazik H, Becchetti F, Mingari MC, Moretta L. Mesenchymal stem cells inhibit natural killer-cell proliferation, cytotoxicity, and cytokine production: role of indoleamine 2,3-dioxygenase and prostaglandin E2. *Blood*. 2008;111:1327-1333.
74. Poggi A, Prevosto C, Massaro AM, et al. Interaction between human NK cells and bone marrow stromal cells induces NK cell triggering: role of NKp30 and NKG2D receptors. *J Immunol*. 2005;175:6352-6360.
75. Spaggiari GM, Capobianco A, Becchetti S, Mingari MC, Moretta L. Mesenchymal stem cell-natural killer cell interactions: evidence that activated NK cells are capable of killing MSCs,

whereas MSCs can inhibit IL-2-induced NK-cell proliferation. *Blood*. 2006;107:1484-1490.

76. Beyth S, Borovsky Z, Mevorach D, et al. Human mesenchymal stem cells alter antigen-presenting cell maturation and induce T-cell unresponsiveness. *Blood*. 2005;105:2214-2219.
77. Nauta AJ, Kruisselbrink AB, Lurvink E, Willemze R, Fibbe WE. Mesenchymal stem cells inhibit generation and function of both CD34+-derived and monocyte-derived dendritic cells. *J Immunol*. 2006;177:2080-2087.
78. Zhang B, Liu R, Shi D, et al. Mesenchymal stem cells induce mature dendritic cells into a novel Jagged-2-dependent regulatory dendritic cell population. *Blood*. 2009;113:46-57.
79. Chabannes D, Hill M, Merieau E, et al. A role for heme oxygenase-1 in the immunosuppressive effect of adult rat and human mesenchymal stem cells. *Blood*. 2007;110:3691-3694.
80. De Miguel MP, Fuentes-Julian S, Blazquez-Martinez A, et al. Immunosuppressive properties of mesenchymal stem cells: advances and applications. *Curr Mol Med*. 2012;12:574-591.
81. Nasef A, Chapel A, Mazurier C, et al. Identification of IL-10 and TGF-beta transcripts involved in the inhibition of T-lymphocyte proliferation during cell contact with human mesenchymal stem cells. *Gene Expr*. 2007;13:217-226.
82. Najar M, Fayyad-Kazan H, Faour WH, et al. Immunological modulation following bone marrow-derived mesenchymal stromal cells and Th17 lymphocyte co-cultures. *Inflamm Res*. 2019;68:203-213.
83. Zimmermann JA, Hettiaratchi MH, McDevitt TC. Enhanced immunosuppression of T cells by sustained presentation of bioactive interferon-gamma within three-dimensional mesenchymal stem cell constructs. *Stem Cells Transl Med*. 2017;6:223-237.
84. Francois M, Romieu-Mourez R, Li M, Galipeau J. Human MSC suppression correlates with cytokine induction of indoleamine 2,3-dioxygenase and bystander M2 macrophage differentiation. *Mol Ther*. 2012;20:187-195.
85. Nemeth K, Leelahavanichkul A, Yuen PS, et al. Bone marrow stromal cells attenuate sepsis via prostaglandin E(2)-dependent reprogramming of host macrophages to increase their interleukin-10 production. *Nat Med*. 2009;15:42-49.
86. Philipp D, Suhr L, Wahlers T, Choi YH, Paunel-Gorgulu A. Preconditioning of bone marrow-derived mesenchymal stem cells highly strengthens their potential to promote IL-6-dependent M2b polarization. *Stem Cell Res Ther*. 2018;9:286.
87. Hodges C, Kirkland JG, Crabtree GR. The many roles of BAF (mSWI/SNF) and PBAF complexes in Cancer. *Cold Spring Harb Perspect Med*. 2016;6.
88. Hargreaves DC, Crabtree GR. ATP-dependent chromatin remodeling: genetics, genomics and mechanisms. *Cell Res*. 2011;21:396-420.
89. Vignali M, Hassan AH, Neely KE, Workman JL. ATP-dependent chromatin-remodeling complexes. *Mol Cell Biol*. 2000;20:1899-1910.
90. Chatterjee SS, Biswas M, Boila LD, Banerjee D, Sengupta A. SMARCB1 deficiency integrates epigenetic signals to oncogenic gene expression program maintenance in human acute myeloid leukemia. *Mol Cancer Res*. 2018;16:791-804.
91. Sinha S, Chatterjee SS, Biswas M, et al. SWI/SNF subunit expression heterogeneity in human aplastic anemia stem/progenitors. *Exp Hematol*. 2018;62(39–44):e32.
92. Hota SK, Bruneau BG. ATP-dependent chromatin remodeling during mammalian development. *Development*. 2016;143:2882-2897.
93. Clapier CR, Iwasa J, Cairns BR, Peterson CL. Mechanisms of action and regulation of ATP-dependent chromatin-remodelling complexes. *Nat Rev Mol Cell Biol*. 2017;18:407-422.
94. Yoo AS, Crabtree GR. ATP-dependent chromatin remodeling in neural development. *Curr Opin Neurobiol*. 2009;19:120-126.
95. Chen T, Dent SY. Chromatin modifiers and remodellers: regulators of cellular differentiation. *Nat Rev Genet*. 2014;15:93-106.
96. Gaspar-Maia A, Alajem A, Meshorer E, Ramalho-Santos M. Open chromatin in pluripotency and reprogramming. *Nat Rev Mol Cell Biol*. 2011;12:36-47.
97. El Hadidy N, Uversky VN. Intrinsic disorder of the BAF complex: roles in chromatin remodeling and disease development. *Int J Mol Sci*. 2019;20:5260.
98. Alfert A, Moreno N, Kerl K. The BAF complex in development and disease. *Epigenetics Chromatin*. 2019;12:19.
99. Wang Z, Zhai W, Richardson JA, et al. Polybromo protein BAF180 functions in mammalian cardiac chamber maturation. *Genes Dev*. 2004;18:3106-3116.
100. Young DW, Pratap J, Javed A, et al. SWI/SNF chromatin remodeling complex is obligatory for BMP2-induced, Runx2-dependent skeletal gene expression that controls osteoblast differentiation. *J Cell Biochem*. 2005;94:720-730.
101. Nguyen KH, Xu F, Flowers S, Williams EA, Fritton JC, Moran E. SWI/SNF-mediated lineage determination in mesenchymal stem cells confers resistance to osteoporosis. *Stem Cells*. 2015;33:3028-3038.
102. Villagra A, Cruzat F, Carvallo L, et al. Chromatin remodeling and transcriptional activity of the bone-specific osteocalcin gene require CCAAT/enhancer-binding protein beta-dependent recruitment of SWI/SNF activity. *J Biol Chem*. 2006;281:22695-22706.
103. Pan J, McKenzie ZM, D'Avino AR, et al. The ATPase module of mammalian SWI/SNF family complexes mediates subcomplex identity and catalytic activity-independent genomic targeting. *Nat Genet*. 2019;51:618-626.
104. Alver BH, Kim KH, Lu P, et al. The SWI/SNF chromatin remodelling complex is required for maintenance of lineage specific enhancers. *Nat Commun*. 2017;8:14648.
105. Wilson BG, Roberts CW. SWI/SNF nucleosome remodellers and cancer. *Nat Rev Cancer*. 2011;11:481-492.
106. Flowers S, Nagl NG Jr, Beck GR Jr, Moran E. Antagonistic roles for BRM and BRG1 SWI/SNF complexes in differentiation. *J Biol Chem*. 2009;284:10067-10075.
107. Grandy R, Sepulveda H, Aguilar R, et al. The Ric-8B gene is highly expressed in proliferating preosteoblastic cells and down-regulated during osteoblast differentiation in a SWI/SNF- and C/EBPbeta-mediated manner. *Mol Cell Biol*. 2011;31:2997-3008.
108. Nagl NG Jr, Patsialou A, Haines DS, Dallas PB, Beck GR Jr, Moran E. The p270 (ARID1A/SMARCF1) subunit of mammalian SWI/SNF-related complexes is essential for normal cell cycle arrest. *Cancer Res*. 2005;65:9236-9244.
109. van de Peppel J, Strini T, Tilburg J, Westerhoff H, van Wijnen AJ, van Leeuwen JP. Identification of three early phases of cell-fate determination during osteogenic and adipogenic differentiation by transcription factor dynamics. *Stem Cell Reports*. 2017;8:947-960.

110. Salma N, Xiao H, Mueller E, Imbalzano AN. Temporal recruitment of transcription factors and SWI/SNF chromatin-remodeling enzymes during adipogenic induction of the peroxisome proliferator-activated receptor gamma nuclear hormone receptor. *Mol Cell Biol*. 2004;24:4651-4663.
111. Agrawal Singh S, Lerdrup M, Gomes AR, et al. PLZF targets developmental enhancers for activation during osteogenic differentiation of human mesenchymal stem cells. *Elife*. 2019;8.
112. Meyer MB, Benkusky NA, Sen B, Rubin J, Pike JW. Epigenetic plasticity drives adipogenic and osteogenic differentiation of marrow-derived mesenchymal stem cells. *J Biol Chem*. 2016;291:17829-17847.
113. Rauch A, Haakonsson AK, Madsen JGS, et al. Osteogenesis depends on commissioning of a network of stem cell transcription factors that act as repressors of adipogenesis. *Nat Genet*. 2019;51:716-727.
114. Olave IA, Reck-Peterson SL, Crabtree GR. Nuclear actin and actin-related proteins in chromatin remodeling. *Annu Rev Biochem*. 2002;71:755-781.
115. Kapoor P, Shen X. Mechanisms of nuclear actin in chromatin-remodeling complexes. *Trends Cell Biol*. 2014;24:238-246.
116. Sen B, Xie Z, Uzer G, et al. Intranuclear actin regulates osteogenesis. *Stem Cells*. 2015;33:3065-3076.
117. Giancotti V, Bergamin N, Cataldi P, Rizzi C. Epigenetic contribution of high-mobility group A proteins to stem cell properties. *Int J Cell Biol*. 2018;2018:3698078.
118. Mashtalir N, D'Avino AR, Michel BC, et al. Modular organization and assembly of SWI/SNF family chromatin remodeling complexes. *Cell*. 2018;175(1272–1288):e1220.
119. He L, Tian X, Zhang H, et al. BAF200 is required for heart morphogenesis and coronary artery development. *PLoS One*. 2014;9:e109493.
120. Kaeser MD, Aslanian A, Dong MQ, Yates JR 3rd, Emerson BM. BRD7, a novel PBAF-specific SWI/SNF subunit, is required for target gene activation and repression in embryonic stem cells. *J Biol Chem*. 2008;283:32254-32263.
121. Yan Z, Cui K, Murray DM, et al. PBAF chromatin-remodeling complex requires a novel specificity subunit, BAF200, to regulate expression of selective interferon-responsive genes. *Genes Dev*. 2005;19:1662-1667.
122. Wang W. The SWI/SNF family of ATP-dependent chromatin remodelers: similar mechanisms for diverse functions. *Curr Top Microbiol Immunol*. 2003;274:143-169.
123. Nie Z, Xue Y, Yang D, et al. A specificity and targeting subunit of a human SWI/SNF family-related chromatin-remodeling complex. *Mol Cell Biol*. 2000;20:8879-8888.
124. Greenblatt SM, Man N, Hamard PJ, et al. CARM1 is essential for myeloid leukemogenesis but dispensable for normal hematopoiesis. *Cancer Cell*. 2018;34:868.
125. Xu F, Flowers S, Moran E. Essential role of ARID2 protein-containing SWI/SNF complex in tissue-specific gene expression. *J Biol Chem*. 2012;287:5033-5041.
126. Marfella CG, Imbalzano AN. The Chd family of chromatin remodelers. *Mutat Res*. 2007;618:30-40.
127. Sun F, Yang Q, Weng W, et al. Chd4 and associated proteins function as corepressors of Sox9 expression during BMP-2-induced chondrogenesis. *Journal Bone Miner Res*. 2013;28:1950-1961.
128. Baumgart SJ, Najafova Z, Hossan T, et al. CHD1 regulates cell fate determination by activation of differentiation-induced genes. *Nucleic Acids Res*. 2017;45:7722-7735.
129. Lee HW, Suh JH, Kim AY, Lee YS, Park SY, Kim JB. Histone deacetylase 1-mediated histone modification regulates osteoblast differentiation. *Mol Endocrinol*. 2006;20:2432-2443.
130. Kumar A, Salimath BP, Schieker M, Stark GB, Finkenzeller G. Inhibition of metastasis-associated gene 1 expression affects proliferation and osteogenic differentiation of immortalized human mesenchymal stem cells. *Cell Prolif*. 2011;44:128-138.
131. Zhou C, Zou J, Zou S, Li X. INO80 is required for osteogenic differentiation of human mesenchymal stem cells. *Sci Rep*. 2016;6:35924.
132. Breiling A, Lyko F. Epigenetic regulatory functions of DNA modifications: 5-methylcytosine and beyond. *Epigenetics Chromatin*. 2015;8:24.
133. Bork S, Pfister S, Witt H, et al. DNA methylation pattern changes upon long-term culture and aging of human mesenchymal stromal cells. *Aging Cell*. 2010;9:54-63.
134. Yang R, Yu T, Kou X, et al. Tet1 and Tet2 maintain mesenchymal stem cell homeostasis via demethylation of the P2rX7 promoter. *Nat Commun*. 2018;9:2143.
135. Zhang RP, Shao JZ, Xiang LX. GADD45A protein plays an essential role in active DNA demethylation during terminal osteogenic differentiation of adipose-derived mesenchymal stem cells. *J Biol Chem*. 2011;286:41083-41094.
136. Shen WC, Lai YC, Li LH, et al. Methylation and PTEN activation in dental pulp mesenchymal stem cells promotes osteogenesis and reduces oncogenesis. *Nat Commun*. 2019;10:2226.
137. Ying J, Xu T, Wang C, et al. Dnmt3b ablation impairs fracture repair through upregulation of Notch pathway. *JCI insight*. 2020;5.
138. Stachecka J, Lemanska W, Noak M, Szczerbal I. Expression of key genes involved in DNA methylation during in vitro differentiation of porcine mesenchymal stem cells (MSCs) into adipocytes. *Biochem Biophys Res Comm*. 2020;522:811-818.
139. Zhou C, Liu Y, Li X, Zou J, Zou S. DNA N(6)-methyladenine demethylase ALKBH1 enhances osteogenic differentiation of human MSCs. *Bone Res*. 2016;4:16033.
140. Zhang Z, Hou Y, Wang Y, et al. Regulation of adipocyte differentiation by METTL4, a 6 mA methylase. *Sci Rep*. 2020;10:8285.
141. Thaler R, Agsten M, Spitzer S, et al. Homocysteine suppresses the expression of the collagen cross-linker lysyl oxidase involving IL-6, Fli1, and epigenetic DNA methylation. *J Biol Chem*. 2011;286:5578-5588.
142. Li B, Zhao J, Ma JX, et al. Overexpression of DNMT1 leads to hypermethylation of H19 promoter and inhibition of Erk signaling pathway in disuse osteoporosis. *Bone*. 2018;111:82-91.
143. Tsai CC, Su PF, Huang YF, Yew TL, Hung SC. Oct4 and Nanog directly regulate Dnmt1 to maintain self-renewal and undifferentiated state in mesenchymal stem cells. *Mol Cell*. 2012;47:169-182.
144. Li G, An J, Han X, Zhang X, Wang W, Wang S. Hypermethylation of microRNA-149 activates SDF-1/CXCR4 to promote osteogenic differentiation of mesenchymal stem cells. *J Cell Physiol*. 2019;234:23485-23494.
145. Taylor SM, Jones PA. Multiple new phenotypes induced in 10T1/2 and 3T3 cells treated with 5-azacytidine. *Cell*. 1979;17:771-779.
146. Bowers RR, Kim JW, Otto TC, Lane MD. Stable stem cell commitment to the adipocyte lineage by inhibition of DNA methylation: Role of the BMP-4 gene. *Proc Nat Acad Sci*. 2006;103(35):13022-13027. https://doi.org/10.1073/pnas.0605789103

147. Chen YS, Wu R, Yang X, et al. Inhibiting DNA methylation switches adipogenesis to osteoblastogenesis by activating Wnt10a. *Sci Rep*. 2016;6:25283.
148. Ma X, Kang S. Functional implications of DNA methylation in adipose biology. *Diabetes*. 2019;68:871-878.
149. Yang X, Wu R, Shan W, Yu L, Xue B, Shi H. DNA methylation biphasically regulates 3T3-L1 preadipocyte differentiation. *Mol Endocrinol*. 2016;30:677-687.
150. Zhang R, Wang N, Zhang LN, et al. Knockdown of DNMT1 and DNMT3a promotes the angiogenesis of human mesenchymal stem cells leading to arterial specific differentiation. *Stem Cells*. 2016;34:1273-1283.
151. Liu K, Li QM, Pan LH, et al. The effects of lotus root amylopectin on the formation of whey protein isolate gels. *Carbohyd Polym*. 2017;175:721-727.
152. Shen J, Hovhannisyan H, Lian JB, et al. Transcriptional induction of the osteocalcin gene during osteoblast differentiation involves acetylation of histones h3 and h4. *Mol Endocrinol*. 2003;17:743-756.
153. Tsuda M, Takahashi S, Takahashi Y, Asahara H. Transcriptional co-activators CREB-binding protein and p300 regulate chondrocyte-specific gene expression via association with Sox9. *J Biol Chem*. 2003;278:27224-27229.
154. van Beekum O, Brenkman AB, Grontved L, et al. The adipogenic acetyltransferase Tip60 targets activation function 1 of peroxisome proliferator-activated receptor gamma. *Endocrinology*. 2008;149:1840-1849.
155. Sui BD, Zheng CX, Li M, Jin Y, Hu CH. Epigenetic regulation of mesenchymal stem cell homeostasis. *Trends Cell Biol*. 2020;30:97-116.
156. Farmer SR. Transcriptional control of adipocyte formation. *Cell Metab*. 2006;4:263-273.
157. Sierra J, Villagra A, Paredes R, et al. Regulation of the bone-specific osteocalcin gene by p300 requires Runx2/Cbfa1 and the vitamin D3 receptor but not p300 intrinsic histone acetyltransferase activity. *Mol Cell Biol*. 2003;23:3339-3351.
158. Jing H, Liao L, Su X, et al. Declining histone acetyltransferase GCN5 represses BMSC-mediated angiogenesis during osteoporosis. *FASEB J*. 2017;31:4422-4433.
159. Zhang P, Liu Y, Jin C, et al. Histone H3K9 acetyltransferase PCAF is essential for osteogenic differentiation through bone morphogenetic protein signaling and may be involved in osteoporosis. *Stem Cells*. 2016;34:2332-2341.
160. Gao F, Chiu SM, Motan DA, et al. Mesenchymal stem cells and immunomodulation: current status and future prospects. *Cell Death Dis*. 2016;7:e2062.
161. Huang S, Wang S, Bian C, et al. Upregulation of miR-22 promotes osteogenic differentiation and inhibits adipogenic differentiation of human adipose tissue-derived mesenchymal stem cells by repressing HDAC6 protein expression. *Stem Cells Dev*. 2012;21:2531-2540.
162. Wang Y, Shi ZY, Feng J, Cao JK. HDAC6 regulates dental mesenchymal stem cells and osteoclast differentiation. *BMC Oral Health*. 2018;18:190.
163. Rimando MG, Wu HH, Liu YA, et al. Glucocorticoid receptor and Histone deacetylase 6 mediate the differential effect of dexamethasone during osteogenesis of mesenchymal stromal cells (MSCs). *Sci Rep*. 2016;6:37371.
164. Picard F, Kurtev M, Chung N, et al. Sirt1 promotes fat mobilization in white adipocytes by repressing PPAR-gamma. *Nature*. 2004;429:771-776.
165. Backesjo CM, Li Y, Lindgren U, Haldosen LA. Activation of Sirt1 decreases adipocyte formation during osteoblast differentiation of mesenchymal stem cells. *Cells, tissues, organs*. 2009;189:93-97.
166. Qu P, Wang L, Min Y, McKennett L, Keller JR, Lin PC. Vav1 regulates mesenchymal stem cell differentiation decision between adipocyte and chondrocyte via Sirt1. *Stem Cells*. 2016;34:1934-1946.
167. Tseng PC, Hou SM, Chen RJ, et al. Resveratrol promotes osteogenesis of human mesenchymal stem cells by upregulating RUNX2 gene expression via the SIRT1/FOXO3A axis. *J Bone Miner Res*. 2011;26:2552-2563.
168. Yoon DS, Choi Y, Jang Y, et al. SIRT1 directly regulates SOX2 to maintain self-renewal and multipotency in bone marrow-derived mesenchymal stem cells. *Stem Cells*. 2014;32:3219-3231.
169. Simic P, Zainabadi K, Bell E, et al. SIRT1 regulates differentiation of mesenchymal stem cells by deacetylating beta-catenin. *EMBO Mol Med*. 2013;5:430-440.
170. Sun H, Wu Y, Fu D, Liu Y, Huang C. SIRT6 regulates osteogenic differentiation of rat bone marrow mesenchymal stem cells partially via suppressing the nuclear factor-kappaB signaling pathway. *Stem Cells*. 2014;32:1943-1955.
171. Zhang P, Liu Y, Wang Y, et al. SIRT6 promotes osteogenic differentiation of mesenchymal stem cells through BMP signaling. *Sci Rep*. 2017;7:10229.
172. Dudakovic A, Samsonraj RM, Paradise CR, et al. Inhibition of the epigenetic suppressor EZH2 primes osteogenic differentiation mediated by BMP2. *J Biol Chem*. 2020;295:7877-7893.
173. Zhu XX, Yan YW, Chen D, et al. Long non-coding RNA HoxA-AS3 interacts with EZH2 to regulate lineage commitment of mesenchymal stem cells. *Oncotarget*. 2016;7:63561-63570.
174. Hemming S, Cakouros D, Codrington J, et al. EZH2 deletion in early mesenchyme compromises postnatal bone microarchitecture and structural integrity and accelerates remodeling. *FASEB J*. 2017;31:1011-1027.
175. Camilleri ET, Dudakovic A, Riester SM, et al. Loss of histone methyltransferase Ezh2 stimulates an osteogenic transcriptional program in chondrocytes but does not affect cartilage development. *J Biol Chem*. 2018;293:19001-19011.
176. Dudakovic A, Camilleri ET, Paradise CR, et al. Enhancer of zeste homolog 2 (Ezh2) controls bone formation and cell cycle progression during osteogenesis in mice. *J Biol Chem*. 2018;293:12894-12907.
177. Dudakovic A, Camilleri ET, Riester SM, et al. Enhancer of zeste homolog 2 inhibition stimulates bone formation and mitigates bone loss caused by ovariectomy in skeletally mature mice. *J Biol Chem*. 2016;291:24594-24606.
178. Dudakovic A, Camilleri ET, Xu F, et al. Epigenetic control of skeletal development by the histone methyltransferase Ezh2. *J Biol Chem*. 2015;290:27604-27617.
179. Wei Y, Chen YH, Li LY, et al. CDK1-dependent phosphorylation of EZH2 suppresses methylation of H3K27 and promotes osteogenic differentiation of human mesenchymal stem cells. *Nat Cell Biol*. 2011;13:87-94.
180. Zhu L, Xu PC. Downregulated LncRNA-ANCR promotes osteoblast differentiation by targeting EZH2 and regulating Runx2 expression. *Biochem Biophys Res Comm*. 2013;432:612-617.
181. Hernandez-Munoz I, Taghavi P, Kuijl C, Neefjes J, van Lohuizen M. Association of BMI1 with polycomb bodies is dynamic and requires PRC2/EZH2 and the maintenance DNA methyltransferase DNMT1. *Mol Cell Biol*. 2005;25:11047-11058.

182. Sengupta A, Ficker AM, Dunn SK, Madhu M, Cancelas JA. Bmi1 reprograms CML B-lymphoid progenitors to become B-ALL-initiating cells. *Blood*. 2012;119:494-502.
183. Jung Y, Nolta JA. BMI1 regulation of self-renewal and multipotency in human mesenchymal stem cells. *Curr Stem Cell Res Ther*. 2016;11:131-140.
184. Boila LD, Chatterjee SS, Banerjee D, Sengupta A. KDM6 and KDM4 histone lysine demethylases emerge as molecular therapeutic targets in human acute myeloid leukemia. *Exp Hematol*. 2018;58(44–51):e47.
185. Biswas M, Chatterjee SS, Boila LD, Chakraborty S, Banerjee D, Sengupta A. MBD3/NuRD loss participates with KDM6A program to promote DOCK5/8 expression and Rac GTPase activation in human acute myeloid leukemia. *FASEB J*. 2019;33:5268-5286.
186. Tran N, Broun A, Ge K. Lysine demethylase KDM6A in differentiation, development and cancer. *Mol Cell Biol*. 2020;40(20): https://doi.org/10.1128/MCB.00341-20.
187. Hemming S, Cakouros D, Isenmann S, et al. EZH2 and KDM6A act as an epigenetic switch to regulate mesenchymal stem cell lineage specification. *Stem Cells*. 2014;32:802-815.
188. Rojas A, Aguilar R, Henriquez B, et al. Epigenetic control of the bone-master Runx2 gene during osteoblast-lineage commitment by the histone demethylase JARID1B/KDM5B. *J Biol Chem*. 2015;290:28329-28342.
189. Ye L, Fan Z, Yu B, et al. Histone demethylases KDM4B and KDM6B promotes osteogenic differentiation of human MSCs. *Cell Stem Cell*. 2012;11:50-61.
190. Takada I, Yogiashi Y, Kato S. Signaling crosstalk between PPARgamma and BMP2 in mesenchymal stem cells. *PPAR Res*. 2012;2012:607141.
191. Takada I, Kouzmenko AP, Kato S. Wnt and PPARgamma signaling in osteoblastogenesis and adipogenesis. *Nat Rev Rheumatol*. 2009;5:442-447.
192. Rodova M, Lu Q, Li Y, et al. Nfat1 regulates adult articular chondrocyte function through its age-dependent expression mediated by epigenetic histone methylation. *J Bone Miner Res*. 2011;26:1974-1986.
193. Yang L, Lawson KA, Teteak CJ, et al. ESET histone methyltransferase is essential to hypertrophic differentiation of growth plate chondrocytes and formation of epiphyseal plates. *Dev Biol*. 2013;380:99-110.
194. Lawson KA, Teteak CJ, Gao J, et al. ESET histone methyltransferase regulates osteoblastic differentiation of mesenchymal stem cells during postnatal bone development. *FEBS Lett*. 2013;587:3961-3967.
195. Wang L, Niu N, Li L, Shao R, Ouyang H, Zou W. H3K36 trimethylation mediated by SETD2 regulates the fate of bone marrow mesenchymal stem cells. *PLoS Biol*. 2018;16:e2006522.
196. Yang J, Kaur K, Ong LL, Eisenberg CA, Eisenberg LM. Inhibition of G9a histone methyltransferase converts bone marrow mesenchymal stem cells to cardiac competent progenitors. *Stem Cells Int*. 2015;2015:270428.
197. Yu BD, Hess JL, Horning SE, Brown GA, Korsmeyer SJ. Altered Hox expression and segmental identity in Mll-mutant mice. *Nature*. 1995;378:505-508.
198. Terranova R, Agherbi H, Boned A, Meresse S, Djabali M. Histone and DNA methylation defects at Hox genes in mice expressing a SET domain-truncated form of Mll. *Proc Natl Acad Sci USA*. 2006;103:6629-6634.
199. Lee J, Saha PK, Yang QH, et al. Targeted inactivation of MLL3 histone H3-Lys-4 methyltransferase activity in the mouse reveals vital roles for MLL3 in adipogenesis. *Proc Natl Acad Sci USA*. 2008;105:19229-19234.
200. Lee YF, Nimura K, Lo WN, Saga K, Kaneda Y. Histone H3 lysine 36 methyltransferase Whsc1 promotes the association of Runx2 and p300 in the activation of bone-related genes. *PLoS One*. 2014;9:e106661.
201. Khani F, Thaler R, Paradise CR, et al. Histone H4 methyltransferase Suv420h2 maintains fidelity of osteoblast differentiation. *J Cell Biochem*. 2017;118:1262-1272.
202. Yin B, Yu F, Wang C, Li B, Liu M, Ye L. Epigenetic control of mesenchymal stem cell fate decision via histone methyltransferase Ash1l. *Stem Cells*. 2019;37:115-127.
203. Ito T, Yadav N, Lee J, et al. Arginine methyltransferase CARM1/PRMT4 regulates endochondral ossification. *BMC Dev Biol*. 2009;9:47.
204. He J, Kallin EM, Tsukada Y, Zhang Y. The H3K36 demethylase Jhdm1b/Kdm2b regulates cell proliferation and senescence through p15(Ink4b). *Nat Struct Mol Biol*. 2008;15:1169-1175.
205. Dong R, Yao R, Du J, Wang S, Fan Z. Depletion of histone demethylase KDM2A enhanced the adipogenic and chondrogenic differentiation potentials of stem cells from apical papilla. *Exp Cell Res*. 2013;319:2874-2882.
206. Fan Z, Yamaza T, Lee JS, et al. BCOR regulates mesenchymal stem cell function by epigenetic mechanisms. *Nat Cell Biol*. 2009;11:1002-1009.
207. Du J, Ma Y, Ma P, Wang S, Fan Z. Demethylation of epiregulin gene by histone demethylase FBXL11 and BCL6 corepressor inhibits osteo/dentinogenic differentiation. *Stem Cells*. 2013;31:126-136.
208. Guo L, Li X, Huang JX, et al. Histone demethylase Kdm4b functions as a co-factor of C/EBPbeta to promote mitotic clonal expansion during differentiation of 3T3-L1 preadipocytes. *Cell Death Differ*. 2012;19:1917-1927.
209. Lu C, Ward PS, Kapoor GS, et al. IDH mutation impairs histone demethylation and results in a block to cell differentiation. *Nature*. 2012;483:474-478.
210. Benevolenskaya EV, Murray HL, Branton P, Young RA, Kaelin WG Jr. Binding of pRB to the PHD protein RBP2 promotes cellular differentiation. *Mol Cell*. 2005;18:623-635.
211. Sinha KM, Yasuda H, Zhou X, deCrombrugghe B. Osterix and NO66 histone demethylase control the chromatin of Osterix target genes during osteoblast differentiation. *Journal Bone Miner Res*. 2014;29:855-865.
212. Sun J, Ermann J, Niu N, et al. Histone demethylase LSD1 regulates bone mass by controlling WNT7B and BMP2 signaling in osteoblasts. *Bone Res*. 2018;6:14.
213. Okuno Y, Ohtake F, Igarashi K, et al. Epigenetic regulation of adipogenesis by PHF2 histone demethylase. *Diabetes*. 2013;62:1426-1434.
214. Shen X, Kim W, Fujiwara Y, et al. Jumonji modulates polycomb activity and self-renewal versus differentiation of stem cells. *Cell*. 2009;139:1303-1314.
215. Liu S, Liu D, Chen C, et al. MSC transplantation improves osteopenia via epigenetic regulation of notch signaling in Lupus. *Cell Metab*. 2015;22:606-618.
216. Kornicka K, Marycz K, Maredziak M, Tomaszewski KA, Nicpon J. The effects of the DNA methyltranfserases inhibitor

5-Azacitidine on ageing, oxidative stress and DNA methylation of adipose derived stem cells. *J Cell Mol Med*. 2017;21:387-401.
217. Grandi FC, Bhutani N. Epigenetic therapies for osteoarthritis. *Trends Pharmacol Sci*. 2020;41(8):557-569. https://doi.org/10.1016/j.tips.2020.05.008
218. Im GI, Choi YJ. Epigenetics in osteoarthritis and its implication for future therapeutics. *Expert Opin Biol Ther*. 2013;13:713-721.
219. Khan NM, Haqqi TM. Epigenetics in osteoarthritis: potential of HDAC inhibitors as therapeutics. *Pharmacol Res*. 2018;128:73-79.
220. Yu T, Liu D, Zhang T, Zhou Y, Shi S, Yang R. Inhibition of Tet1- and Tet2-mediated DNA demethylation promotes immunomodulation of periodontal ligament stem cells. *Cell Death Dis*. 2019;10:780.
221. Azevedo RI, Minskaia E, Fernandes-Platzgummer A, et al. Mesenchymal stromal cells induce regulatory T cells via epigenetic conversion of human conventional CD4 T cells in vitro. *Stem Cells*. 2020;38:1007-1019.
222. Khosravi M, Bidmeshkipour A, Cohen JL, et al. Induction of CD4(+)CD25(+)FOXP3(+) regulatory T cells by mesenchymal stem cells is associated with modulation of ubiquitination factors and TSDR demethylation. *Stem Cell Res Ther*. 2018;9:273.
223. Yang R, Qu C, Zhou Y, et al. Hydrogen Sulfide Promotes Tet1- and Tet2-Mediated Foxp3 Demethylation to Drive Regulatory T Cell Differentiation and Maintain Immune Homeostasis. *Immunity*. 2015;43:251-263.
224. Khosravi M, Bidmeshkipour A, Moravej A, Hojjat-Assari S, Naserian S, Karimi MH. Induction of CD4(+)CD25(+)Foxp3(+) regulatory T cells by mesenchymal stem cells is associated with RUNX complex factors. *Immunol Res*. 2018;66:207-218.
225. Loh C, Park SH, Lee A, Yuan R, Ivashkiv LB, Kalliolias GD. TNF-induced inflammatory genes escape repression in fibroblast-like synoviocytes: transcriptomic and epigenomic analysis. *Ann Rheum Dis*. 2019;78:1205-1214.
226. Ai R, Laragione T, Hammaker D, et al. Comprehensive epigenetic landscape of rheumatoid arthritis fibroblast-like synoviocytes. *Nat Commun*. 2018;9:1921.
227. De Witte SFH, Peters FS, Merino A, et al. Epigenetic changes in umbilical cord mesenchymal stromal cells upon stimulation and culture expansion. *Cytotherapy*. 2018;20:919-929.
228. Teklemariam T, Purandare B, Zhao L, Hantash BM. Inhibition of DNA methylation enhances HLA-G expression in human mesenchymal stem cells. *Biochem Biophys Res Commun*. 2014;452:753-759.
229. Rovira Gonzalez YI, Lynch PJ, Thompson EE, Stultz BG, Hursh DA. In vitro cytokine licensing induces persistent permissive chromatin at the Indoleamine 2,3-dioxygenase promoter. *Cytotherapy*. 2016;18:1114-1128.
230. Netea MG, Dominguez-Andres J, Barreiro LB, et al. Defining trained immunity and its role in health and disease. *Nat Rev Immunol*. 2020;20:375-388.
231. Lee S, Kim HS, Roh KH, et al. DNA methyltransferase inhibition accelerates the immunomodulation and migration of human mesenchymal stem cells. *Sci Rep*. 2015;5:8020.
232. Kim KW, Kim HJ, Kim BM, Kwon YR, Kim HR, Kim YJ. Epigenetic modification of mesenchymal stromal cells enhances their suppressive effects on the Th17 responses of cells from rheumatoid arthritis patients. *Stem Cell Res Ther*. 2018;9:208.
233. Vella S, Conaldi PG, Cova E, et al. Lung resident mesenchymal cells isolated from patients with the Bronchiolitis Obliterans Syndrome display a deregulated epigenetic profile. *Sci Rep*. 2018;8:11167.
234. Lim J, Lee S, Ju H, et al. Valproic acid enforces the priming effect of sphingosine-1 phosphate on human mesenchymal stem cells. *Int J Mol Med*. 2017;40:739-747.
235. Kim SH, In Choi H, Choi MR, et al. Epigenetic regulation of IFITM1 expression in lipopolysaccharide-stimulated human mesenchymal stromal cells. *Stem Cell Res Ther*. 2020;11:16.
236. Inoue S, Popp FC, Koehl GE, et al. Immunomodulatory effects of mesenchymal stem cells in a rat organ transplant model. *Transplantation*. 2006;81:1589-1595.
237. Chen X, Gan Y, Li W, et al. The interaction between mesenchymal stem cells and steroids during inflammation. *Cell Death Dis*. 2014;5:e1009.

How to cite this article: Chakraborty S, Sinha S, Sengupta A. Emerging trends in chromatin remodeler plasticity in mesenchymal stromal cell function. *The FASEB Journal*. 2021;35:e21234. https://doi.org/10.1096/fj.202002232R

STAR Protocols

CellPress
OPEN ACCESS

Protocol

Establishment of a Long-Term Co-culture Assay for Mesenchymal Stromal Cells and Hematopoietic Stem/Progenitors

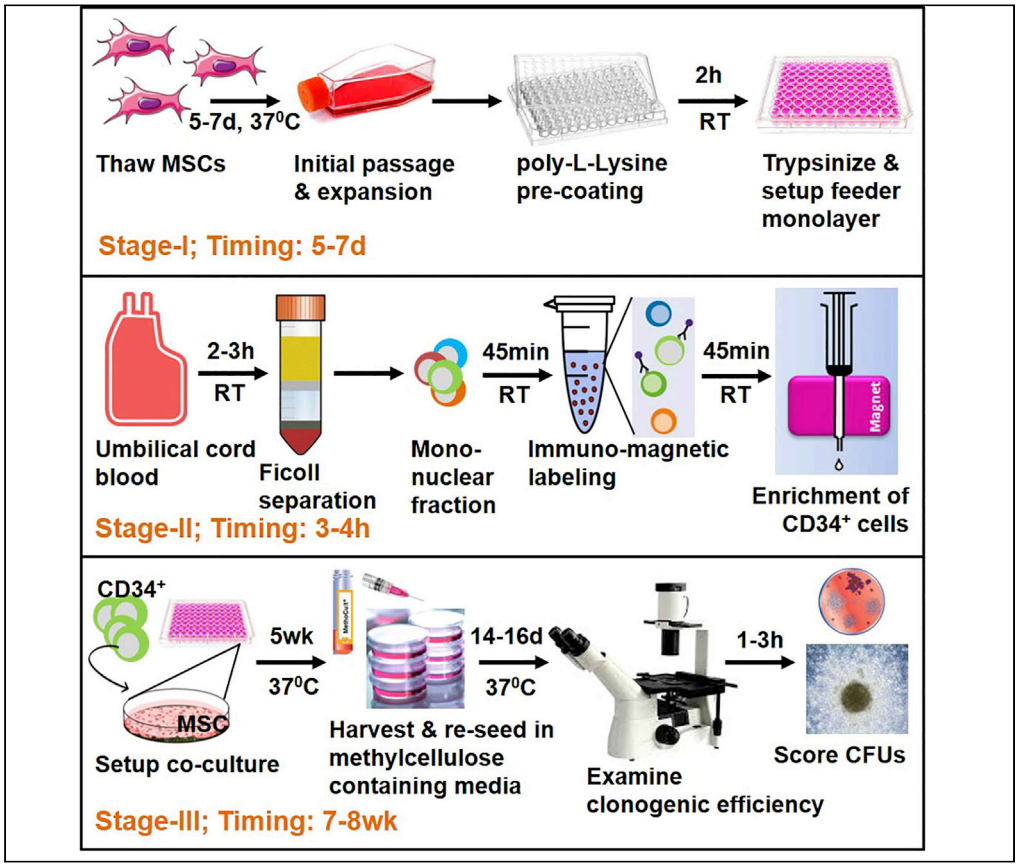

We describe a protocol for a long-term co-culture assay to study the contribution of mesenchymal stromal cells (MSCs) in regulating hematopoietic stem/progenitor cell (HSPC) activity. In addition, we describe the use of a clonogenic assay to determine myelo-erythroid differentiation. This long-term culture-initiating cell assay can be used for qualitative analysis of MSCs capable of supporting hematopoiesis and may also be used as a proxy readout to study HSPC repopulation.

Sayantani Sinha, Sayan Chakraborty, Amitava Sengupta

sayanatani.sinha@csiriicb.res.in (S.S.)
amitava.sengupta@iicb.res.in (A.S.)

HIGHLIGHTS

We report long-term co-culture of mesenchymal stroma and hematopoietic stem/progenitors

End-point colony-forming analysis helps determine myelo-erythroid differentiation

This protocol analyzes mesenchymal stromal cell potential to support hematopoiesis

Long-term culture-initiating cell assay is a surrogate for hematopoietic engraftment

Sinha et al., STAR Protocols 1, 100161
December 18, 2020
https://doi.org/10.1016/j.xpro.2020.100161

STAR Protocols

CellPress
OPEN ACCESS

Protocol

Establishment of a Long-Term Co-culture Assay for Mesenchymal Stromal Cells and Hematopoietic Stem/Progenitors

Sayantani Sinha,[1,2,3,*] Sayan Chakraborty,[1,2] and Amitava Sengupta[1,2,4,*]

[1]Stem Cell & Leukemia Lab, Cancer Biology & Inflammatory Disorder Division, CSIR-Indian Institute of Chemical Biology, 4, Raja S. C. Mullick Road, Kolkata 700032, India

[2]Translational Research Unit of Excellence, CN-6, Sector V, Salt Lake, Kolkata 700091, India

[3]Technical Contact

[4]Lead Contact

*Correspondence: sayanatani.sinha@csiriicb.res.in (S.S.), amitava.sengupta@iicb.res.in (A.S.)
https://doi.org/10.1016/j.xpro.2020.100161

SUMMARY

We describe a protocol for a long-term co-culture assay to study the contribution of mesenchymal stromal cells (MSCs) in regulating hematopoietic stem/progenitor cell (HSPC) activity. In addition, we describe the use of a clonogenic assay to determine myelo-erythroid differentiation. This long-term culture-initiating cell assay can be used for qualitative analysis of MSCs capable of supporting hematopoiesis and may also be used as a proxy readout to study HSPC repopulation. For complete details on the use and execution of this protocol, please refer to Sinha et al. (2020).

BEFORE YOU BEGIN

Prepare Tissue Culture Plates

1. Use 96-well flat-bottomed tissue culture (TC) wells to generate adherent mesenchymal stromal (MSC) monolayer.
2. Pre-coat the TC wells with 100 μL of 0.01% poly-L-lysine at 25°C–30°C for 2 h or 12–16 h at 4°C.

   Note: Pre-coating of the plates must be done just prior to use. For 12–16 h coating of the wells using poly-L-lysine, seal the edges of the plate with parafilm and store in a refrigerator maintained at 4°C. Do not keep the plates for more than 24 h in this condition.

3. Treating wells with poly-L-lysine increases the adherence of the stromal monolayer and prevents peeling off from the surface during subsequent media exchange.
4. Ensure the wells are dry after coating is complete.
5. Seed OP9 cells at a density of 2.5×10^3 cells/cm^2 per well in 200 μL of DMEM supplemented with 20% FBS, Pens-Strep (1×) and L-glutamine (1×). Incubate the cells at 37°C with 5% CO_2 for at least 5 days.
6. If media is turning yellow hemi deplete the media.
7. The cells should reach 100% confluency after 5–7 days.

   ⚠ CRITICAL: Ensure umbilical cord blood (UCB) derived mononuclear cells (freshly prepared or cryopreserved) are in stock. Once the MSC monolayer forms enrich $CD34^+$ hematopoietic stem/progenitor cells (HSPCs) from UCB for immediate use.

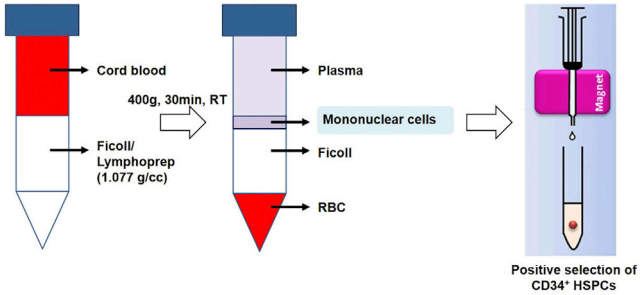

Figure 1. Schema Representing Isolation of Human HSPCs

Establishment of Adherent Feeder Layer Prior to the Addition of HSPCs

Timing: 5–7 days

8. The feeder layer needs to be established 5–7 days prior to the addition of the HSPCs

Isolation of CD34$^+$ Human Hematopoietic Stem and Progenitor Cells (HSPCs)

Timing: 3–5 h

9. Cord blood mononuclear cell preparation from fresh end of term healthy samples
10. Use these mononuclear cells to isolate cord blood-derived CD34$^+$ HSPCs using column-free human progenitor cell isolation kit (Figure 1)

Note: Either process the mononuclear cells for immediate use or cryopreserve them in liquid nitrogen for future use. Cells are cryopreserved in cryogenic media containing 90% FBS and 10% DMSO.

⚠ CRITICAL: Commonly used sources to enrich and isolate human HSPCs are umbilical cord blood, mobilized peripheral blood/apheresis and bone marrow aspiration. This protocol has used human cord blood-derived mononuclear cells as the source of CD34$^+$ cells. For using cryopreserved samples for isolation of CD34$^+$ cells, ensure that cells are viable using hemocytometer and trypan blue before proceeding with progenitor cell isolation. Also ensure that the cells do not form clump during thawing. Avoid clumping by rapid addition of the sample to complete media (IMDM containing 10% FBS, 100 U/mL penicillin, 100 mg/mL streptomycin and 2 mM L-glutamine). Breakdown the cell pellets before adding resuspension media (IMDM containing 10% FBS, 100 U/mL penicillin, 100 mg/mL streptomycin and 2 mM L-glutamine along with 10 ng/mL of SCF, FLT3, and TPO). Remove clumps by passing the cell suspension through a 70 μm filter. This leads to loss of viable cells and may significantly reduce overall yield and quality of CD34$^+$ cells.

KEY RESOURCES TABLE

REAGENT or RESOURCE	SOURCE	IDENTIFIER
Chemicals, Peptides, and Recombinant Proteins		
rh SCF	PeproTech	Cat# 300-07
rh FLT-3	PeproTech	Cat# 300-19
rh TPO	PeproTech	Cat# 300-18

(*Continued on next page*)

Continued

REAGENT or RESOURCE	SOURCE	IDENTIFIER
Ficoll or Lymphoprep	Stem Cell Technology	Cat# 07851
MethoCult	Stem Cell Technology	Cat# H4034
MyeloCult	Stem Cell Technology	Cat# H5100
Hydrocortisone	Stem Cell Technology	Cat# 74142
Horse Serum	Stem Cell Technology	Cat# 06750
β-mercaptoethanol	Sigma	Cat# M3148
DMEM	Thermo	Cat# 11995065
IMDM	Thermo	Cat# 12440053
FBS (heat inactivated)	Thermo	Cat# 10438026
FBS	Thermo	Cat# 16000044
PBS (Ca^{2+} and Mg^{2+} free)	Sigma-Aldrich	N/A
Isopropyl alcohol	Sigma-Aldrich	Cat# I9516
Penicillin/Streptomycin	Thermo	Cat# 15070063
L-Glutamine	Thermo	Cat# 25030081
Trypsin	Thermo	Cat# 25300062
poly-L-Lysine	Sigma-Aldrich	Cat# P4707
Critical Commercial Assays		
Column-Free Human CD34 Positive Selection Kit (for cord blood)	Stem Cell Technology	Cat# 18066A
EasySep™ Buffer	Stem Cell Technology	Cat# 20144
Experimental Models: Cell Lines		
OP9	ATCC	Cat# CRL-2749; RRID: CVCL_4398
Biological Samples		
Human umbilical cord blood	This study	Samples were collected according to CSIR-IICB Human Ethics Committee approval and following guidelines set by Institutional Review Board
Serological pipettes	N/A	N/A
Sterile polystyrene tubes	N/A	N/A
Sterile pipette tips	N/A	N/A
Syringe (5 mL)	N/A	N/A
18 Gauge Blunt-End Needles	N/A	N/A
T-25 tissue culture treated flasks	N/A	N/A
150 mm culture dishes	N/A	N/A
35 mm Gridded Scoring Dish	Thermo	Cat# 174926
Permanent fine-tip marker	N/A	N/A
96-well plates tissue culture treated	N/A	N/A

MATERIALS AND EQUIPMENT

Solutions required

- 0.01% poly-L-Lysine solution
- PBS (Ca^{2+} and Mg^{2+} free)
- 0.05% Trypsin containing 0.05% EDTA
- 1.077 g/mL Ficoll or Lymphoprep
- RBC lysis buffer (optional)

- PBS containing 2% FBS and 1 mM EDTA (Recommended media for $CD34^+$ cell isolation in place of EasySep™ Buffer)

Recipe for Co-culture of Isolated HSPCs with OP9 Cells

Reagent	Final Concentration (mM or μM)	Volume (μL)
Hydrocortisone (10^{-3} M) (2.42 mg)	10^{-5} M (To prepare 10^{-3} M solution of hydrocortisone dissolve 2.42 mg in 5 mL of α-MEM media. Dilute 1:100 to obtain a final concentration of 10^{-5} M)	5 mL of α-MEM media
β-mercaptoethanol	100 μM	N/A
Horse serum	5%	N/A
FBS (Heat Inactivated, HI)	10% (used during co-culture)	N/A

Maintain OP9 cells in DMEM media containing 20% non-heat inactivated FBS and supplemented with 100 U/mL penicillin, 100 mg/mL streptomycin and 2 mM L-glutamine

⚠ CRITICAL: Use β-mercaptoethanol with necessary precaution. Freshly prepare hydrocortisone just before use. Store the stock solutions at 2°C–8°C for up to 1 week. Use hydrocortisone for long-term culture and long-term culture-initiating cell assays

Alternatives: Use MyeloCult in place of IMDM containing 10% FBS during co-culture

Equipment for Isolation of $CD34^+$ HSPCs

Equipment	Source	Identifier
EasySep™ Magnet	Stem Cell Technology	Cat# 18000

STEP-BY-STEP METHOD DETAILS

Establishment of Adherent Cell Layer

Timing: 5–7 days

This step involves adherent feeder layer formation for subsequent co-culture with HSPCs over a period of 5 weeks

1. Culture of OP9 cells
2. Purchase parental OP9 cells from ATCC. Maintain these cells in DMEM media with supplements as mentioned below.

⚠ CRITICAL: It is essential to maintain the cells at 70% confluency for two to three passages in T-25 cm^2 flasks at 37°C with 5% CO_2 and 100% humidity prior to seeding for adherent layer formation (Figure 2).

Reagents for Culturing OP9 Cells

Components	Final Concentration
DMEM	N/A
Non-Heat Inactivated FBS	20%
Penicillin	100 U/mL
Streptomycin	100 mg/mL
L-Glutamine	2 mM

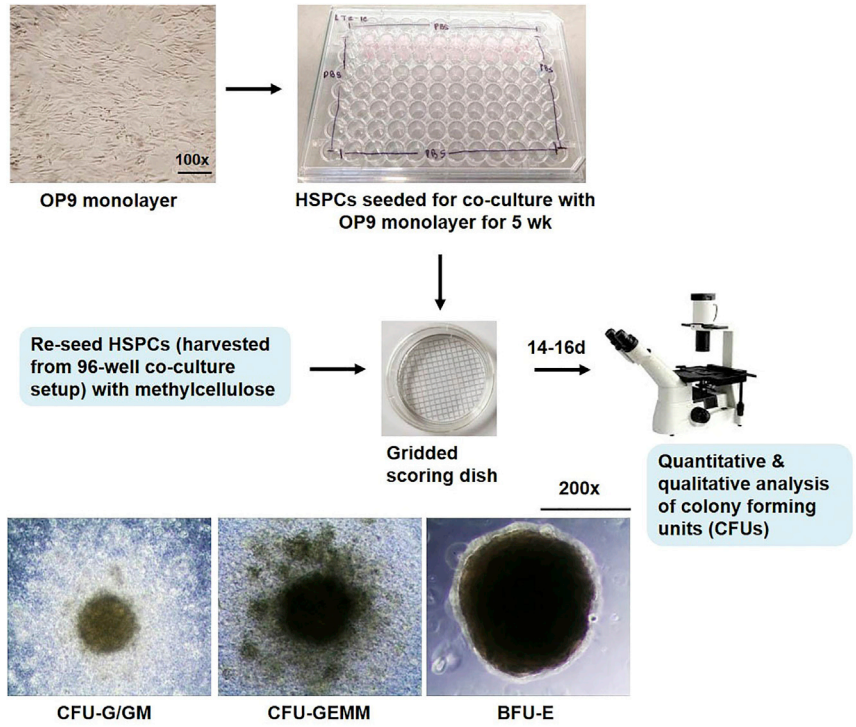

Figure 2. Working Model of Long-Term Co-culture of MSCs and HSPCs and Clonogenic Assay

a. Remove culture media carefully without disrupting the cellular layer.
b. Wash the cellular layer with 1× PBS.
c. Trypsinize the cells using 500 µL of 0.05% Trypsin containing 0.05% EDTA for 2–3 min at 37°C. Observe the flask under microscope to check that the cells have detached. Gently tap the flask incase still there are attached cells in the flask. Add equal volume of OP9 culture media after trypsinization for neutralization. Collect the cell suspension in fresh 15 mL tubes.
d. Pellet down the cells at 125 × *g* for 5 min at 25°C–30°C.
e. Resuspend cells in 5 mL of fresh culture media.
f. Count viable cells using trypan blue and hemocytometer. Mix 10 µL of trypan blue to 10 µL of media containing cells in suspension. Mix carefully and add 10 µL of the mix to hemocytometer for counting trypan blue negative (live) cells using an inverted microscope.
    i. Viable cell count is essential to support the HSPCs for a period of 5 weeks
    ii. Reseed unused cells for subsequent use or cryopreserve

3. Seed cells in poly-L-Lysine coated wells for formation of feeder layer
    a. Pre-coat the TC 96-wells by adding 100 µL of 0.01% poly-L-Lysine for 2 h at 25°C–30°C.
    b. Remove poly-L-lysine completely as residual amount can become toxic for the cells.
    c. Ensure the wells are dry before seeding the cells for adherent layer formation.
    d. Count the number of viable OP9 cells (1f) and seed at a density of 2.5 × 10^{-3}/cm^2 per well in 200 µL of DMEM supplemented with 20% FBS, Pen-Strep (1×) and L-glutamine (1×) per well so that the cells reach confluency of 100% in 5–7 days.
        i. For seeding cells in a 96-well plate, use the inner 60 wells and avoid the peripheral 36 wells.
        ii. Add sterile water or PBS to the unused peripheral 36 wells in order to maintain humidity and preventing evaporation from the wells containing media.
4. Hemi deplete (half media change) after 3 days when the media color partially changes to yellow and cells are 50% confluent.

Note: Adding excess fresh media can lead to over proliferation and detachment of the monolayer. It is essential to maintain the stromal cells as a monolayer, and hemi-depletion helps to maintain an even monolayer. An even, adherent cell monolayer also prevents HSPCs from migrating and adhering to the culture surface of the wells.

Note: Using OP9 cells as stromal support usually does not require the irradiation process. However, use of primary MSCs or FBMD-1 stromal cell line may require further irradiation in order to prevent excessive growth of stroma causing withdrawal of the stromal sheet from the well periphery. Irradiation process commonly involves subjecting nearly confluent stromal layers to 20 Gy radiation using a ^{137}Cs or ^{60}Co γ source. Replace the culture media one day after irradiation with IMDM media containing hydrocortisone and 20% horse serum. Alternatively use Mitomycin C to inhibit excessive growth of the adherent cell layer for long-term culture assays (Ponchio et al., 2000).

Isolate HSPCs once the adherent layer is ready around day 6.

⚠ CRITICAL: Start a fresh experiment if the adherent OP9 layer is not 100% confluent at the end of 7 days. There are many reasons for this: 1. It indicates that cells are not sufficiently healthy; 2. Cells with lower confluency will not be able to support the HSPCs for 5 weeks; 3. If there are empty spaces without the adherent stromal layer, HSPCs will tend to adhere to the TC surface.

Note: Viable cell count at the time of seeding can ensure healthy status of the cells. Live cells will proliferate easily and reach the desired confluency in the stipulated time frame. Essentially this reflects the growth kinetics of OP9 cells (*sh-Control*) that we have recently reported (Sinha et al., 2020; Toksoz et al., 1992). Primary MSCs or FBMD-1 cell line may take longer to reach full confluency.

⚠ CRITICAL: If it takes more than 14 days to reach 100% confluency, we do not advise using these cells for the assays. It is not advisable to keep the cells in culture for more than 7 days (for OP9) and 14 days (for primary MSCs and FBMD-1), without co-culturing once the confluent adherent monolayer is formed.

Isolation of CD34$^+$ HSPCs

Timing: 3–5 h

This step describes processing of fresh umbilical cord blood samples to obtain mononuclear cells and subsequent enrichment of HSPCs. Collect cord blood samples from term pregnancies after informed consent and strictly following human ethics committee guidelines. In the clinical setting the umbilical cord is clamped, wiped with antiseptic, and needle inserted into the vein to withdraw the desired volume of blood. Typically one term pregnancy will help collect about 50 mL of cord blood specimen. With fresh samples, perform density gradient centrifugation and HSPC enrichment on the same day. Otherwise thaw cryopreserved samples for HSPC isolation. Isolate HSPCs one day prior to seeding for the co-culture as they may require 12–16 h pre-stimulation with of recombinant SCF, FLT3L and TPO (10 ng/mL each).

5. Isolation of mononuclear cells from cord blood samples

   a. Gently layer 25 mL of undiluted cord blood sample on top of 25 mL of Lymphoprep or Ficoll (1.077 g/mL) to form the density gradient (Figure 3A).
   b. Thus, for a 50 mL cord blood unit, evenly distribute the sample into two 50 mL centrifugation tubes to perform the density gradient.

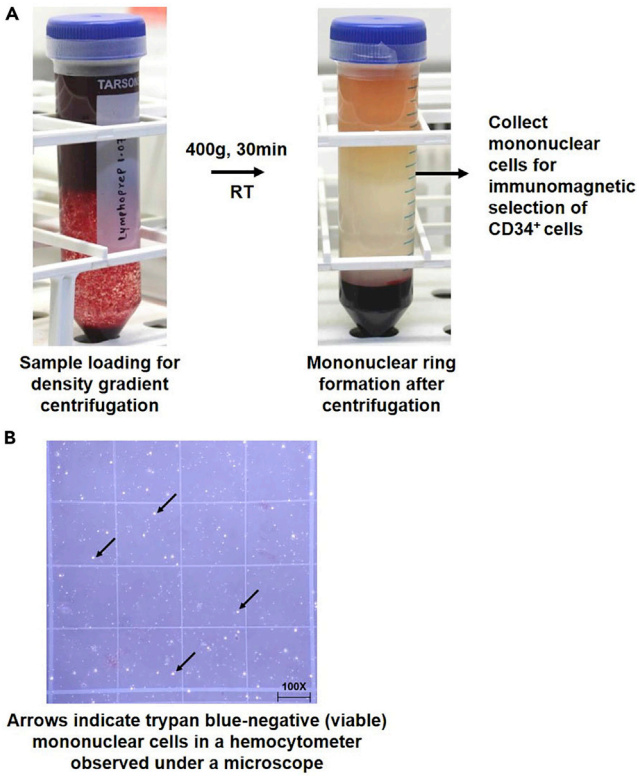

Figure 3. Density Gradient Centrifugation and Viable Cell Counting Analysis

Image showing (A) cord blood density gradient centrifugation and (B) cell counting of mononuclear cells.

c. Perform density gradient centrifugation at 400 × *g* using a horizontal rotor, for 30 min at 25°C–30°C, with an acceleration set at 9 and deceleration at 0. This usually takes around 1.5 h.

d. After the centrifugation carefully collect the mononuclear cells that forms a white ring between the Lymphoprep layer and the plasma using a serological pipette without disturbing the gradient (Methods Video S1). RBCs should have accumulated at the bottom of the tube.
Methods Video S1. Density Gradient Centrifugation, Related to Step 5d

e. Repeat the density gradient centrifugation once more for a total of two times to sufficiently remove RBC contaminants.

f. Wash the mononuclear cells with 40 mL of PBS at 500 × *g* for 5 min at 25°C–30°C to remove residual amount of Lymphoprep.

g. Take viable cell counts using trypan blue and hemocytometer. Mix 10 μL of trypan blue to 10 μL of PBS containing cells in suspension in a separate microcentrifuge tube. Mix rapidly and add 10 μL of the mix to hemocytometer for cell counting using an inverted microscope (Methods Video S2). Live cells should appear as trypan blue negative (Figure 3B).
Methods Video S2. Counting of Trypan Blue Negative Hematopoietic Cells Using a Hemocytometer, Related to Step 5g

h. Proceed with isolation of $CD34^+$ cells or immediately freeze the mononuclear cells. Cryopreserve cells in multiple vials using a cryogenic solution containing 90% FBS and 10% DMSO as the final concentration. Do not freeze more than 10–15 × 10^6 cells per vial. At the beginning resuspend the cell pellets in 100% FBS, total resuspension volume will depend on the number of vials to be used for freezing in accordance with the total number of mononuclear cells obtained from the sample. For each 1.8 mL cryogenic vial add 500 μL of cell suspension, and on the top add 500 μL freezing solution containing 20% DMSO and mix gently. Immediately store

the cryogenic vials, placed within a freezing container, at −80°C. The freezing containers carrying 100% isopropyl alcohol ensure achieve a rate of cooling near −1°C/min, which is the optimal rate for cell preservation. For long-term storage transfer the vials into liquid nitrogen containers in another 24–48 h.

i. For using cryopreserved specimens for isolation of HSPCs, thaw the cells in sufficient quantity (use at least 10–20 mL per vial) of complete media (IMDM containing 10% FBS, 100 U/mL penicillin, 100 mg/mL streptomycin and 2 mM L-glutamine). Ensure that the cells do not form clump during the process by rapidly adding of the sample to complete media with gentle tapping at 25°C–30°C. Centrifuge the cell suspension at 1,000 × *g* for 5 min at 25°C–30°C, aspirate out the media containing DMSO, and wash twice with 50 mL of PBS. Finally resuspend the cells in 1 mL PBS, remove cell clumps if any by passing the cell suspension through a 70 μm filter, and take viable cell count before proceeding for immunomagnetic selection. We did not use DNase to avoid clumping.

Alternatives: Remove RBC contamination by performing RBC lysis after completion of first density gradient centrifugation. Resuspend mononuclear cells in 25 mL of 1× RBC lysis buffer and incubate at 25°C–30°C for 5 min to a maximum of 10 min. After the incubation, top up the tube with sufficient volume of PBS and centrifuge cells at 800 × *g* for 10 min at 25°C–30°C. Wash the cells with PBS to remove residual volume of RBC lysis buffer. Take viable cell counts. Cryopreserve mononuclear cells or immediately proceed for $CD34^+$ cell isolation. Alternatively, perform a second round of density gradient centrifugation. Performing two consecutive rounds of density gradient centrifugation can be a better method to obtain good quality of cells.

Composition of RBC Lysis Buffer (10×)

Components	Amount (For 100 mL)
NH_4Cl	8.02 g
$NaHCO_3$	0.84 g
EDTA (disodium)	0.37 g
H_2O	100 mL

Filter and store at 4°C for up to 6 months, and warm before use. The pH of the buffer should be between 7.1 and 7.4.

6. Isolation of $CD34^+$ cells

a. Resuspend the mononuclear cells in 500 μL of EasySep™ buffer or the recommended media (PBS containing 2% FBS and 1 mM EDTA). Medium should be free of $Ca^{2+}$and Mg^{2+}.
b. Isolate $CD34^+$ cells using Column-free human CD34 progenitor isolation kit.
c. Add $CD34^+$ selection cocktail from Column-Free Human CD34 Positive Selection Kit (for cord blood) to the cell suspension at a concentration of 100 μL/mL.
d. Mix and incubate at 25°C–30°C for 15 min.
e. Mix magnetic particles thoroughly to obtain even distribution by pipetting up and down at least five times.
f. Add magnetic particles at a concentration of 50 μL/mL of sample.
g. Incubate at 25°C–30°C for 10 min.
h. Add EasySep™ buffer or the recommended media to the tube up to 2.5 mL and mix thoroughly 2–3 times. Use either EasySep™ buffer or recommended media for the process.
i. Place the tube in the magnet and incubate for 5 min.
j. Pick up the magnet and in one continuous motion invert the magnet and tube to discard the supernatant. Leave the tube in inverted position for an additional 2–3 s. Do not shake of the drops adhered to the side walls of the tube. This might lead to loss of enriched cells (Methods Video S3).

Methods Video S3. Immunomagnetic Selection of CD34+ HSPCs, Related to Step 6j

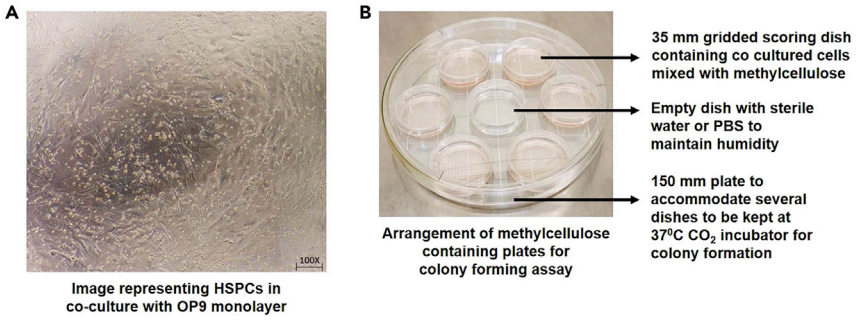

Figure 4. Co-culture and Clonogenic Assay Setup

Photomicrograph images for (A) HSPCs in co-culture with OP9 monolayer and (B) clonogenic assay setup.

k. Repeat steps (h) to(j) for a total of five times.

l. Remove the tube from the magnet. This contains isolated $CD34^+$ cells.

m. Top up with 4 mL of recommended media (defined in 5a as per manufacturer's instruction) and centrifuge at 300 × *g* for 10 min at 25°C–30°C, keeping acceleration 9 and deceleration 0.

n. Resuspend the cell pellet in IMDM media supplemented with 10% heat inactivated FBS, 100 U/mL penicillin, 100 mg/mL streptomycin and 2 mM L-glutamine.

o. Pre-stimulate cells 12–16 h with 10 ng/mL of each of recombinant human SCF, FLT3L and TPO in IMDM complete media (supplemented with 10% FBS, 100 U/mL penicillin, 100 mg/mL streptomycin and 2 mM L-glutamine). We usually pre-stimulate cord blood-derived $CD34^+$ cells prior to *in vitro* co-culture experiments. However, we avoid pre-stimulation for gene expression analysis of $CD34^+$ cells. Absolute number of viable cells does not significantly change after 10–12 h of pre-stimulation.

7. Co-culture assay set up

a. Take viable cell counts immediately after immunomagnetic separation and also after overnight pre-stimulation. Absolute number of viable cells does not significantly change after 10–12 h of pre-stimulation.

b. Ensure that the adherent cell layer is 100% confluent.

c. Seed 25 × 10^3 $CD34^+$ cells per well over the stromal monolayer in 200 μL of IMDM supplemented with 10% heat inactivated FBS, β-mercaptoethanol, 5% horse serum, 10^{-5} M hydrocortisone, 100 U/mL penicillin, 100 mg/mL streptomycin and 2 mM L-glutamine (co-culture media), and co-culture at 37°C in presence of 5% CO_2 for 5 weeks (Figure 4).

d. Add PBS or sterile water to the peripheral wells to prevent evaporation of media and maintain humidity.

e. Check plate every three days under the microscope to ensure that cells appear healthy and enough volume of media is present in all the wells.

f. Replenish one half of the co-culture media (100 μL) every week without disturbing the adherent feeder layer and the HSPCs. Collect media from the wells in microfuge tubes, spin down at 500 × *g* for 5 min at 25°C–30°C to avoid loss of HSPCs during media change. Resuspend in 100 μL of fresh co-culture media and gently add back to the wells, so that each well has a total of 200 μL of co-culture media.

8. Harvest cells for clonogenic assay

a. Remove media and add to fresh microfuge tubes as this media can contain non-adherent hematopoietic cells.

b. Rinse each well with PBS and add this PBS to the tubes containing media previously removed from the wells. Collect PBS that is used to rinse the wells as it might contain hematopoietic cells.

c. Trypsinize the wells with 100 μL of 0.05% trypsin containing 0.05% EDTA per well for 3–5 min at 37°C. Check the wells under microscope to ensure that the adherent layer has started to detach from the surface.
d. Stop trypsinization by addition of 100 μL of IMDM supplemented with 20% heat inactivated FBS, 100 U/mL penicillin, 100 mg/mL streptomycin and 2 mM L-glutamine.
e. Collect the cell suspension in tubes which already contain media and PBS collected from the wells prior to trypsinization and spin down at 500 × *g*, for 7–10 min at 25°C–30°C.
f. Remove the media.
g. Wash with PBS and spin at 500 × *g*, for 7–10 min at 25°C–30°C.
h. Resuspend the cell pellet in 200 μL of basal IMDM media.
i. Meanwhile thaw MethoCult and aliquot 3 mL in 14 mL round bottom tubes.
j. Add 100 U/mL penicillin, 100 mg/mL streptomycin and 2 mM L-glutamine to each tube containing 3 mL of MethoCult.
k. Add the entire single cell suspension from each well to the tube containing 3 mL of Methocult using cut tips. We do not use blunt-end needles in this step. [In this long-term co-culture assay we are only interested to understand qualitative effect of stromal cells in regulating HSPC clonogenic potential. Therefore, we did not perform limiting dilution-based LTC-IC analysis].
l. Vortex the tube thoroughly.
m. Allow the tube to stand for 5 min so that the bubbles rise up to the top.
n. Aliquot the MethoCult containing the cells into 35 mm gridded tissue culture scoring dish using 5 mL syringe fitted with 18-gauge blunt-end needles (Figure 4).
o. Ensure minimum bubble formation by slowly adding MethoCult to the gridded dish and even spreading of the MethoCult.
p. Place the plates in a 150 mm dish along with a 35 mm dish containing sterile water to reduce evaporation.
q. Incubate at 37°C in 5% CO_2 with $\geq$ 95% humidity for 14–16 days.
r. Score the number and type of colonies at the end of the incubation period.
s. Count the well as positive if you can detect one or more CFU-G/GM, CFU-GEMM or BFU-E colonies or score as negative if no colonies are present (Figures 2 and 4).

EXPECTED OUTCOMES

After incubation with methylcellulose-based media different types of colonies should form. The frequency of the types of colonies formed can vary according to the treatment of the HSPCs during co-culture or due to the influence of the stromal layer on the HSPCs. The types of colonies formed usually include CFU-G/GM, CFU-GEMM, and BFU-E (Figure 2). CFU-G/GM colonies are smaller and more scattered while CFU-GEMM colonies are larger and more compact. BFU-E colonies are compact, with well-defined boundaries and dark in color as they differentiate into erythroid lineage. Flow cytometry (FACS) analysis using single cell suspension of these colonies can determine cell surface marker expression. In addition, one can determine frequency of long-term colony-initiating cells (LTC-IC) using limiting dilution assay during co-culture and Poisson statistics (Cancelas et al., 2005; Liu et al., 2013; Sengupta et al., 2010).

Note: Figure 2 shows representative images for CFU-G/GM, CFU-GEMM, and BFU-E. We did not observe CFU-Es in our assays since CFU-Es are more frequently obtained for cultures established from peripheral blood than human umbilical cord blood samples.

CFU-G/GM (Colony-Forming Unit-Granulocyte, Macrophage)

20 or more granulocytes and/or macrophages form these colonies. Cells in these colonies are not hemoglobinized and hence do not appear red in color. Individual cells can be identified along the periphery of the colony. One or more dark dense core can be observed in case of larger colonies. They do not require erythropoietin to support their growth. Colonies obtained from cord blood samples are usually larger in size than those obtained from bone marrow or mobilized peripheral blood.

CFU-GEMM (Colony-Forming Unit-Granulocyte, Erythroid, Macrophage, Megakaryocyte)

A colony that is formed of erythroid cells (containing hemoglobin) and higher number of non-erythroid (do not contain hemoglobin) cells that includes megakaryocytes, granulocytes, and macrophages. Usually the core region of these colonies is made up of erythroid cells and peripheral regions are made up of non-erythroid cells. In certain cases, non-erythroid cells can accumulate on one side of the erythroid cells. Size of CFU-GEMM colonies are usually larger than CFU-GM or BFU-E. The frequency of CFU-GEMM type of colonies is higher in case of cord blood samples than in case of bone marrow. However, variation is usually observed in between samples.

BFU-E (Burst Forming Unit-Erythroid)

More than 200 erythroblasts either singly or in multiple clusters accumulate to form this type of colony. They are hemoglobinized and thus appear deep brown to red in color. Individual cells cannot be identified within the cluster. IL-3, SCF, and EPO containing media support their growth. Cord blood-derived colonies have higher frequency and are larger in size than peripheral blood-derived colonies.

CFU-E (Colony-Forming Unit-Erythroid)

One to two clusters are formed by erythroblasts that are lesser than 200 in number. Colonies appear red or brown in color due to accumulation of hemoglobin. Individual cells cannot be identified within the colony. Presence of EPO in media is essential for its growth. This is more frequently obtained for cultures established from peripheral blood than human umbilical cord blood samples.

LIMITATIONS

The protocol described above is suitable for studying myeloid differentiation of HSPCs when co-cultured with stromal feeder layer. Adapt newer protocols to study lymphoid and NK cell clonogenic efficiencies (Bock, 1997; Lemieux and Eaves, 1996; Lemieux et al., 1995; Miller et al., 1998; Punzel et al., 1999). It is essential to use low cell numbers for culture assay and during colony formation. Using high cell density can lead to formation of large number of colonies that will be difficult to score. Also, if cell density is higher the Methocult may not be sufficient to support the growth of the colonies and they may undergo senescence before analysis. Always use freshly prepared cytokines at recommended concentration for best results.

TROUBLESHOOTING

Problem

50 mL of cord blood sample usually yields 5 × 105 CD34+ cells. However, CD34+ cell number is low.

Potential Solution

Pool more than one umbilical cord blood specimens.

Problem

There is overgrowth of macrophages during co-culture.

Potential Solution

Always use horse serum *by default* during co-culture as it restricts macrophage proliferation.

> *Note:* OP9 cells do not produce M-CSF, which can help reduce macrophage proliferation in the co-culture setup.

Problem

Feeder layer is not confluent.

Potential Solution

OP9 cells may not be healthy, thaw another frozen vial of OP9 and start afresh.

Problem
HSPCs are not healthy.

Potential Solution
Use fresh set of cytokines at recommended concentration for pre-stimulation and co-culture. In addition, freshly prepare hydrocortisone every week and use at defined concentration. Changing concentration can alter possible outcomes.

Problem
Feeder layer is detached during co-culture.

Potential Solutions
During media change keep a residual volume of media in the wells and add fresh media on top of the residual volume.

Ensure that the pointed end of the tips do not come in direct contact with the feeder layer, thus disrupting the continuity and leading to detachment of the monolayer.

Problem
Wells become contaminated.

Potential Solution
In case any of the wells become contaminated, add 200 μL of 1 N NaOH solution to the contaminated well (to prepare 1 N NaOH solution, add 40 g of NaOH to 100 mL of distilled water). Dispose of the well contents using aspiration device. Refill the well with 1 N NaOH. Identify the well on top of the lid. Keep checking the plate for possible contamination.

Problem
Absolute number of CFUs is too low or high. Typically 1 mL of human umbilical cord blood specimens generate between 13,000 and 24,000 CFU-GM (which is 15 times higher than that present in the bone marrow or peripheral blood), between 1,000 and 10,000 of CFU-GEMM, and about 8,000 BFU-E (3 times more than that present in the bone marrow or peripheral blood) (Hordyjewska et al., 2015).

Potential Solution
Ensure proper trypsinization while harvesting cells for the clonogenic assay. It is essential to collect all the cells to avoid loss of positive colonies. Single cell suspension ensures that the colonies have developed from clonogenic precursors.

It is essential to include additional wells or dish containing PBS/H_2O to maintain proper humidity. Do not disturb the plates for the first 10 days. One can check the dish after 10 days to see if colonies have formed. This is an optional step, which is to ensure that the culture system is sufficiently hydrated and there is no contamination.

If stromal layer is not fully confluent then HSPCs will start adhering to the culture well surface. So final colony obtained may not reflect the real clonogenic potential of the HSPCs.

While scoring the plates ensure that colonies formed from the feeder layer are not included.

RESOURCE AVAILABILITY

Lead Contact
Further information and requests for resources and reagents should be directed to and will be fulfilled by Amitava Sengupta (amitava.sengupta@iicb.res.in; amitava.iicb@gmail.com).

Materials Availability

This study did not generate new unique reagents.

Data and Code Availability

This study did not generate/analyze any datasets or code.

SUPPLEMENTAL INFORMATION

Supplemental Information can be found online at https://doi.org/10.1016/j.xpro.2020.100161.

ACKNOWLEDGMENTS

This study is supported by funding from Council for Scientific & Industrial Research (CSIR) (NWP/BIOCERAM/ESC-0103 and Sickle Cell Anemia-Mission Mode Program/HCP-0008 to A.S.), Department of Biotechnology (DBT) (BT/RLF/RE-ENTRY/06/2010), Ramalingaswami Fellowship (to A.S.), DBT (BT/PR13023/MED/31/311/2015) (to A.S.), and Science & Engineering Research Board-Department of Science & Technology (SERB-DST) (SB/SO/HS-053/2013), Government of India (to A.S.). A.S. is a recipient of Indian Council of Medical Research-Department of Health Research (ICMR-DHR) International Fellowship for Indian Biomedical Scientists (INDO/FRC/452/S-11/2019-20-IHD). S.S. and S.C. acknowledge research fellowships from CSIR and UGC, Government of India, respectively. The authors thank Dr. Prasanta Mukhopadhyay for providing umbilical cord blood samples.

AUTHOR CONTRIBUTIONS

Experiments and analysis: S.S. and S.C.; Manuscript design, writing, and editing: S.S. and A.S.; Conception, data interpretation, illustration, and overall direction: A.S.

DECLARATION OF INTERESTS

The authors declare no competing interests.

REFERENCES

Bock, T.A. (1997). Assay systems for hematopoietic stem and progenitor cells. Stem Cells *15* (*Suppl 1*), 185–195.

Cancelas, J.A., Lee, A.W., Prabhakar, R., Stringer, K.F., Zheng, Y., and Williams, D.A. (2005). Rac GTPases differentially integrate signals regulating hematopoietic stem cell localization. Nat. Med. *11*, 886–891.

Hordyjewska, A., Popiolek, L., and Horecka, A. (2015). Characteristics of hematopoietic stem cells of umbilical cord blood. Cytotechnology *67*, 387–396.

Lemieux, M.E., and Eaves, C.J. (1996). Identification of properties that can distinguish primitive populations of stromal-cell-responsive lympho-myeloid cells from cells that are stromal-cell-responsive but lymphoid-restricted and cells that have lympho-myeloid potential but are also capable of competitively repopulating myeloablated recipients. Blood *88*, 1639–1648.

Lemieux, M.E., Rebel, V.I., Lansdorp, P.M., and Eaves, C.J. (1995). Characterization and purification of a primitive hematopoietic cell type in adult mouse marrow capable of lymphomyeloid differentiation in long-term marrow "switch" cultures. Blood *86*, 1339–1347.

Liu, M., Miller, C.L., and Eaves, C.J. (2013). Human long-term culture initiating cell assay. Methods Mol. Biol. *946*, 241–256.

Miller, J.S., McCullar, V., and Verfaillie, C.M. (1998). Ex vivo culture of CD34+/Lin-/DR- cells in stroma-derived soluble factors, interleukin-3, and macrophage inflammatory protein-1alpha maintains not only myeloid but also lymphoid progenitors in a novel switch culture assay. Blood *91*, 4516–4522.

Ponchio, L., Duma, L., Oliviero, B., Gibelli, N., Pedrazzoli, P., and Robustelli della Cuna, G. (2000). Mitomycin C as an alternative to irradiation to inhibit the feeder layer growth in long-term culture assays. Cytotherapy *2*, 281–286.

Punzel, M., Wissink, S.D., Miller, J.S., Moore, K.A., Lemischka, I.R., and Verfaillie, C.M. (1999). The myeloid-lymphoid initiating cell (ML-IC) assay assesses the fate of multipotent human progenitors in vitro. Blood *93*, 3750–3756.

Sengupta, A., Arnett, J., Dunn, S., Williams, D.A., and Cancelas, J.A. (2010). Rac2 GTPase deficiency depletes BCR-ABL+ leukemic stem cells and progenitors in vivo. Blood *116*, 81–84.

Sinha, S., Biswas, M., Chatterjee, S.S., Kumar, S., and Sengupta, A. (2020). Pbrm1 steers mesenchymal stromal cell osteolineage differentiation by integrating PBAF-dependent chromatin remodeling and BMP/TGF-beta signaling. Cell Rep. *31*, 107570.

Toksoz, D., Zsebo, K.M., Smith, K.A., Hu, S., Brankow, D., Suggs, S.V., Martin, F.H., and Williams, D.A. (1992). Support of human hematopoiesis in long-term bone marrow cultures by murine stromal cells selectively expressing the membrane-bound and secreted forms of the human homolog of the steel gene product, stem cell factor. Proc. Natl. Acad. Sci. U S A *89*, 7350–7354.

THE FASEB JOURNAL • RESEARCH • www.fasebj.org

MBD3/NuRD loss participates with KDM6A program to promote *DOCK5/8* expression and Rac GTPase activation in human acute myeloid leukemia

Mayukh Biswas,[*,†,1] Shankha Subhra Chatterjee,[*,†,1] Liberalis Debraj Boila,[*,†] Sayan Chakraborty,[*,†] Debasis Banerjee,[‡] and Amitava Sengupta[*,†,2]

[*]Stem Cell and Leukemia Laboratory, Council of Scientific and Industrial Research (CSIR)—Indian Institute of Chemical Biology (IICB), Translational Research Unit of Excellence (TRUE), Salt Lake, Kolkata, West Bengal, India; [†]Cancer Biology and Inflammatory Disorder Division, CSIR-IICB, Jadavpur, Kolkata, West Bengal, India; and [‡]Park Clinic, Gorky Terrace, Kolkata, West Bengal, India

ABSTRACT: Cancer genome sequencing studies have focused on identifying oncogenic mutations. However, mutational profiling alone may not always help dissect underlying epigenetic dependencies in tumorigenesis. Nucleosome remodeling and deacetylase (NuRD) is an ATP-dependent chromatin remodeling complex that regulates transcriptional architecture and is involved in cell fate commitment. We demonstrate that loss of MBD3, an important NuRD scaffold, in human primary acute myeloid leukemia (AML) cells associates with leukemic NuRD. Interestingly, CHD4, an intact ATPase subunit of leukemic NuRD, coimmunoprecipitates and participates with H3K27Me3/2-demethylase KDM6A to induce expression of atypical guanine nucleotide exchange factors, dedicator of cytokinesis (DOCK) 5 and 8 (DOCK5/8), promoting Rac GTPase signaling. Mechanistically, MBD3 deficiency caused loss of histone deacytelase 1 occupancy with a corresponding increase in KDM6A, CBP, and H3K27Ac on *DOCK5/8* loci, leading to derepression of gene expression. Importantly, the Cancer Genome Atlas AML cohort reveals that *DOCK5/8* levels are correlated with *MBD3* and *KDM6A*, and *DOCK5/8* expression is significantly increased in patients who are *MBD3* low and *KDM6A* high with a poor survival. In addition, pharmacological inhibition of DOCK signaling selectively attenuates AML cell survival. Because *MBD3* and *KDM6A* have been implicated in metastasis, our results may suggest a general phenomenon in tumorigenesis. Collectively, these findings provide evidence for MBD3-deficient NuRD in leukemia pathobiology and inform a novel epistasis between NuRD and KDM6A toward maintenance of oncogenic gene expression in AML.—Biswas, M., Chatterjee, S. S., Boila, L. D., Chakraborty, S., Banerjee, D., Sengupta, A. MBD3/NuRD loss participates with KDM6A program to promote *DOCK5/8* expression and Rac GTPase activation in human acute myeloid leukemia. FASEB J. 33, 5268–5286 (2019). www.fasebj.org

KEY WORDS: chromatin remodeling · KDM6A · epistasis

Acute myeloid leukemia (AML) is the second most common leukemia worldwide with a median age of ~65 yr at diagnosis. Myelodysplastic syndromes (MDS) are hematopoietic stem and progenitor cell (HSPC)–initiated clonal preleukemic disorders of aged individuals that may transform into secondary AML (1, 2). Despite progress in our understanding of AML pathogenesis, the overall 5-yr survival is ~20% because of low remission and high incidence of relapse (3, 4). Over the past decade, genome sequencing studies have identified that recurrent somatic

ABBREVIATIONS: 7-AAD, 7-aminoactomycin-D; ACN, acetonitrile; ambic, ammonium bicarbonate; AML, acute myeloid leukemia; BM, bone marrow; BMNC, BM nuclear cell; $CD34^+$, CD34 positive; ChIP, chromatin immunoprecipitation; ChIP-seq, ChIP sequencing; CPYPP, 4-[3-(2-chlorophenyl)-2-propen-1-ylidene]-1-phenyl-3,5-pyrazolidinedione; CXCL12, CXC motif chemokine ligand 12; DAVID, Database for Annotation, Visualization and Integrated Discovery; DOCK5/8, dedicator of cytokinesis 5/8; FBS, fetal bovine serum; GAPDH, glyceraldehyde-3-phosphate dehydrogenase; GEF, guanine nucleotide exchange factor; GFP, green fluorescent protein; GFP^+, GFP positive; GO, gene ontology; GSEA, gene set enrichment analysis; HDAC, histone deacetylase; HQ, high quality; HSPC, hematopoietic stem and progenitor cell; IC_{50}, median inhibitory concentration; IMDM, Iscove's modified Dulbecco's medium; LC-MS/MS, liquid chromatography with MS/MS; LSD1, lysine-specific demethylase 1; MBD3, methyl-CpG binding domain protein 3; MDS, myelodysplastic syndrome; MoI, multiplicity of infection; MS, mass spectrometry; MS/MS, tandem MS; NuRD, nucleosome remodeling and deacetylase; qPCR, quantitative PCR; qRT-PCR, quantitative RT-PCR; RNA-seq, RNA sequencing; sh-KDM6A, KDM6A-targeted shRNA; sh-MBD3, MBD3-targeted shRNA; shRNA, short hairpin RNA; T-ALL, T-cell acute lymphoblastic leukemia; TCGA, The Cancer Genome Atlas

[1] These authors contributed equally to this work.

[2] Correspondence: Council of Scientific and Industrial Research–Indian Institute of Chemical Biology, CN-6, Sector V, Salt Lake, Kolkata 700091, India. E-mail: amitava.iicb@gmail.com

doi: 10.1096/fj.201801035R

This article includes supplemental data. Please visit *http://www.fasebj.org* to obtain this information.

0892-6638/19/0033-5268 © FASEB

mutations in genes encoding chromatin regulators frequently contribute to tumorigenesis (2, 5). Nonetheless, mutational profiling alone may not suffice to identify tumor-associated transcriptional plasticity (6), one of the major hallmarks of cancer biology.

ATP-dependent chromatin remodelers play an important role in pluripotency and cellular reprogramming (7, 8). Recent studies, including ours, have highlighted that specific members in ATP-dependent chromatin remodelers have critical regulatory roles in hematopoiesis and leukemia pathogenesis (9–14). Nucleosome remodeling and deacetylase (NuRD) is an ATP-dependent chromatin remodeling complex that critically regulates cell fate commitment and transcriptional architecture of murine embryonic stem cells (7). Conditional inactivation of Mi-2β of the NuRD complex caused erythroid leukemia in mice (15). NuRD-mediated *Runx1* repression has been implicated in *Setbp1*-induced murine myeloid leukemia development (16). In lymphoid cells, Mi-2β activity is regulated by Ikaros, and release of NuRD in Ikaros-deficient cells results in lymphoid leukemia (14).

Methyl-CpG binding domain protein 3 (MBD3) is a ubiquitously expressed important scaffold of the NuRD complex that regulates cell fate commitment (7, 8, 17). MBD2, another subunit of the NuRD complex, was originally identified as a transcriptional repressor belonging to the MeCP1 histone deacetylase (HDAC) complex (18). MBD3 and MBD2 may assemble into mutually exclusive distinct NuRD complexes (19). Depletion of *Mbd3*, together with transduction of induced pluripotency–promoting factors, result in complete deterministic reprogramming (8). Paradoxically, Mbd3/NuRD, in synergy with Nanog, augments reprogramming of epiblast stem cells to naive pluripotency, suggesting that NuRD's contribution to regulating stem cell activity is context dependent (17).

NuRD complex has been predominantly associated with H3K4Me2/1 demethylase lysine-specific histone demethylase 1 (LSD1), regulating transcriptional repression (20). LSD1 and NuRD are involved in breast cancer metastasis and *SALL4*-mediated transcriptional repression in HSPCs (20). A growing body of evidence highlights involvement of histone demethylases in tumorigenesis (21). KDM6-family H3K27Me3/2 demethylases have been shown to play antagonistic roles in T-cell acute lymphoblastic leukemia (T-ALL) development (22). KDM6A (*UTX*) acts as a tumor suppressor and is frequently mutated in T-ALL, whereas KDM6B (*JMJD3*) is essential for the initiation and maintenance of T-ALL (22). However, a subgroup of T-ALL expressing TAL1 is uniquely vulnerable to KDM6A inhibition (23). Recently we have identified KDM6 histone demethylases as molecular therapeutic targets in human primary AML (24). However, the net contribution of KDM6A in hematopoiesis and particularly in MDS and AML development has remained contentious, and it largely depends on the cellular microenvironment (25–29). KDM6B regulates transcriptional elongation, and overexpression of *KDM6B* is reported in MDS HSPCs (30).

We investigated the contribution of NuRD complex to human AML pathobiology. We identified that loss of MBD3 in primary AML cells associates with leukemic NuRD, which retains its CHD4 ATPase subunit. CHD4/NuRD interacts and participates with KDM6A to transcriptionally regulate the expression of Rac GTPase guanine nucleotide exchange factors (GEFs), dedicator of cytokinesis (DOCK) 5 and 8 (*DOCK5/8*), in AML cells, and deficiency of MBD3 derepresses *DOCK5/8* expression that involves locus-specific loss of HDAC1 occupancy. *DOCK5/8* expression is significantly increased in *MBD3*-low, *KDM6A*-high patients with relatively poor survival compared with *MBD3*-high, *KDM6A*-low AML, and pharmacological inhibition of DOCK signaling selectively attenuates AML cell survival. Together, our results illustrate a hitherto unidentified epistasis between NuRD and KDM6A toward maintenance of oncogenic gene expression in AML.

MATERIALS AND METHODS

Patient cohort

Human MDS (n = 24) or AML (n = 63) bone marrow (BM) aspirates (1–2 ml each) were obtained from Park Clinic, Kolkata, India, from untreated, freshly diagnosed patients after informed consent according to Institutional Human Ethics Committee approval and following guidelines set by the Council of Scientific and Industrial Research–Indian Institute of Chemical Biology Institutional Review Board. Sample collection was part of routine diagnosis, and the inclusion criterion for this study was histopathological confirmation of BM aspirates or biopsies, karyotyping, and immunophenotypic analyses. Array comparative genomic hybridization analysis of AML samples and subtyping were previously reported (9, 24). BM aspirates were also collected from age-matched normal individuals (n = 6) after informed consent, who were found to be pathologically negative for MDS and AML. Umbilical cord blood (n = 10) samples (40 ml each) were obtained from Deb Shishu Nursing Home, Howrah, India, from term pregnancies after informed consent according to Council of Scientific and Industrial Research–Indian Institute of Chemical Biology Human Ethics Committee approval and following Institutional Review Board guidelines. Low-density (1.077 gm/cc) nuclear cells from normal or AML BM or cord blood samples were isolated by Ficoll (MilliporeSigma, Burlington, MA, USA) separation and cryopreserved in liquid nitrogen. Peripheral blood nucleated cells were also isolated from healthy volunteers and used as normal controls.

Quantitative RT-PCR

Total RNA was isolated by using Trizol (Thermo Fisher Scientific, Waltham, MA, USA) according to the manufacturer's recommendation. RNase free DNase treatment was carried out to remove any genomic DNA contamination using a DNase I recombinant, RNase free kit (Roche, Basel, Switzerland). The RNA amount was quantified, and cDNA was prepared using TaqMan Reverse Transcription Reagents (Thermo Fisher Scientific). Gene expression levels were determined by quantitative PCR (qPCR) performed using cDNA with SYBR Select Master Mix (Thermo Fisher Scientific) on the 7500 Fast Real-Time PCR System (Thermo Fisher Scientific). Glyceraldehyde-3-phosphate dehydrogenase (*GAPDH*) was used as a housekeeping gene. Relative expression levels were calculated using the $2^{-\Delta\Delta Ct}$ method.

Co-immunoprecipitation and immunoblotting

Nuclear extracts for immunoprecipitation experiments were prepared using NE-PER Nuclear and Cytoplasmic Extraction Reagents (Thermo Fisher Scientific) and diluted in 1× RIPA (Cell Signaling Technology, Danvers, MA, USA) containing protease and phosphatase inhibitor cocktails. About 300 μg extracts were incubated with 2.0 μg of antibodies against CHD4 (clone 3F2/4, ab70469; Abcam, Cambridge, MA, USA), MTA1/2 (clone C-20, sc-9447; Santa Cruz Biotechnology, Dallas, TX, USA), KDM6A (A302-374A; Bethyl Laboratories, Montgomery, TX, USA) or rabbit IgG (P120-101; Bethyl Laboratories) and incubated overnight at 4°C with gentle rocking. Fifty microliters of protein A/G agarose beads (Cell Signaling Technology) were added and incubated for 3–4 h at room temperature. The beads were then washed 6 times with 1× RIPA supplemented with 300–500 mM NaCl and resuspended in 1× SDS gel loading buffer. The proteins were separated in SDS-PAGE and transferred to PVDF membrane (MilliporeSigma) and subsequently probed with respective antibodies. For co-immunoprecipitation with DNase I treatment, 300 μg extracts were incubated with 300 U of DNase I at 37°C for 1 h. The reaction was stopped by adding EDTA to a final concentration of 10 mM. All antibodies were used at a dilution of 1:1000 unless otherwise specified. Total cell lysate for immunoblotting was prepared by incubating cells in 1× RIPA for 15 min followed by brief sonication. Supernatants were collected following centrifugation at 16,000 *g* for 15 min at 4°C. Protein concentration was determined using the Pierce BCA Protein Assay Kit (Thermo Fisher Scientific). SDS-PAGE was used to separate proteins, which were transferred to PVDF membrane and probed using respective antibodies. Densitometry analyses were performed using ImageJ software (National Institutes of Health, Bethesda, MD, USA).

Sucrose density gradient centrifugation

Seven hundred micrigrams to 1.0 mg nuclear extracts, isolated from pooled (n = 5–7) primary AML BM nuclear cells (BMNCs), were prepared and diluted in 300 μl of 1× RIPA. The extracts were overlaid on a 10 ml 20–50% sucrose gradient (in 1× RIPA) in 13 × 89 mm polyallomer tubes (Beckman Coulter, Brea, CA, USA). The tubes were then centrifuged in a SW-41 Ti swing-out rotor at 30,000 rpm for 12 h at 4°C. Fractions of 500 ml were collected and separated in SDS-PAGE, transferred to a PVDF membrane, and subsequently probed with specific antibodies.

Mass spectrometry analysis

Cells were lysed in cytoplasmic extraction buffer (10 mM HEPES, 60 mM KCl, 1 mM EDTA, 1 mM DTT, 0.1% v/v Nonidet P-40 (NP40), protease inhibitors) for 20 min on ice with intermittent vortexing. Nuclei were isolated by centrifuging cells at 16,000 *g* for 15 min at 4°C. Nuclear lysis were performed in nuclear extraction buffer (20 mM Tris-Cl, 100 mM NaCl, 1.5 mM $MgCl_2$, 0.2 mM EDTA, 20% v/v glycerol, protease inhibitors) for 30 min with intermittent vortexing and centrifugation at 18,000 *g* for 15 min at 4°C. Nuclear proteins in excess of 5.0 mg in 250 μl of buffer were precleared with 30 μl of protein A/G agarose beads for 2 h at 4°C with gentle rocking. After preclearing, the samples were incubated with 8–10 μg of antibodies against MTA2 (clone F-9, sc-55566; Santa Cruz Biotechnology) and UTX/KDM6A (A302-374A; Bethyl Laboratories) for 16 h at 4°C with end-to-end rotation. Fifty microliters of protein A/G agarose beads was added to the samples and further incubated for 4 h at 4°C. The beads were then washed 3–5 times in PBS supplemented with 150 mM of NaCl and were incubated with 60 μl of 1× loading buffer at 98°C for 10 min. The supernatant was resolved in a 10% polyacrylamide gel, and silver staining (Bio-Rad, Hercules, CA, USA) was performed according to the manufacturer's protocol. The lanes containing the immunoprecipitated samples were excised, cut into several pieces, and destained. The gel pieces were dried, and reduction was performed in 200 μl of 10 mM DTT in 100 mM ammonium bicarbonate (ambic) for 30 min at 56°C. Subsequent alkylation was done by adding 200 μl of 55 mM iodoacetamide in 100 mM ambic and incubated for 30 min in the dark. In-gel tryptic digestion was performed by incubating gel slices in 20 μg/ml of modified trypsin (New England Biolabs, Ipswich, MA, USA) in a digestion buffer [40 mM ambic/10% acetonitrile (ACN)] for 14–16 h at 37°C. Each gel digest was extracted twice by keeping slices in 200 μl of 50% ACN/5% TFA for 1 h at room temperature with gentle mixing. The extracts were pooled and lyophilized and resuspended in 75 μl of mass spectrometry (MS)–grade ultrapure water and 25 μl of sample buffer (2% TFA in 20% ACN). Sample clean-up was performed using Pierce C18 spin columns (Thermo Fisher Scientific). The spin columns were washed twice with activation buffer (0.5% TFA in 5% ACN) before sample loading. The resin-bound peptides were recovered by spinning 20 μl of elution buffer (70% ACN) at 1500 *g* for 1 min.

The peptides were lyophilized, reconstituted in 10 μl of 0.1% formic acid, and analyzed in online nano–liquid chromatography (Easy-nLC-1000; Thermo Fisher Scientific) with tandem MS (MS/MS) (LTQ-Orbitrap-XL; Thermo Fisher Scientific). The samples were run through a C18 trap column (Acclaim PepMap 100, 75 μm internal diameter × 2 cm, C18, 3 μm, 100 Å) and separated through an analytical column (Easy-Spray, PepMap C18, 3 μm, 75 μm × 15 cm, 100 Å) in a gradient of ACN (5% for 5 min, 35% for 5 min, 95% for 40 min, 35% for 10 min, and 5% for 5 min) and 0.1% formic acid. The MS was performed with a Top 6 data-dependent acquisition mode, and the preview mode for Fourier transform MS master scan was enabled. The MS full scan was set at 350–2000 *m/z* score with a resolution of 60,000 and automatic gain control at 1×10^6 with a maximum injection time of 100 ms. The minimal signal acquired was above 500 counts with the automatic gain control set at 1000 and maximum injection time of 100 ms in ion trap. The collision energy for the MS/MS was at 35% with an isolation width of 2 Da and exclusion duration of 30 s. MS analyses were performed using Proteome Discoverer software, and peptide identification and validation were performed using SEQUEST against the Uniprot Swiss-Prot database. For semiquantitative analyses of KDM6A interaction with NuRD, the peptide enrichment score of KDM6A was normalized to MTA2 (bait protein) as determined from the MS interactome profiles in the respective cells.

NuRD and KDM6A *in vitro* interaction assay

KDM6A-deficient U937 cells were generated using lentivirus transduction with short hairpin RNA (shRNA) targeting KDM6A (sh-KDM6A) and coexpressing green fluorescent protein (GFP) followed by flow cytometry sorting of GFP-positive (GFP^+) cells. CHD4/NuRD was immunoprecipitated as described earlier. Briefly, the protein A/G agarose beads were washed 4 times with wash buffer supplemented with 300 mM NaCl. The bound NuRD complex was eluted by incubating the beads with 50 μl of elution buffer (glycine-HCl buffer, pH 2.7) and neutralizing the supernatant with equal volume of 1 M Tris buffer (pH 8.0). 293T cells were transiently transfected with plasmids containing full-length *KDM6A* (RC210861L4; OriGene Technologies, Rockville, MD, USA), and KDM6A was isolated using co-immunoprecipitation using 10 μg of antibody against KDM6A (A302-374A; Bethyl Laboratories).

To assess the interaction between CHD4/NuRD complex and KDM6A, 5.0 μg of each of the eluted fractions was incubated together in 200 μl of 1× RIPA buffer supplemented with 1× each

of protease and phosphatase inhibitors (Roche) for 16 h at 4°C with gentle rocking. Co-immunoprecipitation was performed as previously described with 5 μg of antibodies against CHD4, KDM6A, and IgG. The beads from each immunoprecipitation set were washed 5 times with wash buffer supplemented with 300, 500, and 1000 mM of NaCl, respectively. The bound proteins were eluted by incubating the beads with 30 μl of elution buffer (glycine-HCl buffer, pH 2.7) and neutralizing the supernatant with equal volume of 1 M Tris buffer (pH 8.0). The eluted fractions were resolved using denaturing PAGE, transferred to a PVDF membrane, and subsequently probed with specified antibodies.

H3K27Me3/2 demethylase assay

Endogenous CHD4 or KDM6A or IgG co-immunoprecipitated fractions were eluted from primary AML BMNCs or AML lines or 293T cells using 80 μl of 0.1 M glycine-HCl buffer (pH 2.7), neutralized with equal volume of 1 M Tris (pH 8.0), and stored at −80°C. Eluted fractions (150 ng) were used for H3K27Me3/2 demethylase assay following the manufacturer's recommendation (P-3084; Epigentek, Farmingdale, NY, USA). Briefly, 150 ng of the eluted protein fraction was added with completed histone demethylase assay buffer and substrate (P-3084; Epigentek) and incubated at 37°C for 60 min. The wells were washed 3 times and incubated with capture antibody at room temperature for 60 min. Detection antibody was added to each well after washing and incubated at room temperature for 30 min. The wells were washed 4 times and incubated for 1–10 min at room temperature with detection solution. The absorbance was read using a microplate reader at 450 nm within 10 min. A standard curve was generated using given standards, and the values of the test samples were calculated from the curve.

Chromatin immunoprecipitation sequencing, chromatin immunoprecipitation–qPCR, and analyses

Chromatin immunoprecipitation (ChIP) sequencing (ChIP-seq) experiments were carried out at Core Technologies Research Initiative, National Institute of Biomedical Genomics, Kalyani, India. For each ChIP set, 10×10^6 primary BMNCs, isolated from 3 independent (biologic replicates) AML patients, or 10×10^6 normal blood nucleated cells or 10×10^6 U937 cells (transduced with lentiviral particles expressing sh-KDM6A or sh-Control and coexpressing GFP) were crosslinked with formaldehyde (MilliporeSigma) in culture media. After cross-linking, chromatin was extracted and sonicated to fragment lengths between 150 and 900 bp in chromatin extraction buffer containing 10 mM Tris pH 8.0, 1 mM EDTA pH 8.0, and 0.5 mM EGTA pH 8.0. Chromatin was incubated with antibodies to CHD4 (clone 3F2/4, ab70469; Abcam), KDM6A (A302-374A; Bethyl Laboratories), H3K27Ac (ab4729; Abcam), HDAC1 (A300-713A; Bethyl Laboratories), CBP (D6C5; Cell Signaling Technology), and rabbit IgG (clone P120-101; Bethyl Laboratories) or mouse IgG (clone G3A1; 5415S; Cell Signaling Technology) overnight at 4°C with rotation. All antibodies were used at 1:1000 dilution. Protein A/G agarose beads (Cell Signaling Technology) were then added and incubated for 2 h at 4°C. The beads were washed with chromatin extraction buffer and by increasing salt concentration 4×. The chromatin was eluted from the beads in chromatin elution buffer at 65°C with gentle vortexing. The eluted chromatin was treated with RNase for 30 min at 37°C. Reverse cross-linking was performed by treating the eluted chromatin with Proteinase K (MilliporeSigma) at 65°C for 2 h. The DNA was finally precipitated by phenol-chloroform extraction; precipitated DNA was dissolved in Tris-EDTA buffer and subjected to ChIP-seq analyses. For ChIP-qPCR experiments, 4–5 $\times$ 10^6 293T cells or AML cells and 2 μg of antibody or ChIP DNA obtained from primary AML BMNCs were used.

Size distribution of the ChIP-enriched DNA was checked using high-sensitivity chips in the 2100 Bioanalyzer (Agilent Technologies, Santa Clara, CA, USA) for each sample, and quantitation was performed in the Qubit Fluorometer (Thermo Fisher Scientific) by the picogreen method. ChIP-seq library preparation was performed using the TruSeqChIP Sample Prep Kit (Illumina, San Diego, CA, USA) according to the manufacturer's instructions. Ten nanograms of input ChIP-enriched DNA was used for ChIP-seq library preparation. Final libraries were checked using high-sensitivity chips in the 2100 Bioanalyzer. The average fragment size of the final libraries was found to be 280 $\pm$ 8 bp. Paired-end sequencing (2 $\times$ 100 bp) of these libraries were performed in the HiSeq 2500 (Illumina). Quality control analysis of the raw data using the NGS QC ToolKit was done, and high-quality (HQ) reads with filter criteria of bases having ≥20 Phred score and reads with ≥70% were filtered. Paired end reads (.fastq format) were aligned with Bowtie software using –best and –m 2 [*i.e.*, mismatches against reference genome Ensembl build GrCh37/hg19 (considering 2% input as the baseline)], and saved in SAM format, which was then converted to a sorted BAM file using SAMTools. PCR duplicates were removed using SAMTools rmdup. Peak calling was performed using MACS14 model building with a *P* value cutoff of 0.05. Annotation of the identified peaks was performed with PeakAnalyzer. Functional enrichment analysis [gene ontology (GO) and pathway] was done using the Database for Annotation, Visualization and Integrated Discovery (DAVID) v.6.8 (*https://david.ncifcrf.gov/*). The gene list was uploaded and converted to respective gene identifiers from the U.S. National Center for Biotechnology Information. The converted gene list was submitted to DAVID, and functional annotation clustering was carried out, which comprises GO and pathway analysis. The R bioconductor package ChiPseeker (*https://guangchuangyu.github.io/software/ChIPseeker/*) was used to generate heatmaps, average profile distibutions, and pie charts. Bigwig/bed files were imported into the Integrative Genomics Viewer (*http://software.broadinstitute.org/software/igv/home*), and snapshots of particular genomic loci were captured.

Gene-enrichment and functional annotation analysis

GO analysis of the shared *gene set* was carried out using DAVID v.6.8. This analysis uses a modified *P* value, termed the Expression Analysis Systematic Explorer score threshold (maximum probability). The threshold of this score is a modified Fisher's exact *P* value used for gene-enrichment analysis. It ranges from 0 to 1. Fisher's exact *P* value of 0 represents perfect enrichment. Usually a $P \leq 0.05$ is considered strongly enriched in the annotation categories.

RNA sequencing–based transcriptional profiling and analyses

RNA sequencing (RNA-seq) experiments were performed by Bionivid Technology, Bangalore, India. Total RNA was isolated from BMNCs from the identical AML cohort (n = 3) and age-matched normal (n = 2) hematopoietic cells using Trizol (Thermo Fisher Scientific) according to the manufacturer's instructions. DNase treatment was carried out to remove any genomic DNA contamination using a DNase I recombinant, RNase free kit (Roche). The RNA amount was quantified, and the sequencing library was prepared using the TruSeq RNA Sample Prep Kit v.2 (Illumina). Paired-end sequencing was performed on the HiSeq 4000 using the TruSeq 3000 4000 SBS Kit v.3 (Illumina).

Raw data resulted in an average of 35.39 $\times$ 10^6 reads in normal hematopoietic cells and 36.86 $\times$ 10^6 reads of 101 bp length in primary AML cells. Quality control using the NGS QC Toolkit

yielded around 34.28×10^6 HQ reads in normal hematopoietic cells and 36.05×10^6 HQ reads in primary AML cells. Around 88.2% of the HQ reads from normal cells and 85.12% of the HQ reads from primary AMLs could be mapped to the *Homo sapiens* (hg 38) genome reference sequence using TopHat, suggesting a good quality of RNA-seq. Transcripts were given a score for their expression by Cufflinks-based maximum likelihood method. Cuffdiff validation identified 24,784 transcripts as expressed in either normal or primary AML cells, representing 13,847 genes. Transcript type analysis revealed 95.5% of the transcripts to be "Full Length" or "Known Transcripts" and 4.5% to be "Potentially Novel Isoforms" transcripts as per Cufflinks Class Code distribution. This indicates a largely complete transcription machinery activity in both normal and AML cells. Significant biology analysis for differentially expressed transcripts was performed with GO-Elite v.1.2.5 Software (*http://www.genmapp.org/go_elite/*). A cutoff of *P* value less than 0.05 was considered significant for filtering the significantly enriched GO pathways. In testing for differential expression, we considered $\log_2$ FC >2 (up-regulation) and $\log_2$ FC < -2 (down-regulation). For gene set enrichment analysis (GSEA), differentially expressed genes from individual comparisons were preranked based on fold change such that maximally up-regulated genes fell topmost in the list. This was used as an input for GSEA (GeneSpring, Agilent, Santa Clara, CA, USA). GSEA was performed on the "H: Hallmark gene set" representing well-defined biologic states or processes available on the Molecular Signature Database (*http://software.broadinstitute.org/gsea/msigdb*).

ChIP-seq, RNA-seq data accession

All sequencing data have been submitted to databases with accession numbers as follows. ChIP-seq: GSE108976. RNA-seq: Sequence Read Archive accession: SRP127783; BioProject identifier: PRJNA428149.

Plasmids

shRNA-expressing lentiviral constructs targeting against *MBD3* (pLKO.1-puro-CMV-TGFP, TRCN0000285209) and *KDM6A* (pGFP-C-sh-Lenti, TL300596A and TL300596B) were purchased from MilliporeSigma and OriGene, respectively. *Mbd3*-overexpressing vector *F75* was a kind gift from Dr. Jose Silva, University of Cambridge, Cambridge, United Kingdom. Full-length *Mbd3* was amplified from the plasmid using the primers 5′-ATAGAATTCATGGAGCGGAAGAGGTGG-3′ (forward primer) and 5′-ATAGAATTCCTACACTCGCTCTGGCTC-3′ (reverse primer) and subcloned into a MSCV Puro-IRES-GFP retroviral vector (18751; Addgene, Watertown, MA, USA) using the *Eco*RI restriction enzyme (New England Biolabs). *KDM6A* human shRNA plasmid was purchased from OriGene (TL300596). Scrambled vector sh-Control (pGFP-C-sh-Lenti, TR30021) was purchased from OriGene. Lentiviral and retroviral packaging constructs PAX2 (12260; Addgene), pMD2.G (12259; Addgene), and pHCMV-AmphoEnv (15799) were purchased from Addgene.

HSPC isolation and lentiviral transduction

CD34-positive ($CD34^+$) HSPCs were isolated from freshly collected MDS BMNCs or normal BMNCs and cord blood nuclear cells or from cryopreserved specimens using the CD34 Microbead Positive Selection Kit (Miltenyi Biotec, Bergisch Gladbach, Germany) following the manufacturer's protocol. Cells were prestimulated overnight in Iscove's modified Dulbecco's medium (IMDM), 10% fetal bovine serum (FBS), 100 U/ml penicillin, 100 μg/ml streptomycin, and 2 mM L-glutamine (all from Thermo Fisher Scientific) supplemented with 10 ng/ml stem cell factor, 10 ng/ml FMS-like tyrosine kinase 3 ligand, and 10 ng/ml thrombopoietin (R&D Systems, Minneapolis, MN, USA, or PeproTech, Rocky Hill, NJ, USA). 293T cells (obtained from Dr. Jose Cancelas, Cincinnati Children's Hospital, OH, USA), were maintained in DMEM supplemented with 10% FBS, 100 U/ml penicillin, 100 μg/ml streptomycin, and 2 mM L-glutamine (all from Thermo Fisher Scientific) at 37°C with 5% CO_2. Cells were seeded in T-225 flasks at 70% confluence and transfected with the target plasmid DNA, PAX2, and pMD2.G using the calcium phosphate transfection method. After overnight incubation, butyrate induction was given for 8 h. Supernatant-containing lentiviral particles were collected after 36–40 h of incubation at 37°C with 5% CO_2 and ultracentrifuged at 25,000 rpm for 90 min at 4°C using (Sorvall WX Ultra 90; Thermo Fisher Scientific). Virus pellet was resuspended in X-VIVO (Lonza, Basel, Switerland), aliquoted, and stored at −80°C. HL60, U937, and THP1 cells were transduced with lentiviral particles expressing sh-Control, MBD3-targeted shRNA (sh-MBD3), or sh-KDM6A and coexpressing GFP in a U-bottom 96-well non–tissue-culture treated plate. 1×10^5 cells were incubated overnight with virus particles at a multiplicity of infection (MoI) of 5–10, and polybrene (8 μg/ml) was added to initiate lentiviral infection.

Retroviral transduction

Retrovirus packaging Phoenix GP cells were transfected with Gag-Pol, AmphoEnv, and the target plasmid at 70% confluency using calcium phosphate. Supernatants were collected 48 and 72 h post-transfection and stored at −80°C. For transduction of AML cells and normal hematopoietic cells, retroviral supernatants expressing *MIGR1* and *MBD3* were centrifuged at 3700 rpm for 2 h at room temperature in wells of 6-well non–tissue-culture-treated plate precoated with retronectin (10 μg/ml, 16 h at 4°C). After discarding the supernatant, cells were centrifuged for 1200 rpm for 10 min at room temperature and incubated for 12–16 h at 37°C with 5% CO_2. The second round of transduction was performed by incubating the cells with supernatant-containing retroviral particles at a MoI of 5–10 at 37°C with 5% CO_2 for 16 h. After discarding the viral supernatant, fresh culture media were added to the cells and further incubated for 48 h at 37°C with 5% CO_2.

Flow cytometric sorting of *KDM6A*-deficient AML cells

AML cell lines were transduced with lentiviral particles expressing sh-KDM6A or sh-Control and coexpressing GFP. Cells were harvested at 1000 *g* for 5 min, washed with ice-cold PBS, and resuspended in 500 μl of PBS supplemented with 2% FBS and 1 μg/ml of 7-Aminoactinomycin D (7-AAD; BD Biosciences, San Jose, CA, USA). GFP^+, 7-AAD-negative cells were sorted using the MoFlo XDP Cell Sorter (Beckman Coulter). Postsorting enrichment of HL60 and U937 was 93 and 95%, respectively. In a different experimental setup, AML cell lines were transduced with lentiviral particles expressing sh-MBD3 or sh-Control and coexpressing GFP. Cells were harvested at 1000 *g* for 5 min and washed with ice-cold PBS and resuspended in 500 μl of PBS supplemented with 2% human serum. GFP^+, 7-AAD-negative (BD Biosciences) cells were analyzed in LSRFortessa (Becton Dickinson, San Diego, CA, USA) using FACSDiva software (Becton Dickinson).

Rac GTPase pulldown assay

AML cells were transduced with sh-MBD3 or MBD3-OE or control virus particles and subjected to PAK1 pulldown analysis. 293T cells or A549 cells were transiently transfected with plasmids expressing sh-MBD3_A, sh-MBD3_B, or sh-Control.

Thirty-six hours post-transfection, cells were cultured in the presence of DMEM, penicillin, streptomycin, and glutamine supplemented with either 0.5% FBS (starved) or 10% FBS (basal) for another 12 h. Starved cells were induced with fresh DMEM, penicillin, streptomycin, and glutamine supplemented with 10% FBS for 10 min (serum$^+$; serum induced). Immediately after induction, cells were washed in ice-cold PBS and trypsinized. Cells were lysed using 400 μl of 1× Mg2+ Lysis/Wash Buffer (MLB) with repeated pipetting and centrifuged at 14,000 *g* for 5 min at 4°C, and supernatants were used for PAK1 pulldown assay (MilliporeSigma) as previously described. To the supernatant, 10 μl of Rac1 conjugated agarose beads were added and incubated for 45 min at 4°C with gentle rocking. The beads were centrifuged at 14,000 *g* for 10 s at 4°C. After the supernatants were removed, the beads were washed 3 times with 1× MLB buffer and resuspended in 40 μl of protein loading buffer, boiled for 5 min, separated in 12% polyacrylamide gel, transferred to PVDF membrane, and probed using respective antibodies. The presence of active Rac GTP was determined by using antibody against Rac GTP in the pulldown fraction and normalized against total Rac present in the lysate. Densitometry analyses were performed using ImageJ software.

Migration assay

AML cells or normal hematopoietic cells were transduced with lentivirus or retrovirus particles (at a MoI of 1–2), expressing sh-MBD3 or MBD3-OE or control and coexpressing GFP, and subjected to transwell migration assay toward CXC motif chemokine ligand 12 (CXCL12). Briefly, after 48 h of transduction, 50,000 cells were seeded in 100 μl of IMDM (serum-free) in duplicate in the upper chamber of 0.5 μ-pore sized 24-well Transwell (Corning, Corning, NY, USA), and cells were allowed to migrate toward 10 ng/ml CXCL12 (PeproTech) present in the lower chamber (600 μl). After 4 h of incubation at 37°C with 5% CO_2, the absolute number of GFP$^+$ cells migrated to the lower chamber was enumerated using flow cytometry. The percentage of cell migration was determined by normalizing with GFP$^+$ cells present in the input. In a different experimental setup, overnight prestimulated AML BMNCs were cultured in low-serum (0.5%) media in presence of 100 μM 4-[3-(2-chlorophenyl)-2-propen-1-ylidene]-1-phenyl-3,5-pyrazolidinedione (CPYPP) or DMSO for 1 h, and a migration assay was performed (31).

Phalloidin staining

AML cells were seeded onto Poly-L-Lysine (MilliporeSigma)–coated coverslips in serum-starved media (0.5% FBS) with either CPYPP (100 μM) or DMSO (vehicle) and incubated for 60 min at 37°C with 5% CO_2. Cells were washed with cold PBS, fixed with 4% paraformaldehyde, and permeabilized using 0.2% Triton X-100 (MilliporeSigma) for 10 min at room temperature. Cells were then blocked for 30 min at room temperature using 0.1% Triton X and then incubated with phalloidin conjugated to AlexaFluor 546 (Thermo Fisher Scientific) for 60 min at room temperature. Cells were stained with DAPI (1 μg/ml) and mounted onto slides using Vectashield (Vector Laboratories, Burlingame, CA, USA). Immunofluorescence imaging was performed using a confocal laser scanning microscope (TCS SP8; Leica Microsystems, Buffalo Grove, IL, USA).

Cells, drug treatments and survival, proliferation assays

Cord blood-derived, immortalized AML cells CB-AML1/ETO (CB-AE) and CB-MLL/AF9 (CB-MA9) were kind gifts from Dr. James Mulloy, Cincinnati Children's Hospital Medical Center (32, 33). CB-AE and CB-MA9 cells were grown in IMDM supplemented with 20% Bovine serum albumin (BSA), insulin, and transferrin in Iscove's MDM (BIT) (StemCell Technologies, Vancouver, BC, Canada) and 10 ng/ml of each of 5 cytokines KTF-36 (R&D, PeproTech). MDS-L cells were kindly provided by Dr. Daniel Starczynowski, Cincinnati Children's Hospital Medical Center, with consent from Dr. Kaoru Tohyama, Kurashiki, Japan (34, 35). MDS-L cells were grown in IMDM supplemented with 10% FBS and 10 ng/ml IL-3 (PeproTech). Human AML cell lines HL60, U937, HEL, and THP1 were maintained in IMDM supplemented with 10% FBS, 100 U/ml penicillin, 100 μg/ml streptomycin, and 2 mM L-glutamine (all from Thermo Fisher Scientific) at 37°C with 5% CO_2. Phoenix GP, 293T (obtained from Dr. Jose Cancelas, Cincinnati Children's Hospital), and A549 cells were maintained in DMEM supplemented with 10% FBS, 100 U/ml penicillin, 100 μg/ml streptomycin, and 2 mM L-glutamine (all from Thermo Fisher Scientific) at 37°C with 5% CO_2. Adherent cells were transfected at 70% confluency using the calcium phosphate transfection method.

CPYPP was purchased from Tocris Bioscience (4568; Bristol, United Kingdom). For calculating median inhibitory concentration (IC_{50}), cells were treated with varying doses of CPYPP from 0.1 to 100 μM. Viable cell counts were taken after 24 h of drug treatment. Cell counts were normalized to DMSO and plotted against the logarithm of CPYPP concentration using GraphPad Prism v.5 to measure the IC_{50}. For proliferation assay, cells were allowed to grow in triplicate in regular media supplemented with cytokines in presence of 5 μM CPYPP or DMSO (vehicle) for 5 d. Media were calibrated with fresh cytokines and CPYPP after every 2 d. Trypan blue–negative cell numbers were determined at respective time points. For survival assay, cells were cultured in the presence of 5 μM CPYPP or DMSO (vehicle) for 6 and 18 h. Total RNA was isolated using Trizol (Thermo Fisher Scientific), and expression of survival genes and apoptotic genes was determined using quantitative RT-PCR (qRT-PCR; Thermo Fisher Scientific).

Analysis of TCGA AML cohort

Heatmap cluster of *MBD3*, *KDM6A*, *DOCK5*, and *DOCK8* expression from TCGA AML cohort was derived using cBioPortal for Cancer Genomics interface. For correlation analysis, mRNA expression (RNA Seq v.2 RSEM) was obtained and plotted using GraphPad Prism v.5. Kaplan-Meier survival plots were generated using TCGA clinical data derived from cBioPortal for Cancer Genomics interface. For correlation as well as survival analysis, only samples with "Normal Karyotype" were considered. Grouping of samples was done based on mRNA expression (RNA Seq v.2 RSEM); all samples showing expression level above median value for the particular gene were considered "high," whereas all samples showing expression level below median value were considered "low." Kaplan-Meier survival probability plots for *MBD3*, *KDM6A*, and *DOCK8* from different AML datasets were derived using prediction of clinical outcomes from genomic profiles.

Statistical analyses

Statistical analyses were performed using GraphPad Prism v.5. Statistics were calculated with Student's *t* test. Quantitative data are expressed as means ± SEM unless specified otherwise. For IC_{50} calculation, cell counts were normalized and plotted against logarithm of CPYPP concentration using GraphPad Prism v.5. Densitometry analyses were performed using ImageJ software. For all statistical analyses, the level of significance was set at 0.05.

RESULTS

Loss of *MBD3* in human primary AML cells associates with leukemic NuRD

We sought to identify NuRD's contribution to human myeloid leukemia pathobiology. Gene expression analysis identified a significant loss of *MBD3* in a cohort (9, 10, 24) of primary AML BMNCs ($P < 0.001$, $n = 58$) and MDS $CD34^+$ HSPCs ($P < 0.01$, $n = 24$) compared with age-matched normal BM $CD34^+$ cells (**Fig. 1*A***). In addition, expression of *MBD2*, *CHD3*, *RBBP7*, and *MTA1/2/3* was significantly down-regulated in primary AML but not in MDS (Fig. 1*B* and Supplemental Fig. S1*A*). Established MDS (34, 35) and AML lines further demonstrated reduced *MBD3* expression (Fig. 1*C*). Consistent with gene expression analysis, MBD3 protein was dramatically reduced in primary AML cells (Fig. 1*D*). However, expression of CHD4, an ATPase subunit of NuRD, remained unaltered in AML (Fig. 1*B*, *D*). This was in contrast to a recent report that demonstrated MBD3 dependency for CHD4 expression and NuRD formation (36), which prompted us to explore NuRD complex in AML cells. Endogenous CHD4 and MTA1/2 were co-immunoprecipitated in AML BMNCs and normal $CD34^+$ cells (Fig. 1*E* and Supplemental Fig. S1*B*). Sucrose density gradient centrifugation analysis confirmed the presence of endogenous, MBD3-deficient, residual nuclear NuRD complex (hereafter called leukemic NuRD) in primary AML cells (Fig. 1*F*). Taken together, our AML discovery cohort indicates that hematopoietic loss of MBD3 is an interesting molecular phenomenon observed in myeloid leukemia.

NuRD co-immunoprecipitates with KDM6A

We reasoned that leukemic NuRD, devoid of specificity factor MBD3, may aberrantly target and regulate genes in myeloid malignancies. NuRD complex is generally considered to be a transcriptional corepressor (37). However, reports have identified NuRD to also be present at actively transcribed loci and to be essential for the expression of certain genes, like *CD4* in mice (38). Importantly, NuRD acts as transcriptional coactivator of GATA-1/FOG-1 genes during hematopoietic development (39). MBD3 mediates association of the MTA2 subunit of NuRD complex with the core HDAC complex, integral to its repressive function (40). Loss of MBD3 may therefore disrupt this association and give rise to a transcriptionally permissive NuRD. NuRD is frequently associated with "poised" genes, which are marked by H3K4Me3 and H3K27Me3 (41). Activation of poised genes requires removal of H3K27 methylation, which is catalyzed by the KDM6 family of H3K27Me3/2 demethylases (42, 43). KDM6B (*JMJD3*) has already been implicated in the development of MDS and T-ALL (22, 30).

We therefore wanted to explore whether NuRD associates with KDM6 in AML. Interestingly, co-immunoprecipitation studies performed using antibody against endogenous MTA1/2, followed by MS [liquid chromatography with MS/MS (LC-MS/MS)] analysis, identified interaction between NuRD complex and KDM6A, but not KDM6B, in 293T cell nuclear fraction (**Fig. 2*A***). A reciprocal co-immunoprecipitation experiment using antibody against endogenous KDM6A followed by MS analysis further demonstrated KDM6A interaction with NuRD complex in 293T cells (Fig. 2*B*). Reciprocal co-immunoprecipitation studies followed by immunoblot analyses further confirmed interaction between mammalian endogenous nuclear NuRD complex with KDM6A in human primary AML cells, in established AML lines as well as in normal hematopoietic cells (Fig. 2*C* and Supplemental Fig. S1*C*). Co-immunoprecipitation experiments failed to find any interaction of KDM6B with NuRD (Fig. 2*C* and Supplemental Fig. S1*C*). NuRD-KDM6A interaction was stably maintained even under stringent high salt concentration (up to 500 mM NaCl) and was independent of the presence of DNA template (Supplemental Fig. S1*D*). In addition, we also observed an *in vitro* interaction between KDM6A and NuRD complex (Supplemental Fig. S1*E*). Overall, these findings identify a novel and unappreciated interaction of mammalian NuRD complex with KDM6A demethylase.

Because KDM6A association with NuRD complex was present in normal hematopoietic cells, nonhematopoietic cells, and MBD3-deficient AML cells, we asked whether loss of MBD3 might cause a change in the affinity or stoichiometry of NuRD interaction with KDM6A. To understand this, 293T cells were transiently transfected with shRNA-expressing construct against *MBD3*, nuclear fractions were co-immunoprecipitated, using antibodies against MTA1/2 or KDM6A, from both control cells or *MBD3*-deficient cells, and were subjected to MS analysis (Fig. 2*D* and Supplemental Fig. S1*F–H* and **Table 1**). Although KDM6A was co-immunoprecipitated with NuRD complex in both control and MBD3-deficent cells, interestingly, the enrichment of KDM6A (normalized with respect to score of bait protein MTA1/2) bound to NuRD was significantly higher in MBD3-deficent cells compared with the control (Fig. 2*E* and Supplemental Fig. S1*H*). We further extended these studies in normal hematopoietic cells and MBD3-deficient AML cells. Consistent with these findings, both MBD3-deficient primary AML cells and HL60 cells had a significantly higher enrichment of endogenous KDM6A co-immunprecipitated with NuRD complex compared with normal hematopoietic cells (Fig. 2*F*, *G* and Supplemental Figs. S2 and S3). MS studies revealed lower enrichment of MBD3 protein co-immunoprecipitated with NuRD complex in primary AML cells (~0.1 fold) and HL60 cells (~0.2 fold) compared with normal (considered as 1-fold) hematopoietic cells (Supplemental Fig. S3). Co-immunoprecipitation using MTA1/2 followed by LC-MS/MS studies further revealed unique NuRD-interacting partners in MBD3-deficient primary AML cells, HL60 cells, and non-hematopoietic cells compared with the respective control cells (Fig. 2*D*, *F* and Supplemental Figs. S2 and S3).

Next, we performed a co-immunoprecipitation experiment of endogenous CHD4 or KDM6A in both AML cells and nonhematopoietic cells; fractions were eluted and analyzed for *in vitro* H3K27Me3/2 demethylase activity.

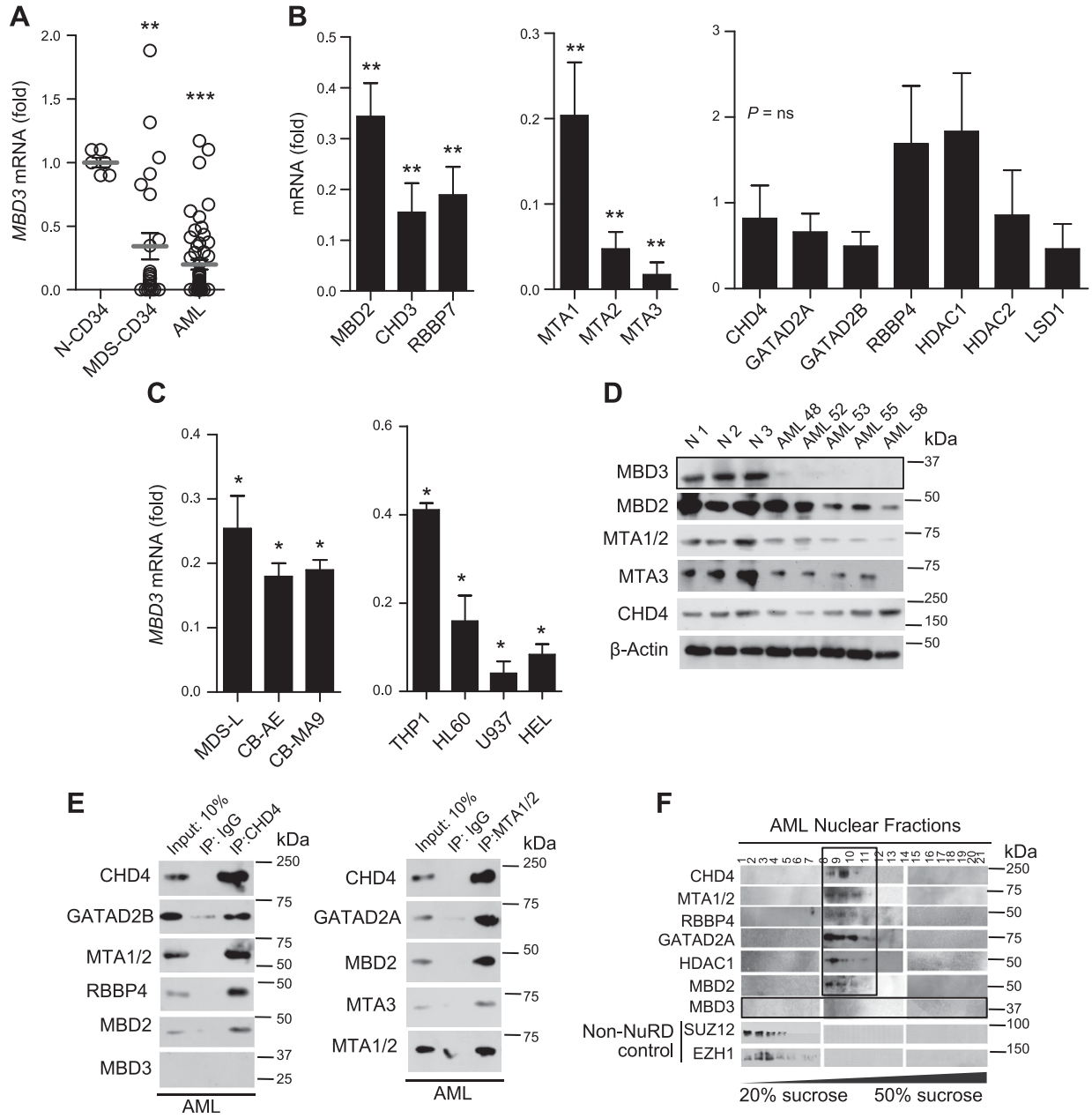

Figure 1. *MBD3* loss in human AML cells associates with leukemic NuRD. *A*) qRT-PCR expression of *MBD3* in MDS ($n = 24$) BM $CD34^+$ HSPCs or AML ($n = 58$) low-density BMNCs compared with age-matched normal (considered as 1-fold) BM ($n = 6$) $CD34^+$ HSPCs. *B*) qRT-PCR expression of NuRD subunits in AML ($n = 15$–20) BMNCs compared with normal (considered as 1-fold) BM ($n = 6$) $CD34^+$ HSPCs. *C*) qRT-PCR analysis of *MBD3* in MDS-L cells and cord blood (CB)–derived CB-AML1/ETO (CB-AE) and CB-MLL/AF9 (CB-MA9) cells (left) and in other established AML cells (right), compared with normal (considered as 1-fold) BM $CD34^+$ HSPCs. *D*) Immunoblot analysis of NuRD in primary AML cells and normal hematopoietic cells. *E*) Co-immunoprecipitation of endogenous CHD4 (left) or MTA1/2 or IgG (right) in nuclear lysate of primary AML BMNC. *F*) Sucrose density gradient analysis of primary AML (pooled from $n = 7$) BMNC-derived nuclear lysates, immunoblotted with respective NuRD antibodies. PRC antibodies were used as non-NuRD controls. qRT-PCR values were normalized to *GAPDH*. Co-immunoprecipitation and immunoblots are representatives of 2–3 independent experiments with similar results. Ns, not significant. Statistics were calculated with Student's *t* test; error bars represent means ± SEM. $^*P < 0.05$, $^{**}P < 0.01$, $^{***}P < 0.001$ were considered to be statistically significant.

Both KDM6A and CHD4 co-immunoprecipitated fractions independently showed H3K27Me3/2 demethylase activities (Supplemental Fig. S4*A*). As a negative control, we used *KDM6A* stable knockdown HL60 and U937 cells, which did not show appreciable histone demethylase activity (Supplemental Fig. S4*B*, *C*). Then, we asked whether loss of *MBD3* could affect H3K27 demethylase activity. To answer this question, 293T cells were transiently transfected with 2 different shRNA-expressing constructs against *MBD3*, and nuclear lysates were co-immunoprecipitated with CHD4 or KDM6A and checked for H3K27Me3/2 demethylase activity. *MBD3*

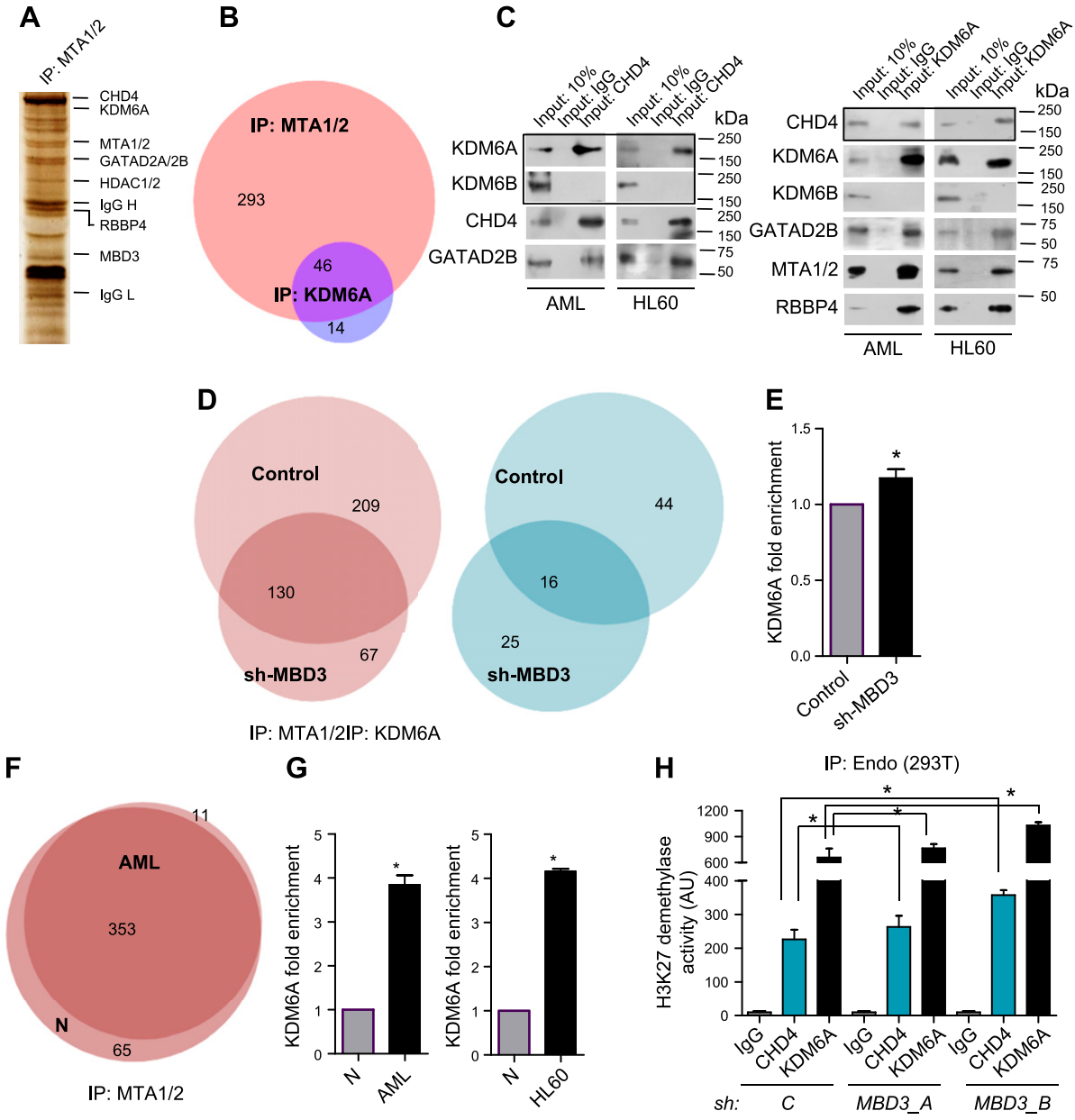

Figure 2. NuRD interacts with KDM6A. *A*) Representative silver staining showing endogenous MTA1/2 co-immunoprecipitated nuclear proteins in 293T cells. *B*) Venn diagram analysis of MS (LC-MS/MS) identified nuclear proteins co-immunoprecipitated using antibodies against endogenous MTA1/2 and KDM6A in 293T cells. MS data are representative of 1 of 2 independent experiments. *C*) Reciprocal co-immunoprecipitation of endogenous CHD4 (left) or KDM6A or IgG (right) in nuclear lysate of primary AML BMNC and HL60 cells. *D*) Venn diagram analysis of LC-MS/MS identified MTA1/2 co-immunoprecipitated proteins (left) and KDM6A co-immunoprecipitated proteins (right) isolated from nuclear lysates of control or *MBD3*-deficient 293T cells. MS data are representative of 1 of 2 independent experiments. *E*) MS quantitation of KDM6A enrichment in MTA1/2 co-immunoprecipitated nuclear fraction in *MBD3*-deficient 293T cells compared with control. KDM6A enrichment was normalized with respect to bait (MTA1/2) score (considered as 1-fold). MS data are representative of 1 of 2 independent experiments. *F*) Venn diagram analysis of LC-MS/MS identified nuclear proteins co-immunoprecipitated using antibodies against endogenous MTA1/2 in normal hematopoietic (blood nucleated) cells and human primary AML (pooled from $n = 7$–9) blasts. *G*) MS quantitation of KDM6A enrichment in MTA1/2 co-immunoprecipitated nuclear fraction in *MBD3*-deficient human primary AML cells (left) or HL60 cells (right) compared with human normal primary hematopoietic cells. KDM6A enrichment was normalized with respect to bait (MTA1/2) score (considered as 1-fold). *H*) H3K27Me3/2 demethylase activity of endogenous CHD4, KDM6A, or IgG co-immunoprecipitated and eluted fractions from 293T cells transiently transfected with sh-Control or 2 different constructs expressing sh-MBD3 (sh-MBD3_A and sh-MBD3_B). Demethylase activity was normalized with respect to individual IgGs. Statistics were calculated with Student's *t* test; error bars represent means ± SD. $^*P < 0.05$ was considered to be statistically significant.

loss resulted in ~1.5-fold increase of *in vitro* demethylase activity (Fig. 2*H*). Importantly, so far, NuRD function has been linked with LSD1/H3K4Me2/1 demethylase activity regulating transcriptional repression (20). To our knowledge, for the first time, we report KDM6A demethylase activity associated with the mammalian NuRD complex.

TABLE 1. *LC-MS/MS analysis of MTA1/2 co-immunoprecipitated proteins isolated from nuclear lysates of control or MBD3-deficient 293T cells*

Description	293T Proteins	Accession ID (UniProtKB)	Control (IP: MTA1/2)			sh-MBD3 (IP: MTA1/2)		
			Score	Coverage	Unique peptides	Score	Coverage	Unique peptides
NuRD subunits	MTA2	O94776	417.89	26.8	12	669.38	31	13
	MTA1	Q13330	127.84	10.35	4	320.44	15.8	6
	CHD4	Q14839	32.18	2.88	1	58.66	4.76	3
	HDAC1	Q13547	465.1	25.52	4	376.13	22.61	3
	HDAC2	Q92769	415.09	25.2	3	667.64	43.03	8
	MBD3	O95983	348.9	15.12	4	—	—	—
	GATAD2A	Q86YP4	32.62	3.16	1	—	—	—
	GATAD2B	Q8WXI9	32.82	2.7	1	28.39	7.59	1
Novel associated factors	KDM6A	O15550	317.69	4.5	2	575.76	17.66	2
	KDM6B	—	—	—	—	—	—	—

CHD4 colocalizes with KDM6A on Rac GTPase *GEFs* in primary AML cells

Interaction of NuRD with KDM6A prompted us to investigate their genome-wide co-occupancy in primary AML cells using ChIP-seq. CHD4 (an intact ATPase subunit of leukemic NuRD) ChIP-seq identified about 10,000 genes on average in 3 independent (biologic replicates) primary AML (AML 01, AML 02, AML 03) BMNCs (**Fig. 3*A, B***). To identify genes coregulated by KDM6A and NuRD, we performed ChIP-seq with KDM6A and H3K27Ac. KDM6A removes the methylation mark from H3K27 residues, which are then subsequently acetylated by either p300 or CBP, permitting transcription (44, 45). Thus, co-occupancy of CHD4, KDM6A, and H3K27Ac would indicate transcription activation of target genes by KDM6A/NuRD. Venn diagram analysis indicated that CHD4, KDM6A, and H3K27Ac ChIP-seq co-occupied 1063 genes that were shared among the 3 biologic replicates of AML, of which nearly 40% binding occurred at the transcription start site–distal intergenic region and 60% occupancy was at promoter proximal and gene body loci (Fig. 3*C–E* and Supplemental Figs. S5 and S6*A*). Transcriptome analysis of the matched AML cohort was carried out to determine differentially expressed genes (Supplemental Fig. S6*B*). Functional annotation clustering of the CHD4, KDM6A, and H3K27Ac co-occupied genes in AML samples using GO terms identified an enrichment of transcripts associated with Rac GTPase activation (Fig. 3*E*). The shared 1063 co-occupied genes also showed significant up-regulation in the RNA-seq analysis (Supplemental Fig. S6*B*).

Importantly, among the Rac GTPase *GEF*s, we noted co-occupancy of CHD4, KDM6A, and H3K27Ac at *DOCK5* and *DOCK8* (*DOCK5/8*) loci in AML (Supplemental Fig. S6*C*). We performed ChIP-seq analysis of CHD4, KDM6A, and H3K27Ac in normal hematopoietic cells (Supplemental Fig. S6*D*). ChIP-qPCR analysis confirmed an increased co-occupancy of CHD4, KDM6A, and H3K27Ac in several primary AML blasts, as well as in AML lines, compared with normal hematopoietic cells (Fig. 3*F* and Supplemental Fig. S6*E*). In agreement with this, gene expression analysis confirmed that *DOCK5/8* expression levels were increased in AML blasts compared with normal $CD34^+$ cells. We did not observe similar regulation operating at other *DOCK* loci in our AML samples. The quality, and hence specificity, of commercially available KDM6A antibodies for ChIP studies is often questioned. Therefore, as a negative control of KDM6A ChIP, we used *KDM6A*-stably silenced AML lines, which confirmed absence of KDM6A occupancy on target loci (Supplemental Fig. S7*A–C*). In addition, our ChIP-seq–based genome colocalization results are in agreement with a recent study, demonstrating that Kdm6a and ATP-dependent chromatin remodelers interact to maintain locus-specific chromatin accessibility in murine hematopoietic cells (26). We also performed CHD4–ChIP-seq analysis in control or *KDM6A*-deficient U937 cells (Supplemental Fig. S7*D*). There was an appreciable loss of CHD4 occupancy on target *GEF* loci in *KDM6A*-deficient AML cells compared with control (Supplemental Fig. S7*D*). Subsequently, we focused our analysis on MBD3/NuRD and KDM6A regulation of Rac GTPase *GEF* expression in AML.

Next, we investigated the mechanism of MBD3 loss–associated increase in the expression of *DOCK5/8* in AML cells. We reasoned that loss of MBD3 would cause relief from HDAC/NuRD–mediated transcriptional repression at target loci. Indeed, deficiency of *MBD3* caused a significant decrease in HDAC1 occupancy, with a corresponding increase in KDM6A, H3K27Ac, and CBP levels at *DOCK5/8* genomic loci (Fig. 3*G*). Taken together, these results suggest that NuRD and KDM6A crosstalk toward *DOCK5/8* regulation in myeloid leukemia.

MBD3-low, *KDM6A*-high AML is correlated with increased *DOCK5*, *DOCK8* expression, and poor prognosis

DOCK proteins are evolutionarily conserved atypical GEFs for Rho GTPase activation, regulating cell motility (31). We and others previously demonstrated that Rac GTPases regulate myeloid leukemia cell survival and engraftment *in vivo* (46, 47). Importantly, DOCK proteins play a key role in Ras-mediated activation of the Rac pathway, which promotes cancer cell survival (48). We asked whether MBD3-mediated regulation of *DOCK* is of

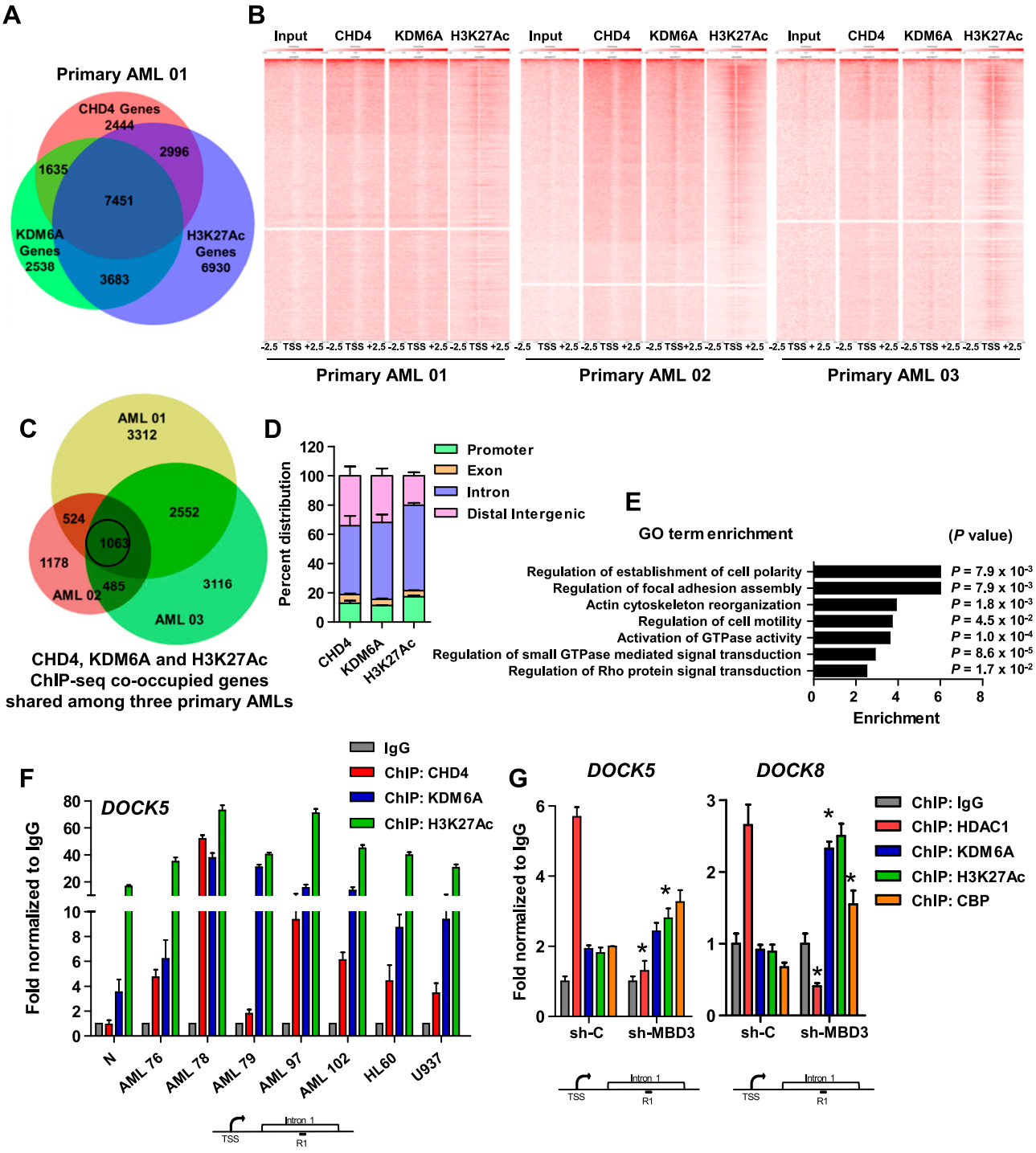

Figure 3. CHD4 colocalizes with KDM6A on Rac GTPase *GEFs* in AML BMNCs. *A*) Representative ChIP-seq Venn diagram analysis showing overlap of genes identified from CHD4 (pink), KDM6A (green), and H3K27Ac (gray) in primary AML (AML 01) BMNC. Number of co-occupied genes (7451) is shown in the intersection. *B*) ChIP-seq ($P < 0.05$) heatmaps showing occupancy of CHD4 or KDM6A or H3K27Ac peaks 2.5 kb upstream or downstream from transcription start site (TSS) in primary AML ($n = 3$; AML 01, AML 02, and AML 03 as biologic replicates) BMNCs. *C*) Venn diagram analysis showing CHD4, KDM6A, and H3K27Ac ChIP-seq co-occupied genes that are shared (1063) among the 3 biologic replicates of AML BMNCs. *D*) ChIP-seq average genomic distribution of CHD4, KDM6A, and H3K27Ac on the shared (1063) gene set in AML. *E*) GO term analysis of the 1063 gene set in AML. Co-immunoprecipitation and immunoblots are representatives of 2–3 independent experiments with similar results. *F*) ChIP-qPCR analysis showing occupancy of CHD4, KDM6A, and H3K27Ac on *DOCK5* loci in primary individual AML cells, AML cell lines, and normal hematopoietic mononuclear cells. ChIP-qPCR values were normalized to IgG; error bars represent means ± SD. Location of ChIP-qPCR primers are represented in the schema. *G*) ChIP-qPCR analysis showing respective chromatin occupancy on *DOCK5* and *DOCK8* loci in 293T cells that were transiently transfected with sh-MBD3 or sh-Control. ChIP-qPCR values were normalized to IgG; error bars represent means ± SD. Location of ChIP-qPCR primers are represented in the schema. Statistics were calculated with Student's *t* test; error bars represent means ± SD. *$P < 0.05$ was considered to be statistically significant.

potential clinical significance. Interestingly, the Cancer Genome Atlas (TCGA) AML cohort revealed a significant negative correlation in expression of *MBD3* with *KDM6A* and *DOCK5/8* (**Fig. 4*A***). In addition, *DOCK5* and *KDM6A* expression was positively correlated in our AML cohort (Fig. 4*B*). Overall, TCGA gene expression analysis indicated that expression of *DOCK5/8* is correlated with inverse *MBD3* and *KDM6A* levels (Fig. 4*C*). A cross-cancer summary of *KDM6A* showed that it is maximally expressed in AML among all cancer types (49); in addition, we recently identified an increased expression of *KDM6A* in primary AML (24).

To further elucidate clinical significance of *MBD3*, we performed survival analysis on TCGA AML dataset with a normal karyotype. Interestingly, *DOCK5/8* expression was significantly increased in the *MBD3*-low, *KDM6A*-high AML cohort compared with *MBD3*-high, *KDM6A*-low AML (Fig. 4*D*). *MBD3*-low, *KDM6A*-high patients have relatively poor overall survival and disease-free survival compared with *MBD3*-high, *KDM6A*-low individuals (Fig. 4*E*). High *DOCK5* expression correlates with an even poorer prognosis in *MBD3*-low, *KDM6A*-high individuals (Fig. 4*F*). Survival prediction in several other AML datasets highlights the significance of *MBD3*, *KDM6A*, and *DOCK5/8* expression levels (Supplemental Fig. S8). Together, these data suggest that *MBD3*-low, *KDM6A*-high AML is correlated with elevated *DOCK5/8* expression and poor prognosis, highlighting the importance of MBD3 as a potential tumor suppressor in leukemia.

MBD3 regulates *DOCK5/8* expression that involves KDM6A program

Having identified KDM6A and NuRD interaction, genome colocalization, and its relevance in AML pathobiology, we further investigated mechanisms of crosstalk between *MBD3* and *KDM6A* programs in *DOCK5/8* regulation. Lentivirus-mediated silencing of *MBD3* in established AML cell lines, which still express residual *MBD3*, induced *DOCK5/8* expression (**Fig. 5*A*** and Supplemental Fig. S9*A–C*). There was no significant change in expression of other *DOCK*s in *MBD3*-deficient cells (Supplemental Fig. S9*D*). We asked whether *MBD3*-mediated *DOCK5/8* expression depends on KDM6A. We therefore generated HL60 and U937 cells that were stably transduced with multiple sh-KDM6A constructs or sh-Control, coexpressing GFP, and sorted using flow cytometry (Supplemental Figs. S4*B* and S7*A*). Interestingly, silencing of *MBD3* in *KDM6A*-deficient background did not induce *DOCK5/8* expression (Fig. 5*A* and Supplemental Fig. S9*E*). *KDM6A*-null THP1 cells also did not show *DOCK5/8* induction upon loss of *MBD3* (Supplemental Fig. S9*F*). Mechanistically, down-regulation of *DOCK5/8* expression in *KDM6A*-deficient cells was associated with reduced occupancy of H3K27Ac and CBP on *DOCK5/8* loci compared with control (Fig. 5*B* and Supplemental Fig. S9*G*). Collectively, these data highlight interdependency of *MBD3* and *KDM6A* programs toward regulation of selective Rac GTPase *GEF* expression in AML.

Deficiency of *MBD3* augments Rac GTPase activation and AML cell migration

DOCK proteins are integral for activation of the Rac pathway. We therefore investigated whether increased *DOCK5/8* expression, secondary to loss of *MBD3*, would result in Rac GTPase activation. Indeed, loss of *MBD3* resulted in ~2.5-fold increase in active Rac GTP compared with control (Fig. 5*C*). Consistent with its effect on *DOCK* expression, silencing of *KDM6A* restored Rac GTPase level in *MBD3*-deficient cells (Fig. 5*D*). To determine whether Rac activation induces migration or cell trafficking, sh-Control– or sh-MBD3–treated AML cells were allowed to migrate *in vitro* toward a CXCL12 gradient. In agreement with Rac GTPase activation, deficiency of *MBD3* promoted migration of AML cells (Fig. 5*E*). In addition, pharmacological inhibition of DOCKs using CPYPP (50, 51) reversed hypermigration of *MBD3*-deficient AML cells (Fig. 5*F*). Essentially, this confirmed that *MBD3*-deficient migration induction was dependent on DOCK activation. Retrovirus-mediated overexpression of *Mbd3* into HL60 and U937 cells resulted in reversal of *DOCK5/8* expression, Rac activation, and AML cell migration (Supplemental Fig. S10*A–C*). To further confirm whether KDM6A is required for loss of *MBD3*-induced cell migration, we transduced *KDM6A*-deficient AML cells with sh-MBD3 or sh-Control and subjected them to transwell migration assay. Importantly, consistently with functional epistasis between *MBD3* and *KDM6A*, absence of *KDM6A* significantly reversed the hypermigratory phenotype of *MBD3*-deficient AML cells (Fig. 5*G*). *MBD3* and *KDM6A* epistasis toward expression of *DOCK5/8* and chemokine-directed cell migration were similarly observed in normal primary hematopoietic cells (Supplemental Fig. S10*D*, *E*). Together, these data illustrate a novel cooperation between MBD3 and KDM6A toward *DOCK5/8* expression and Rac activation.

Pharmacological inhibition of DOCK signaling selectively attenuates AML cell survival

In our AML discovery cohort, DOCK genes emerged as a focal point of NuRD activity. We interrogated whether pharmacological inhibition of DOCK signaling would affect AML cell survival and proliferation. Unlike other GEFs, DOCKs do not possess a Dbl homology/Pleckstrin homology domain; instead, a DOCK homology region domain located at the C terminus is responsible for GEF activity. CPYPP, a commercially available small molecule inhibitor, binds to the DOCK homology region domain and inhibits activity of DOCK family proteins (31, 50). DOCK inhibition reversed F-actin polymerization, attenuated AML cell migration, and induced apoptotic gene expression (Supplemental Fig. S10*F–H*). The IC_{50} of CPYPP was determined in AML and normal HSPCs (**Fig. 6*A***). CPYPP treatment for 24 h dramatically inhibited survival of established AML lines and primary AML blasts with an average IC_{50} of ~5 μM (Fig. 6*A*). $CD34^+$ normal HSPCs were substantially less sensitive (IC_{50} ~57 μM) to CPYPP (Fig. 6*A*). Mechanistically, CPYPP inhibition in

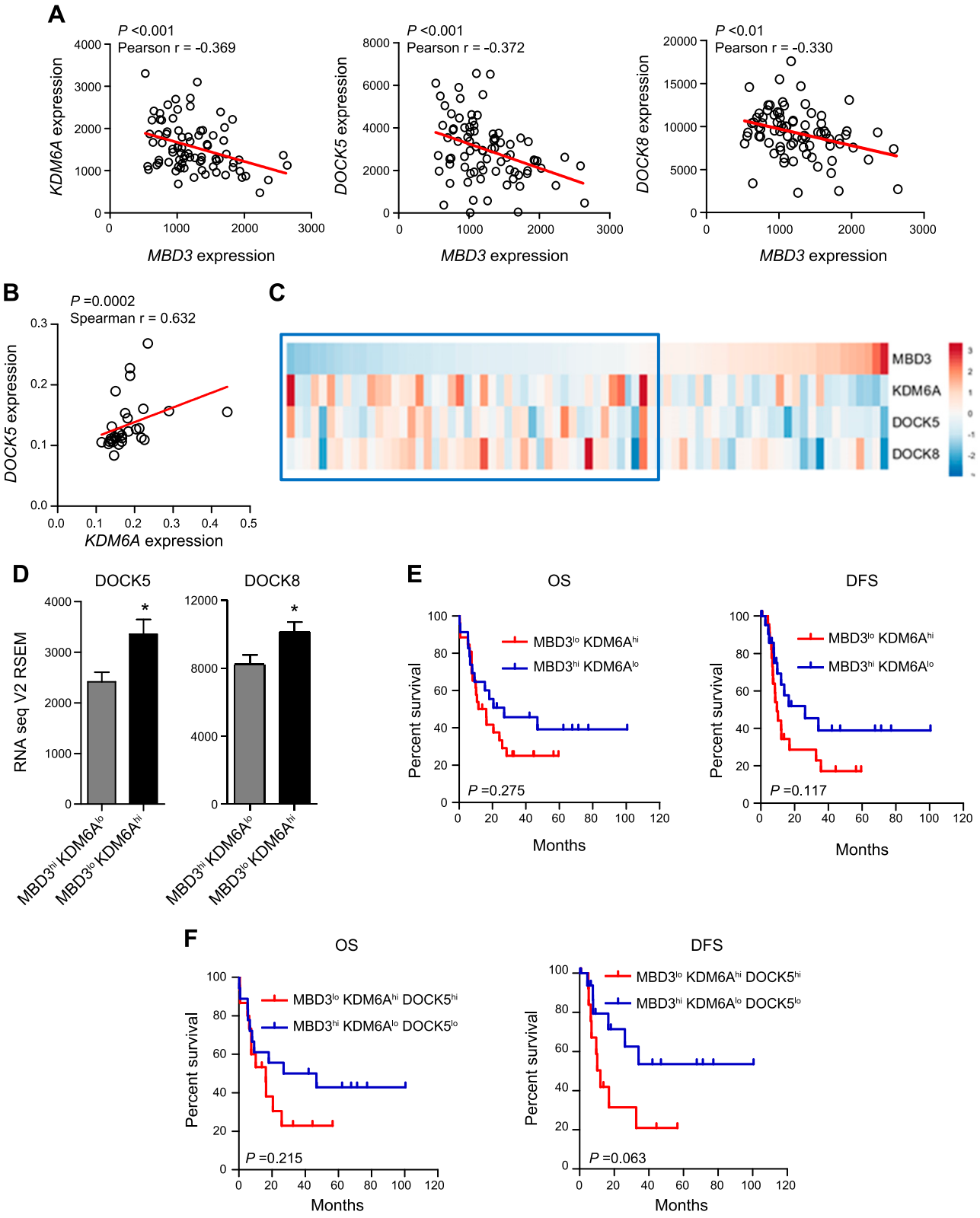

Figure 4. *MBD3*-low (*MBD3*^{lo}), *KDM6A*-high (*KDM6A*^{hi}) AML is correlated with increased *DOCK5*, *DOCK8* expression, and poor prognosis. *A*) *MBD3* gene expression correlation plots with *KDM6A*, *DOCK5*, and *DOCK8* in AML cohort ($n = 80$) from TCGA dataset. *B*) *KDM6A* and *DOCK5* gene expression correlation plot in our AML ($n = 35$) cohort. *C*) mRNA expression z-scores (RNA Seq v.2 RSEM) heatmap cluster from TCGA AML dataset ($n = 80$) of *MBD3*, *KDM6A*, *DOCK5*, and *DOCK8*. Highlighted blue box shows up-regulated (red) *DOCK5* or *DOCK8* in samples with low (blue) *MBD3* and high (red) *KDM6A* expression. *D*) Bar graph showing difference in *DOCK5* or *DOCK8* expression between *MBD3*-high (*MBD3*^{hi}), *KDM6A*-low (*KDM6A*^{lo}) ($n = 23$) and *MBD3*^{lo}*KDM6A*^{hi} ($n = 26$) AML samples from TCGA dataset. *E*) Kaplan-Meier survival plots showing overall survival (OS) (left) or disease-free survival (DFS) (right) of *MBD3*^{hi}*KDM6A*^{lo} ($n = 23$) and *MBD3*^{lo}*KDM6A*^{hi} ($n = 26$) AML samples from TCGA dataset.

(*continued on next page*)

MBD3-deficient cells, but not in wild-type cells, significantly reduced active Rac GTP level, demonstrating that CPYPP sensitivity was dependent on loss of *MBD3* (Fig. 6*B*). In a time-dependent proliferation assay, CPYPP treatment selectively inhibited survival of multiple AML cells (Fig. 6*C*). *KDM6A* deficiency further sensitized (2-fold) AML cells to CPYPP inhibition (Supplemental Fig. S10*I*). Collectively, our findings provide evidence for a hitherto unrecognized functional epistasis between NuRD and KDM6A toward maintenance of Rac GTPase *GEF* expression and Rac activation in human AML pathobiology (Fig. 6*D*) and may suggest a rationale for DOCK inhibition in AML. *In vivo* genetic characterization of *MBD3* as a potential tumor suppressor precisely in AML maintenance was beyond the scope of this present study and warrants future investigations.

DISCUSSION

Transcriptional plasticity is an evolving phenomenon in cancer biology. Tumor cell type–specific transcriptional dependencies cannot be addressed using only genome sequencing studies. In the present study, we took a focused mechanistic approach toward understanding gene control programs operating within human primary leukemia cells in order to identify novel epigenetic vulnerability. Overall, our findings indicate a tumor suppressor function of MBD3, a subunit of the NuRD complex, in human myeloid leukemia. Gut-specific conditional inactivation of *Mbd3* causes increased susceptibility to tumorigenesis, highlighting its tumor suppressor role (52, 53). Loss of *MBD3* has been also linked with pancreatic cancer cell invasion and metastasis (54). One recent study has demonstrated that pan-hematopoietic loss of *Mbd3 in vivo* (*Mbd3*$^{f/f}$; *Vav-Cre*) results in the development of T-cell acute lymphoblastic lymphoma (36). Using this model, the authors have shown that Mbd3 was necessary for maintenance of normal levels of Chd4 and that *Mbd3* loss prevented formation of stable NuRD complex (36). In contrast, our data indicate that both CHD4 expression and NuRD complex integrity were maintained despite the complete absence of MBD3 in human primary AML blasts. It is is noteworthy to mention that although conditional inactivation of Mi-2β (*Chd4*) caused erythroid leukemia in mice (15), CHD4 depletion selectively sensitizes human AML blasts to genotoxic stress and reduces tumor burden *in vivo* (3). Together, these results essentially suggest that epigenetic regulation and dependence on specific chromatin regulatory complex are cell type–specific and context-dependent phenomena; herein, loss of *MBD3* in human myeloid leukemia participates with KDM6A program toward maintenance of oncogenic gene expression.

NuRD is commonly considered as a transcriptional corepressor, although NuRD complex can also act as enhancers and superenhancers and mediate transcription factor–induced gene activation (55, 56). MBD3 mediates association of the MTA2 subunit of NuRD complex with the core HDAC complex, integral for its repressive function (37, 40). Mbd3 interaction with Evi1 was shown to inhibit *in vitro* HDAC activity of the NuRD complex (57). In a separate study, it was shown that NuRD-mediated H3K27 deacetylation facilitated recruitment of polycomb repressive complex to direct gene repression in embryonic stem cells (41). In agreement with these findings, we provide evidence that deficiency of *MBD3* causes locus-specific loss of HDAC1 chromatin occupancy, which is accompanied by a corresponding increase in occupancy of KDM6A/H3K27Ac/CBP, leading to derepression of gene expression. Given that leukemic NuRD retains the catalytic ATPase subunit CHD4, which co-immunoprecipitates with KDM6A and colocalizes with KDM6A/H3K27Ac on target loci, it would be tempting to speculate that MBD3 deficiency may therefore harness the potential of CHD4 toward transcriptional activation associated chromatin remodeling.

Our results illustrate that NuRD interacts with KDM6A to regulate *DOCK5/8* expression in human AML cells. MS studies indicate that MBD3-deficient AML cells have a higher enrichment of endogenous KDM6A co-immunoprecipitated with NuRD complex compared with normal hematopoietic cells. Our finding is consistent with a current study highlighting interaction among Kdm6a and chromatin remodelers toward gene expression regulation in murine hematopoiesis (26). KDM6A participates with mixed lineage leukemia 2 and 3 complexes and creates a transcription-permissive chromatin state. Although KDM6A was predominantly implicated as a tumor suppressor, as evidenced by its H3K27 demethylase–dependent catalytic function in murine T-ALL pathogenesis and demethylase-independent transcriptional regulatory activity in murine AML (22, 26), emerging evidence also highlights its oncogenic function (23, 25, 58). Recently, we have identified KDM6 demethylases as molecular therapeutic targets in human primary AML (24). Inhibition of KDM6A is proposed as a selective epigenetic therapy against TAL1-driven T-ALL (23). Attenuation of H3K27 demethylase activity of KDM6A has also been shown to enhance tumor cell radiosensitivity (25). It is important to mention that, unlike in primary AML, low *KDM6A* expression has been observed in relapsed AML patients (28), which further suggests that the overall contribution of KDM6A in tumorigenesis is spatiotemporally regulated.

Analysis of TCGA database revealed that *DOCK5/8* expression is positively dependent on *KDM6A* expression

F) Kaplan-Meier survival plots showing overall survival (OS) (left) or disease-free survival (DFS) (right) of *MBD3*^{hi}*KDM6A*^{lo}, *DOCK5*-low (*DOCK5*^{lo}) (n = 18) and *MBD3*^{lo}*KDM6A*^{hi}, *DOCK5*-high (*DOCK5*^{hi}) (n = 15) AML samples from TCGA dataset. For TCGA data analyses, only AML samples with normal karyotype (NK) were considered. qRT-PCR values were normalized to *GAPDH*. Statistics were calculated with Student's t test; error bars represent means ± SEM. *$P < 0.05$ was considered to be statistically significant.

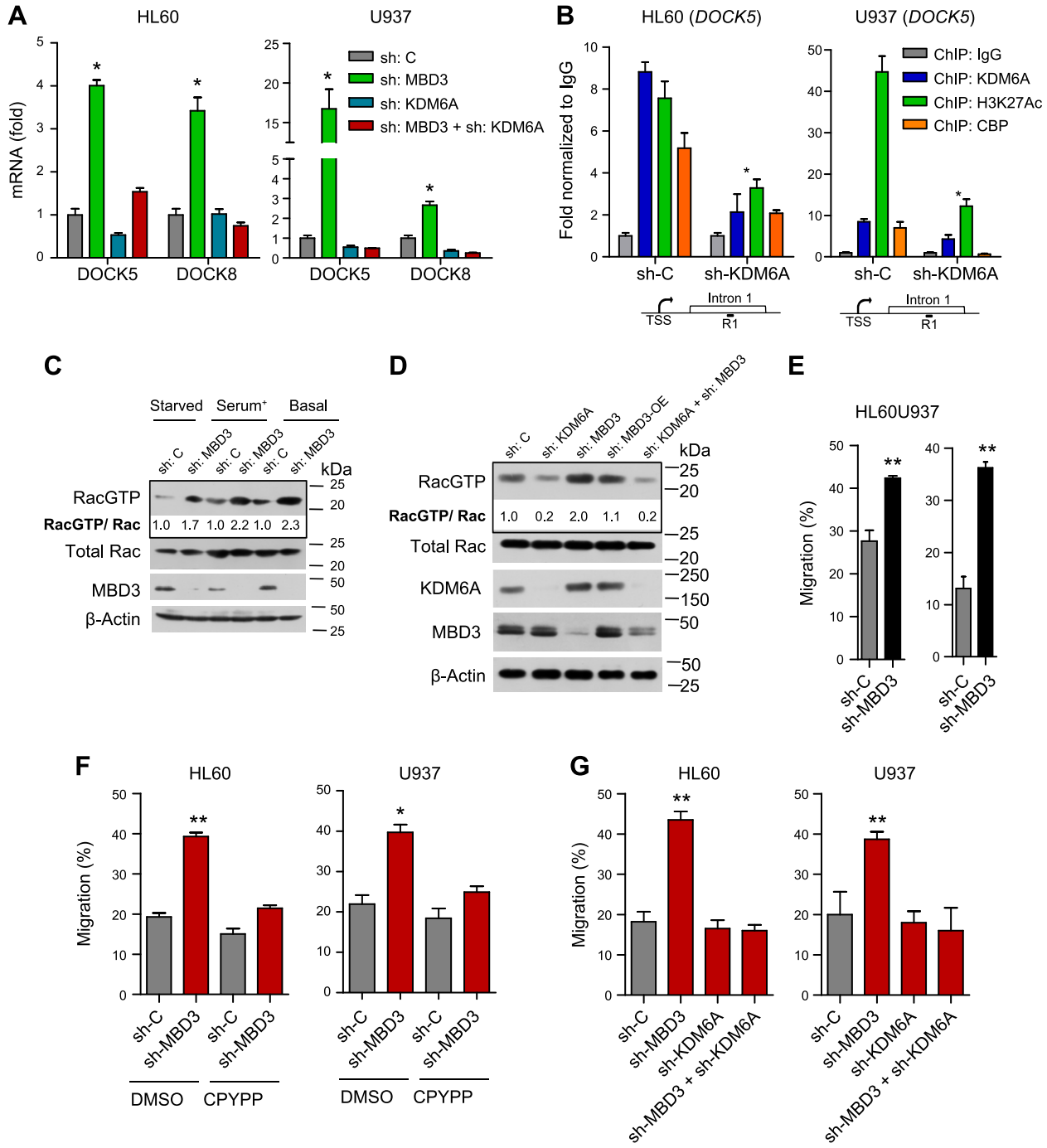

Figure 5. MBD3 regulates *DOCK5/8* expression in KDM6A-dependent mechanism; deficiency of *MBD3* translates into Rac GTPase activation and AML cell hypermigration. *A*) qRT-PCR expression of *DOCK5* and *DOCK8* in HL60 cells (left) and U937 cells (right) expressing sh-MBD3 or sh-KDM6A or both compared with sh-Control–expressing cells (considered as 1-fold). *B*) ChIP-qPCR analysis showing respective chromatin occupancy on *DOCK5* loci in *KDM6A*-deficient HL60 cells (left) and U937 cells (right). ChIP-qPCR values were normalized to IgG; error bars represent means ± SD. Location of ChIP-qPCR primers are represented in the schema. *C*) PAK1 pulldown assay in A549 cells transiently transfected with sh-Control or sh-MBD3 under different conditions. Densitometry represents ratio of Rac GTP *vs.* total Rac normalized to sh-Control. *D*) PAK1 pulldown assay in 293T cells transiently transfected with different constructs. Densitometry represents ratio of Rac GTP *vs.* total Rac normalized to sh-Control. *E*) Migration of HL60 and U937 cells expressing sh-Control or sh-MBD3 and coexpressing *GFP*. Data represent 2 independent experiments with similar results. *F*) Migration of control or *MBD3*-deficient HL60 cells (left) and U937 cells (right) that were treated with CPYPP (100 μM for 1 h) or DMSO (vehicle). Data represent 2 independent experiments with similar results. *G*) Migration of *MBD3*-deficient or *KDM6A*-deficient or doubly deficient HL60 cells (left) and U937 cells (right). Pulldown and immunoblots are representative of 2–3 independent experiments with similar results. Statistics were calculated with Student's *t* test; error bars represent means ± SD. $^{*}P < 0.05$, $^{**}P < 0.01$, were considered to be statistically significant.

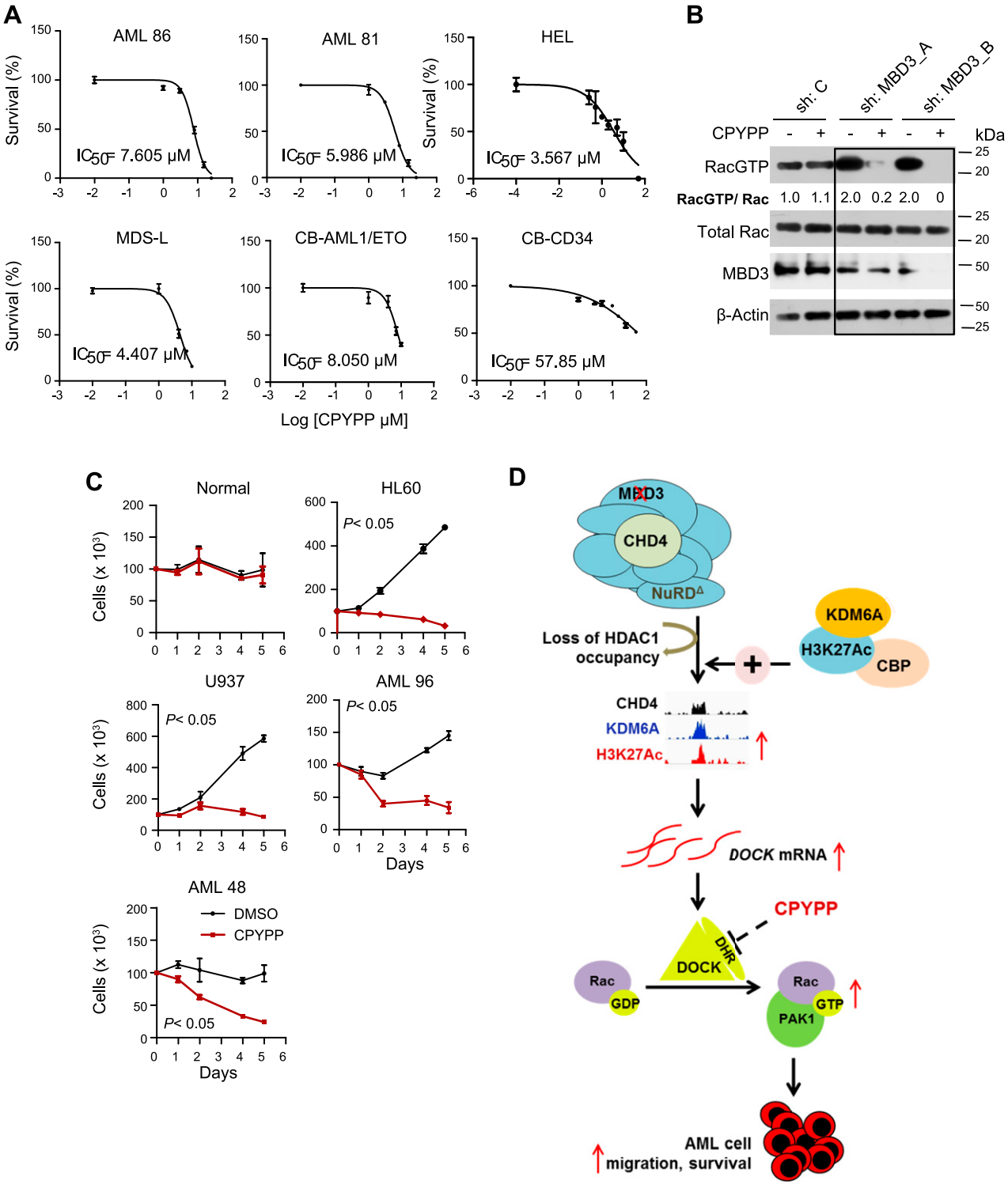

Figure 6. Pharmacological inhibition of DOCK signaling selectively attenuates AML cell survival. *A*) IC_{50} of CPYPP (normalized to DMSO) in AML cells and $CD34^+$ normal HSPCs. *B*) PAK1 pulldown assay of wild type or *MBD3*-deficient (carrying 2 different shRNA–expressing constructs against *MBD3*) 293T cells that were treated with CPYPP or DMSO (vehicle). Densitometry represents ratio of Rac GTP *vs.* total Rac normalized to sh-Control. *C*) Survival of AML cells and normal hematopoietic cells cultured for 5 d in the presence of CPYPP (5 μM) or DMSO control. Data represent 2 independent experiments with similar results. *D*) Schema representing MBD3 loss–associated molecular crosstalk among CHD4, KDM6A, H3K27Ac, and CBP toward induction of *DOCK5/8* expression and maintenance of Rac GTPase program in AML cells. MBD3-deficient leukemic NuRD is represented with $NuRD^{\Delta}$. Pulldown and immunoblots are representative of 2–3 independent experiments with similar results. Statistics were calculated with Student's *t* test; error bars represent means ± SD.

and negatively correlated with *MBD3* expression. TCGA dataset shows *DOCK5/8* expression to be significantly increased in *MBD3*-low, *KDM6A*-high AML cohort with a normal karyotype compared with the *MBD3*-high, *KDM6A*-low AML cohort, and patients with *MBD3*-low, *KDM6A*-high AML have a relatively poor survival compared with the *MBD3*-high, *KDM6A*-low cohort. *DOCK5/8* is similarly up-regulated in our AML cohort. We have demonstrated that pharmacological inhibition of DOCK signaling preferentially attenuated AML cell survival compared with normal hematopoietic cells, and DOCK inhibition was associated with *MBD3* expression level. An earlier report by Hwei *et al.* suggested that overexpression of *DOCK1* (or *DOCK180*) is significantly associated with a poor prognosis in AML patients (60). Because CPYPP is a pan-DOCK inhibitor, we cannot completely rule out the possibility of inhibition of other DOCK family proteins in this study. However ChIP-seq and transcriptome analysis, along with *MBD3 loss of function* studies, indicated selective enrichment of CHD4-KDM6A-H3K27Ac on *DOCK5/8* loci. DOCKs have been shown to promote Rac GTPase activity and Rac GTPase–dependent cell migration. We and others previously demonstrated that Rac GTPases regulate myeloid leukemia cell survival and engraftment *in vivo*. Together, our data position DOCK proteins as important targets of leukemic NuRD in human AML cells and underscore the rationale of pharmacological inhibition of DOCK in human myeloid leukemia.

In this study, for the first time, we report that KDM6A program is associated with NuRD function in human primary AML cells, and our data illustrate that NuRD-associated targeting of KDM6A is a novel component of epigenetic regulation. So far, NuRD function has been linked with LSD1/H3K4Me2/1 demethylase activity, promoting gene repression (20, 59). We have mechanistically identified that loss of MBD3 causes relief from HDAC1-associated transcriptional repression in a locus-specific manner, which in turn results in increased occupancy of KDM6A, H3K27Ac, and CBP, leading to derepression of *DOCK5/8* expression. Therefore, MBD3 deficiency exerts its tumor suppressive function in human primary AML in a 2-hit mechanism. In summary, our results reveal that leukemic NuRD cooperates with KDM6A to amplify Rac GTPase *GEF* expression, and Rac activation, AML cell trafficking, and pharmacological targeting of DOCK signaling may selectively inhibit AML cell survival. In order to characterize an *in vivo* genetic epistatic relationship between *MBD3* and *KDM6A* toward AML pathogenesis, tissue-specific conditional knockout mice models would be instrumental, which was beyond the scope of our present study. Overall, the contribution of KDM6A in AML pathobiology appears to be context dependent and probably contentious, warranting further investigation. Nevertheless, our current findings based on a human AML discovery cohort along with mechanistic and functional insights may lead to even more interesting future investigations to fully appreciate and understand this epistatic relation within an *in vivo* genetic context. FJ

ACKNOWLEDGMENTS

The authors thank Dr. Prasanta Mukhopadhyay for providing umbilical cord blood samples; Dr. Jose Silva (University of Cambridge, Cambridge, United Kingdom), Dr. Keisuke Kaji (The University of Edinburgh, Edinburgh, United Kingdom), and Dr. Jose Cancelas (Cincinnati Children's Hospital, OH, USA) for sharing plasmids; and Addgene (Watertown, MA, USA) for shipping DNA constructs. CB-AE and CB-MA9 acute myeloid leukemia cells were generous gifts from Dr. James Mulloy (Cincinnati Children's Hospital Medical Center, Cincinnati, OH, USA). MDS-L cells were obtained from Dr. Daniel Starczynowski (Cincinnati Children's Hospital Medical Center) with consent from Dr. Kaoru Tohyama (Kawasaki Medical School, Kurashiki, Japan). The authors thank Dr. Arindam Maitra and Dr. Subrata Patra [Core Technologies Research Initiative (CoTERI), National Institute of Biomedical Genomics (NIBMG), Kalyani, India] for chromatin immunoprecipitation sequencing (ChIP-seq) and next-generation sequencing experiments and Dr. Madavan Vasudevan and Shemi Ramesh (Bionivid Technology, Bangalore, India) for RNA sequencing (RNA-seq) experiments, ChIP-seq, and RNA-seq analysis; and Indian Institute of Chemical Biology (IICB) flow cytometry and mass spectrometry cores for services. This study is supported by funding from the Council of Scientific and Industrial Research (CSIR) (NWP/BioDiscovery, BSC 0120), Department of Biotechnology (DBT) (BT/RLF/RE-ENTRY/06/2010), Ramalingaswami Fellowship (to A.S.), DBT (BT/PR13023/MED/31/311/2015) (to A.S.), and Department of Science and Technology (DST) (SB/SO/HS-053/2013), Government of India (to A.S.). M.B., S.C., and S.S.C. acknowledge fellowships from the University Grants Commission (UGC) and CSIR, respectively. L.D.B. is CSIR–Shyama Prasad Mukherjee Fellow. The authors declare no conflicts of interest.

AUTHOR CONTRIBUTIONS

M. Biswas and S. S. Chatterjee performed all experiments and analyzed data; L. D. Boila generated *KDM6A* knockdown cells and *MBD3-OE* construct, performed The Cancer Genome Atlas survival analysis, and participated in manuscript editing; S. Chakraborty participated in processing of human acute myeloid leukemia (AML) bone marrow specimens and helped in lentivirus preparation; D. Banerjee performed pathological analyses of human myelodysplastic syndromes and AML bone marrow samples; and A. Sengupta conceived and designed research, interpreted data, wrote the manuscript, and directed the overall study.

REFERENCES

1. Raza, A., and Galili, N. (2012) The genetic basis of phenotypic heterogeneity in myelodysplastic syndromes. *Nat. Rev. Cancer* **12**, 849–859
2. Papaemmanuil, E., Gerstung, M., Malcovati, L., Tauro, S., Gundem, G., Van Loo, P., Yoon, C. J., Ellis, P., Wedge, D. C., Pellagatti, A., Shlien, A., Groves, M. J., Forbes, S. A., Raine, K., Hinton, J., Mudie, L. J., McLaren, S., Hardy, C., Latimer, C., Della Porta, M. G., O'Meara, S., Ambaglio, I., Galli, A., Butler, A. P., Walldin, G., Teague, J. W., Quek, L., Sternberg, A., Gambacorti-Passerini, C., Cross, N. C., Green, A. R., Boultwood, J., Vyas, P., Hellstrom-Lindberg, E., Bowen, D., Cazzola, M., Stratton, M. R., and Campbell, P. J.; Chronic Myeloid Disorders Working Group of the International Cancer Genome Consortium. (2013) Clinical and biological implications of driver mutations in myelodysplastic syndromes. *Blood* **122**, 3616–3627; quiz 3699

3. Sperlazza, J., Rahmani, M., Beckta, J., Aust, M., Hawkins, E., Wang, S. Z., Zu Zhu, S., Podder, S., Dumur, C., Archer, K., Grant, S., and Ginder, G. D. (2015) Depletion of the chromatin remodeler CHD4 sensitizes AML blasts to genotoxic agents and reduces tumor formation. *Blood* **126**, 1462–1472
4. Appelbaum, F. R., Gundacker, H., Head, D. R., Slovak, M. L., Willman, C. L., Godwin, J. E., Anderson, J. E., and Petersdorf, S. H. (2006) Age and acute myeloid leukemia. *Blood* **107**, 3481–3485
5. Papaemmanuil, E., Gerstung, M., Bullinger, L., Gaidzik, V. I., Paschka, P., Roberts, N. D., Potter, N. E., Heuser, M., Thol, F., Bolli, N., Gundem, G., Van Loo, P., Martincorena, I., Ganly, P., Mudie, L., McLaren, S., O'Meara, S., Raine, K., Jones, D. R., Teague, J. W., Butler, A. P., Greaves, M. F., Ganser, A., Döhner, K., Schlenk, R. F., Döhner, H., and Campbell, P. J. (2016) Genomic classification and prognosis in acute myeloid leukemia. *N. Engl. J. Med.* **374**, 2209–2221
6. Bradner, J. E., Hnisz, D., and Young, R. A. (2017) Transcriptional addiction in cancer. *Cell* **168**, 629–643
7. Kaji, K., Caballero, I. M., MacLeod, R., Nichols, J., Wilson, V. A., and Hendrich, B. (2006) The NuRD component Mbd3 is required for pluripotency of embryonic stem cells. *Nat. Cell Biol.* **8**, 285–292
8. Rais, Y., Zviran, A., Geula, S., Gafni, O., Chomsky, E., Viukov, S., Mansour, A. A., Caspi, I., Krupalnik, V., Zerbib, M., Maza, I., Mor, N., Baran, D., Weinberger, L., Jaitin, D. A., Lara-Astiaso, D., Blecher-Gonen, R., Shipony, Z., Mukamel, Z., Hagai, T., Gilad, S., Amann-Zalcenstein, D., Tanay, A., Amit, I., Novershtern, N., and Hanna, J. H. (2013) Deterministic direct reprogramming of somatic cells to pluripotency. *Nature* **502**, 65–70; erratum: 520, 710
9. Chatterjee, S. S., Biswas, M., Boila, L. D., Banerjee, D., and Sengupta, A. (2018) SMARCB1 deficiency integrates epigenetic signals to oncogenic gene expression program maintenance in human acute myeloid leukemia. *Mol. Cancer Res.* **16**, 791–804
10. Sinha, S., Chatterjee, S. S., Biswas, M., Nag, A., Banerjee, D., De, R., and Sengupta, A. (2018) SWI/SNF subunit expression heterogeneity in human aplastic anemia stem/progenitors. *Exp. Hematol.* **62**, 39–44. e2
11. Witzel, M., Petersheim, D., Fan, Y., Bahrami, E., Racek, T., Rohlfs, M., Puchałka, J., Mertes, C., Gagneur, J., Ziegenhain, C., Enard, W., Stray-Pedersen, A., Arkwright, P. D., Abboud, M. R., Pazhakh, V., Lieschke, G. J., Krawitz, P. M., Dahlhoff, M., Schneider, M. R., Wolf, E., Horny, H. P., Schmidt, H., Schäffer, A. A., and Klein, C. (2017) Chromatin-remodeling factor SMARCD2 regulates transcriptional networks controlling differentiation of neutrophil granulocytes. *Nat. Genet.* **49**, 742–752
12. Priam, P., Krasteva, V., Rousseau, P., D'Angelo, G., Gaboury, L., Sauvageau, G., and Lessard, J. A. (2017) SMARCD2 subunit of SWI/SNF chromatin-remodeling complexes mediates granulopoiesis through a CEBPε dependent mechanism. *Nat. Genet.* **49**, 753–764
13. Shi, J., Whyte, W. A., Zepeda-Mendoza, C. J., Milazzo, J. P., Shen, C., Roe, J. S., Minder, J. L., Mercan, F., Wang, E., Eckersley-Maslin, M. A., Campbell, A. E., Kawaoka, S., Shareef, S., Zhu, Z., Kendall, J., Muhar, M., Haslinger, C., Yu, M., Roeder, R. G., Wigler, M. H., Blobel, G. A., Zuber, J., Spector, D. L., Young, R. A., and Vakoc, C. R. (2013) Role of SWI/SNF in acute leukemia maintenance and enhancer-mediated Myc regulation. *Genes Dev.* **27**, 2648–2662
14. Zhang, J., Jackson, A. F., Naito, T., Dose, M., Seavitt, J., Liu, F., Heller, E. J., Kashiwagi, M., Yoshida, T., Gounari, F., Petrie, H. T., and Georgopoulos, K. (2011) Harnessing of the nucleosome-remodeling-deacetylase complex controls lymphocyte development and prevents leukemogenesis. *Nat. Immunol.* **13**, 86–94
15. Yoshida, T., Hazan, I., Zhang, J., Ng, S. Y., Naito, T., Snippert, H. J., Heller, E. J., Qi, X., Lawton, L. N., Williams, C. J., and Georgopoulos, K. (2008) The role of the chromatin remodeler Mi-2beta in hematopoietic stem cell self-renewal and multilineage differentiation. *Genes Dev.* **22**, 1174–1189
16. Vishwakarma, B. A., Nguyen, N., Makishima, H., Hosono, N., Gudmundsson, K. O., Negi, V., Oakley, K., Han, Y., Przychodzen, B., Maciejewski, J. P., and Du, Y. (2016) Runx1 repression by histone deacetylation is critical for Setbp1-induced mouse myeloid leukemia development. *Leukemia* **30**, 200–208
17. Dos Santos, R. L., Tosti, L., Radzisheuskaya, A., Caballero, I. M., Kaji, K., Hendrich, B., and Silva, J. C. (2014) MBD3/NuRD facilitates induction of pluripotency in a context-dependent manner. *Cell Stem Cell* **15**, 102–110
18. Ng, H. H., Zhang, Y., Hendrich, B., Johnson, C. A., Turner, B. M., Erdjument-Bromage, H., Tempst, P., Reinberg, D., and Bird, A. (1999) MBD2 is a transcriptional repressor belonging to the MeCP1 histone deacetylase complex. *Nat. Genet.* **23**, 58–61
19. Le Guezennec, X., Vermeulen, M., Brinkman, A. B., Hoeijmakers, W. A., Cohen, A., Lasonder, E., and Stunnenberg, H. G. (2006) MBD2/NuRD and MBD3/NuRD, two distinct complexes with different biochemical and functional properties. *Mol. Cell. Biol.* **26**, 843–851
20. Wang, Y., Zhang, H., Chen, Y., Sun, Y., Yang, F., Yu, W., Liang, J., Sun, L., Yang, X., Shi, L., Li, R., Li, Y., Zhang, Y., Li, Q., Yi, X., and Shang, Y. (2009) LSD1 is a subunit of the NuRD complex and targets the metastasis programs in breast cancer. *Cell* **138**, 660–672
21. Højfeldt, J. W., Agger, K., and Helin, K. (2013) Histone lysine demethylases as targets for anticancer therapy. *Nat. Rev. Drug Discov.* **12**, 917–930
22. Ntziachristos, P., Tsirigos, A., Welstead, G. G., Trimarchi, T., Bakogianni, S., Xu, L., Loizou, E., Holmfeldt, L., Strikoudis, A., King, B., Mullenders, J., Becksfort, J., Nedjic, J., Paietta, E., Tallman, M. S., Rowe, J. M., Tonon, G., Satoh, T., Kruidenier, L., Prinjha, R., Akira, S., Van Vlierberghe, P., Ferrando, A. A., Jaenisch, R., Mullighan, C. G., and Aifantis, I. (2014) Contrasting roles of histone 3 lysine 27 demethylases in acute lymphoblastic leukaemia. *Nature* **514**, 513–517
23. Benyoucef, A., Palii, C. G., Wang, C., Porter, C. J., Chu, A., Dai, F., Tremblay, V., Rakopoulos, P., Singh, K., Huang, S., Pflumio, F., Hébert, J., Couture, J. F., Perkins, T. J., Ge, K., Dilworth, F. J., and Brand, M. (2016) UTX inhibition as selective epigenetic therapy against TAL1-driven T-cell acute lymphoblastic leukemia. *Genes Dev.* **30**, 508–521
24. Boila, L. D., Chatterjee, S. S., Banerjee, D., and Sengupta, A. (2017) KDM6 and KDM4 histone lysine demethylases emerge as molecular therapeutic targets in human acute myeloid leukemia. *Exp. Hematol.*
25. Rath, B. H., Waung, I., Camphausen, K., and Tofilon, P. J. (2018) Inhibition of the histone H3K27 demethylase UTX enhances tumor cell radiosensitivity. *Mol. Cancer Ther.* **17**, 1070–1078
26. Gozdecka, M., Meduri, E., Mazan, M., Tzelepis, K., Dudek, M., Knights, A. J., Pardo, M., Yu, L., Choudhary, J. S., Metzakopian, E., Iyer, V., Yun, H., Park, N., Varela, I., Bautista, R., Collord, G., Dovey, O., Garyfallos, D. A., De Braekeleer, E., Kondo, S., Cooper, J., Göttgens, B., Bullinger, L., Northcott, P. A., Adams, D., Vassiliou, G. S., and Huntly, B. J. P. (2018) UTX-mediated enhancer and chromatin remodeling suppresses myeloid leukemogenesis through noncatalytic inverse regulation of ETS and GATA programs. *Nat. Genet.* **50**, 883–894
27. Ezponda, T., Dupéré-Richer, D., Will, C. M., Small, E. C., Varghese, N., Patel, T., Nabet, B., Popovic, R., Oyer, J., Bulic, M., Zheng, Y., Huang, X., Shah, M. Y., Maji, S., Riva, A., Occhionorelli, M., Tonon, G., Kelleher, N., Keats, J., and Licht, J. D. (2017) UTX/KDM6A loss enhances the malignant phenotype of multiple myeloma and sensitizes cells to EZH2 inhibition. *Cell Rep.* **21**, 628–640
28. Greif, P. A., Hartmann, L., Vosberg, S., Stief, S. M., Mattes, R., Hellmann, I., Metzeler, K. H., Herold, T., Bamopoulos, S. A., Kerbs, P., Jurinovic, V., Schumacher, D., Pastore, F., Bräundl, K., Zellmeier, E., Ksienzyk, B., Konstandin, N. P., Schneider, S., Graf, A., Krebs, S., Blum, H., Neumann, M., Baldus, C. D., Bohlander, S. K., Wolf, S., Görlich, D., Berdel, W. E., Wörmann, B. J., Hiddemann, W., and Spiekermann, K. (2018) Evolution of cytogenetically normal acute myeloid leukemia during therapy and relapse: an exome sequencing study of 50 patients. *Clin. Cancer Res.* **24**, 1716–1726
29. Thieme, S., Gyárfás, T., Richter, C., Özhan, G., Fu, J., Alexopoulou, D., Muders, M. H., Michalk, I., Jakob, C., Dahl, A., Klink, B., Bandola, J., Bachmann, M., Schröck, E., Buchholz, F., Stewart, A. F., Weidinger, G., Anastassiadis, K., and Brenner, S. (2013) The histone demethylase UTX regulates stem cell migration and hematopoiesis. *Blood* **121**, 2462–2473
30. Wei, Y., Chen, R., Dimicoli, S., Bueso-Ramos, C., Neuberg, D., Pierce, S., Wang, H., Yang, H., Jia, Y., Zheng, H., Fang, Z., Nguyen, M., Ganan-Gomez, I., Ebert, B., Levine, R., Kantarjian, H., and Garcia-Manero, G. (2013) Global H3K4me3 genome mapping reveals alterations of innate immunity signaling and overexpression of JMJD3 in human myelodysplastic syndrome CD34+ cells. *Leukemia* **27**, 2177–2186
31. Laurin, M., Huber, J., Pelletier, A., Houalla, T., Park, M., Fukui, Y., Haibe-Kains, B., Muller, W. J., and Côté, J. F. (2013) Rac-specific guanine nucleotide exchange factor DOCK1 is a critical regulator of HER2-mediated breast cancer metastasis. *Proc. Natl. Acad. Sci. USA* **110**, 7434–7439
32. Wei, J., Wunderlich, M., Fox, C., Alvarez, S., Cigudosa, J. C., Wilhelm, J. S., Zheng, Y., Cancelas, J. A., Gu, Y., Jansen, M., Dimartino, J. F., and Mulloy, J. C. (2008) Microenvironment determines lineage fate in a human model of MLL-AF9 leukemia. *Cancer Cell* **13**, 483–495

33. Mizukawa, B., Wei, J., Shrestha, M., Wunderlich, M., Chou, F. S., Griesinger, A., Harris, C. E., Kumar, A. R., Zheng, Y., Williams, D. A., and Mulloy, J. C. (2011) Inhibition of Rac GTPase signaling and downstream prosurvival Bcl-2 proteins as combination targeted therapy in MLL-AF9 leukemia. *Blood* **118**, 5235–5245
34. Rhyasen, G. W., Wunderlich, M., Tohyama, K., Garcia-Manero, G., Mulloy, J. C., and Starczynowski, D. T. (2014) An MDS xenograft model utilizing a patient-derived cell line. *Leukemia* **28**, 1142–1145
35. Fang, J., Liu, X., Bolanos, L., Barker, B., Rigolino, C., Cortelezzi, A., Oliva, E. N., Cuzzola, M., Grimes, H. L., Fontanillo, C., Komurov, K., MacBeth, K., and Starczynowski, D. T. (2016) A calcium- and calpain-dependent pathway determines the response to lenalidomide in myelodysplastic syndromes. *Nat. Med.* **22**, 727–734
36. Loughran, S. J., Comoglio, F., Hamey, F. K., Giustacchini, A., Errami, Y., Earp, E., Gottgens, B., Jacobsen, S. E. W., Mead, A. J., Hendrich, B., and Green, A. R. (2017) Mbd3/NuRD controls lymphoid cell fate and inhibits tumorigenesis by repressing a B cell transcriptional program. *J. Exp. Med.* **214**, 3085–3104
37. Lai, A. Y., and Wade, P. A. (2011) Cancer biology and NuRD: a multifaceted chromatin remodelling complex. *Nat. Rev. Cancer* **11**, 588–596
38. Williams, C. J., Naito, T., Arco, P. G., Seavitt, J. R., Cashman, S. M., De Souza, B., Qi, X., Keables, P., Von Andrian, U. H., and Georgopoulos, K. (2004) The chromatin remodeler Mi-2beta is required for CD4 expression and T cell development. *Immunity* **20**, 719–733
39. Miccio, A., Wang, Y., Hong, W., Gregory, G. D., Wang, H., Yu, X., Choi, J. K., Shelat, S., Tong, W., Poncz, M., and Blobel, G. A. (2010) NuRD mediates activating and repressive functions of GATA-1 and FOG-1 during blood development. *EMBO J.* **29**, 442–456
40. Zhang, Y., Ng, H. H., Erdjument-Bromage, H., Tempst, P., Bird, A., and Reinberg, D. (1999) Analysis of the NuRD subunits reveals a histone deacetylase core complex and a connection with DNA methylation. *Genes Dev.* **13**, 1924–1935
41. Reynolds, N., Salmon-Divon, M., Dvinge, H., Hynes-Allen, A., Balasooriya, G., Leaford, D., Behrens, A., Bertone, P., and Hendrich, B. (2012) NuRD-mediated deacetylation of H3K27 facilitates recruitment of polycomb repressive complex 2 to direct gene repression. *EMBO J.* **31**, 593–605
42. Dhar, S. S., Lee, S. H., Chen, K., Zhu, G., Oh, W., Allton, K., Gafni, O., Kim, Y. Z., Tomoiga, A. S., Barton, M. C., Hanna, J. H., Wang, Z., Li, W., and Lee, M. G. (2016) An essential role for UTX in resolution and activation of bivalent promoters. *Nucleic Acids Res.* **44**, 3659–3674
43. Li, Q., Zou, J., Wang, M., Ding, X., Chepelev, I., Zhou, X., Zhao, W., Wei, G., Cui, J., Zhao, K., Wang, H. Y., and Wang, R. F. (2014) Critical role of histone demethylase Jmjd3 in the regulation of CD4+ T-cell differentiation. *Nat. Commun.* **5**, 5780
44. Zha, L., Li, F., Wu, R., Artinian, L., Rehder, V., Yu, L., Liang, H., Xue, B., and Shi, H. (2015) The histone demethylase UTX promotes brown adipocyte thermogenic program via coordinated regulation of H3K27 demethylation and acetylation. *J. Biol. Chem.* **290**, 25151–25163
45. Tie, F., Banerjee, R., Conrad, P. A., Scacheri, P. C., and Harte, P. J. (2012) Histone demethylase UTX and chromatin remodeler BRM bind directly to CBP and modulate acetylation of histone H3 lysine 27. *Mol. Cell. Biol.* **32**, 2323–2334
46. Sengupta, A., Arnett, J., Dunn, S., Williams, D. A., and Cancelas, J. A. (2010) Rac2 GTPase deficiency depletes BCR-ABL+ leukemic stem cells and progenitors in vivo. *Blood* **116**, 81–84
47. Thomas, E. K., Cancelas, J. A., Chae, H. D., Cox, A. D., Keller, P. J., Perrotti, D., Neviani, P., Druker, B. J., Setchell, K. D., Zheng, Y., Harris, C. E., and Williams, D. A. (2007) Rac guanosine triphosphatases represent integrating molecular therapeutic targets for BCR-ABL-induced myeloproliferative disease. *Cancer Cell* **12**, 467–478
48. Tajiri, H., Uruno, T., Shirai, T., Takaya, D., Matsunaga, S., Setoyama, D., Watanabe, M., Kukimoto-Niino, M., Oisaki, K., Ushijima, M., Sanematsu, F., Honma, T., Terada, T., Oki, E., Shirasawa, S., Maehara, Y., Kang, D., Côté, J. F., Yokoyama, S., Kanai, M., and Fukui, Y. (2017) Targeting ras-driven cancer cell survival and invasion through selective inhibition of DOCK1. *Cell Rep.* **19**, 969–980
49. Gao, J., Aksoy, B. A., Dogrusoz, U., Dresdner, G., Gross, B., Sumer, S. O., Sun, Y., Jacobsen, A., Sinha, R., Larsson, E., Cerami, E., Sander, C., and Schultz, N. (2013) Integrative analysis of complex cancer genomics and clinical profiles using the cBioPortal. *Sci. Signal.* **6**, pl1
50. Nishikimi, A., Uruno, T., Duan, X., Cao, Q., Okamura, Y., Saitoh, T., Saito, N., Sakaoka, S., Du, Y., Suenaga, A., Kukimoto-Niino, M., Miyano, K., Gotoh, K., Okabe, T., Sanematsu, F., Tanaka, Y., Sumimoto, H., Honma, T., Yokoyama, S., Nagano, T., Kohda, D., Kanai, M., and Fukui, Y. (2012) Blockade of inflammatory responses by a small-molecule inhibitor of the Rac activator DOCK2. *Chem. Biol.* **19**, 488–497
51. Watanabe, M., Terasawa, M., Miyano, K., Yanagihara, T., Uruno, T., Sanematsu, F., Nishikimi, A., Côté, J. F., Sumimoto, H., and Fukui, Y. (2014) DOCK2 and DOCK5 act additively in neutrophils to regulate chemotaxis, superoxide production, and extracellular trap formation. *J. Immunol.* **193**, 5660–5667
52. Aguilera, C., Nakagawa, K., Sancho, R., Chakraborty, A., Hendrich, B., and Behrens, A. (2011) c-Jun N-terminal phosphorylation antagonises recruitment of the Mbd3/NuRD repressor complex. *Nature***469**, 231–235
53. Li, R., He, Q., Han, S., Zhang, M., Liu, J., Su, M., Wei, S., Wang, X., and Shen, L. (2017) MBD3 inhibits formation of liver cancer stem cells. *Oncotarget* **8**, 6067–6078
54. Xu, M., He, J., Li, J., Feng, W., Zhou, H., Wei, H., Zhou, M., Lu, Y., Zeng, J., Peng, W., Du, F., and Gong, A. (2017) Methyl-CpG-binding domain 3 inhibits epithelial-mesenchymal transition in pancreatic cancer cells via TGF-β/Smad signalling. *Br. J. Cancer* **116**, 91–99
55. Hnisz, D., Abraham, B. J., Lee, T. I., Lau, A., Saint-André, V., Sigova, A. A., Hoke, H. A., and Young, R. A. (2013) Super-enhancers in the control of cell identity and disease. *Cell* **155**, 934–947
56. Reynolds, N., O'Shaughnessy, A., and Hendrich, B. (2013) Transcriptional repressors: multifaceted regulators of gene expression. *Development* **140**, 505–512
57. Spensberger, D., Vermeulen, M., Le Guezennec, X., Beekman, R., van Hoven, A., Bindels, E., Stunnenberg, H., and Delwel, R. (2008) Myeloid transforming protein Evi1 interacts with methyl-CpG binding domain protein 3 and inhibits in vitro histone deacetylation by Mbd3/Mi-2/NuRD. *Biochemistry* **47**, 6418–6426
58. Boila, L. D., Chatterjee, S. S., Banerjee, D., and Sengupta, A. (2018) KDM6 and KDM4 histone lysine demethylases emerge as molecular therapeutic targets in human acute myeloid leukemia. *Exp. Hematol.* **58**, 44–51.e7
59. Li, Q., Shi, L., Gui, B., Yu, W., Wang, J., Zhang, D., Han, X., Yao, Z., and Shang, Y. (2011) Binding of the JmjC demethylase JARID1B to LSD1/NuRD suppresses angiogenesis and metastasis in breast cancer cells by repressing chemokine CCL14. *Cancer Res.* **71**, 6899–6908
60. Hwei, L. S., and Chou, W.-C. (2016) The clinical and biological effects of the expression of dedicator of cytokinesis 1 (DOCK1) in acute myeloid leukemia. *Blood.* **128**, 1695

Received for publication May 23, 2018.
Accepted for publication January 2, 2019.

Mutation Research 809 (2016) 50–56

Contents lists available at ScienceDirect

Mutation Research/Genetic Toxicology and Environmental Mutagenesis

journal homepage: www.elsevier.com/locate/gentox
Community address: www.elsevier.com/locate/mutres

Association of single nucleotide polymorphism with arsenic-induced skin lesions and genetic damage in exposed population of West Bengal, India

Nandana Das[a], Allan Giri[b,1], Sayan Chakraborty[a], Pritha Bhattacharjee[b,*]

[a] Molecular Genetics Division, Indian Institute of Chemical Biology, Kolkata-700032, India
[b] Department of Environmental Science, University of Calcutta, Kolkata-700019, India

ARTICLE INFO

Article history:
Received 15 June 2016
Received in revised form 1 September 2016
Accepted 7 September 2016
Available online 9 September 2016

Keywords:
Arsenic toxicity
Drinking water
Skin lesions
Single nucleotide polymorphism
Genetic damage

ABSTRACT

Long term consumption of arsenic contaminated water causes a number of dermatological and non-dermatological health problems and cancer. In a Genome Wide Association Study (GWAS) on Bangladesh population, a significant association of asingle nucleotide polymorphism (SNP) in the C10orf32 region (rs 9527; G > A) with urinary metabolites and arsenic induced skin lesions was reported. This study aims to evaluate the association of the C10orf32 G to A polymorphism (rs9527), concerned with As3MT read-through transcription, with the development of arsenic induced skin lesions in the arsenic exposed individuals of West Bengal, India. A total of 157 individuals with characteristic skin lesions (cases) and 158 individuals without any skin lesion (controls) were recruited for this study. The G > A polymorphism (rs9527) having at least one minor allele 'A' was found to be significantly higher in cases compared to controls, implying increased risk toward the development of skin lesions. The risk genotype was also found to be significantly associated with cytogenetic damage as measured by chromosomal aberrations and micronuclei formation in lymphocytes. Hence, it can be concluded that G > A change in the C10orf32 region plays an important role in arsenic induced toxicity and susceptibility.

1. Introduction

Arsenic contamination in ground water became a global concern as 70 countries across 5 continents, with around 150 million people are suffering from arsenic toxicity [1,2]. Among them, about 50 million individuals are from India and Bangladesh alone. West Bengal is regarded as one of the most severely affected states in India, where over 26 million individuals are exposed to arsenic primarily through drinking water, above the permissible limit of 10 μg/ml recommended by both WHO and USEPA [3–5]. Chronic exposure to arsenic causes several patho-physiological disorders that include pigmentation changes, pre-malignant as well as malignant dermatological lesions and cancers of skin along with other internal organs [6].

The metabolism of arsenic is mediated by methylation and the intermediate metabolites (like MMA^{III} or trivalent monomethylarsonic acid) are found to be even more toxic compared to the inorganic parent compounds (arsenite or As^{III} and arsenate or As^{V}). The formation of metabolites is enzymatically catalyzed and generates reactive oxygen species (ROS) which imparts genomic instability, either by inducing DNA damage, inhibiting repair enzymes, mitotic dysregulation or other mechanisms as described in detail elsewhere [7]. Chromosomal instability (CIN) is well known biomarker for assessing genotoxicity. It is noteworthy to mention here that the toxic insult by arsenic, even at a similar extent, do not induce similar cellular alteration and disease manifestation. It is observed from our study that, although a large number of individuals are exposed to arsenic through contaminated drinking water, only 15–20% show evidence of arsenic-induced skin lesions; which might be due to inter-individual genetic variations [8]. Studies from India [9] and Bangladesh [10,11] have investigated SNPs in the arsenic metabolizing enzymeAs3MT (arsenite methyltransferase), which is the key enzyme of the arsenic biotransformation pathway, and explored its association with arsenic-induced skin lesion.

However, the most interesting study reported so far, is to observe the genome wide association study in Bangladesh population that revealed significant association of 10q24.32 chromosomal

* Corresponding author at: Department of Environmental Science, University of Calcutta 35, Ballygunge Circular Road Kolkata–700019, India.
E-mail address: 777.pritha@gmail.com (P. Bhattacharjee).
[1] Present address: Queens College, 65-30 Kissena Blvd, Flushing, NY 11367, United States of America.

http://dx.doi.org/10.1016/j.mrgentox.2016.09.006
1383-5718/

region (containing five SNPs) with urinary arsenic metabolites [12]. The variants fall in the transcription read through of *As3MT* gene, 10q24.32, and one of the five reported variants (rs9527) was also found to be associated with arsenic induced skin lesions, hallmarks of arsenicosis. The SNP within C10orf 32 (rs9527; G > A polymorphism) was associated with both urinary arsenic metabolites and *As3MT* expression in the Bangladeshi population [12]. rs9527 is positioned within reading frames coding the C10orf32 transcripts which includes the naturally occurring C10orf32-As3MT read through transcript. Very few information regarding the C10orf32 transcripts, both in regulatory and functional level, are available in the databases and the mechanism by which they may affect the expression of *As3MT* gene is not known. Moreover, till date there is no report of an association of this SNP (rs9527; G > A polymorphism) of C10orf32 region with arsenic toxicity in population other than Bangladesh. So here we have studied the association of this SNP (rs9527; G > A polymorphism) of C10orf32 with arsenic induced skin lesions and genetic damage as measured by chromosomal aberrations (CA) and micronuclei formation (MN) in our Indian population exposed to arsenic through drinking water.

2. Materials and methods

2.1. Study sites and subject selection

North 24 Parganas, Nadia and Murshidabad are most critically affected. Accordingly, the arsenic exposed study subjects were selected from different villages within these three districts, including 5 villages of Murshidabad district (across 5 different blocks), four villages of North 24 Parganas (encompassing four administrative blocks), and two villages from Nadia (Haringhata block) (Fig. 1). Urine arsenic content of participants was measured as it is known to be one of the best indicators to assess recent arsenic exposure [13]. Trained volunteers went to the villages and identified individuals with skin lesions, requested them to attend the medical camp and to participate in the study. Thorough information about age, gender, tobacco usage (both smoking and chewing), food habits, occupation, source of drinking water along with volume of intake, and medical history were acquired through a structured questionnaire. All samples were collected after having informed consent of the study participants. Included study participants were confirmed to have at least 10 years of arsenic exposure through drinking water. Detailed procedures of field survey, sample collection, and strategies for selection of genetically unrelated case-controls are described in our previous studies [9]. Dermatologists examined and detected various types of arsenic-related skin lesions among the study participants. According to WHO, arsenic induced skin lesions are regarded as hallmark symptoms of As-toxicity and exposed individuals were categorized on the basis of this criteria (individuals having skin lesions or without skin lesions). The present study included a total of 315 arsenic-exposed individuals, of which 157 individuals had characteristic arsenic-induced skin lesions (cases) and 158 individuals were devoid of any such lesions (controls). Both cases and controls included genetically unrelated individuals with similar level of arsenic exposure through drinking water. Study protocols were approved by the Institutional Review Board and abide by the policy of the Declaration of Helsinki II.

2.2. Arsenic exposure assessment

Arsenic exposure and the overall load of arsenic in the body were assessed by the estimation of total arsenic content in drinking water from tube wells and urine samples from exposed individuals respectively. Each study participant was provided with acid-washed [nitric acid:water (1:1)] plastic bottles (100 ml) for the collection of drinking water samples and nitric acid (1.0 ml/l) was added as preservative. Approximately100 ml first morning voids were collected in pre-coded polypropylene bottles. The total arsenic content in the samples was estimation by the previously described procedure [14,15]. A flow injection hydride generation–atomic absorption spectrometry (FI-HG-AAS) was used for the estimation of arsenic concentration in drinking water and urine samples in combination with Model Analyst-700 spectrometer equipped with a Hewlett-Packard Vectra computer with GEM software (Hewlett-Packard, Houston, TX, USA), and arsenic lamp (lamp current 380 mA).

2.3. C10orf32 SNP (rs9527) genotyping

About 6 ml venous blood was drawn from each individual. DNA extraction from blood (about 4.5 ml) was carried out following standard protocol [16]. PCR amplifications were performed in a 25 μl reaction volume using standard PCR buffer, MgCl2 (1.5 mM), deoxyribonucleotides (200 μM) and Taq polymerase from Takara (Otsu, Shiga, Japan). The sequences of flanking primers were designed in the laboratory by the PRIMER 3 software (Sense: 5′-ACCTCTGCCACAATCACTCA-3′; Antisense: 5′-AGAAGAAGCGAGGTGGTTGA-3′). PCR amplification was performed in Eppendorf Mastercycler (Hamburg, Germany) as follows: a pre-PCR step of 5 min denaturation at 94 °C, followed by 30 cycles of 30 s denaturation at 94 °C, 30 s annealing at 58 °C(Tm), 30 s extension at 72 °C, and finally 5 min incubation at 72 °C. PCR products were analyzed by polyacrylamidegel (8%) electrophoresis and by bi-directional DNA sequencing in an ABI prism 3100 DNA sequencer (Applied Biosystems) as previously described [17].

2.4. Chromosomal aberrations (CA) assay and detection of micronucleus (MN) formation

For lymphocyte culture, whole blood (0.7 ml) was added to 7 ml of RPMI-1640 supplemented with L-glutamine, 15% FCS (fetal calf serum), penicillin (100 IU/ml), streptomycin (100 mg/ml) and 2% PHA-M form, following the standard protocol as previously described [17]. The cultures were incubated at 37 °C and harvested at 72 h (as arsenic is known to induce cell cycle delay, hence it is customary to carry out these cultures for 72 h instead of the routine 48 h to get a sufficient population of first and second division cells for scoring aberrations) [15,18]. Upon harvesting, slide was prepared from each culture and duly coded. On availability of good scoring metaphases, 50–100 metaphases from each slide were randomly scored for both chromatid type and chromosome type of aberrations [19]. Gaps were not included as aberrations. Results were expressed as CA per cell and also as percentage of aberrant cells.

Lymphocyte cultures for micronuclei analysis were carried out following the standard protocol of Fenech [20] and Migliore et al. [21]. Whole blood cultures were incubated for 44 h at 37 °C. Then Cytochalasin B (a cytokinesis blocker) was added to each culture to give a final concentration of 6 μg/ml and the culture was incubated at 37 °C for an additional 28 h to induce binucleated cell formation. After a total of 72 h incubation, cells were harvested following previously described protocol [22]. Slides were prepared from each culture, duly coded and stained with 5% Giemsa in phosphate buffer (pH 6.8). Approximately 2000 binucleated cells from each subject were examined for micronuclei under the microscope.

All slides were first examined with low-power (20×) magnification using a Nikon Eclipse 80*i* microscope to discard those infected with bacteria, fungi, and polymorphonuclear leukocytes and then scored at 100× oil immersion lens. Only those micronuclei were noted which were (a) rounded or oval shaped; (b) less than one-third the diameter of the main nucleus; (c) in the same focal plane

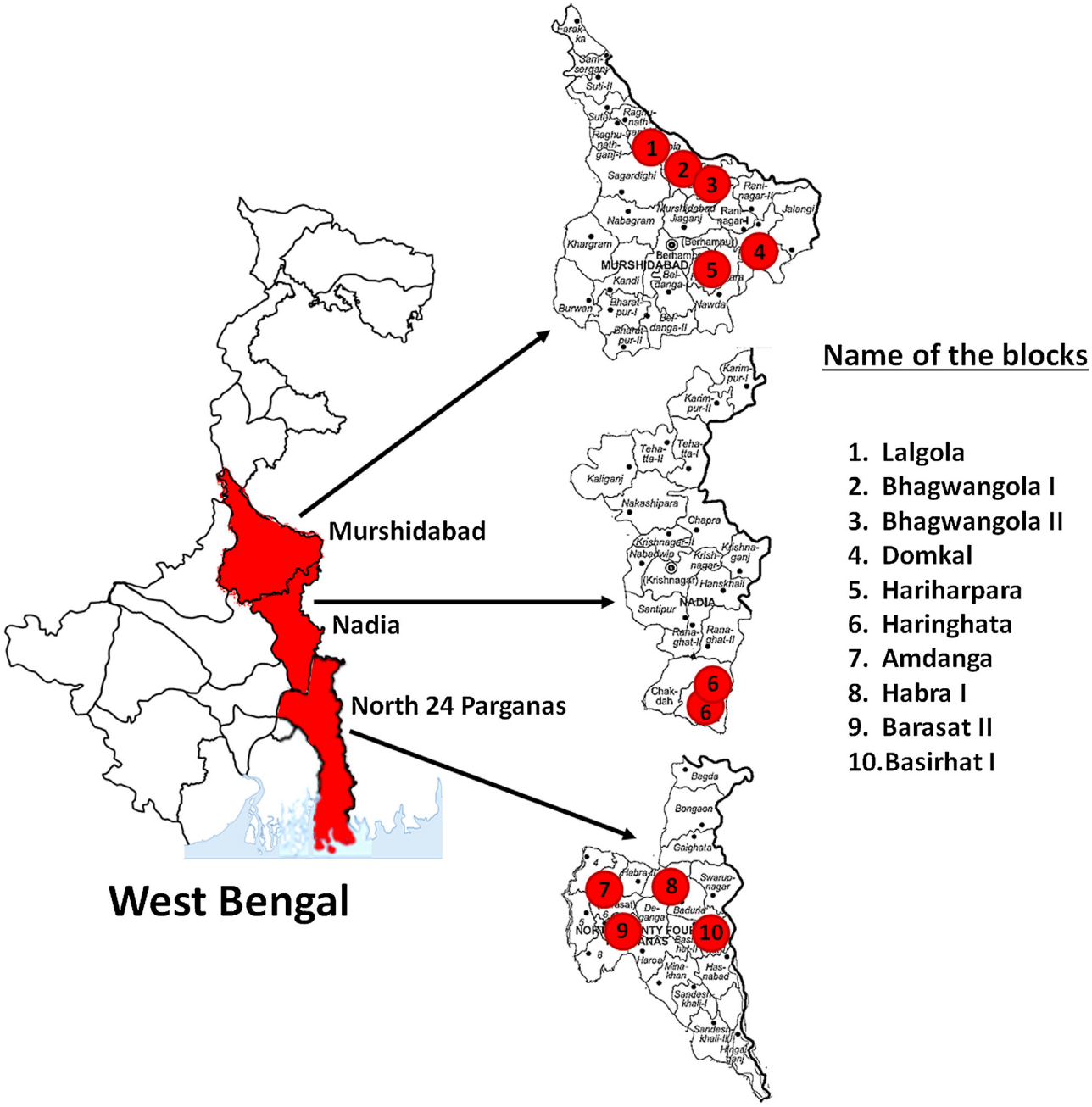

Fig. 1. Arsenic exposed study area and sampling sites in West Bengal.

as the nucleus; (d) of the same color, texture, and refraction as the main nucleus; and (e) clearly separated from the main nucleus. Two trained research fellows cross-checked all micronuclei scores to obviate the risk of bias. The values so obtained were averaged [23].

2.5. Statistical analysis

Mann–Whitney test was performed to compare the central tendencies of continuous independent variables (like age, arsenic content in water, urine) between cases and controls, as data for these parameters does not follow normal distribution. Chi-square test was used to compare the distribution of gender and tobacco usage between the two groups. Mean and standard deviation were calculated for chromosomal aberration (measured in percentage of aberrant cells, and CA/cell). The risk of the variant genotype towards the development of skin lesions was calculated as the odds ratio (OR) with a 95% confidence interval (CI) and the two-tailed p value was assessed. All statistical analyses were performed using GraphPad InStat Software (GraphPad Software Inc., San Diego, CA).

3. Results

3.1. Demographic features of the study population

Detailed characteristics of the total arsenic exposed study population are summarized in Table 1, which shows the age, gender and socio-demographic characteristics of the study participants included in case (N = 157) and control groups (N = 158). Occupationally, majority of the male individuals were farmers and females were housewives. It was observed that both the case and control groups are well matched in all concerned parameters.

Table 1
Demographic characteristics of the arsenic-exposed study population.

Parameters	Arsenic-exposed no skin lesion group (Control)	Arsenic-exposed skin lesion group (Case)
Total Subjects (N)	158	157
Gender [N (%)]		
Male	73 (46.20)	88 (56.05)
Female	85 (52.80)	69 (43.95)
Age (in years, Mean ± SD)	37.54 ± 11.95	39.62 ± 13.11
Occupation [N (%)]		
Farmer	51 (32.28)	74 (47.13)
Daily wage earner	13 (8.23)	10 (6.37)
Business	9 (5.70)	11 (7.01)
Teacher	2 (1.27)	3 (1.91)
Student	20 (12.66)	16 (10.19)
Service	1(0.63)	3 (1.91)
Housewife	55 (34.81)	36 (22.93)
Unemployed	3 (1.90)	1 (0.64)
Retired	4 (2.53)	3 (1.91)
Tobacco Consumption [N (%)]		
Tobacco user	42 (26.58)	45 (28.66)
Tobacco non-user	116 (73.42)	112 (71.34)

3.2. Arsenic content in drinking water and urine samples of the study groups

Both the cases and controls have similar levels of arsenic exposure, as evident by the arsenic content in their drinking water (Table 2). The cumulative water and food intake for the study participants were found to be similar in cases and controls. However, the arsenic concentration in urine of the control group was observed to be higher (although not statistically significant) compared to the cases. Higher prevalence of skin lesions despite similar exposure level might be due to the higher susceptibility towards arsenic toxicity in individuals with skin lesions (Table 2).

3.3. G > A polymorphism within C10orf32 (rs9527) is associated with increased incidence of arsenic induced skin lesions

The G > A polymorphism in C10orf32 (rs9527) was recorded in all 315 samples (cases and controls) and it was observed that this SNP has a statistically significant association with arsenic induced skin lesions. The genotype distribution of major and minor alleles for this particular variant (rs9527) in the control and case groups is shown in Table 3. We have found a total of 253 individuals with GG genotype, of which 55.73% are control and 44.27% are cases. Thus we found individuals with at least one minor allele (genotype GA and AA); in which 27.42% were control and 72.58% were cases. The distribution of the minor allele A (in the form of G/A + A/A) was found to be significantly higher in cases, thus having an association with the increased risk toward the development of skin lesions [OR = 3.332, 95% CI: 1.81–6.14; p-value < 0.0001]. As no additional risk was offered by A/A genotype over the G/A genotype, the genotypes for the variant allele were combined (G/A + A/A taken together), and subsequently the effect of this combined genotype on arsenic induced cytogenetic damage was evaluated with GG as the reference genotype (Fig. 2).

3.4. rs9527 variant allele is associated with higher level of chromosomal aberrations (CA) and micronucleus (MN) formation

To explore whether this SNP has any association with cytogenetic damage induced by arsenic, we categorized the extent of chromosomal aberrations (CA) and micronucleus (MN) formation according to the genotype. The distribution of CA in individuals having variant rs9527genotype is shown in Table 4. A statistically significant increase in CA, considering both CA/cell (p-value = 0.0038) and% aberrant cells (p-value = 0.0019) was observed in individuals having at least one of the variant allele (G/A andA/A genotypes taken together) compared to those having G/G genotype within our exposed study population. It was also observed that individuals with G/A and A/A had significantly higher number of micronuclei formation in their lymphocytes (p-value = 0.0214) (Fig. 2).

4. Discussion

Differential arsenic metabolism and retention in the body are one of the key factors behind the difference in susceptibility to arsenic toxicity, and a number of studies, either in vitro or in vivo, highlight the importance of As3MT enzyme in conversion of the inorganic arsenic metabolites to their corresponding methylated products [24,25]. Therefore, it can be expected that altered expression or activities of As3MT may well be a decisive factor behind arsenic susceptibility. However, previous studies have not found any association of Met287Thr (only exonic SNP within the gene) with arsenic-induced skin lesions, when compared to arsenic-exposed no skin lesion individuals in the population of West Bengal [9] and Met287Thr polymorphism had marginal association with skin lesion (p = 0.055) in an arsenic exposed Mexican population compared to individuals without skin lesions [26]. In vitro studies established the link between Met287Thr SNP with high As3MT activity and increased production of methylated arsenicals (MAs) [27,28]. Other epidemiological studies on a Chilean group and a European population showed that individuals having the C allele (Thr287) excrete higher percentage of urinary MAs [29,30]. In addition to this, the Genome Wide Association study on a Bangladeshi population[11]has identified variants in a region of chromosome 10q24.32 that has significant association with urine arsenic metabolites (DMA or dimethylarsinic acid and MMA or monomethylarsonic acid). However, this extensive GWAS study did not find any association between a SNP within the *AS3MT* gene and skin lesions or urinary arsenic metabolites, confirming the observations from other studies [9]. Rather according to the GWAS study, all SNPs that have significant associations with urine arsenicals are positioned within a certain stretch of Chromosome 10 which is nearby to the *AS3MT* gene. One of the SNPs, the G > A change (rs9725), also showed significant association with arsenic induced skin lesions. Moreover, the G > A polymorphism was also found to be associated with the reduced expression of the *AS3MT* gene [12]. Hence polymorphism in the C10orf32-AS3MT read through transcript can be assumed to influence AS3MT enzyme production in a hitherto unknown mechanism. In this study, we have assessed the association C10orf32 SNP (rs9527) with arsenic induced skin lesions within the population of West Bengal, which showed almost

Table 2
Arsenic content in drinking water and urine samples of the study groups.

Parameters	Exposed without skin lesions	Exposed with skin lesions
Drinking Water (μg/L)	196.74 ± 151.54	200.3 ± 132.05
Urine (μg/L)	294.79 ± 224.07	245.94 ± 149.34

Table 3
Association of C10orf32 SNP (rs9527) with arsenic-induced skin lesions.

Genotype	Exposed individuals without skin lesions	Exposed individuals with skin lesions	Odd's ratio [95% CI]	p-Value
GG[N (%)]	141(55.73)	112(44.27)	3.332 [1.81–6.14]	<0.0001[a]
GA + AA[N(%)]	17(27.42)	45(72.58)		

[a] Fisher's exact *t*-test; CI, confidence interval.

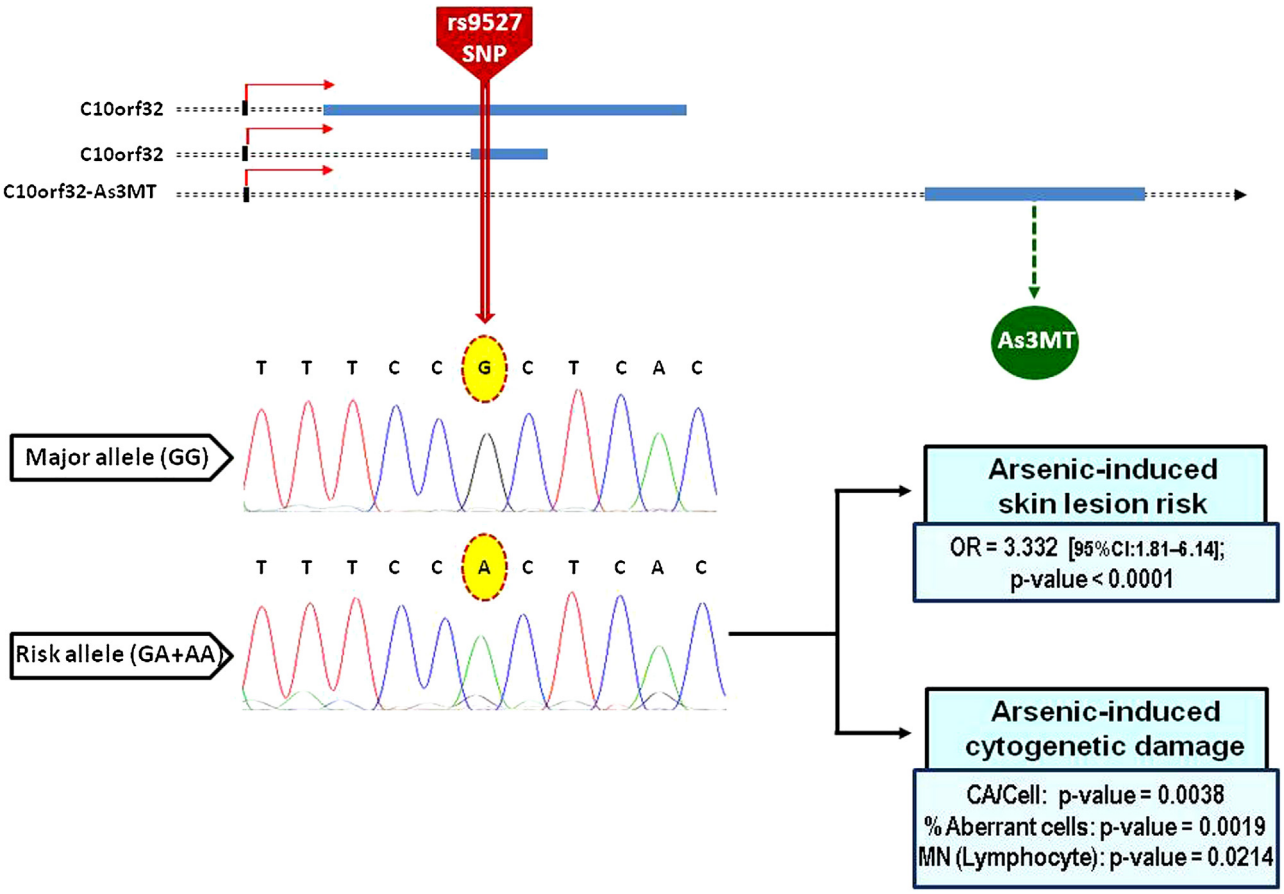

Fig. 2. Association of C10orf32 SNP (rs9527) with arsenic-induced skin lesion risk and increased cytogenetic damage [position of rs9527 is conceptualized from UCSC Genome Browser(https://genome.ucsc.edu/cgi-bin/hgTracks?db=hg38&lastVirtModeType=default&lastVirtModeExtraState=&virtModeType=default&virtMode=0&nonVirtPosition=&position=chr10%3A102863571-102864071&hgsid=505136677_L6zi0pHPJHlwD3BdhPqrp0GO5rIt)].

Table 4
Association of C10orf32 SNP (rs9527) and chromosomal aberration.

Parameters	G/G genotype (N = 177)	A/A + G/A genotype (N = 52)	p-Value
CA/cell (mean ± S.D.)	0.08 ± 0.03	0.09 ± 0.02	0.0038[a]
% Aberrant cells (mean ± S.D.)	7.57 ± 2.51	8.7 ± 2.4	0.0019[a]
MN (Lymphocyte) (mean ± S.D.)	8.07 ± 2.67	9.16 ± 2.41	0.0214[a]

[a] Mann-Whitney *U* test.

three times higher risk toward development of these skin lesions, further confirming the potential of rs9527 variant as a predictive biomarker for arsenicosis.

It is important to mention here that although several studies have shown that urinary metabolites are strong indicator of primary/secondary methylation index and associated risk of cancer [31–33], it is difficult to perform speciation for biomonitoring purpose where a large population is exposed. A more simpler and efficient way to measure the magnitude of arsenic induced toxicity is to assess the level of genetic damage. Arsenic and its metabo-

lites induce ROS and cause DNA damage. The genotoxic potential of arsenic is well examined by the elevated frequency of chromosomal aberration and/or micronuclei frequency [7]. Structural chromosomal aberrations (CA) includes ring formation, chromatid exchanges, end-to-end fusion, translocation, chromatid break and deletions, acentric fragment formation etc. and previous studies have reported an increase in all these aberrations within arsenic exposed populations [15,34–36]. Alternatively, formation of micronuclei (MN), which are nuclear fragments formed around the nucleus due to errors in chromosome segregation during mitosis, is an important marker to observe genetic damage at the nuclear level rather than individual chromosomes. Various studies have associated MN formation in lymphocytes, oral and urothelial cells with arsenic toxicity [37–39]. Among all cell types, MN in lymphocyte is observed to be a more efficient marker for the assessment of arsenic induced cytogenetic damage [22,39]. Attempt has also been made to find out the association, if any with the risk allele individuals with their cytogenetic damage as measured by both CA and MN in lymphocytes. We found that individuals with the risk allele (AA/GA) of C10orf32 SNP have significantly higher chromosomal aberrations, both in terms of CA/cell and% of aberrant cells, and increased MN formation in lymphocytes compared to the wild type variant. Thus, the above findings establish the genotype-phenotype correlation and explain the higher susceptibility for individuals with AA/GA genotype. Arsenic induced skin lesions are considered as hallmarks of arsenic toxicity, although it has been reported earlier that about 75% individuals do not show any arsenic-induced skin lesion despite of arsenic exposure at a similar extent. Therefore, the applicability of this research finding is significant, as C10orf32 SNP rs9527 variant can be a predictive biomarker for arsenicosis. The present study indicates that the development of arsenic-induced skin lesions and increased arsenic-induced genetic damage are associated with C10orf32 SNP rs9527 variation, providing us with an indirect measure to assess individual susceptibility to arsenic toxicity.

5. Conclusion

The presence of the C10orf32 SNP (rs9527) variant imparts a risk toward the development of arsenic induced skin lesions and increased cytogenetic damage in the arsenic exposed population of West Bengal. Hence it can be concluded that the C10orf32-G to A polymorphism (rs9527) may have a role in arsenic susceptibility of individuals having chronic arsenic exposure. As the presence of this SNP variant was identified by a GWAS study conducted on a Bangladeshi population of over 1000 individuals and then validated on a population of 315 from West Bengal, both having the highest level of arsenic exposure as per global report, this SNP could be used as a prospective biomarker for assessment of arsenic susceptibility.

Conflicts of interest

None declared.

Acknowledgements

Authors are thankful to the Council of Scientific and Industrial Research (CSIR), Government of India for providing Senior Research Fellowship to ND and Department of Science & Technology (DST), Government of India, for research funding to PI (Project: 2620/2013).

References

[1] British Geological Survey. DWI. 2013. Drinking Water 2012, Private water supplies in England. A report by the Chief Inspector of Drinking Water, July 2013. http://www.bgs.ac.uk/sciencefacilities/laboratories/geochemistry/igf/biomonitoring/arsenicSW.html.
[2] S. Shankar, U. Shanker, U. Shikha, Arsenic contamination of groundwater: a review of sources, prevalence, health risks, and strategies for mitigation, Scientific World J. 2014 (2014) 304524, http://dx.doi.org/10.1155/2014/304524.
[3] WHO, Guidelines for Drinking Water Quality, Health Criteria and Other Supporting Information, 2nd ed., WHO, Geneva, 1996, pp. 940–994 http://www.who.int/water_sanitation_health/dwq/arsenicun5.pdf.
[4] USEPA, Chemical Contaminant Rules, 2000 https://www.epa.gov/dwreginfo/chemical-contaminant-rules.
[5] S. Paul, N. Das, P. Bhattacharjee, M. Banerjee, J.K. Das, N. Sarma, A. Sarkar, A.K. Bandyopadhyay, T.J. Sau, S. Basu, S. Banerjee, P. Majumder, A.K. Giri, Arsenic-induced toxicity and carcinogenicity: a two-wave cress-sectional study in arsenicosis individuals in West Bengal, India, J. Expo. Sci. Environ. Epidemiol. 23 (2013) 156–162.
[6] M. Banerjee, P. Bhattacharjee, A.K. Giri, Arsenic-induced cancers: a review with special reference to gene, environment and their interaction, Genes Environ. 33 (2011) 128–140.
[7] P. Bhattacharjee, M. Banerjee, A.K. Giri, Role of genomic instability in arsenic-induced carcinogenicity: a review, Environ. Int. 53 (2013) 29–40.
[8] A. Hernández, R. Marcos, Genetic variations associated with interindividual sensitivity in the response to arsenic exposure, Pharmacogenomics 8 (2008) 1113–1132.
[9] S. De Chaudhuri, P. Ghosh, N. Sarma, P. Majumdar, T.J. Sau, S. Basu, S. Roychoudhury, K. Ray, A.K. Giri, Genetic variants associated with arsenic susceptibility: study of purine nucleoside phosphorylase,arsenic (+3) methyltransferase, and glutathione S-transferase omega genes, Environ. Health Perspect. 116 (2008) 501–505.
[10] K. Engström, M. Vahter, S.J. Mlakar, G. Concha, B. Nermell, R. Raqib, Polymorphisms in arsenic(+III oxidation state) methyltransferase (AS3MT) predict gene expression of AS3MT as well as arsenic metabolism, Environ. Health Perspect. 119 (2011) 182–188.
[11] B.L. Pierce, L. Tong, M. Argos, J. Gao, J. Farzana, S. Roy, Arsenic metabolism efficiency has a causal role in arsenic toxicity: mendelian randomization and gene-environment interaction, Int. J. Epidemiol. 42 (2013) 1862–1871.
[12] B.L. Pierce, M.G. Kibriya, L. Tong, F. Jasmine, M. Argos, S. Roy, R. Paul-Brutus, R. Rahaman, M. Rakibuz-Zaman, F. Parvez, A. Ahmed, I. Quasem, S.K. Hore, S. Alam, T. Islam, V. Slavkovich, M.V. Gamble, M. Yunus, M. Rahman, J.A. Baron, J.H. Graziano, H. Ahsan, Genome-wide association study identifies chromosome 10q24.32 variants associated with arsenic metabolism and toxicity phenotypes in Bangladesh, PLoS Genet. 8 (2012) e1002522, http://dx.doi.org/10.1371/journal.pgen.1002522.
[13] Agency for Toxic Substances and Disease Registry. Toxic Substances Portal – Arsenic. 1999. http://www.atsdr.cdc.gov/toxprofiles/TP.asp?id=22&tid=3.
[14] P. Ghosh, M. Banerjee, S. De Chaudhuri, R. Chowdhury, J.K. Das, A. Mukherjee, A.K. Sarkar, L. Mondal, K. Baidya, T.J. Sau, A. Banerjee, A. Basu, K. Chaudhuri, K. Ray, A.K. Giri, Comparison of health effects between individuals with and without skin lesions in the population exposed to arsenic through drinking water in West Bengal, India, J. Expo. Sci. Environ. Epidemiol. 17 (2007) 215–223.
[15] M. Banerjee, J. Sarkar, J.K. Das, A. Mukherjee, A.K. Sarkar, L. Mondal, A.K. Giri, Polymorphism in the ERCC2 codon 751 is associated with arsenic-induced premalignant hyperkeratosis and significant chromosome aberrations, Carcinogenesis 28 (2007) 672–676.
[16] J. Sambrook, E.F. Fritsch, T. Maniatis, Molecular Cloning A Laboratory Manual, 2nd ed., Cold Spring Harbor Laboratory Press Cold Spring Harbor, NY, 1989.
[17] S. De Chaudhuri, M. Kundu, M. Banerjee, J.K. Das, P. Majumdar, S. Basu, et al., Arsenic-induced health effects and genetic damage in keratotic individuals: involvement of p53 arginine variant and chromosomal aberrations in arsenic susceptibility, Mutat. Res. 659 (2008) 118–125.
[18] R.E. Rasmussen, D.B. Menzel, Variation in arsenic-induced sister chromatid exchange in human lymphocytes and lymphoblastoid cell lines, Mutat. Res. 386 (1997) 299–306.
[19] P. Ghosh, M. Banerjee, S. De Chaudhuri, J.K. Das, N. Sarma, A. Basu, A.K. Giri, Increased chromosome aberration frequencies in the Bowen's patients compared to non-cancerous skin lesions individuals exposed to arsenic, Mutat. Res. 632 (2007) 104–110.
[20] M. Fenech, Important variables that influence base-line micronucleus frequency in cytokinesis-blocked lymphocytes-a biomarker for DNA damage in human populations, Mutat. Res. 404 (1998) 155–165.
[21] L. Migliore, M. Nieri, S. Amodio, N. Loprieno, The human lymphocyte micronucleus assay: a comparison between whole-blood and separated-lymphocyte cultures, Mutat. Res. 227 (1989) 167–172.
[22] A. Basu, P. Ghosh, J.K. Das, A. Banerjee, K. Ray, A.K. Giri, Micronuclei as biomarkers of carcinogen exposure in populations exposed to arsenic through drinking water in West Bengal, India: a comparative study in three cell types, Cancer. Epidemiol. Biomarkers. Prev. 13 (2004) 820–827.
[23] A. Martelli, L. Robbiano, M. Cosso, C. Perrone, A. Tagliazucchi, L. Giuliano, G.F. Aresca, G. Brambilla, Comparison of micronuclei frequencies in mono- bi- and poly-nucleated lymphocytes from subjects of a residential suburb and subjects living near a metallurgical plant, Mutat. Res. 470 (2000) 211–219.
[24] Z. Drobná, S.B. Waters, V. Devesa, A.W. Harmon, D.J. Thomas, M. Stýblo, Metabolism and toxicity of arsenic in human urothelial cells expressing rat arsenic (+3 oxidation state)-methyltransferase, Toxicol. Appl. Pharmacol. 207 (2005) 147–159.

[25] D.J. Thomas, J. Li, S.B. Waters, W. Xing, B.M. Adair, Z. Drobna, V. Devesa, M. Styblo, Arsenic (+3 oxidation state) methyltransferase and the methylation of arsenical, Exp. Biol. Med. (Maywood) 232 (2007) 3–13.
[26] O.L. Valenzuela, Z. Drobná, E. Hernández-Castellanos, L.C. Sánchez-Peña, G.G. García-Vargas, V.H. Borja-Aburto, M. Styblo, L.M. Del Razo, Association of AS3MT polymorphisms and the risk of premalignant arsenic skin lesions, Toxicol. Appl. Pharmacol. 239 (2) (2009) 200–207.
[27] Z. Drobna, W. Xing, D.J. Thomas, M. Stýblo, shRNA silencing of AS3MT expression minimizes arsenic methylation capacity of HepG2 cells, Chem. Res.Toxicol. 19 (2006) 894–898.
[28] T.C. Wood, O.E. Salavagionne, B. Mukherjee, L. Wang, A.F. Klumpp, B.A. Thomae, B.W. Eckloff, D.J. Schaid, E.D. Wieben, R.M. Weinshilboum, Human arsenic methyltransferase (AS3MT) pharmacogenetics: gene resequencing and functional genomics studies, J. Biol. Chem. 281 (2006) 7364–7373.
[29] A. Hernández, N. Xamena, J. Surrallés, C. Sekaran, H. Tokunaga, D. Quinteros, A. Creus, R. Marcos, Role of the Met(287)Thr polymorphism in the AS3MT gene on the metabolic arsenic profile, Mutat. Res. 637 (2008) 80–92.
[30] A.L. Lindberg, R. Kumar, W. Goessler, R. Thirumaran, E. Gurzau, K. Koppova, P. Rudnai, G. Leonardi, T. Fletcher, M. Vahter, Metabolism of low-dose inorganic arsenic in a central European population: influence of sex and genetic polymorphisms, Environ. Health Perspect. 115 (2007) 1081–1086.
[31] A.L. Lindberg, M. Rahman, L.A. Persson, M. Vahter, The risk of arsenic induced skin lesions in Bangladeshi men and women is affected by arsenicmetabolism and the age at first exposure, Toxicol. Appl. Pharmacol. 230 (2008) 9–16.
[32] M.L. Kile, E. Hoffman, E.G. Rodrigues, C.V. Breton, Q. Quamruzzaman, M. Rahman, G. Mahiuddin, Y.M. Hsueh, D.C. Christiani, A pathway-based analysis of urinary arsenic metabolites and skin lesions, Am. J. Epidemiol. 7 (2011) 778–786.
[33] Y. Chen, F. Parvez, M. Gamble, T. Islam, A. Ahmed, M. Argos, J.H. Graziano, H. Ahsan, Arsenic exposure at low-to-moderate levels and skin lesions, arsenic metabolism neurological functions, and biomarkers for respiratory and cardiovascular diseases: review of recent findings from the health effects of arsenic longitudinal study (HEALS) in Bangladesh, Toxicol. Appl. Pharmacol. 239 (2009) 184–192.
[34] A.T. Natarajan, J.J. Boei, F. Darroudi, P.C. Van Diemen, F. Dulout, M.P. Hande, A.T. Ramalho, Current cytogenetic methods for detecting exposure and effects of mutagens and carcinogens, Environ. Health Perspect. 104 (1996) 445–448.
[35] J. Mahata, A. Basu, S. Ghoshal, J.N. Sarkar, A.K. Roy, G. Poddar, A.K. Nandy, A. Banerjee, K. Ray, A.T. Natarajan, R. Nilsson, A.K. Giri, Chromosomal aberrations and sister chromatid exchanges in individuals exposed to arsenicthrough drinking water in West Bengal India, Mutat. Res. 534 (2003) 133–143.
[36] P. Ghosh, A. Basu, J. Mahata, S. Basu, M. Sengupta, J.K. Das, A. Mukherjee, A.K. Sarkar, L. Mondal, K. Ray, A.K. Giri, Cytogenetic damage and genetic variants in the individuals susceptible to arsenic-induced cancer through drinking water, Int. J. Cancer. 118 (2006) 2470–2478.
[37] L.E. Moore, A.H. Smith, C. Hopenhayn-Rich, M.L. Biggs, D.A. Kalman, M.T. Smith, Micronuclei in exfoliated bladder cells among individuals chronically exposed to arsenic in drinking water, Cancer Epidemiol. Biomark. Prev. 6 (1997) 31–36.
[38] M.E. Gonsebatt, L. Vega, A.M. Salazar, R. Montero, P. Guzmán, J. Blas, L.M. Del Razo, G. García-Vargas, A. Albores, M.E. Cebrián, M. Kelsh, P. Ostrosky-Wegman, Cytogenetic effects in human exposure to arsenic, Mutat. Res. 386 (1997) 219–228.
[39] P. Ghosh, A. Basu, K.K. Singh, A.K. Giri, Evaluation of cell types for assessment of cytogenetic damage in arsenic exposed population, Mol. Cancer 7 (2008), http://dx.doi.org/10.1186/1476-4598-7-45.